ALMA MATER STUDIORUM - UNIVERSITÀ DI BOLOGNA

SCUOLA DI INGEGNERIA E ARCHITETTURA

INGEGNERIA DELL'ENERGIA ELETTRICA

E DELL'INFORMAZIONE "GUGLIELMO MARCONI" - DEI

AUTOMATION ENGINEERING

TESI DI LAUREA

in

DIAGNOSIS AND CONTROL M

CONTROL OF FIVE PHASE DOUBLY FED INDUCTION MACHINES FOR MOTION AND CONTACTLESS POWER TRANSMISSION

CANDIDATO:

Gabriele Fabbri

RELATORE:

Prof. Ing. Andrea Tilli

CORRELATORE:

Ing. Christian Conficoni

Anno Accademico 2016/2017

Sessione II

To my Grandmother Marisa

A mia Nonna Marisa

Table of Contents

Figure Index

Abstract

In questa tesi si mostra come un motore a induzione di tipo doubly fed (DFIM) possa assolvere contemporaneamente le funzioni di motore e di trasmissione di potenza

In particolare questa peculiarità è particolarmente utile laddove sia necessario alimentare dei dispositivi elettrici a bordo di una macchina automatica a giostra, normalmente alimentati tramite contatti striscianti: da quest'ultimi infatti spesso derivano innumerevoli problematiche di usura e sicurezza.

In particolare, in questa tesi verrà trattato un azionamento pentafase: tale scelta è stata dettata dalla possibilità di disaccoppiare la trasmissione di potenza elettrica e quella meccanica. Data la particolarità di tale macchina una lunga sezione è dedicata alla sua descrizione.

Si presentano tre diverse metodologie di funzionamento e controllo della macchina doubly fed: in particolare le prime due, che si avvalgono di modulazioni di coppia o di potenza, potrebbero essere implementate anche su un motore trifase qualora risultasse conveniente; al contrario l'ultimo controllo proposto, che si fonda sull'utilizzo indipendente delle frequenze di statore, è applicabile solo a un DFIM pentafase.

Dai risultati ottenuti in simulazione, ma comprendenti moltissimi gradi di realismo, appare evidente come quest'ultimo dia i risultati migliori e sfrutti al meglio la macchina pentafase.

1 Introduction

A Doubly Fed Induction Machine (DFIM) is a particular induction motor that is characterized by some particular features that can be exploited in different ways.

Roughly speaking the main difference between a typical induction motor and a DFIM is that, instead of short-circuiting the rotor windings, they are open and connected to an inverter.

Doubly Fed Induction Machines are widely used now-a-days in wind pharms and aeolian electric generation: in that case, the rotor windings are connected to an inverter through slips rings. The main advantage of such a choice is that, with a proper control of the rotor inverter, it is possible to connect the stator directly to the electrical network. In other words, you can control the whole energy production, given both by the stator and the rotor, managing just the rotor fraction of energy (generally like a third of the total), leading to an under sizing of the inverter itself.

In this thesis, the motivation that led us to choosing a Doubly Fed Induction Motor is quite different: in order to obtain contactless power transfer, the motor must act also like a transformer closed in the air of the gap between the rotor and the stator. So, it is quite clear that both the extremities of such a transformer must be actively controlled by means of two power converters.

This result is desirable since up to now, if some electrical apparatuses are located on a rotating carousel they must be fed by the mean of slip rings.

This technology is well known as far as its drawbacks: in particular slip rings are subject to wear and often can create electric arcs. These characteristics lead to frequent maintenance operation and safety issues.

Since the main goal of this thesis is to eliminate slip rings and all their drawbacks, the rotor winding end in the rotor inverter that must be placed on board of the rotor itself, in order to feed the equipment placed on it as if they are connected to the grid.

Note that, since in carousel applications the mechanical load is almost only inertial, the machine that will be described has been designed to transmit a much higher quantity of electrical power respect that mechanical.

In the figure below, a generic scheme of the machine is reported, where the use of the two inverters can be recognized. Note that all the grey part is the carousel and so is moving that means that even the data must be transferred contactless.

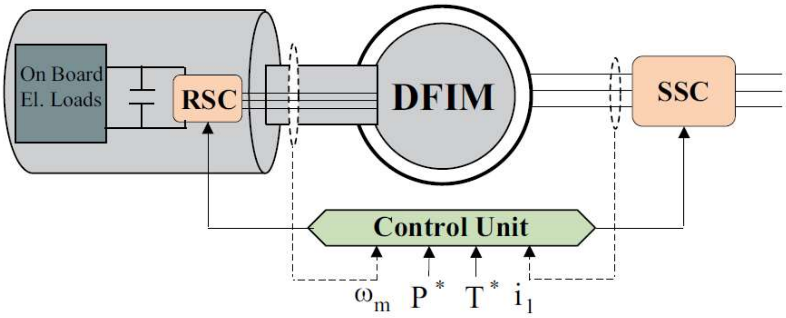

Figure 1-1 DFIM for contactless power transmission

The machine that will be referred to in this thesis is not a standard three phase motor, but it has been chosen, under the advice of expert electrical engineers, a five phase doubly fed induction machine.

This choice, as will be deeply explained in the following chapters, has been driven by the fact that such a machine has two, completely decoupled sets of dynamics: in other words, it is like having two motors acting on the same shaft. In such a way, it is possible to decouple the problem of transmitting motion and power.

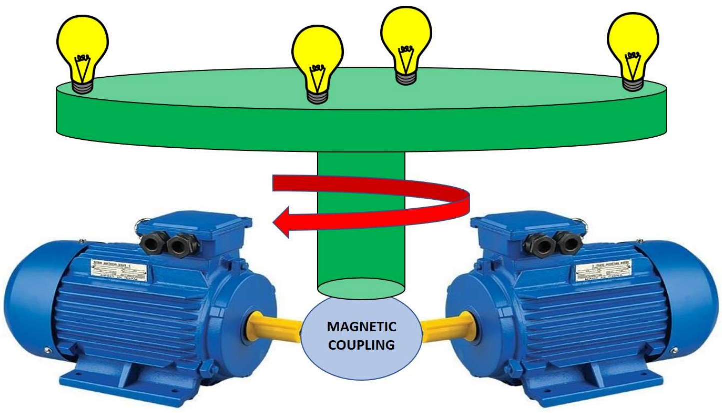

Figure 1-2 Explicative Scheme of a five phase DFIM behaviour

The thesis is structured as follows. First of all, the mathematical model of the DFIM and its simulative implementation is reported. A brief chapter is, then, devoted to describe limitations and issues related to a real implementation and to introduce the proposed controller structure, basically organized in two levels in a cascade fashion. Subsequently, three possible high-level algorithms are explained; then different techniques for tracking the refences generated will be shown. This thesis ends with some simulative results that highlights the characteristics of each high-level algorithm.

2 Model of a Five Phase Doubly Fed Induction Machine

2.1 Generic Principles, Clarke-Park Transformation and Harmonics Decoupling

The main functional principle beside a Doubly Fed Induction Machine is very similar to the classical squirrel cage induction motor.

A sinusoidal current in the stator produce a time varying magnetic flux that induce in the rotor a current in turn produce another field: from the interaction of the two fields comes out the torque.

As already remarked, the main difference between the two type of electric drives is that even the rotor of the DFIM is controllable: this means that the rotor currents are a degree of freedom and so are the fluxes.

For what concerns the torque and the power transmission can be, very roughly and imprecisely, considered in this way. The stator provides a certain amount of power to the rotor; then the rotor, by the means of the inverter, extract from it a certain amount of the power necessary to feed the carousel: the remaining energy is converted in mechanical energy and so in torque.

Before going deeper in the five-phase specification we have to do some assumptions.

The first one is quite common to all the electric drives: the stator and rotor windings must be star connected.

The second instead is trickier: the stator and the rotor windings must be concentrated instead of distributed. This will let the control to injects independent odd harmonics in the system ([2]).

In particular for a five-phase system the decoupled harmonics are the first, the fundamental, and the third.

It is common practices to take the stator frequencies of the two harmonics equal and so the only bound between the harmonics is, the frequency itself. This is due to the fact that in such a way the flux harmonics sum in order to reduce the peeks and so avoid possible magnetic saturation.

As all the three phase machines, even in this case the study of the dynamic of the machine is carried out by the use of the Clark Park transformation that can let us to transform the sinusoidal signals in continuous ones by the mean of a rotating reference frame.

The transformation is linear but dependant on the angle of the fundamental harmonic of the magnetic field's space vector. In particular, holds:

$$v_{dq} = T(\theta)v_{real} \qquad \text{Eq. 1}$$

Where v_{real} is a generic vector in the world reference frame (a sinusoidal signal) and v_{dq} is instead the same signal but in the $d-q$ reference frame.

In particular those vectors are made as

$$v_{real} = [v_a \quad v_b \quad v_c \quad v_d \quad v_e]^T \qquad \text{Eq. 2}$$

Where a, b, c, d, e are the real values in the machine's phases, and

$$v_{dq} = [v_{d1} \quad v_{q1} \quad v_{d3} \quad v_{q3} \quad v_n]^T \qquad \text{Eq. 3}$$

Where the down script 1 and 3 stays for the harmonic number and v_n is the tension of the neutral point, the center of the star.

The matrix $T(\theta)$, as already outlined, is function of the angle and is ([2]-[4])

$$T(\theta) = \frac{2}{5}\begin{bmatrix} \cos(\theta) & \cos\left(\theta - \frac{2\pi}{5}\right) & \cos\left(\theta - \frac{4\pi}{5}\right) & \cos\left(\theta + \frac{4\pi}{5}\right) & \cos\left(\theta + \frac{2\pi}{5}\right) \\ \sin(\theta) & \sin\left(\theta - \frac{2\pi}{5}\right) & \sin\left(\theta - \frac{4\pi}{5}\right) & \sin\left(\theta + \frac{4\pi}{5}\right) & \sin\left(\theta + \frac{2\pi}{5}\right) \\ \cos(3\theta) & \cos 3\left(\theta - \frac{2\pi}{5}\right) & \cos 3\left(\theta - \frac{4\pi}{5}\right) & \cos 3\left(\theta + \frac{4\pi}{5}\right) & \cos 3\left(\theta + \frac{2\pi}{5}\right) \\ \sin(3\theta) & \sin 3\left(\theta - \frac{2\pi}{5}\right) & \sin 3\left(\theta - \frac{4\pi}{5}\right) & \sin 3\left(\theta + \frac{4\pi}{5}\right) & \sin 3\left(\theta + \frac{2\pi}{5}\right) \\ \frac{1}{\sqrt{2}} & \frac{1}{\sqrt{2}} & \frac{1}{\sqrt{2}} & \frac{1}{\sqrt{2}} & \frac{1}{\sqrt{2}} \end{bmatrix} \qquad \text{Eq. 4}$$

Due to the characteristic propriety of T, T^{-1} it follows

$$T^{-1}(\theta) = \frac{5}{2}T(\theta) \qquad \text{Eq. 5}$$

We have to point out that is common practice to choose the angle θ in the transformation equal to the stator flux angle for the stator variables. For the rotoric variables instead θ corresponds to angle of the rotor flux with respect to the rotor itself: it is so equal to the difference between the electrical angle of the stator and the one of the rotor.

At the very end of this process it is obtained that all the variables are written in the same reference frame.

This will allow to write the equations in the sequent chapters.

The model that will be elaborated from now on has as state variables the stator currents i_{sd1}, i_{sq1}, i_{sd3}, i_{sq3} and the rotor magnetic fluxes φ_{rd1}, φ_{rq} , φ_{rd3}, φ_{rq3}.

Due to the need of simulating the machine behaviour the model that will follow was implemented in Simulink, by Mathworks.

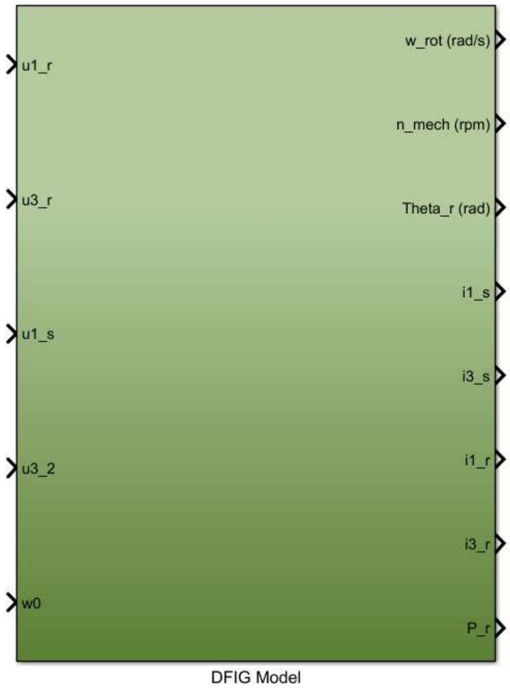

Figure 2.1-1 Outside-view of the Simulink DFIM model

The main inputs of the implemented block are the voltages for both the harmonics and for both the stator and the rotor, since are the best choice for controlling the currents and since is what I can directly apply them through the inverter. Another input is the frequency of the stator, again decided by policy that I will explain later.

The figure below portrays the details of the macro-block shown before.

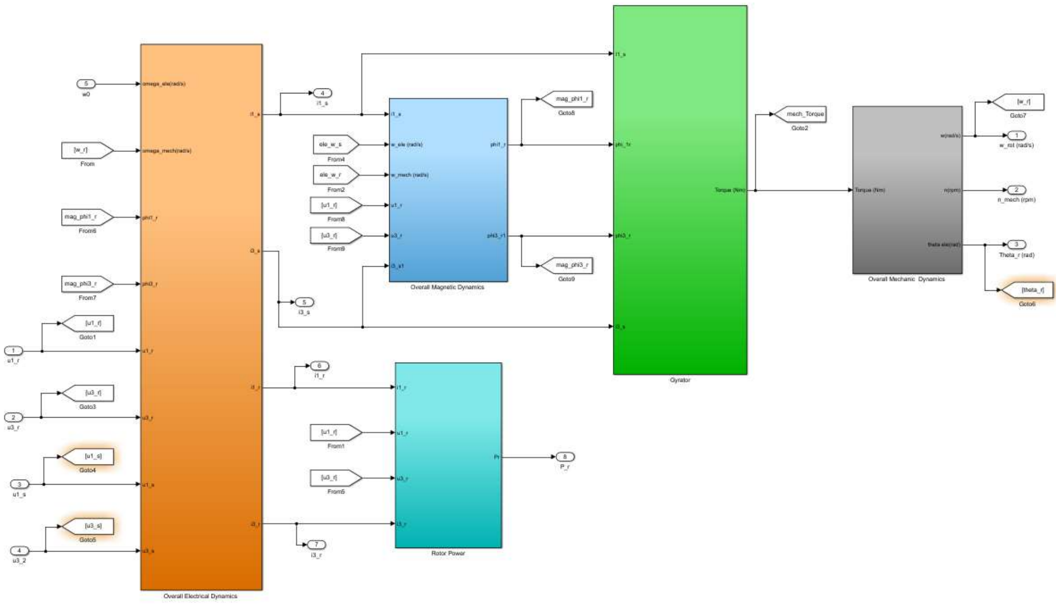

Figure 2.1-2 Inside-view of Overall view of the Simulink DFIM model

The overall model is divided in domains dynamics, mainly electrical (orange in Figure 2.1-2) magnetic (light blue) and mechanic (grey); the other two blocks are the *gyrator* (light green), that converts the interaction between fields in mechanical torque, and the electrical power out (cyan) on the rotor.

Each of the shown blocks shown in Figure 2.1-2 will be explained in detail in the following paragraphs.

2.2 Electrical Dynamics

All the DFIM inputs previously discussed enter the block and encounter the electrical dynamics. This happens for how we have decided to develop the model and then the control.

The block shown in Figure 2.2-1 presents even the two fluxes in input, that are computed by the dedicated block that will be discussed in the next chapter. That is due to the fact that obviously the fields interact with the windings of both the stator and the rotor, producing what is known as back electro-motive force.

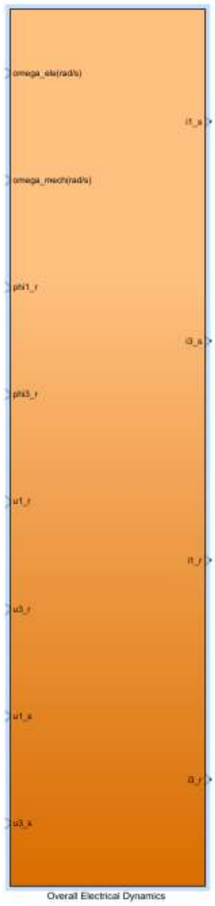

Figure 2.2-1 Outside-view of electrical dynamics

Since the dynamics, both for the stator and the rotor, are very similar for the first and the third harmonic, the model was developed in such a way that the parameters are exposed: to both the harmonics are dedicated identical blocks in which enters different constants.

For this reason, from now on we will go in the details only on the block without saying if it is referenced to the first o the third harmonic.

In any case obviously are present four blocks, even if are identical at couples.

The upper ones in Figure 2.2-2 are the stator dynamics for the first and third harmonic, while the down ones are linked to the rotor.

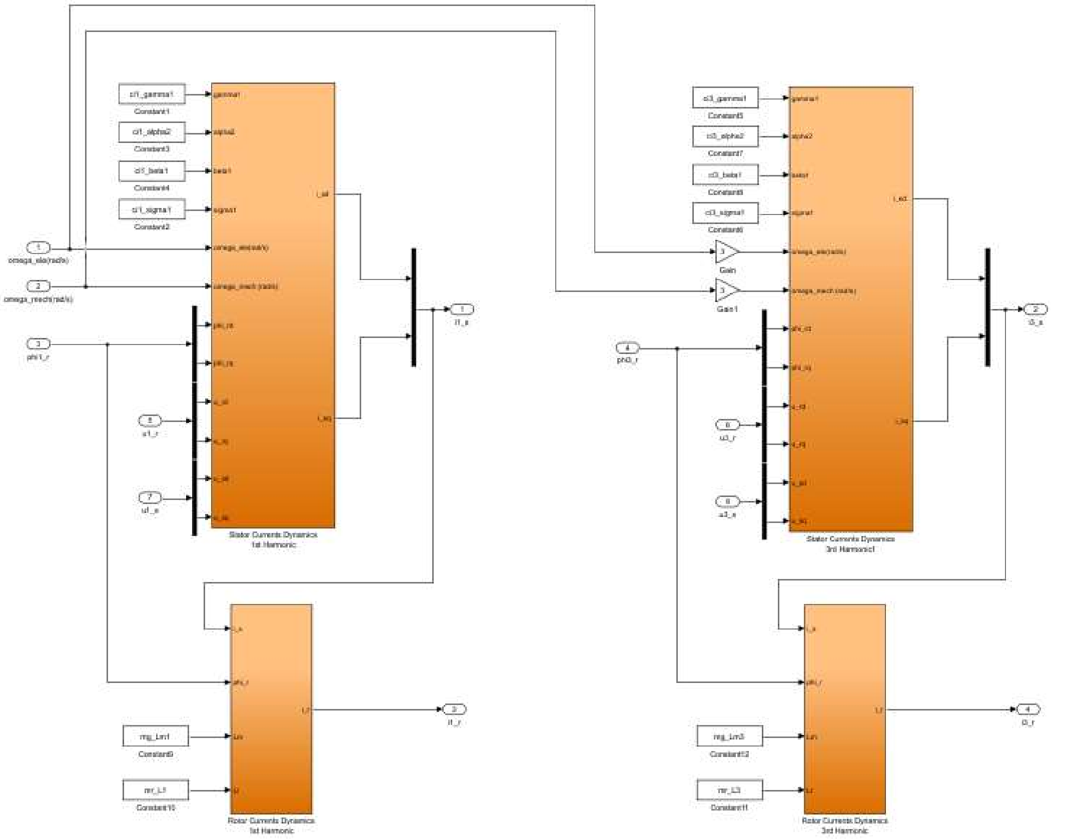

Figure 2.2-2 Inside-view of electrical dynamics

Before continuing let's define some concentrated parameters that will be referenced from now on.

Note again that those definitions are not linked to any harmonic: each harmonic will so have different values.

$$\sigma_1 = L_s\left(1 - \frac{L_m^2}{L_s L_r}\right)$$

$$\alpha_2 = \frac{R_r}{L_r} \qquad \beta_1 = \frac{L_m}{\sigma_1 L_r}$$

$$\gamma_1 = \frac{R_s}{\sigma_1} + \alpha_2 \beta_1 L_m \qquad \eta_1 = \frac{5}{2} p \frac{L_m}{L_r} \qquad \textit{Eq. 6}$$

The meaning of those symbols, even if standard and trivial, is reported in the end of this thesis.

2.2.1 Stator Dynamics

Now we will explore the stator dynamics.

Recalling the definitions before we can write the stator current dynamics of a generic harmonic as ([1]-[7]):

$$\dot{i_{sd}} = -\gamma_1 i_{sd} + \omega_0 i_{sq} + \alpha_2 \beta_1 \varphi_{rd} + \omega_r \beta_1 \varphi_{rq} - \beta_1 u_{rd} + \frac{1}{\sigma_1} u_{sd} \qquad \text{Eq. 7}$$

$$\dot{i_{sq}} = -\gamma_1 i_{sq} - \omega_0 i_{sd} + \alpha_2 \beta_1 \varphi_{rq} - \omega_r \beta_1 \varphi_{rd} - \beta_1 u_{rq} + \frac{1}{\sigma_1} u_{sq} \qquad \text{Eq. 8}$$

Where i are the currents and u are the voltages.

Remember that ω_r is the electrical speed of the rotor that is equal to

$$\omega_r = p\ \omega_m \qquad \text{Eq. 9}$$

Where ω_m is the mechanical speed of the rotor and p the number of pole pairs.

Defining them for the first and the third harmonic it results

$$\dot{i_{sd1}} = -\gamma_{11} i_{sd1} + \omega_0 i_{sq1} + \alpha_{21} \beta_{11} \varphi_{rd1} + \omega_r \beta_{11} \varphi_{rq1} - \beta_{11} u_{rd1} + \frac{1}{\sigma_{11}} u_{sd1} \qquad \text{Eq. 10}$$

$$\dot{i_{sq1}} = -\gamma_{11} i_{sq1} - \omega_0 i_{sd1} + \alpha_{21} \beta_{11} \varphi_{rq1} - \omega_{r1} \beta_{11} \varphi_{rd1} - \beta_{11} u_{rq1} + \frac{1}{\sigma_1} u_{sq1} \qquad \text{Eq. 11}$$

$$\dot{i_{sd3}} = -\gamma_{13} i_{sd3} + 3\omega_0 i_{sq3} + \alpha_{23} \beta_{13} \varphi_{rd3} + 3\omega_r \beta_1 \varphi_{rq3} - \beta_{13} u_{rd3} + \frac{1}{\sigma_{13}} u_{sd3} \qquad \text{Eq. 12}$$

$$\dot{i_{sq3}} = -\gamma_{13} i_{sq3} - 3\omega_0 i_{sd3} + \alpha_{23} \beta_{13} \varphi_{rq3} - 3\omega_r \beta_{13} \varphi_{rd3} - \beta_{13} u_{rq3} + \frac{1}{\sigma_{13}} u_{sq3} \qquad \text{Eq. 13}$$

As said and clearly shown in Figure 2.2-3, in the interface of the blocks there are also the parameters in such a way that the block is transparent respect changing of parameters between the first and the third harmonic.

Going inside the block it shows up two low side blocks, one devoted to the d-axis dynamic and one to the q-axis one. This instead is shown in Figure 2.2-4.

From that figure it is remarkable that most of the inputs are in common, as expected.

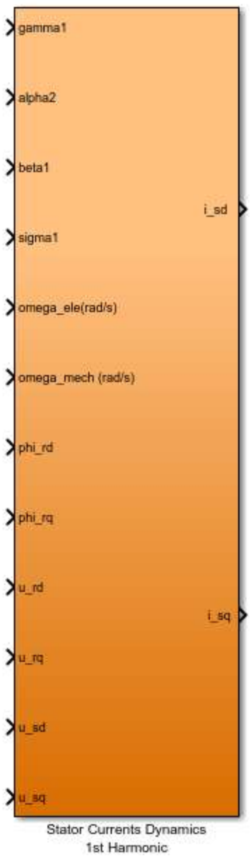

Figure 2.2-3 Outside-view Stator Dynamic

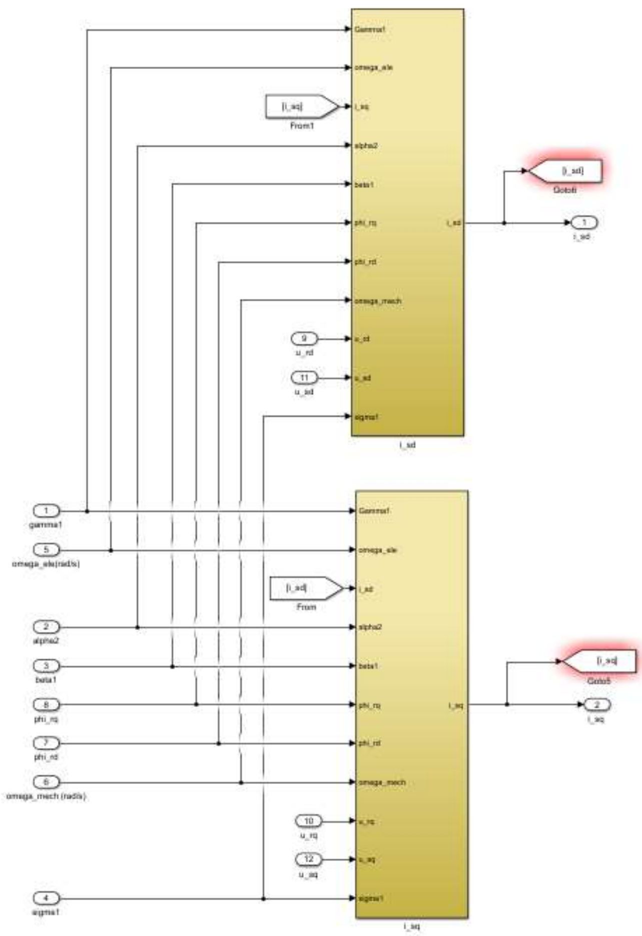

Figure 2.2-4 Inside-view Stator Dynamics

For sake of fast simulation and clear visualization, all the differential equations written in the beginning of this chapter where implemented by the common Simulink blocks and then integrated in time. The usage of Matlab function would have speeded up the implementation but such a component is treated quite badly by the Simulink solver, stuff that have should led to slow and imprecise simulations.

The results of such a choice is shown in the figures below.

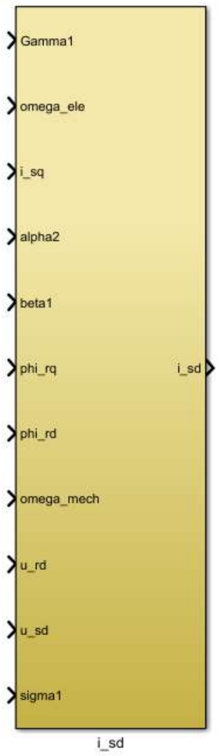

Figure 2.2-5 Outside-view d-axis Stator current

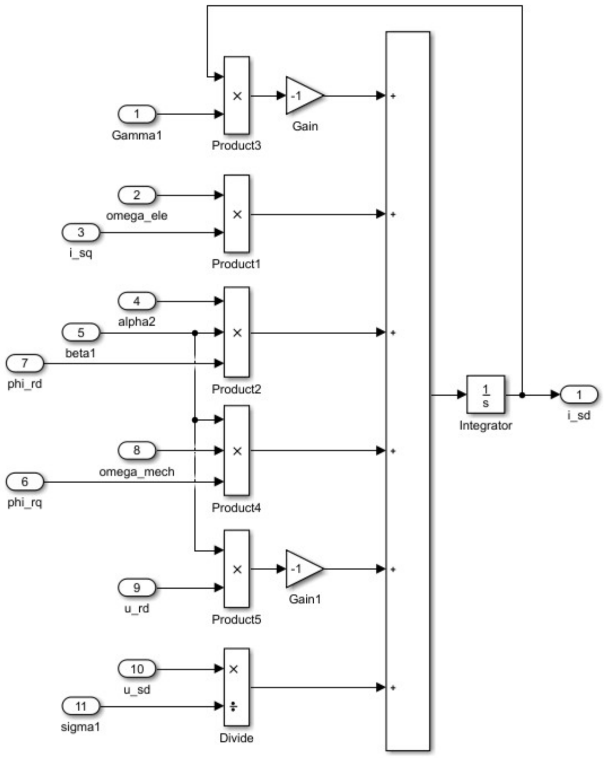

Figure 2.2-6 Inside-view d-axis Stator Current

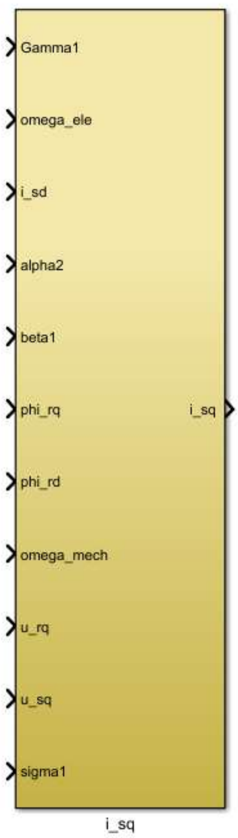

Figure 2.2-7 Outside-view q-axis Stator current

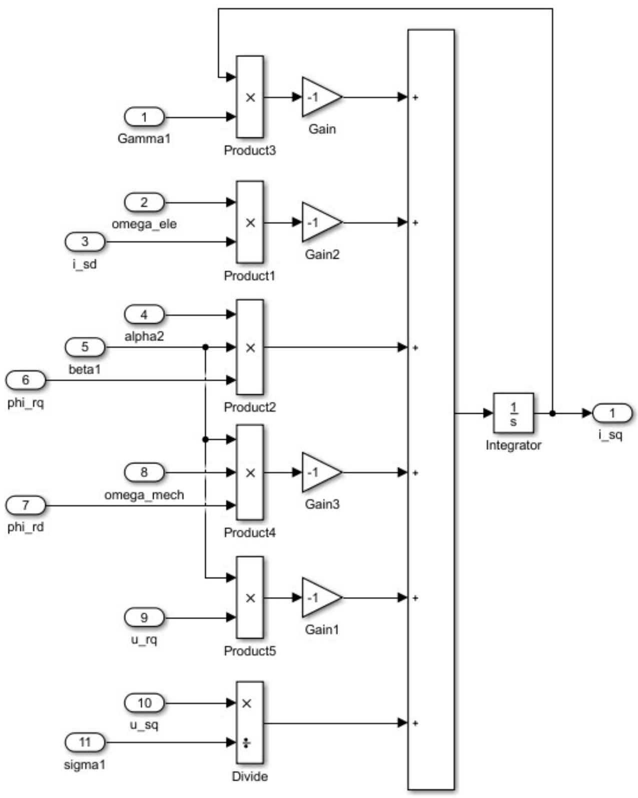

Figure 2.2-8 Inside-view q-axis Stator Current

2.2.2 Rotor Dynamics

As already mentioned the state variables that we have decided to adopt are the stator currents and the rotor fluxes. So only to those variables is associated a first order differential equation.

This implies that, for what concern the rotor currents, it must exist an algebraic relation between the state variable i_s and φ_r and the rotor currents i_r.

In particular, for a generic harmonic it holds ([1]-[7])

$$\varphi_{rd} = L_r i_{rd} + L_m i_{sd} \qquad \text{Eq. 14}$$

$$\varphi_{rq} = L_r i_{rq} + L_m i_{sq} \qquad \text{Eq. 15}$$

So reverting them and expliciting the rotor currents for all the harmonics, it is showable that

$$i_{rd1} = \frac{\varphi_{rd1} - L_{m1} i_{sd1}}{L_{r1}} \qquad \text{Eq. 16}$$

$$i_{rq1} = \frac{\varphi_{rq1} - L_{m1} i_{sq1}}{L_{r1}} \qquad \text{Eq. 17}$$

$$i_{rd3} = \frac{\varphi_{rd3} - L_{m3} i_{sd3}}{L_{r3}} \qquad \text{Eq. 18}$$

$$i_{rq3} = \frac{\varphi_{rq3} - L_{m3} i_{sq3}}{L_{r3}} \qquad \text{Eq. 19}$$

The Simulink implementation is reported in Figure 2.2-8: again, the parameters like the inductances are exposed for transparency respects the harmonics.

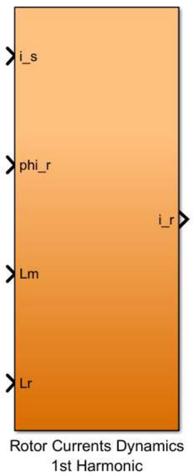

Figure 2.2-9 Outside-view Rotor Dynamics

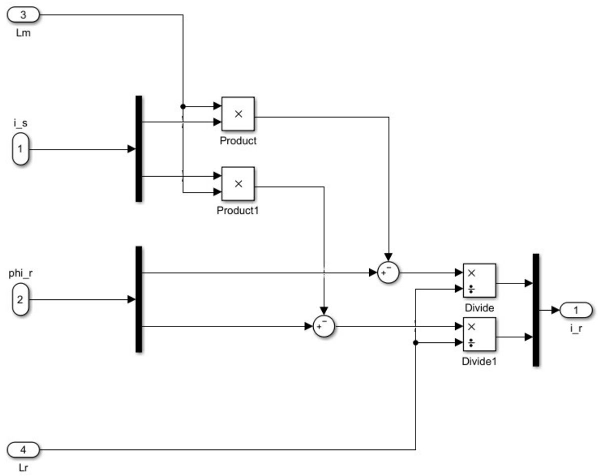

Figure 2.2-10 Inside-view Rotor Dynamics

2.3 Magnetic Dynamics

In this chapter, the rotor flux dynamic will be analysed.

The rotor flux dynamic associated to a generic harmonic has the following form ([1]-[7]):

$$\dot{\varphi_{rd}} = -\alpha_2\varphi_{rd} + (\omega_0 - \omega_r)\varphi_{rq} + \alpha_2 L_m i_{sd} + u_{rd} \qquad \textit{Eq. 20}$$

$$\dot{\varphi_{rq}} = -\alpha_2\varphi_{rq} - (\omega_0 - \omega_r)\varphi_{rd} + \alpha_2 L_m i_{sq} + u_{rq} \qquad \textit{Eq. 21}$$

It is remarkable that is present the difference between the stator and rotor angular speed since, as outlined in the beginning of this chapter, the Clarke Park transformation for the rotor variables involves the difference between the stator and the rotor angle.

Writing them for the first and the third harmonic I get

$$\dot{\varphi_{rd1}} = -\alpha_{21}\varphi_{rd1} + (\omega_0 - \omega_r)\varphi_{rq1} + \alpha_{21} L_{m1} i_{sd1} + u_{rd1} \qquad \textit{Eq. 22}$$

$$\dot{\varphi_{rq1}} = -\alpha_{21}\varphi_{rq1} - (\omega_0 - \omega_r)\varphi_{rd1} + \alpha_{21} L_{m1} i_{sq1} + u_{rq1} \qquad \textit{Eq. 23}$$

$$\dot{\varphi_{rd3}} = -\alpha_{23}\varphi_{rd3} + 3(\omega_0 - \omega_r)\varphi_{rq3} + \alpha_{23} L_{m3} i_{sd3} + u_{rd3} \qquad \textit{Eq. 24}$$

$$\dot{\varphi_{rq3}} = -\alpha_{23}\varphi_{rq3} - 3(\omega_0 - \omega_r)\varphi_{rd3} + \alpha_{23} L_{m3} i_{sq3} + u_{rq3} \qquad \textit{Eq. 25}$$

For what instead concerns the Simulink implementation, again it is has been decided to maintain separate the two harmonics and develop a generic block that can represent the first of the third harmonic dynamic, according to the parameters that are given to it.

According to this, as shown in Figure 2.3-2, all the parameters are exposed.

On the opposite, the interface of the overall magnetic dynamics has just control inputs (u) state variables (i) and the frequencies. This could be seen in Figure 2.3-1.

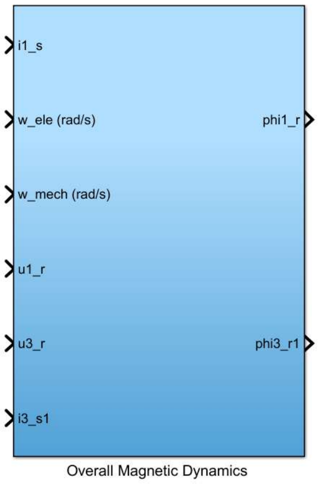

Figure 2.3-1 Outside-view Overall Magnetic dynamics

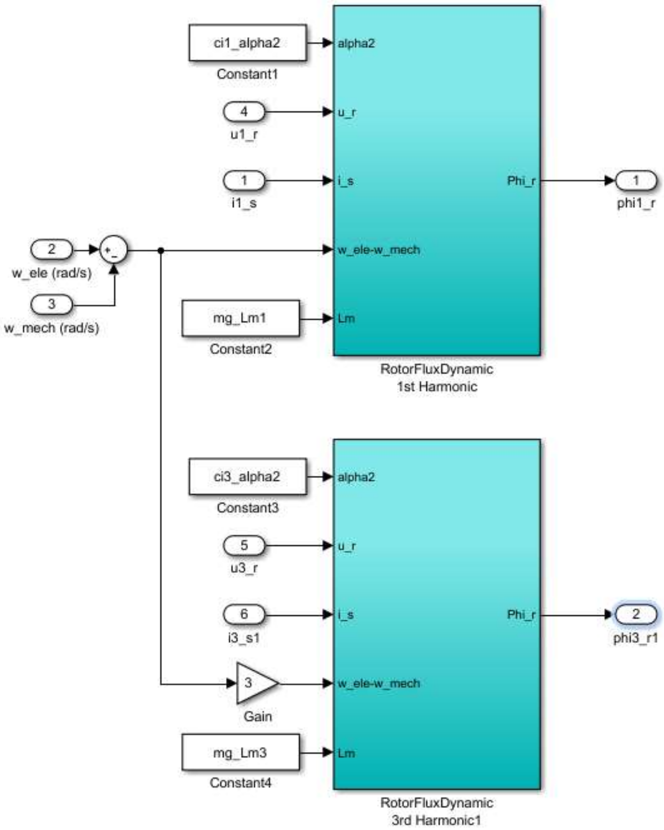

Figure 2.3-2 Inside-view Overall Magnetic dynamics

Going in the deep of a harmonic we will find the $d - q$ dynamics that are cross-coupled. As show in the beginning in the equations both the axis shares the majority of the inputs, since here inputs components $(d - q)$ are united in a single wire: to extract the value I just use a 2-way demux.

Even the two components of the output are muxed together for a more compact notation.

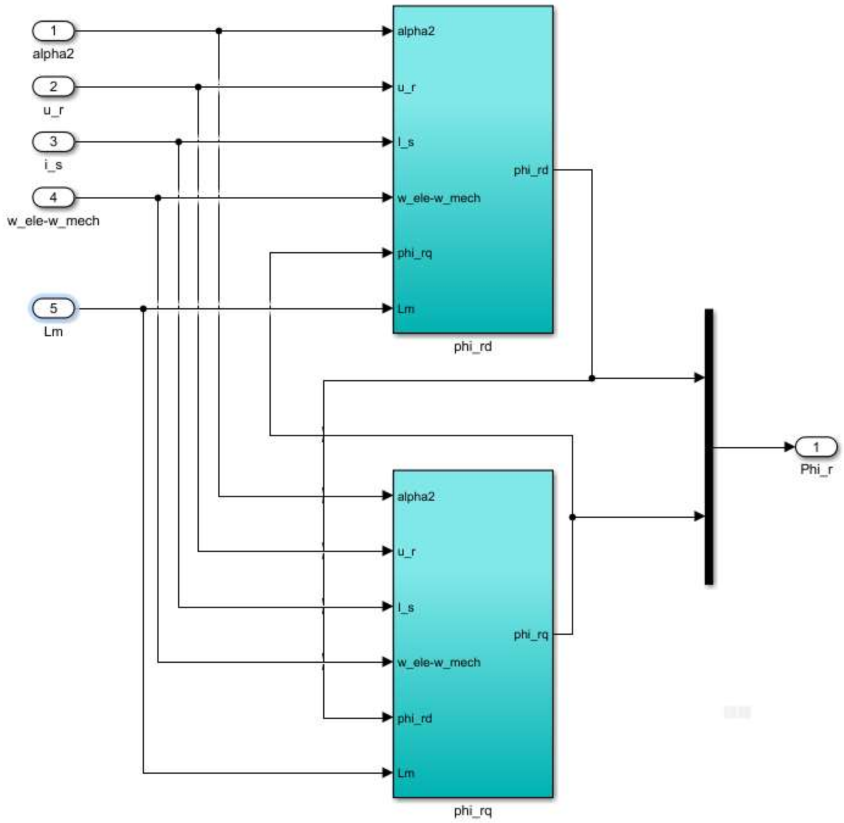

Figure 2.3-3 Inside-view Magnetic dynamic

In the next figures is show the implementation of the state equations of the and magnetic axis.

As in the stator current case it has been decided to use just Simulink blocks to speed up simulations and make them more robust. This was paid with a longer implementation time and a less user-friendly block.

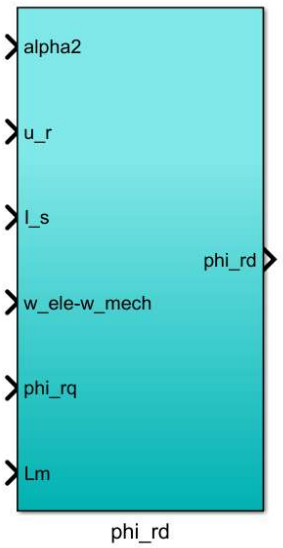

Figure 2.3-4 Outside-view d-axis Rotor Flux

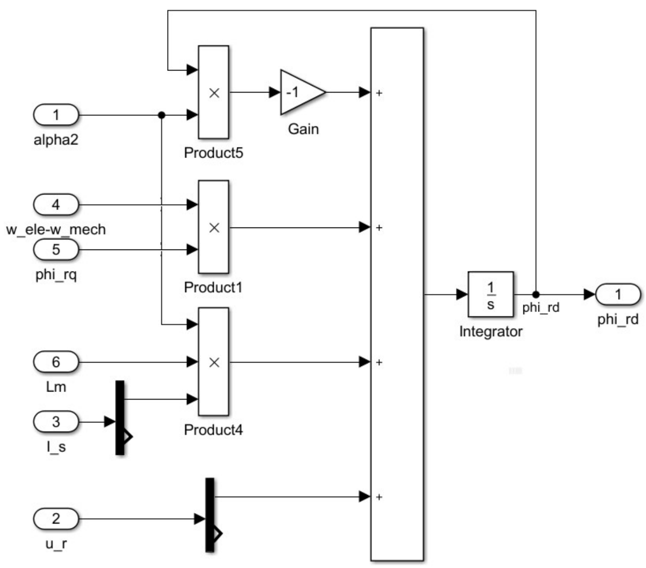

Figure 2.3-5 Inside-view d-axis Rotor Flux

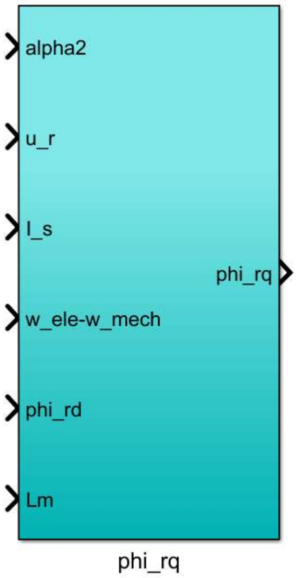

Figure 2.3-6 Outside-view q-axis Rotor Flux

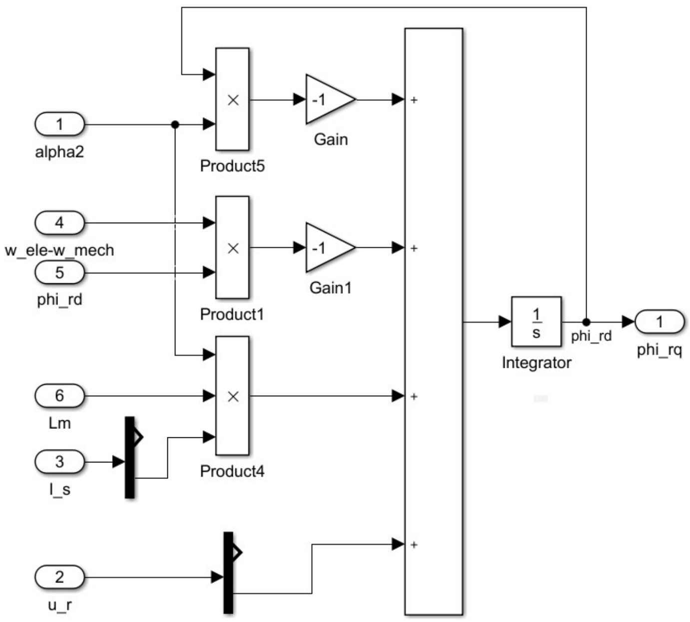

Figure 2.3-7 Inside-view q-axis Rotor Flux

2.4 Gyrator

The gyrator is not touchable part of the machine but is more like part that makes a motor to produce torque.

In fact, it is the part devoted to link the stator currents and the rotor flux in such a way it is possible to compute the torque that is delivered to the mechanical load.

In this case we have to abandon a generic formulation, independent from the harmonic number, and going in the deep of the specific structure of the machine.

In particular it holds ([2]-[4])

$$T = T_1 + 3T_3 \qquad \textit{Eq. 26}$$

$$T = \eta_{11}(\varphi_{rd1} i_{sq1} - \varphi_{rq1} i_{sd1}) + 3\eta_{13}(\varphi_{rd3} i_{sq3} - \varphi_{rq3} i_{sd3}) \qquad \textit{Eq. 27}$$

Where T_1 and T_3 are the torques delivered from the first and the third harmonic.

The Simulink implementation is shown below.

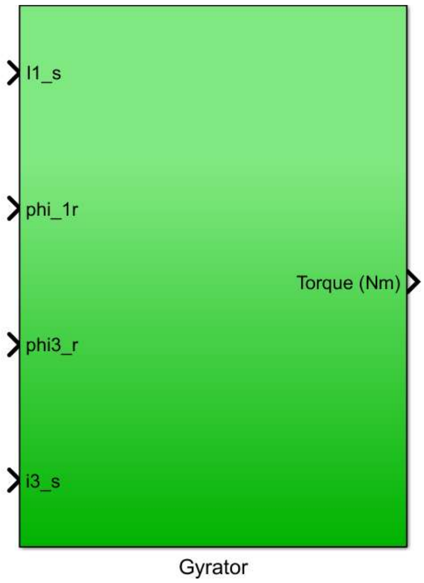

Figure 2.4-1 Outside-view Gyrator

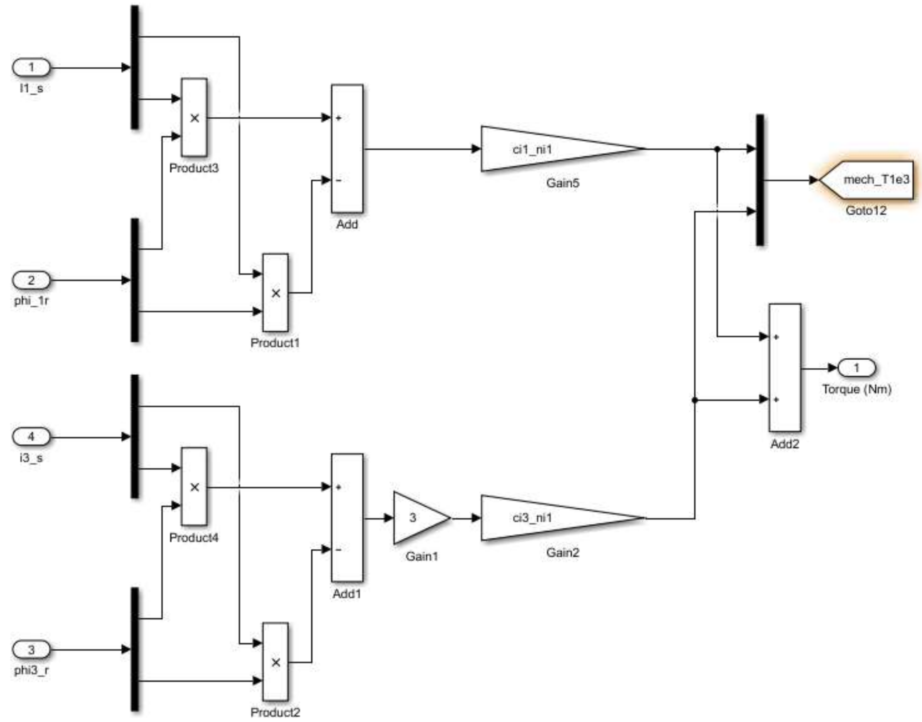

Figure 2.4-2 Inside-view Gyrator

2.5 Electrical Output Power

The electrical power delivered to the electrical load is computed as a generic load, so like the product between the voltage and the current.

Both the harmonics contributes in the same way, so the harmonic number doesn't count in the power delivered.

So in the end it holds ([1])

$$P_r = \frac{5}{2}(P_{r1} + P_{r3}) \quad \textit{Eq. 28}$$

$$P_r = \frac{5}{2}(i_{rd1}v_{rd1} + i_{rq1}v_{rq1} + i_{rd3}v_{rd3} + i_{rq3}v_{rq3}) \quad \textit{Eq. 29}$$

Where P_{r1} and P_{r3} are the power delivered to the rotor DC link by the first and the third harmonic. Note also that the term $\frac{5}{2}$ is present due to the Clarke Park transformation.

For what concerns the implementation in Simulink, since it has been decided to collect the components in a single signal it is possible to obtain a more compact formulation of that using the dot product.

The result is shown in the figure below.

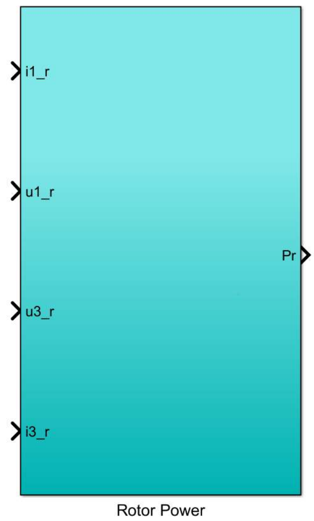

Figure 2.5-1 Outside-view Rotor Power

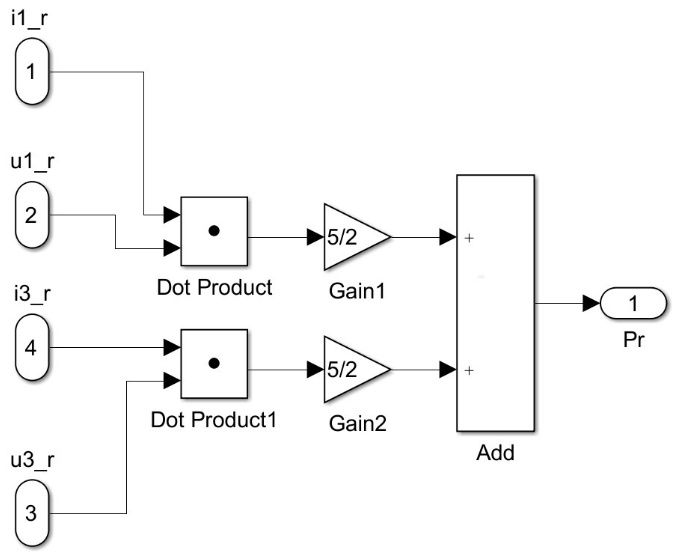

Figure 2.5-2 Inside-view Rotor Power

2.6 Mechanical Dynamics

Really simple is even the mechanical model: in fact, under the assumption of no external forces and viscous friction hold what follows.

$$T = J\dot{\omega_m} + b\omega_m \tag{Eq. 30}$$

Where J is the inertia of the rotor and b the viscous coefficient.

This approximation is quite strong but it is reasonable, in particular the choice of neglecting the elasticity of the system, since it is a direct drive machine, in which no elastic joint or reduction gearbox are necessary ([8]).

In this case is also possible and convenient to derive the transfer function of the mechanical load: this will help when I'll need to tune the velocity regulator.

$$G_m(s) = \frac{1}{Js + b} \tag{Eq. 31}$$

The implementation is now straightforward and follows

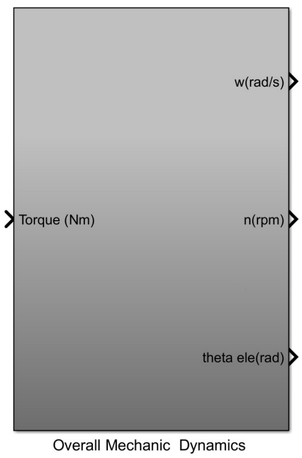

Figure 2.6-1 Outside-view Mechanical Dynamics

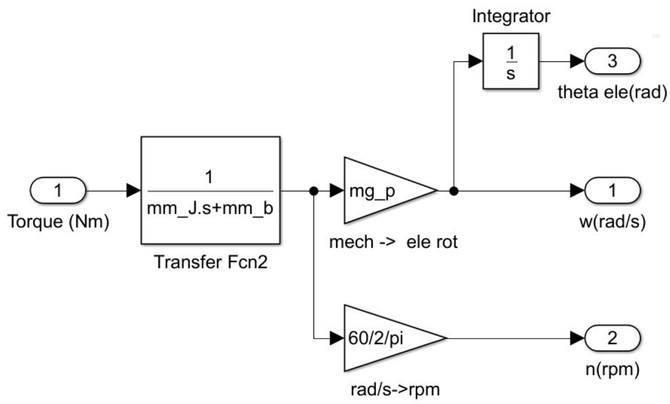

Figure 2.6-2 Inside-view Mechanical Dynamics

Note that, for sake of simplicity, the block outs some indirect measures like the electrical speed and angle.

2.7 Overall Dynamical Model

For sake of completeness in this section it will be reported all the dynamical equation written before in such a way to give a unique vision of the model ([1]-[7]).

$$\dot{i_{sd1}} = -\gamma_{11} i_{sd1} + \omega_0 i_{sq1} + \alpha_{21}\beta_{11}\varphi_{rd1} + \omega_r\beta_{11}\varphi_{rq1} - \beta_{11}u_{rd1} + \frac{1}{\sigma_{11}}u_{sd1} \qquad \text{Eq. 32}$$

$$\dot{i_{sq1}} = -\gamma_{11} i_{sq1} - \omega_0 i_{sd1} + \alpha_{21}\beta_{11}\varphi_{rq1} - \omega_{r1}\beta_{11}\varphi_{rd1} - \beta_{11}u_{rq1} + \frac{1}{\sigma_1}u_{sq1} \qquad \text{Eq. 33}$$

$$\dot{\varphi_{rd1}} = -\alpha_{21}\varphi_{rd1} + (\omega_0 - \omega_r)\varphi_{rq1} + \alpha_{21}L_{m1}i_{sd1} + u_{rd1} \qquad \text{Eq. 34}$$

$$\dot{\varphi_{rq1}} = -\alpha_{21}\varphi_{rq1} - (\omega_0 - \omega_r)\varphi_{rd1} + \alpha_{21}L_{m1}i_{sq1} + u_{rq1} \qquad \text{Eq. 35}$$

$$\dot{i_{sd3}} = -\gamma_{13} i_{sd3} + 3\omega_0 i_{sq3} + \alpha_{23}\beta_{13}\varphi_{rd3} + 3\omega_r\beta_{13}\varphi_{rq3} - \beta_{13}u_{rd3} + \frac{1}{\sigma_{13}}u_{sd3} \qquad \text{Eq. 36}$$

$$\dot{i_{sq3}} = -\gamma_{13} i_{sq3} - 3\omega_0 i_{sd3} + \alpha_{23}\beta_{13}\varphi_{rq3} - 3\omega_r\beta_{13}\varphi_{rd3} - \beta_{13}u_{rq3} + \frac{1}{\sigma_{13}}u_{sq3} \qquad \text{Eq. 37}$$

$$\dot{\varphi_{rd3}} = -\alpha_{23}\varphi_{rd3} + 3(\omega_0 - \omega_r)\varphi_{rq3} + \alpha_{23}L_{m3}i_{sd3} + u_{rd3} \qquad \text{Eq. 38}$$

$$\dot{\varphi_{rq3}} = -\alpha_{23}\varphi_{rq3} - 3(\omega_0 - \omega_r)\varphi_{rd3} + \alpha_{23}L_{m3}i_{sq3} + u_{rq3} \qquad \text{Eq. 39}$$

From these dynamical equations, it is even possible to determine the steady state equations. This is not just a trivial mathematical exercise but really helps to understand the connections between the variables and it will be exploited in the next chapter to determine the physical limits of the machine.

Note that in such conditions the values of currents and fluxes can be considered as the steady state one (i.e. constant in the considered reference frame). After some computations, it results:

$$u_{sd1} = \sigma_{11}(\gamma_{11}i_{sd1} - \omega_0 i_{sq1} - \alpha_{21}\beta_{11}\varphi_{rd1} - \beta_{11}\omega_r\varphi_{rq1} + \beta_{11}u_{rd1}) \qquad \text{Eq. 40}$$

$$u_{sq1} = \sigma_{11}(\gamma_{11}i_{sq1} + \omega_0 i_{sd1} - \alpha_{21}\beta_{11}\varphi_{rq1} + \beta_{11}\omega_r\varphi_{rd1} + \beta_{11}u_{rq1}) \qquad \text{Eq. 41}$$

$$u_{rd1} = \alpha_{21}\varphi_{rd1} - (\omega_0 - \omega_r)\varphi_{rq1} - \alpha_{21}L_{m1}i_{sd1} \qquad \text{Eq. 42}$$

$$u_{rq1} = \alpha_{21}\varphi_{rq1} + (\omega_0 - \omega_r)\varphi_{rd1} - \alpha_{21}L_{m3}i_{sq1} \qquad \text{Eq. 43}$$

$$u_{sd3} = \sigma_{13}(\gamma_{13}i_{sd3} - 3\omega_0 i_{sq3} - \alpha_{23}\beta_{13}\varphi_{rd3} - 3\beta_{13}\omega_r\varphi_{rq3} + \beta_{13}u_{rd3}) \qquad \text{Eq. 44}$$

$$u_{sq3} = \sigma_{13}(\gamma_{13}i_{sq3} + 3\omega_0 i_{sd3} - \alpha_{23}\beta_{13}\varphi_{rq3} + 3\beta_{13}\omega_r\varphi_{rd3} + \beta_{13}u_{rq3}) \qquad \text{Eq. 45}$$

$$u_{rd3} = \alpha_{23}\varphi_{rd3} - 3(\omega_0 - \omega_r)\varphi_{rq3} - \alpha_{23}L_{m3}i_{sd3} \qquad \text{Eq. 46}$$

$$u_{rq3} = \alpha_{23}\varphi_{rq3} + 3(\omega_0 - \omega_r)\varphi_{rd3} - \alpha_{23}L_{m3}i_{sq3} \qquad \text{Eq. 47}$$

2.8 State Space Model

As already remarked, the model shown up to now presents a really strong coupling between the current and the fluxes.

That is quite obvious if we consider the fact that the torque production is related to the interaction between stator and rotor fluxes.

It is also remarkable that, if we consider the stator and the rotor frequency ω_0 and ω_r constant, or in general dynamically decoupled, the model is made up by four first order differential equations. That is quite obvious for the rotor one, since is proportional to the mechanical speed: it is well known that the mechanical dynamics is much slower than the electrical one. For what concerns, instead, the stator frequency the control should take care of not changing it too quickly.

Under those assumptions, it is possible to write the system of equation of the model in the state space form like

$$\begin{aligned} \dot{x} &= Ax + Bu \\ y &= I_4 x \end{aligned} \qquad \textit{Eq. 48}$$

Where x are the states of the machine and u the inputs.

This framework will never be used for modelling purpose but could come back useful for control tuning and in particular MIMO control.

Note that, under the assumption of linear inductances, measuring the stator currents and the rotor fluxes is equivalent to measure the stator and the rotor currents. So the matrix C that usually links the states and the outputs is the identity, as reported.

Again, even in this case will be reported the result for a generic harmonic.

For what concerns x and u is straightforward

$$x = [i_{sd} \quad i_{sq} \quad \varphi_{rd} \quad \varphi_{rq}] \qquad \textit{Eq. 49}$$

$$u = [u_{sd} \quad u_{sq} \quad u_{rd} \quad u_{rq}] \qquad \textit{Eq. 50}$$

The matrixes A and B are instead equal to

$$A = \begin{bmatrix} -\gamma_1 & \omega_0 & \alpha_2\beta_1 & \beta_1\omega_r \\ -\omega_0 & -\gamma_1 & -\beta_1\omega_r & -\alpha_2\beta_1 \\ \alpha_2 L_m & 0 & -\alpha_2 & \omega_0 - \omega_r \\ 0 & \alpha_2 L_m & -(\omega_0 - \omega_r) & -\alpha_2 \end{bmatrix} \qquad \textit{Eq. 51}$$

$$B = \begin{bmatrix} \frac{1}{\sigma_1} & 0 & -\beta_1 & 0 \\ 0 & \frac{1}{\sigma_1} & 0 & -\beta_1 \\ 0 & 0 & 1 & 0 \\ 0 & 0 & 0 & 1 \end{bmatrix} \qquad \text{Eq. 52}$$

It has to be underlined that only the matrix A is dependant over the frequencies; B instead is time invariant.

2.9 Model in the Measurable Variables

As already often recalled the overall system has been developed using as states the stator currents and the rotor flux. This formulation is very useful once you have to define the references to produces a certain torque and a certain power, since these quantities are usually expressed referring to the variables mentioned; it is no more useful once you have to develop a low-level controller since the flux is not directly measurable.

It has so been converted the state space model in such a way the state variables are the stator and the rotor currents. Let's so now define for a generic harmonic

$$z(t) = [i_{sd} \quad i_{sq} \quad i_{rd} \quad i_{rq}]^T \qquad \textit{Eq. 53}$$

And note that exists the following relation between $z(t)$ and $x(t)$, the vector composed by the stator currents and the rotor fluxes

$$x(t) = \begin{bmatrix} 1 & 0 & 0 & 0 \\ 0 & 1 & 0 & 0 \\ L_m & 0 & L_r & 0 \\ 0 & L_m & 0 & L_r \end{bmatrix} z(t) \qquad \textit{Eq. 54}$$

Let's call this matrix, as in the chapter before, $T_{isir2isphi}$ and its invers $T_{isphir2isi}$.

Now, if we substitute that expression in the continuous time state space model

$$\dot{x}(t) = Ax(t) + Bu(t) \qquad \textit{Eq. 55}$$

We get

$$\dot{z}(t) = T_{isphir2isir}AT_{isir2isphir}z(t) + T_{isphir2isir}Bu(t) \qquad \textit{Eq. 56}$$

And so defining

$$\begin{gathered} A_i = T_{isphir2isir}AT_{isir2isphir} \\ B_i = T_{isphir2isir}B \end{gathered} \qquad \textit{Eq. 57}$$

It is possible to write

$$\dot{z}(t) = A_i z(t) + B_i u(t) \qquad \textit{Eq. 58}$$

For a generic harmonic A_i and B_i have the following shape

$$A_{i\#} =$$

$$\begin{bmatrix} -\frac{R_s}{\sigma_1} & \omega_0 + L_m\beta_1\omega_r & L_r\alpha_2\beta_1 & L_r\beta_1\omega_r \\ -\omega_0 - L_m\beta_1\omega_r & -\frac{R_s}{\sigma_1} & -L_r\beta_1\omega_r & L_r\alpha_2\beta_1 \\ \frac{L_m R_s}{L_r\sigma_1} & -\frac{L_m(1+L_m\beta_1)\omega_r}{L_r} & -\alpha_2(1+L_m\beta_1) & \omega_0 - (1+L_m\beta_1)\omega_r \\ \frac{L_m(1+L_m\beta_1)\omega_r}{L_r} & \frac{L_m R_s}{L_r\sigma_1} & -\omega_0 + (1+L_m\beta_1)\omega_r & -\alpha_2(1+L_m\beta_1) \end{bmatrix}$$

Eq. 59

$$B_{i\#} = \begin{bmatrix} \frac{1}{\sigma_1} & 0 & -\beta_1 & 0 \\ 0 & \frac{1}{\sigma_1} & 0 & -\beta_1 \\ -\frac{L_m}{L_r\sigma_1} & 0 & \frac{1+L_m\beta_1}{L_r} & 0 \\ 0 & -\frac{L_m}{L_r\sigma_1} & 0 & \frac{1+L_m\beta_1}{L_r} \end{bmatrix}$$

Eq. 60

2.10 Operative Limits

In this section, the operative limits of the machine will be explored.

The analysis will be carried out independently from the harmonic number: for that reason, in this chapter won't be reported the harmonic number in the equations. Furthermore, a single harmonic will be analysed. Furthermore, to do not make confusion it has been decided to use the symbol ϕ for the flux and to omit the lowscript s for the stator current.

Substituting the expression of the rotor currents as function of the fluxes and the stator currents (reported in chapter 2.2.2) and the steady state rotor tension in the power expression comes out

$$P = \frac{5}{2}\left(\frac{(-i_q L_m + \phi_q)(-i_q L_m \alpha_2 + \alpha_2 \phi_q + \phi_d \omega_0 - \phi_d \omega_r)}{L_r} + \frac{(-i_d L_m + \phi_d)(-i_d L_m \alpha_2 + \alpha_2 \phi_d - \phi_q \omega_0 + \phi_q \omega_r)}{L_r}\right) \qquad \textit{Eq. 61}$$

On the other side the torque is still

$$T = \eta_1(\phi_d i_q - \phi_q i_d) \qquad \textit{Eq. 62}$$

Now compute i_d from the torque expression and substitute it in the power expression: a completely messy and meaningless expression pops out and for this reason won't be reported.

The important thing is that is quadratic in i_q: this implies that the square that compares solving it must exists. This impose some restrictions.

In particular, i_q is equal to

$$i_q^a = \frac{\phi_q}{L_m} + \frac{T\phi_d}{\eta_1(\phi_d^2 + \phi_q^2)} - \frac{\sqrt{L_m^2 \alpha_2 \eta_1^2 \phi_q^2 (2PL_r \eta_1^2(\phi_d^2 + \phi_q^2) - 5TL_m(TL_m\alpha_2 + \eta_1(\phi_d^2 + \phi_q^2)(-\omega_0 + \omega_r)))}}{\sqrt{5} L_m^2 \alpha_2 \eta_1^2 (\phi_d^2 + \phi_q^2)} \qquad \textit{Eq. 63}$$

$$i_q^b = \frac{\phi_q}{L_m} + \frac{T\phi_d}{\eta_1(\phi_d^2 + \phi_q^2)} + \frac{\sqrt{L_m^2 \alpha_2 \eta_1^2 \phi_q^2 (2PL_r \eta_1^2(\phi_d^2 + \phi_q^2) - 5TL_m(TL_m\alpha_2 + \eta_1(\phi_d^2 + \phi_q^2)(-\omega_0 + \omega_r)))}}{\sqrt{5} L_m^2 \alpha_2 \eta_1^2 (\phi_d^2 + \phi_q^2)} \qquad \textit{Eq. 64}$$

Since the only elements that links the first and the third harmonic is the frequency let's try to grant the existence of that square root through ϕ_d.

$$\phi_d < -\frac{\sqrt{-2PL_r\eta_1^2\phi_q^2 + 5TL_m(TL_m\alpha_2 + \eta_1\phi_q^2(-\omega_0 + \omega_r))}}{\sqrt{\eta_1(2PL_r\eta_1 + 5TL_m(\omega_0 - \omega_r))}}$$

Or

$$\phi_d > \frac{\sqrt{-2PL_r\eta_1^2\phi_q^2 + 5TL_m(TL_m\alpha_2 + \eta_1\phi_q^2(-\omega_0 + \omega_r))}}{\sqrt{\eta_1(2PL_r\eta_1 + 5TL_m(\omega_0 - \omega_r))}} \quad \text{Eq. 65}$$

If T is different from zero both the square roots are satisfied by the same condition on ω_0 that follows and depends on the sign of T.

If $T > 0$

$$\omega_0 - \omega_r > -\frac{2PL_r\eta_1}{5TL_m} \quad \text{Eq. 66}$$

If $T < 0$

$$\omega_0 - \omega_r < -\frac{2PL_r\eta_1}{5TL_m} \quad \text{Eq. 67}$$

This result is very important since gives a bound over the fundamental frequency ω_0 that is, as often remarked, the unique link between the first and the third harmonic.

Let's point out that the power is always negative ($P \leq 0$) since the rotor takes energy in order to supply the on board devices: those expression says that the sign of the slip must be equal to sign of the torque.

Since the slip is the same for all the harmonics this implies that one harmonic can't produce an opposite torque respect another harmonic unless I allow to produce a positive power.

This could be a cute mathematical trick but doesn't make a lot of sense this means that the system is transferring power from the rotor to the stator.

In any case even this functional mode was explored and turns out to not solve some other problems that will be clarified in the next chapters.

2.11 Chapter References

[1] A. TILLI, A. BOSSO, C. CONFICONI A. HASHEMI, Integrated Control of Motion and Contactless Power Transfer for Doubly-Fed Induction Machine in Complex Rotary Apparatus, 20th IFAC Congress, 2017

[2] A. TANI, Slides of the seminar on multiphase modelling and control, UNIBO internal material, 2017

[3] M. J. DURAN, F. SALAS, Bifurcation Analysis of Five-Phase Induction Motor Drives With Third Harmonic Injection, IEEE transactions on industrial electronics, vol. 55, no. 5, may 2008

[4] H. XU, H.A. TOLIYAT, L.J. PETERSEN, Rotor Field Oriented Control of Five-Phase Motor with the Combined Fundamental and Third Harmonic Currents, IEEE APEC, 2001

[5] L. A. PEREIRA, C. C. SCHRLAU, L. F. A. PEREIRA, J. F. HAFFNER, Model of a Five-Phase Induction Machine Allowing for Harmonics in the Air-Gap Field. Part 1: Parameter Determination and General Equations, The 30th Annual Conference of the IEEE lndustrial Electronics Soclety, November 2 - 6, 2004

[6] L. A. PEREIRA, C. C. SCHRLAU, L. F. A. PEREIRA, J. F. HAFFNER, Model of a Five-Phase Induction Machine Allowing for Harmonics in the Air-Gap Field. Part 2: Transformation of Co-Ordinates and d-q Models, The 30th Annual Conference of the IEEE lndustrial Electronics Soclety, November 2 - 6, 2004

[7] G. RENUKADEVI, K. RAJAMBAL, Generalized Model of Multi-Phase Induction Motor Drive using Matlab/Simulink, IEEE PES Innovative Smart Grid Technologies, 2011

[8] E. FUNAIOLI, A. MAGGIORE, U. MENEGHETTI, Lezioni di Meccanica Applicata alle Macchine", Patron, 2005

3 Control Solutions

In this chapter and in the following ones, the proposed control solutions of the DFIM are explained in details. First of all, we have to underline that all of the proposed versions are dived in two main blocks: the high-level and the low-level one.

The first one is in charge of generating the adequate references for stator currents and rotor fluxes; its inputs are the references generated by operators or supervisory systems, namely the velocity trajectory and the transmitted power setpoint. No feedback is involved, except for the real velocity of the machine, value that is necessary to compute the reference for the torque request.

Since the velocity dynamic is very slow the mechanical velocity can be seen as a quasi-stationary signal to the high-level control that makes it as a pure algebraic block without any dynamic.

On the other side, the low-level control is in charge of tracking the references given by the high level one: this implies that obviously the electromagnetic dynamics of the machine are involved and so even the controllers are dynamic.

Due to the architecture of the machine it is not possible to have a tangible connection from the stator and the rotor: what is possible is a wireless connection between the two. A problem with that is that a wireless communication is much slower than an on board one, up to two orders of magnitude of difference.

This make impossible to have a centralized controller, for instance on the stator, that command even the rotor inverter: it is so necessary to have a distributed control. This means that will be two controllers, one for the stator and one for the rotor, that can work close to independently or with rare communications.

The high-level control will reside on one of the two boards, for instance the stator one.

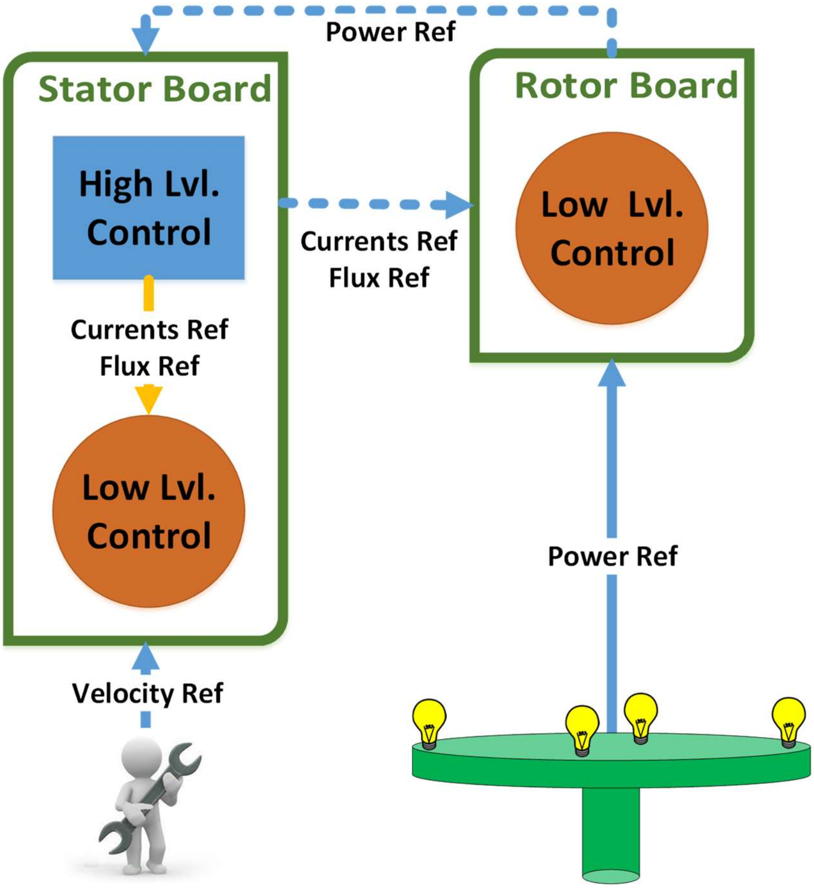

Figure 3-1 Graphical Representation of the division of the controllers

3.1 Real Implementation Limitation and Problems

In this chapter the limitation of a discrete time, distributed, Wi-Fi connected control will be analysed.

The very first one is the fact that, since the control is digital and time discrete, a delay appears between the acknowledge of a tracking error and the actuation of the response: from the control design point of view it is like adding a e^{jT_s}, where T_s is the period of the controller, to the model of the system shown in the chapter before.

It is well known from the SISO (single input single output) control theory that this delay leads to a loss in the phase margin of $180° * \frac{\omega_c}{\omega_s}$, where ω_c is the open loop crossover frequency and ω_s is the sampling frequency. This fact can be generalized for the MIMO system has the appearance of unexpected oscillations in the tracking of the references.

Another issue in the control in this DFIM is, as already mentioned, the fact that the control must be distributed and the communications must take place on a wireless connection.

Such kind of communications has two main drawbacks: the first one is that the communication is not very robust to the noise and disturbances. It can in facts happen that sometimes the data that arrives is corrupted and so the it must be retransmitted, and this implies an unpredictable delay; note that, in any case, once the data are accepted by the protocol is sure the data are not corrupted and then are good for the control.

The second big issue of a wireless communication is that is very slow in respect with the controller frequency: this means that each board has to work without communicate with the other side of the machine for the majority of the time, up to the 90% of the overall time.

The last degree of realism is that, due again to the discretization of the controller, the rotation that transform the references expressed in $d - q$ axes into $abcde$ can deal with the electrical and mechanical angles that are considered constant during all along the T_s: obviously those angles vary during the time lapse and this will lead to some error in the tracking.

3.2 Coordinates Transformation

As already remarked, all the model developed so far, and all the control algorithms that will be analysed in the next chapters, are expressed in the two $d-q$ reference frames: this is a common practice in the control of electric drives since it permit to transform the quantities from sinusoidal to constant that are much easier to be analysed.

This practice is very useful for modelling and controlling but it has to be recalled that it is just a mathematical method: it doesn't exit a machine that can be fed with $d-q$ voltages. It is so necessary to transform the two couples of voltages expressed in the two reference frames $d-q$ in $abcde$ voltages. Furthermore, even the currents are measured by the control boards in $abcde$ coordinates and so must be transformed to get the $d-q$ values.

This operation is a common coordinate transformation that, under the assumption of flux synchronization can be represented by the following matrix.

$$u_{dq0} = T(\theta)v_{abcde} \qquad \text{Eq. 68}$$

$$T(\theta) = \frac{2}{5}\begin{bmatrix} \cos(\theta) & \cos\left(\theta-\frac{2\pi}{5}\right) & \cos\left(\theta-\frac{4\pi}{5}\right) & \cos\left(\theta+\frac{4\pi}{5}\right) & \cos\left(\theta+\frac{2\pi}{5}\right) \\ \sin(\theta) & \sin\left(\theta-\frac{2\pi}{5}\right) & \sin\left(\theta-\frac{4\pi}{5}\right) & \sin\left(\theta+\frac{4\pi}{5}\right) & \sin\left(\theta+\frac{2\pi}{5}\right) \\ \cos(3\theta) & \cos 3\left(\theta-\frac{2\pi}{5}\right) & \cos 3\left(\theta-\frac{4\pi}{5}\right) & \cos 3\left(\theta+\frac{4\pi}{5}\right) & \cos 3\left(\theta+\frac{2\pi}{5}\right) \\ \sin(3\theta) & \sin 3\left(\theta-\frac{2\pi}{5}\right) & \sin 3\left(\theta-\frac{4\pi}{5}\right) & \sin 3\left(\theta+\frac{4\pi}{5}\right) & \sin 3\left(\theta+\frac{2\pi}{5}\right) \\ \frac{1}{\sqrt{2}} & \frac{1}{\sqrt{2}} & \frac{1}{\sqrt{2}} & \frac{1}{\sqrt{2}} & \frac{1}{\sqrt{2}} \end{bmatrix}$$

Eq. 69

This matrix, since is a rotational matrix, has an important propriety that concerns its invers, and in particular holds

$$T^{-1}(\theta) = \frac{5}{2}T^{T}(\theta) \qquad \text{Eq. 70}$$

Note that the fifth element in the vector u_{dq0} is the common mode voltage that can be computed according any modulation technique: in any case it doesn't affect the behaviour of the machine.

Note that, if it will be decided to not use the flux synchronization, two angles will appear θ_1 and θ_3, that are linked to the first and the third harmonic. In particular θ_3 will substitute θ in all the terms that are multiplied by 3.

A problem appears when you have to implement this transformation in discrete time. In fact, in the continuous time modelling the angle θ is the continuous time integral of the stator frequency (or relative frequency, if we are talking about rotor quantities): this means that at each time instant θ is different from the instant before, under the assumption of non-null stator frequency.

This can no more happen in a discrete time controller board since the value of θ can be updated, by a discrete time integration, just every sampling time.

Due to this there will be an error in the approximation of θ and so in the coordinate transformation.

To cope with to the actuation delay discussed in the section above, I should have to add to the actual value of the stator angle a quantity equal to $\omega_0 T_s$ for the stator control, or similarly $(\omega_0 - \omega_r)T_s$ for the rotor control.

To try to cope as much as possible to the problem described before it is possible to add $1.5 * \omega_0 T_s$ or $1.5 * (\omega_0 - \omega_r)T_s$ and it is possible to see from basic simulations that slightly better results are achieved.

4 High Level Control with Pulsating Torque

4.1 Velocity Regulator

What is given by the user is a set point of velocity beside the amount of electrical power transmitted from the rotor and the stator: this crush with the proper nature of an electric motor that is a source of torque.

In any case is well known that there exists a relation between the torque and the velocity that has already been recalled in chapter 2.6: in other words, we need a device that converts a velocity request in a torque one.

In particular it has to be pointed out that, if we can assume, or by the means of a proper tuning of the low-level regulators, that the torque response and the overall velocity response have frequentially decoupled dynamics, a simple PI regulator is enough to control the speed since, under that assumption, the dynamic oh the motor is negligible for the purpose of controlling the velocity of the rotor.

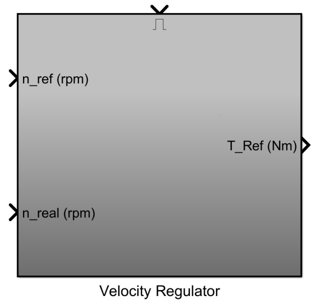

Figure 4.1-1 Outside-view Velocity Regulator

It is well know that, if the mechanical load has been considered with some friction applied, as is reasonable to be, a PI controller grants null steady state error just if the reference becomes constant: to help the regulator to follow different signal a feed forward action has been added in order to compensate the inertial forces.

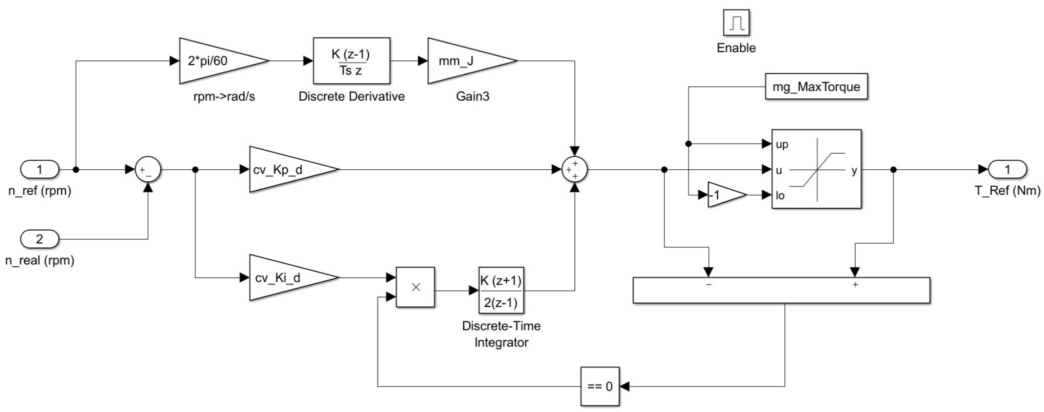

Figure 4.1-2 Inside-view Velocity Regulator

For what concerns the tuning of that regulator, standard cancellation procedure has been used: this technique grants to have minimal assessment tails and the less number of overall internal dynamic ([3]).

In particular, has already reported, no external load is assumed to be applied to the rotor that can be modelled through a transfer function as

$$G_m(s) = \frac{1}{Js + b} \qquad \textit{Eq. 71}$$

Since the regulator $R(s)$ has the following continuous time form

$$R(s) = P + \frac{I}{s} \qquad \textit{Eq. 72}$$

Where P and I are correspondingly the proportional and integral gain of the controller

To get the zero-pole cancellation it is so necessary that

$$P = I\frac{J}{b} \qquad \textit{Eq. 73}$$

This choice will lead to the best behaviour of the machine since now the resultant open loop transfer function L is a single integrator with I as degree of freedom, that can be exploited to determine the closed loop bandwidth.

$$L = I\frac{1}{bs} \qquad \textit{Eq. 74}$$

Note that, in order to not request too stressfully torque and to maintain valid the assumption of frequential decoupling between mechanical and electrical world, the chosen bandwidth must be reasonably low: a proper value, that has been selected, is 4 rad/s.

4.2 Torque pre elaboration

As mathematically remarked in paragraph 2.10, given a maximum stator frequency and a mechanical velocity, and under the assumption of synchronous fluxes, there exists a limit over the ratio between the torque produced and the electrical power transmitted from the stator to the rotor.

In other words, given the setpoint of power to be transmitted, there exists a minimum quantity of torque that must be produced, and this is due to the limit of the inverters, in particular the maximum switching frequency and the DC-link voltages.

Unfortunately, for the structure itself of the machine, the only resistive torque applied to the table is the rotational friction: this means that usually the requested load, at least at constant speed, is quite small.

We have now to underline how much this structure is rigid: in fact, is a bulky, direct drive, carousel: this means that the torsional stiffness is very high so it doesn't really care about vibrations.

This leads to the possibility to provide to the rotor very sharp torque profiles: the inertia itself will provide a low-pass filter effect that will smooth the sharp torque in a mild velocity profile.

The idea is that if the requested torque T_{ref}, needed to reach a setpoint velocity and generated by the controller discussed before, is under the mentioned limit, the torque request is modulated in a way very similar to the PWM.

Now refer to the minimum torque T_{Min}: instantaneously the torque request can be both or T_{Min} or $-T_{Min}$ but on the period the mean value of the torque is the desired one.

The square signal is generated by comparing the reference signal, T_{ref},with a triangular wave: while the signal is bigger than the triangular wave the system asks for T_{Min}, while instead the triangular wave is bigger, it ask for $-T_{Min}$.

An explicative Example is now reported.

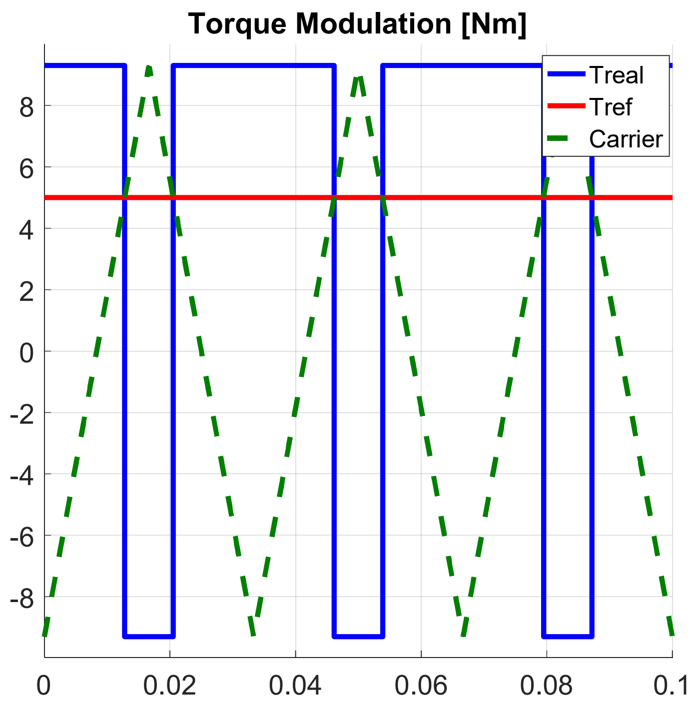

Figure 4.2-1 Example of Torque Modulation

Obviously, this approach will lead to some ripple in the velocity but, if the frequency of the triangular wave is enough high and the low-level control is enough fast to follow the profile imposed, it will result enough small to be assumed negligible, or in any case like a second order effect.

Note that T_{Min} depends on lots of parameter and could be possible to generate it at run time. On the other side, this limit must be as fixed as possible since from it depends al the setpoint of the machine; it has so been calculated a look up table that takes as only input the most significant one, the requested electrical power.

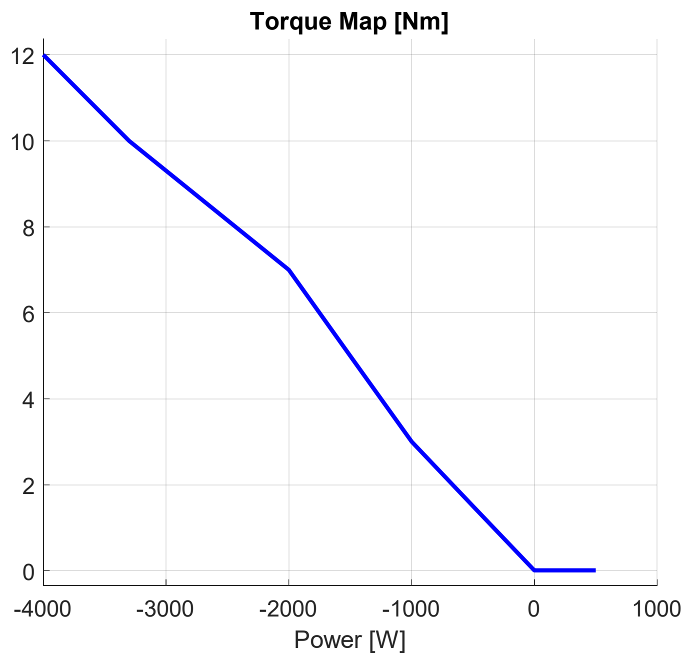

Figure 4.2-2 Minimum Torque Map

Now follows the Simulink implementation.

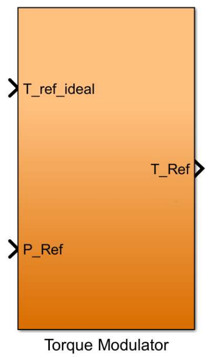

Figure 4.2-3 Outside-view Torque Modulator

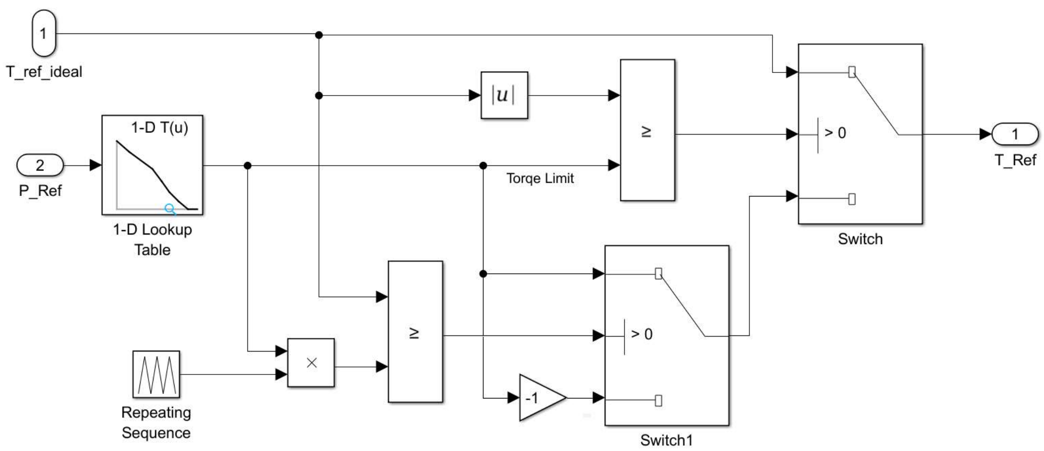

Figure 4.2-4 Inside-view Torque Modulator

4.3 Torque Splitting Policy

As already remarked many times, a five phase machine acts like two decoupled machines with the only constrain, under the assumption of synchronous fluxes, that the stator frequency of the third harmonic machine must be three times the frequency of the fundamental harmonic one.

Obviously, it must hold

$$T = T_1 + 3T_3 \tag{Eq. 75}$$

Where T obviously is the overall requested torque.

This leads to a degree of freedom that can be exploited in order to optimize the behaviour of the motor. In any case it is important to remark how the modelling that we have done doesn't take in account second order effects such as magnetic saturation and hysteresis.

Many studies suggest to divide the torque in $85\% - 15\%$: the first harmonic will deliver so the 85% and the third just the 15%.

Since that is to complex going in the deep of the magnetic behaviour of the hysteresis of this machine it has been decided to follow this rule since it appears reasonable and it will be shown to provide good results.

So it results

$$\begin{cases} T_1 = 0.85\,T \\ T_3 = \dfrac{0.15}{3}\,T \end{cases} \tag{Eq. 76}$$

Now it is reported the Simulink implementation

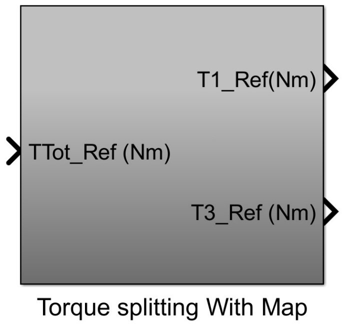

Figure 4.3-1 Outside-view Torque Splitting Map

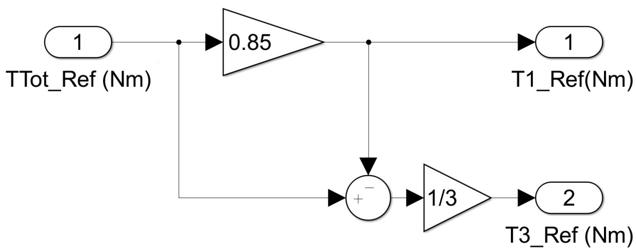

Figure 4.3-2 Inside-view Torque Splitting Map

4.4 Electrical Frequency Selection

As usually done in any *Field oriented control* for induction machine, the stator frequency has been selected in order to kill the component of the rotor flux: in other words, we choose the stator frequency in such a way to align the rotor flux along the d axis.

Note now that in a five-phase machine two rotor fluxes are present: it has been decided to use the first one as reference for the computation of ω_0.

The equation that rules the component of the first harmonic of the rotor flux,φ_{rq1} is, as already reported in section 2.3, ([1], [2])

$$\dot{\varphi_{rq1}} = -\alpha_{21}\varphi_{rq1} - (\omega_0 - \omega_r)\varphi_{rd1} + \alpha_{21}L_{m1}i_{sq1} + u_{rq1} \qquad \textit{Eq. 77}$$

Now assume that the system has already reached the steady state condition and so both the derivate of the flux and the flux itself are already equal to 0 and solve for ω_0.

What comes out is

$$\omega_0 = \omega_r + \frac{\alpha_{21}L_{m1}i_{sq1} + u_{rq1}}{\varphi_{rd1}} \qquad \textit{Eq. 78}$$

This expression is valid and really leads φ_{rq1} to zero but it is strongly connected to some of the actual states of the system, as the component of the stator current and the rotor flux and those values are not known by the high-level control.

This in reality, is not a big deal since the convergence of φ_{rq1} is granted even if, instead of using the actual states of the currents and flux, the reference values are used: note that the reference values are known to the high-level control and so can be exploited to generate the stator frequency. What is not really known instead the rotor voltage u_{rq1}: a reformulation is needed.

Now let is recall the definition of the rotor power

$$P_r = P_{r1} + P_{r3} = \frac{5}{2}(i_{rd1}u_{rd1} + i_{rq1}u_{rq1} + i_{rd3}u_{rd3} + i_{rq3}u_{rq3}) \qquad \textit{Eq. 79}$$

Where P_{r1} and P_{r3} are respectively the power produced by the first and third harmonic. Now let's focus on the first one

$$P_{r1} = \frac{5}{2}(i_{rd1}u_{rd1} + i_{rq1}u_{rq1}) \qquad \textit{Eq. 80}$$

In this expression compares the rotor currents i_{rd1} and i_{rq1} that are not directly controllable according to the choice as control variables the stator currents and the rotor flux.

Fortunately, a relation links those three variables and is the flux definition where φ_{rq1} has been already considered 0 since Eq. 81 grants it:

$$\varphi_{rd1} = L_{r1} i_{rd1} + L_{m1} i_{sd1} \quad \textit{Eq. 82}$$

$$0 = L_{r1} i_{rq1} + L_{m1} i_{sq1} \quad \textit{Eq. 83}$$

Solving for the rotor currents and substituting in the expression of the power it results

$$P_{r1} = \frac{5}{2}\left(u_{rd1} \frac{\varphi_{rd1} - L_{m1} i_{sd_1}}{L_{r1}} - \frac{L_{m1}}{L_{r1}} u_{rq1} i_{sq1}\right) \quad \textit{Eq. 84}$$

Since all the power produced by u_{rd1} is positive this means that it will be dissipated by Joule losses and not driven to the load: so the control will take care of lead it to 0. Assuming it already at steady state is now possible to solve it by u_{rq1} and so holds

$$u_{rq1} = -P_{r1} \frac{2L_{r1}}{5L_{m1} i_{sq1}} \quad \textit{Eq. 85}$$

The fact that we have imposed that $\varphi_{rq1} = 0$ by a proper choice of ω_0 as effects even on the torque delivered by the first harmonic whose simplifies into

$$T_1 = \eta_{11} \varphi_{rd1} i_{sq1} \quad \textit{Eq. 86}$$

Now solving for $i_{sq1,}$ and substituting what results in the expression of u_{rq1} previously reported, yields

$$i_{sq1} = \frac{T_1}{\eta_{11} \varphi_{rd1}} \quad \textit{Eq. 87}$$

$$u_{rq1} = -P_{r1} \frac{2L_{r1} \eta_{11} \varphi_{rd1}}{5L_{m1} T_1} \quad \textit{Eq. 88}$$

Now all the low-level variables have been expressed according to the power and torque reference and so it is possible to replace them ([1]).

$$\omega_0 = \omega_r + \frac{\alpha_{21} L_{m1} T_1}{\eta_{11} \varphi_{rd1}^2} - \frac{2P_{r1} L_{r1} \eta_{11}}{5L_{m1} T_1} \quad \textit{Eq. 89}$$

Note that the stator frequency depends on the electrical power that must be delivered by the fundamental harmonic that will be specified in the following chapter.

Now follows the Simulink implementation:

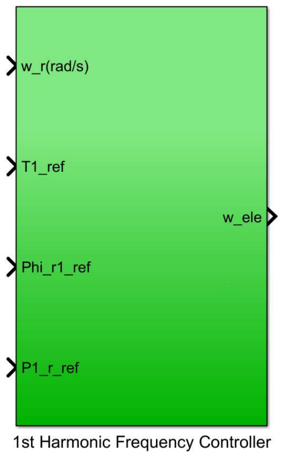

Figure 4.4-1 Outside-view Frequency Controller

Note that, due to technical limits, ω_0 must be bounded, and so a saturation has been implemented in the control scheme.

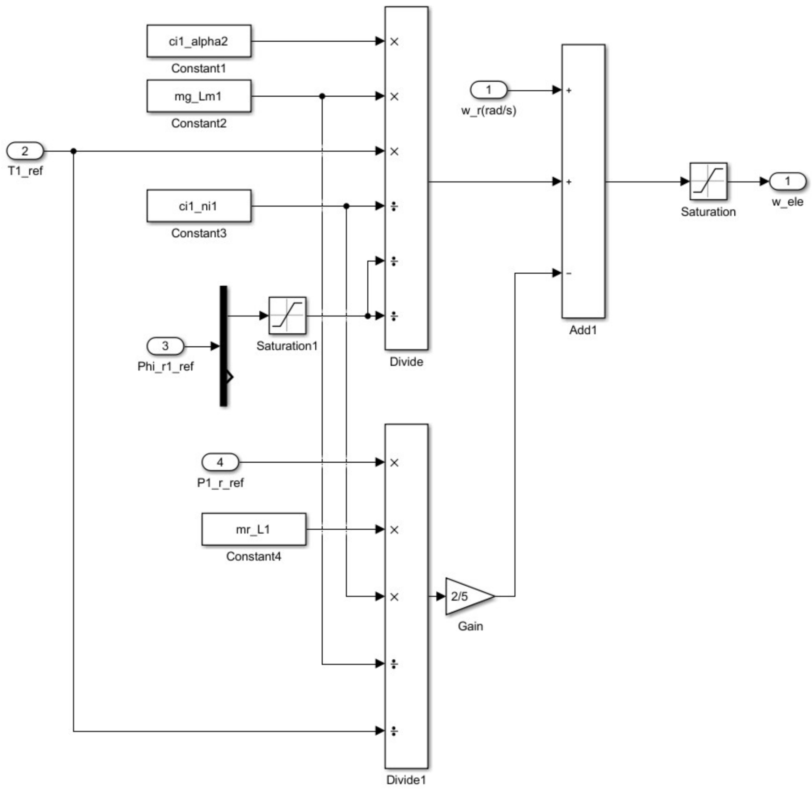

Figure 4.4-2 Inside-view Frequency Controller

4.5 Power Splitting Policy

It is now necessary to analyse how the division of the power to be transmitted between the first and the third harmonic can happen.

Unfortunately, accordingly to the flux synchronization assumption, it is not a degree of freedom since the condition of harmonicity must subsist: in practice, I have to grant that the third harmonic is really the third harmonic of the fundamental frequency and not just a spurious multiple.

Recalling the choice of ω_0 done in chapter 4.4 for the first harmonic holds

$$\omega_0 = \omega_r + \frac{\alpha_{21} L_{m1} T_1}{\eta_{11} \varphi_{rd1}^2} - \frac{2 P_{r1} L_r \eta_{11}}{5 L_m T_1} \qquad \textit{Eq. 90}$$

It is so straightforward that for the third the following relation must be verified

$$3\omega_0 = 3\omega_r + \frac{\alpha_{23} L_{m3} T_3}{\eta_{13} \varphi_{rd3}^2} - \frac{2 P_{r3} L_{r3} \eta_{13}}{5 L_{m3} T_3} \qquad \textit{Eq. 91}$$

Furthermore, must hold that the sum of the produced power by the two harmonics, P_{r1} and P_{r3}, is equal to the required one.

$$P = P_{r1} + P_{r3} \qquad \textit{Eq. 92}$$

Note that neither of P_{r1} and P_{r3} has been decide up to now, and so even ω_0 is not known.

Mathematically speaking, we have a set of three equations in three unknowns, that is so, out of singular conditions, solvable. Note that ω_0 has already been expressed as function of P_{r1} and it is trivial to express P_{r3}according to the first harmonic power. So, what has to be done is to express P_{r1} according to T_1, T_3 and the constants.

After some computation, substituting P_{r3} and ω_0 in the second equation, it is possible to find out

$$P_{r1} = \frac{5 L_{m1} L_{m3}}{2} \frac{T_1 T_3}{3\eta_{11} L_{r1} L_{m3} T_3 + \eta_{13} L_{m1} T_1 L_{r3}} \left(\frac{3\alpha_{11} L_{m1} T_1}{\eta_{11} \varphi_{rd}^2} - \frac{\alpha_{13} L_{m3} T_3}{\eta_{13} \varphi_{rd3}^2} + \frac{2 L_{r3} \eta_{13}}{5 L_{m3} T_3} P \right) \qquad \textit{Eq. 93}$$

Obviously now it is possible to compute ω_0 according to Eq. 90 and P_{r3} as

$$P_{r3} = P - P_{r1} \qquad \textit{Eq. 94}$$

In Simulink this has been implemnted as:

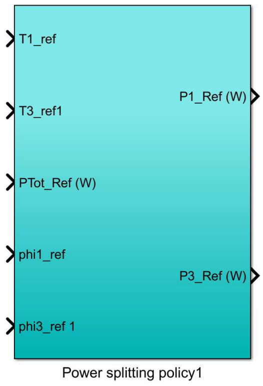

Figure 4.5-1 Outside-view Power Splitting Policy

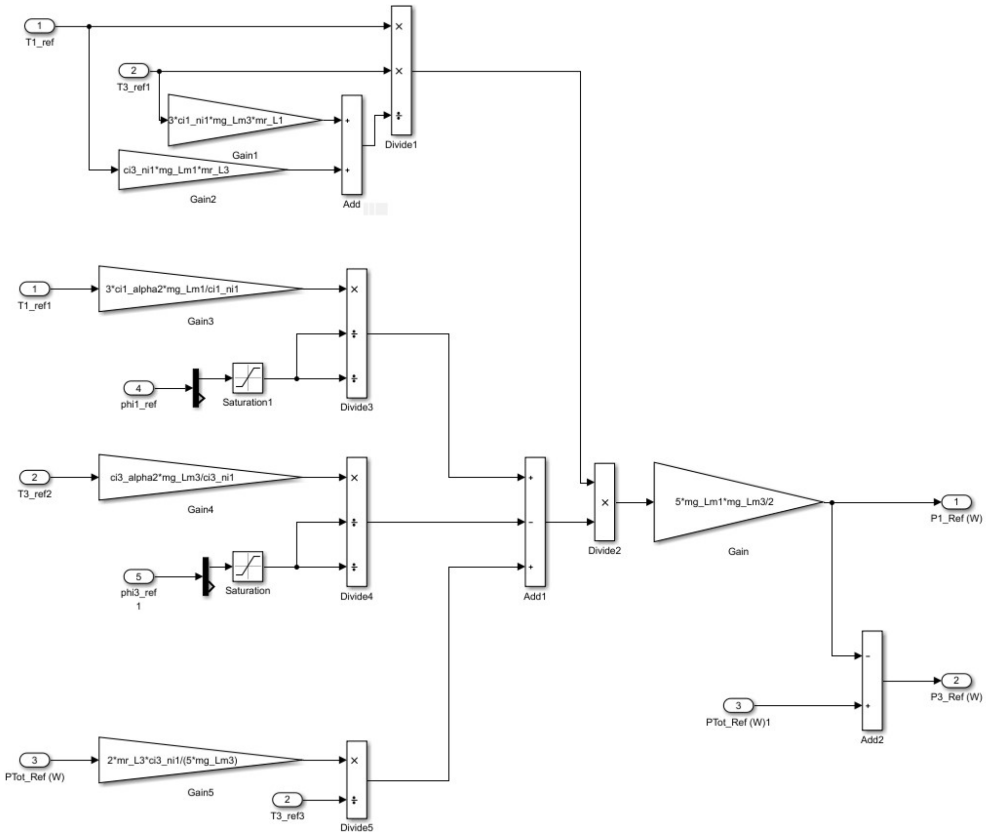

Figure 4.5-2 Inside-view Power Splitting Policy

4.6 Flux Reference Generation

Now comes out the problem of defining a proper reference for the rotor flux for the fundamental and the third harmonic.

For deciding a proper value for the magnetic flux, we have to take into account the limits of the system, in particular the maximum values of the voltages that can be produced by the inverter and the maximum stator frequency.

Let's now consider the first harmonic: the basic formulation for the produced power is, as already reported

$$P_{r1} = \frac{5}{2}(i_{rd1}u_{rd1} + i_{rq1}u_{rq1}) \qquad \textit{Eq. 95}$$

We have already found out that u_{rd1} must be equal to 0, at least at steady state, since to it are associated just the losses.

Furthermore, the stator electrical frequency has already been selected in such a way the q component of the rotor flux is 0. It so straightforward that

$$0 = L_{r1}i_{rq1} + L_{m1}i_{sq1} \qquad \textit{Eq. 96}$$

Solving for i_{sq} and substituting in Eq. 95 can be shown that results

$$P_{r1} = \frac{5}{2}(-\frac{L_{m1}}{L_{r1}}i_{sq1}u_{rq1}) \qquad \textit{Eq. 97}$$

In this expression φ_{rd1} is still missing but it is known that is related, along with i_{sq1} to the torque, and in particular holds

$$T_1 = \eta_{11}\varphi_{rd1}i_{sq1} \qquad \textit{Eq. 98}$$

Now let's make the ratio between those two expressions in order to make i_{sq} disappear and so results

$$\frac{T_1}{P_{r1}} = \frac{\eta_{11}\varphi_{rd1}}{\frac{5}{2}\left(-\frac{L_{m1}}{L_{r1}}u_{rq1}\right)} \qquad \textit{Eq. 99}$$

Now we have to point out two very important results: in the very first place it looks like we need a feedback from the low-level controller to know u_{rd1} but this should vanish our effort to verticalize hierarchically the control. Furthermore, this should create a possible instable algebraic loop.

To cope with this problem, we will use as value of u_{rd} the maximum voltage value that the inverter can produce, multiply by a safety coefficient in order to not saturate during transitory condition: in facts we have to outline that even the real u_{rd1} will converge to that value at steady state. This value is $V_{r_{Max}}$.

The second result that must be pointed out is that even the stator frequency ω_0 appears in the equation since it is strongly related to the ratio between T_1 and P_{r1}, as shown in the chapter before.

Furthermore, in order to be conservative, let's now consider the torque and the power of the fundamental harmonic as the whole required ones.

So now it is possible to solve that expression in order to get a good value for φ_{rd1}

$$\varphi_{rd1} = -\frac{5}{2}\frac{L_{m1}}{L_{r1}\eta_{11}}\frac{T}{P}V_{r_{Max}} \quad \textit{Eq. 100}$$

It has to be pointed out that the model developed assumes that the magnetic behaviour is linear and so the values found with the previous formula must be saturated between proper values.

For what concerns the third harmonic similar consideration can be carried out: the only difference is that, since

$$T_3 = 3\eta_{13}\varphi_{rd3}i_{sq3} \quad \textit{Eq. 101}$$

The requested flux is

$$\varphi_{rd3} = \frac{\varphi_{rd1}}{3} \quad \textit{Eq. 102}$$

$$\varphi_{rd3} = -\frac{5}{6}\frac{L_{m3}}{L_{r3}\eta_{13}}\frac{T}{P}V_{r_{Max}} \quad \textit{Eq. 103}$$

Now follows the Simulink implementation

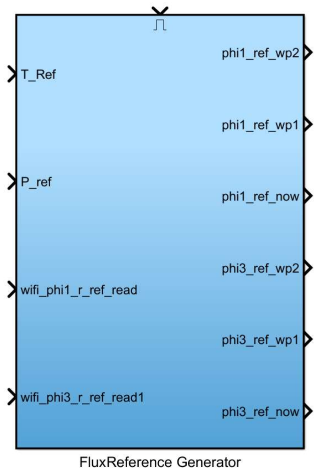

Figure 4.6-1 Outside-view Flux Reference Generator

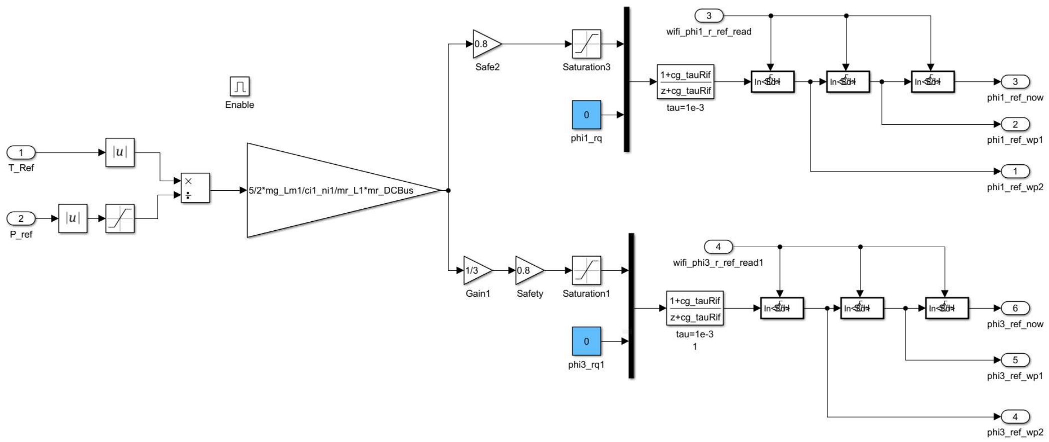

Figure 4.6-2 Inside-view Flux Reference Generator

As can be seen it is has been implemented a filter, to not have discontinuities or rapid changes in the flux reference and also a shift-register of three elements: this has been done in order to know, for instance, at time t the reference at time $t + 1$, where t is expressed in Wi-Fi sample units.

This is useful for both cope with the Wi-Fi delay due to the transmission and to provide possible feedforward actions in the low-level control.

4.7 Stator Current Reference generation

The other reference that must be built for both the harmonics in order to get the desired power and torque is the stator current one.

In this case is very simple to generate since, for each harmonic, is already known both the reference rotor flux φ_{rd} and the torque that must be generated T.

Since it is not desirable that on the rotor flows some current on the d axis the machine must be fluxed all with the d component of the stator current. Recalling the definition the rotor flux of a generic harmonic

$$\varphi_{rd\#} = L_{r\#} i_{rd\#} + L_{m\#} i_{sd\#} \qquad \textit{Eq. 104}$$

And imposing that no current must flux in that component on the rotor it is possible to show that the wanted value of the d component of the stator current is:

$$i_{sd\#} = \frac{\varphi_{rd\#}}{L_{m\#}} \qquad \textit{Eq. 105}$$

For what concerns the q component instead is well known that is the torque generating one and so for a generic harmonic must hold

$$T_{\#} = \eta_{1\#} \varphi_{rd\#} i_{sq\#} \qquad \textit{Eq. 106}$$

So it is possible to invert that relation and get a suitable value for $i_{sq\#}$.

$$i_{sq\#} = \frac{T_{\#}}{\eta_{1\#} \varphi_{rd\#}} \qquad \textit{Eq. 107}$$

Note that $T_{\#}$ is equal, for the third harmonic, to $\frac{T_3}{3}$ in order to have a more uniform development: this has been already performed by the torque splitting block.

For what concerns, instead, the implementation just one block has been reported since that, according to what has been shown so far, the two blocks for the fundamental and the third harmonic are exactly equal.

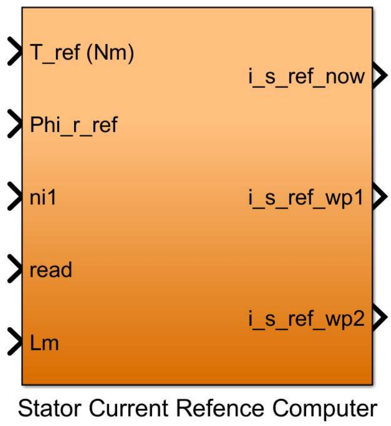

Figure 4.7-1 Outside-view Current Reference Generator

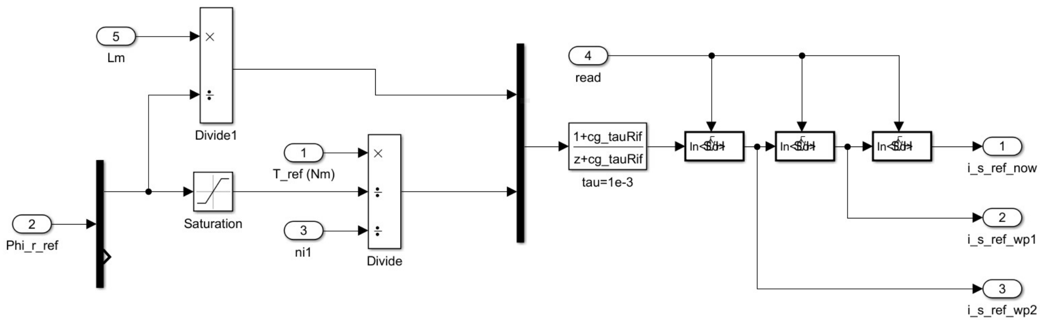

Figure 4.7-2 Inside-view Current Reference Generator

As for the flux reference a filter and a shift register have been implemented in order to synchronize with the rotor and have the possibility to build feed forward actions for the low-level control.

Furthermore, a saturation on the value of the flux has been implemented since, at the very beginning of the simulation the reference flux is equal to 0 according to what has been shown in the chapter before and the trackability of the references: this should generate a division by 0 error. The saturation avoids this possibility.

4.8 Prefluxing Procedure

In the control of induction machines, it is common practice to flux the machine before letting it to produce torque.

This has the purpose of increasing the dynamical response of the machine to a torque request: in facts, since the torque depends on the product of both the stator current and the rotor flux, if this last one is already at steady state (and the control takes it to the setpoint), the overall torque response depends just on the current behaviour.

In order to do so, a simple finite state machine has been implemented with two main inputs and outputs: the inputs are the requests for start the fluxing and the torque production, and the outputs are the corresponding enables.

The flux enable enables the block *Flux reference generator* and so the flux reference pops out. On the other side the torque enable enables all the other blocks seen so far like the *velocity regulator*, *frequency controller* and the *Stator current reference generator*.

Even if a finite state machine is not strictly necessary in order to perform the actions described before it has been implemented in order to grant a well-defined, safe, sequence of actions.

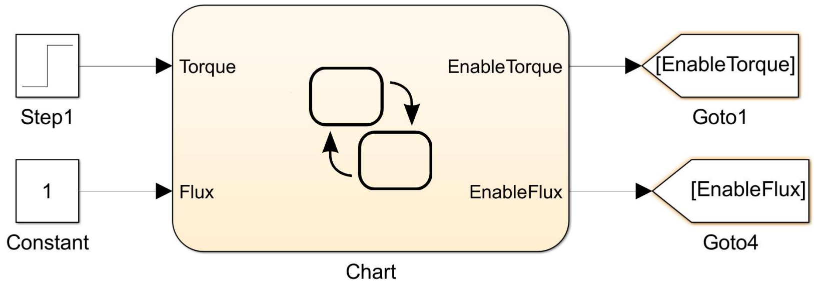

Figure 4.8-1 Outside-view Finite state machine

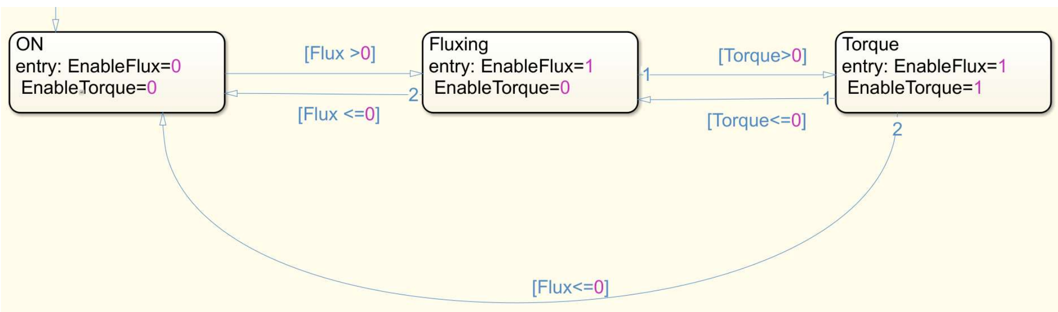

Figure 4.8-2 Inside-view Finite state machine

4.9 Chapter References

[1] A. TILLI, A. BOSSO, C. CONFICONI A. HASHEMI, Integrated Control of Motion and Contactless Power Transfer for Doubly-Fed Induction Machine in Complex Rotary Apparatus, 20th IFAC Congress, 2017

[2] A. TANI, Slides of the seminar on multiphase modelling and control, UNIBO internal material, 2017

[3] C. ROSSI, Notes of the course of Controlli 2, Personal material, 2009

5 High Level Control with Pulsating Flux

5.1 General Description and Methodologies

The power transmission methodology presented in the chapter before is very effective when the machine is mechanically loaded, situation that takes place for example when the rotor must be accelerated.

On the other side if we assume that the machine is quite unloaded, a very common situation that takes place not only when the rotor is still, but even when is rotating to a constant speed, it is necessary to modulate the torque with the technique shown before. This solution is very effective for high inertial load, since this last one acts like a low filter on the torque; if the load is no more so massive the velocity ripple can become important.

So it has been developed a control strategy that decouples the power transmission and the torque production.

Unfortunately, it has been shown in section 2.10 that at steady state there exists a lower limit to the power to be transmitted: the idea is to transmit power exploiting the derivative parts of the dynamical model.

In general, we will exploit the first harmonic to the power transfer since is the more “robust”: in fact, the doubly fed machine has to provide a quantity of electrical power that is three times the quantity of the mechanical one. The exact parameters take in account for this machine will be reported lately, in section 9.1.

The main idea is that a sinusoidal flux will generate a current, and so a voltage, in phase with it: it is known from basic trigonometric that the product of two in phase sinusoidal quantities produces a cosinusoidal quantity plus a bias ([1]).

In particular let’s now consider φ_{rd1} formed by a constant part and a sinusoidal part

$$\varphi_{rd1} = \bar{\varphi} + k(P)\bar{\varphi}\sin(\bar{\omega}t) \qquad \textit{Eq. 108}$$

Where $\bar{\varphi}$ is the constant bias of the rotor flux and $k(P)$, function of the power to be transmitted, is the amplitude of the oscillation.

Now let’s analyse the power formulas, and in particular the power of the first harmonic.

$$P = \frac{5}{2}(i_{rd1}u_{rd1} + i_{rq1}u_{rq1}) \qquad \textit{Eq. 109}$$

Since the first harmonic doesn’t have to produce torque that is

$$T = \eta_{11}\varphi_{rd1}i_{sq1} \qquad \textit{Eq. 110}$$

It follows that

$$i_{sq1} = 0 \qquad \textit{Eq. 111}$$

Furthermore, the control will provide field oriented control, that leads to $\varphi_{rq1} = 0$, and since that holds

$$\varphi_{rq1} = 0 = L_{r1} i_{rq1} + L_{m1} i_{sq1} \qquad \textit{Eq. 112}$$

Follows that even the rotor q component of the current is equal to 0

$$i_{rq1} = 0 \qquad \textit{Eq. 113}$$

So the expression of the electrical power P simplifies and becomes

$$P = \frac{5}{2} i_{rd1} u_{rd1} \qquad \textit{Eq. 114}$$

Recalling the definition of φ_{rd1} according to the stator and rotor currents

$$\varphi_{rd1} = L_{r1} i_{rd1} + L_{m1} i_{sd1} \qquad \textit{Eq. 115}$$

And substituting it in the previously found expression of the power it can be shown that

$$P = \frac{5}{2L_{r1}} u_{rd1} (\varphi_{rd1} - L_{m1} i_{sd1}) \qquad \textit{Eq. 116}$$

Let's now recall the dynamical equation of the d component of the rotor flux: note that now the derivative part is no more negligible since the flux is sinusoidal and so the derivative never vanishes.

From that equation let's isolate i_{sd1}

$$i_{sd1} = \frac{\dot{\varphi_{rd1}} + \alpha_{21} \varphi_{rd1} - u_{rd1}}{\alpha_{21} L_{m1}} \qquad \textit{Eq. 117}$$

Substituting it in the power expression it turns out that

$$P = \frac{5}{2\alpha_{21} L_{r1}} u_{rd1} (u_{rd1} - \dot{\varphi_{rd1}}) \qquad \textit{Eq. 118}$$

Obviously, the power produced in this way will be sinusoidal too that leads to the need of having an active rectifier on the rotor and a DC-link enough big to cope with the power oscillations.

For what concerns the implementation note that just a few data has to be transmitted: in particular the rotor has to transmit to the stator the power request, while the stator has to send the electrical frequency and the rotational speed to the rotor.

This is much less data than before since no low-level reference has to be transmitted: for the third harmonic, the torque generating one, that is trivial since the rotor has to act like a short circuit.

For what concerns instead the first harmonic, the one that has to transmit physically the electrical power from the stator to the rotor, the references are just power and time dependant: if the low-level hardware grants that both the boards have the same time, it is possible to generate two, in phase, sinusoids once I have transmitted the power request.

Finally, it has to be mentioned that, even in this control system, it has been prepared a prefluxing phase in which the machine just flux itself, without producing any power or torque. The implementation won't be reported since it is exactly the same that the one reported in section 4.8.

Similar argumentations can be carried out about the velocity regulation, whose controller has not been modified too.

5.2 Flux Reference Generator

As already reported the flux has to have the form ([1])

$$\varphi_{rd1} = \bar{\varphi} + k(P)\bar{\varphi}\sin(\bar{\omega}t) \qquad \textit{Eq. 119}$$

Where $\bar{\omega}$ is a degree of freedom, tuneable in order to reduce the amplitude of the oscillation $k(P)$ and the DC-link.

Obviously, it is derivate is

$$\dot{\varphi}_{rd1} = k(P)\bar{\varphi}\bar{\omega}\cos(\bar{\omega}t) \qquad \textit{Eq. 120}$$

Now let's make a, reasonable, assumption over u_{rd1}, and in particular let's assume that is proportional to the flux time derivate. So holds

$$u_{rd1} = k_u\dot{\varphi}_{rd1} = k_u k(P)\bar{\varphi}\bar{\omega}\cos(\bar{\omega}t) \qquad \textit{Eq. 121}$$

What is now missing is an expression for $k(P)$: to get it substitute the two last equations in

$$P = \frac{5}{2\alpha_{21}L_{r1}} u_{rd1}(u_{rd1} - \dot{\varphi_{rd1}}) \qquad \textit{Eq. 122}$$

That now can be written just as function of $k(P)$.

$$P = \frac{5}{2\alpha_{21}L_{r1}}(k_u^2 k^2(P)\bar{\varphi}^2\bar{\omega}^2\cos^2(\bar{\omega}t) - k_u k^2(P)\bar{\varphi}^2\bar{\omega}^2\cos^2(\bar{\omega}t)) \qquad \textit{Eq. 123}$$

And just collecting the common terms

$$P = \frac{5}{2\alpha_{21}L_{r1}}(k_u^2 - k_u)k^2(P)\bar{\varphi}^2\bar{\omega}^2\cos^2(\bar{\omega}t) \qquad \textit{Eq. 124}$$

This expression represents the instantaneous value of the delivered power and so it is function of time: with this control strategy, as already remarked, is not possible to have a continuous power transmission but we can control it is mean value by controlling the value of $k(P)$.

From basic trigonometric it is known that

$$\cos^2(\bar{\omega}t) = \frac{1 + \cos(2\bar{\omega}t)}{2} \qquad \textit{Eq. 125}$$

And so it is straightforward that

$$Mean(\cos^2(\bar{\omega}t)) = \frac{2\pi}{\bar{\omega}}\int_0^{\frac{2\pi}{\bar{\omega}}} \cos^2(\bar{\omega}t)\,dt = \frac{1}{2} \qquad \textit{Eq. 126}$$

With these results, it is possible to compute the mean power transferred $\bar{P}$ from the stator to the rotor that turns out to be

$$\bar{P} = \frac{5}{4\alpha_{21}L_{r1}}(k_u^2 - k_u)k^2(P)\bar{\varphi}^2\bar{\omega}^2 \qquad \textit{Eq. 127}$$

So is now possible to impose that the mean power is equal to the reference one by a proper choice of $k(P_{ref})$ and in particular

$$k(P_{ref}) = \frac{1}{\bar{\varphi}\bar{\omega}}\sqrt{\frac{4P_{ref}\alpha_{21}L_{r1}}{k_u^2 - k_u}} \qquad \textit{Eq. 128}$$

The last degree of freedom is represented by k_u: for sure it is value must be between 0 and 1 in order to have a real square root (the power is negative). Furthermore, the value of k_u that minimize $k(P_{ref})$ is 0.5: this value in any case is not a good choice since it will lead to small u_{rd} whose value tends to reduce the current i_{ds}.

A proper choice could be so around 0.9 that appears to be a good trade-off between high currents and big flux oscillations.

For what concerns instead the third harmonic, a constant flux on the d-axis is requested.

Now it follows the Simulink implementation.

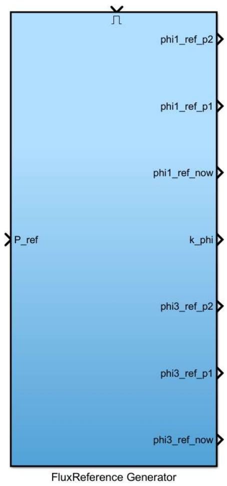

Figure 5.2-1 Outside-view Flux Reference Generator

Note that is present an enable signal to strict to zero the flux references when the machine is not working.

Furthermore, as usual, are present the outputs of the two time steps ahead references in order to provide some feedforward actions.

Finally note that, to compute $\bar{\omega}t$, is not used an integrator, that goes to infinitive as far as the time flows but a counter that wraps between 0 and 2π.

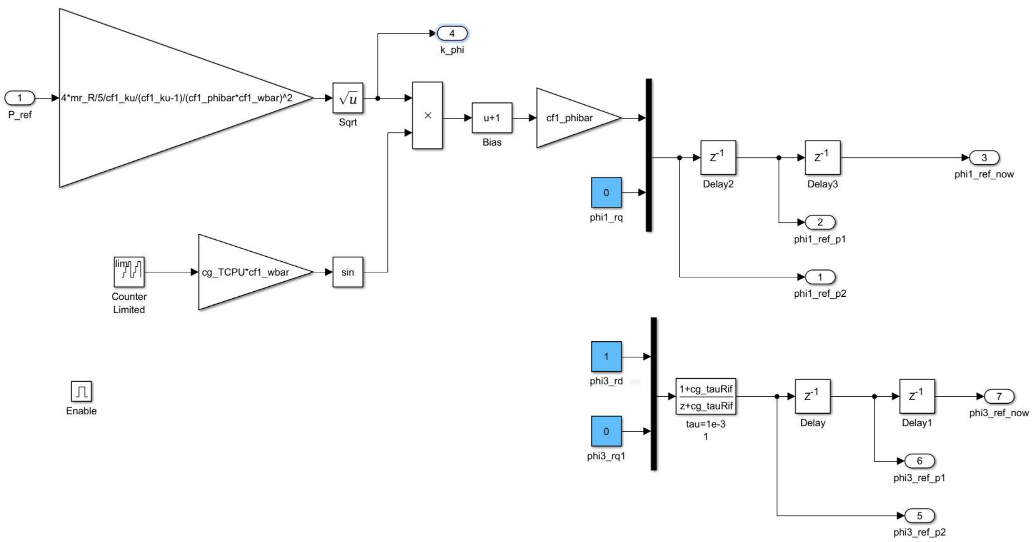

Figure 5.2-2 Inside-view Flux Reference Generator

5.3 First Harmonic Current Reference Generator

Often has been said that the first harmonic has to not transmit power and this is achievable just imposing

$$i_{qs1} = 0 \qquad \text{Eq. 129}$$

For what concerns, instead, the current i_{ds1} is already been shown that is obtainable by the inversion of the dynamical model of the d component of the rotor flux, and so is equal to ([1])

$$i_{sd1} = \frac{\dot{\varphi_{rd1}} + \alpha_{21}\varphi_{rd1} - u_{rd1}}{\alpha_{21}L_{m1}} \qquad \text{Eq. 130}$$

Now all those quantities are known since

$$\varphi_{rd1} = \bar{\varphi} + k(P)\bar{\varphi}\sin(\bar{\omega}t) \qquad \text{Eq. 131}$$

$$\dot{\varphi}_{rd1} = k(P)\bar{\varphi}\bar{\omega}\cos(\bar{\omega}t) \qquad \text{Eq. 132}$$

$$u_{rd1} = k_u k(P)\bar{\varphi}\bar{\omega}\cos(\bar{\omega}t) \qquad \text{Eq. 133}$$

And so it is possible to have the following closed form for i_{sd1}

$$i_{sd1} = \frac{\bar{\varphi}}{\alpha_{21}L_{m1}}\left(k(P)\bar{\omega}(1-k_u)\cos(\bar{\omega}t) + \big(1+k(P)\big)\sin(\bar{\omega}t)\right) \qquad \text{Eq. 134}$$

Note that we have built the reference of i_{sd1} according even with the assumption made on u_{rd1} in the chapter before: this leads to the facts that, if the reference is tracked, the real voltage of the d component is exactly the one supposed.

Now follows the Simulink implementation.

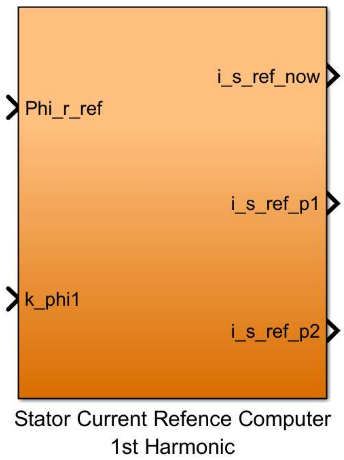

Figure 5.3-1 Outside-view First Harmonic Stator Current Reference Generator

Note that, to simplify the physical implementation and reduce the computational cost, the actual value of φ_{rd} has been exploited to get the refence for the stator current. Obviously the two formulations are equivalent from a theoretical point of view and so it should not affect the overall behaviour.

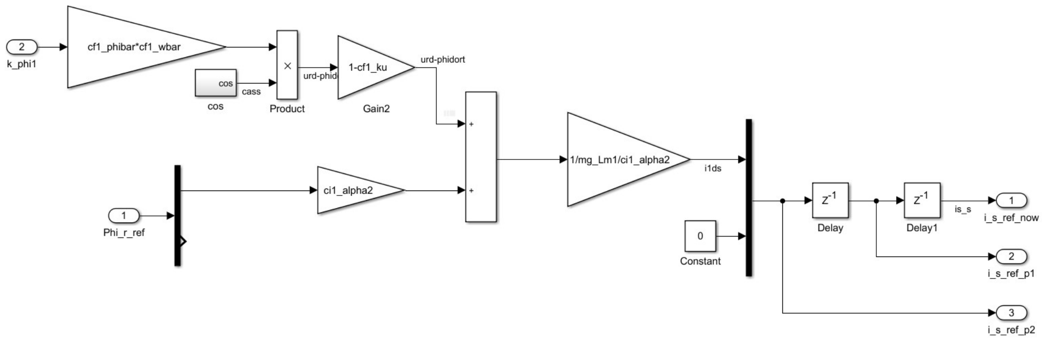

Figure 5.3-2 Inside-view First Harmonic Stator Current Reference Generator

5.4 Third Harmonic Current Reference Generator

The third harmonic is the one devoted to the torque production and it must work as a simple induction motor. This implies that the rotor is short circuited and so even the fluxing must be done by the stator.

Let's now recall the dynamical model of the d component of the rotor flux

$$\dot{\varphi_{rd3}} = -\alpha_{23}\varphi_{rd3} + 3(\omega_0 - \omega_r)\varphi_{rq3} + \alpha_{23}L_{m3}i_{sd3} + u_{rd3} \qquad \textit{Eq. 135}$$

Assuming field orientation ($\varphi_{rq3} = 0$) and rotor short circuit ($u_{rd3} = 0$) it comes out

$$\dot{\varphi_{rd3}} = -\alpha_{23}\varphi_{rd3} + \alpha_{23}L_{m3}i_{sd3} \qquad \textit{Eq. 136}$$

This differential equation is linear and scalar and so can be rewritten as a transfer function

$$G_{phi_{rd3}}(s) = \frac{\varphi_{rd3}}{i_{ds3}} = \frac{L_{m3}}{\frac{s}{\alpha_{23}} + 1} \qquad \textit{Eq. 137}$$

So, as known, at steady state, the state has to provide $i_{ds3} = \frac{\varphi_{rd3}}{L_{m3}}$ to flux the machine: in any case to improve the dynamical response, and so to flux the machine more quickly, I can filter this value with the inverse of the model.

Unfortunately, $1/G_{phi_{rd3}}(s)$ should be an anticipative system since the numerator has a higher degree respect the denominator: it has been so added a reliability pole of time constant τ_φ, according to witch it is possible to control the flux dynamic. Note that imposing a too fast dynamic of the flux should lead to very high currents.

So, the reference for i_{ds3} can be expressed as

$$i_{ds3} = \frac{1}{L_{m3}} \frac{\frac{s}{\alpha_{23}} + 1}{\tau_\varphi s + 1} \varphi_{rd3} \qquad \textit{Eq. 138}$$

For what instead concerns the q component, it is proportional to the torque request according to the very well-known formulation.

$$T = 3T_3 = 3\eta_{13}\varphi_{rd3}i_{sq3} \qquad \textit{Eq. 139}$$

It is so possible to invert that expression to get i_{sq3}, assuming that the flux is already at steady state.

$$i_{sq3} = \frac{T_3}{3\eta_{13}\varphi_{rd3}} \qquad \textit{Eq. 140}$$

It is now reported the Simulink implementation, in which are presents the enable for the fluxing and the enable for the torque production.

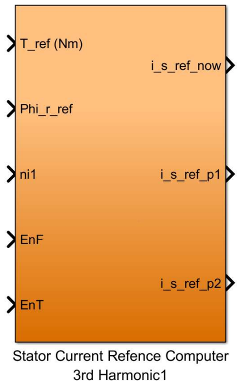

Figure 5.4-1 Outside-view Third Harmonic Stator Current Reference Generator

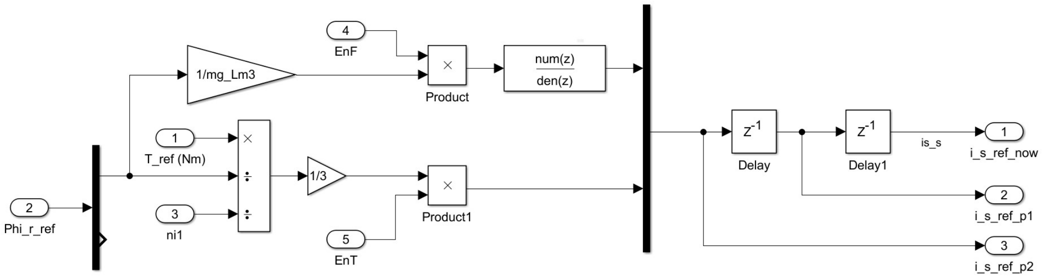

Figure 5.4-2 Inside-view Third Harmonic Stator Current Reference Generator

5.5 Electrical Frequency Selection

As already pointed out in the previous sections, the power transmission role is completely delivered to the fundamental harmonic while the third acts like a normal asynchronous motor. Furthermore, with this methodology of power transmission the $d - q$ references for the first harmonic is completely independent respect the stator frequency ω_0.

That leads to the possibility to select ω_0 as a standard field oriented indirect control but with the remark that we are exploiting the third harmonic.

Now let's recall the dynamic of the q component of the rotor flux associated to the third harmonic already introduced in chapter 2.

$$\dot{\varphi_{rq3}} = -\alpha_{23}\varphi_{rq3} - 3(\omega_0 - \omega_r)\varphi_{rd3} + \alpha_{23}L_{m3}i_{sq3} + u_{rq3} \qquad \textit{Eq. 141}$$

As said the third harmonic will be controlled as a standard induction motor with the short-circuited rotor windings: this implies, as already mentioned, $u_{r3} = 0$.

Now assume steady state conditions ($\dot{\varphi_{r\#3}} = 0$) and already aligned frame ($\varphi_{rq3} = 0$): what we got is an expression in which all the variables can be known as references.

$$0 = -3(\omega_0 - \omega_r)\varphi_{rd3} + \alpha_{23}L_{m3}i_{sq3} \qquad \textit{Eq. 142}$$

It is so possible to express ω_0 as function of i_{sq3} and φ_{rd3}, in particular their reference values.

$$\omega_0 = \omega_r + \frac{\alpha_{23}L_{m3}}{3\varphi_{rd3}}\, i_{sq3} \qquad \textit{Eq. 143}$$

Now is very well known that the reference value of the q component of the stator current is directly related to the torque request. In facts, in field oriented condition ($\varphi_{rq3} = 0$) holds

$$T = 3T_3 = 3\eta_{13}\varphi_{rd3}i_{sq3} \qquad \textit{Eq. 144}$$

It is so possible to solve that expression for i_{sq3} substitute it in the formula that provides the stator frequency and so results:

$$\omega_0 = \omega_r + \frac{\alpha_{23}L_{m3}}{9\eta_{13}\varphi_{rd3}^2}T \qquad \textit{Eq. 145}$$

Now it is reported the Simulink implementation.

Note that again a shift register is present to permit to generate smooth passages between the frequencies and to not have step references.

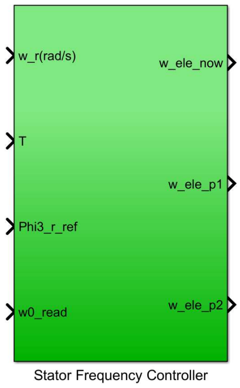

Figure 5.5-1 Outside-view Stator Frequency Controller

Furthermore, the reference so generated is saturated between its own maximum values that the inverter can physically reproduce. In any case this limit with this control strategy is no more so strict as before since is a direct drive machine: this implies that the contribute of the rotor frequency expressed in electrical radians ω_r is in any case limited since the rotor rotates quite slowly.

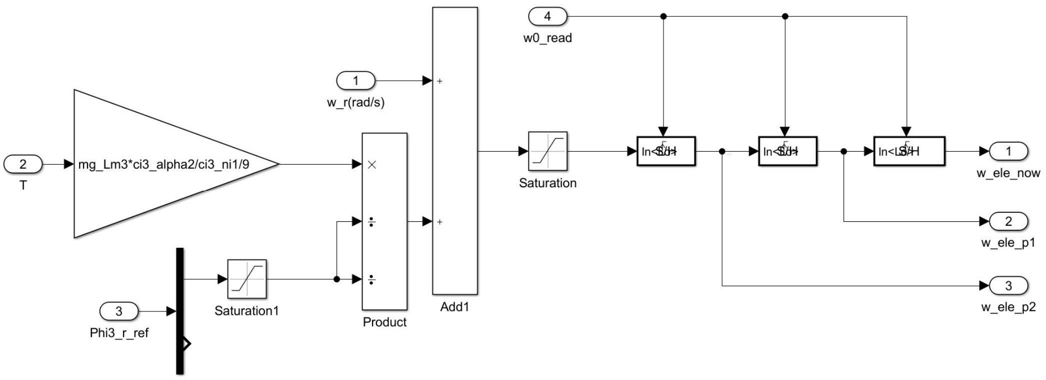

Figure 5.5-2 Inside-view Stator Frequency Controller

5.6 Chapter References

[1] A. TILLI, A. BOSSO, C. CONFICONI A. HASHEMI, Integrated Control of Motion and Contactless Power Transfer for Doubly-Fed Induction Machine in Complex Rotary Apparatus, 20th IFAC Congress, 2017

6 High Level Control with Decoupled Harmonic Frequencies

6.1 Introduction to the Harmonic Decoupling

Up to now we have considered the stator frequencies of the two harmonics, the first and the third, equal. This is a common practice since, in common electrical machine that works as motors, leads to some quite important advantages.

In particular in normal drives, that act just like motor or generator, it is possible to increase the specific torque per amps since it is possible to increase the amplitude of the first harmonic flux. This is because the third harmonic flux tends to reduce the peak of the first one: the optimal value to get the best behaviour of the overall flux is that the third harmonic flux is the 15% of the first harmonic one ([2]).

This can be seen in a graphical representation in the figure below.

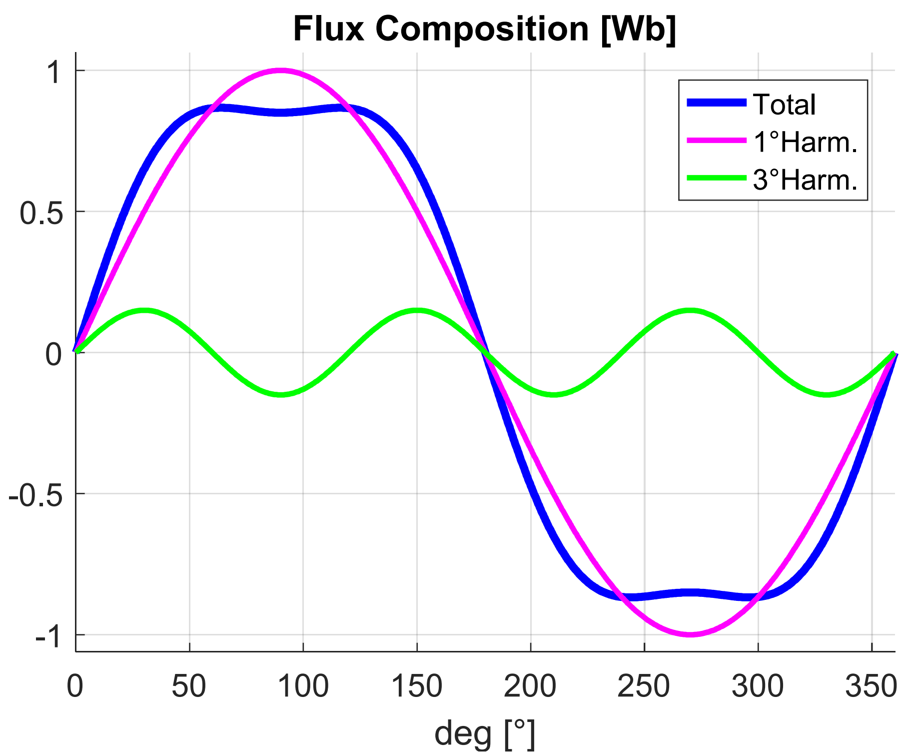

Figure 6.1-1 Flux Composition with Synchronization

This particular and interesting composition of the rotor flux happens if, as already remarked, if the two couples of reference frames $d-q$, have the same speed and the same orientation: in other word if all the quantities of first and third harmonics are expressed in the same space, called space one.

It has to be remarked that this space is in common with even the three-phase machine: this implies that the two control techniques shown up to now, that exploit just the space one, can be used with some minor modification even with a three phase doubly fed induction motor.

The control that will be proposed in this chapter instead expects to have two different stator frequencies for the first and the third harmonic: in other words, this control will exploit even the space three.

This will lead to the fact that the two fluxes won't no more compose in the way that has been shown before but in a more chaotic and time variant way.

In particular we will exploit this new degree of freedom to let the first harmonic produce the requested power while the third will be exploited as a standard induction machine with short circuited rotor windings.

Note that, the production of the power by the first harmonic will lead to the production of some torque that must be compensated by the third harmonic: this thematic will be deeply covered by a following section.

In any case some parts of the control will remain unchanged respect before and in particular the speed regulation, the prefluxing state machine and the electrical frequency selection of an induction machine (discussed in section 5.5): all these parts of the high-level control won't be discussed further.

In addition to this, even the stator currents reference generator is exactly equal to the one used in the pulsating torque solution and reported in section 4.7.

Finally, it has to be pointed out that the high-level control will need to transmit just the mechanical speed from the stator to the rotor and the power request from the rotor to the stator, that is a really low quantity of bytes to be transmitted.

6.2 Flux Reference

As already pointed out, if we don't impose that the first and third harmonic fluxes are synchronized, the two fluxes can compose in undesirable way on the going of the time.

Obviously, the way in which they compose is deterministic and well known: it is so possible to think to a variable amplitude flux that tries to maximize the overall flux in order to have smaller currents.

Unfortunately, we are dealing with a distributed control and, as already often reported, the communications are sporadic.

In any case the maximum peek of the overall flux, that takes place when the two flux sinusoids are delayed of 90° one respect the other, is the sum of the two magnitudes.

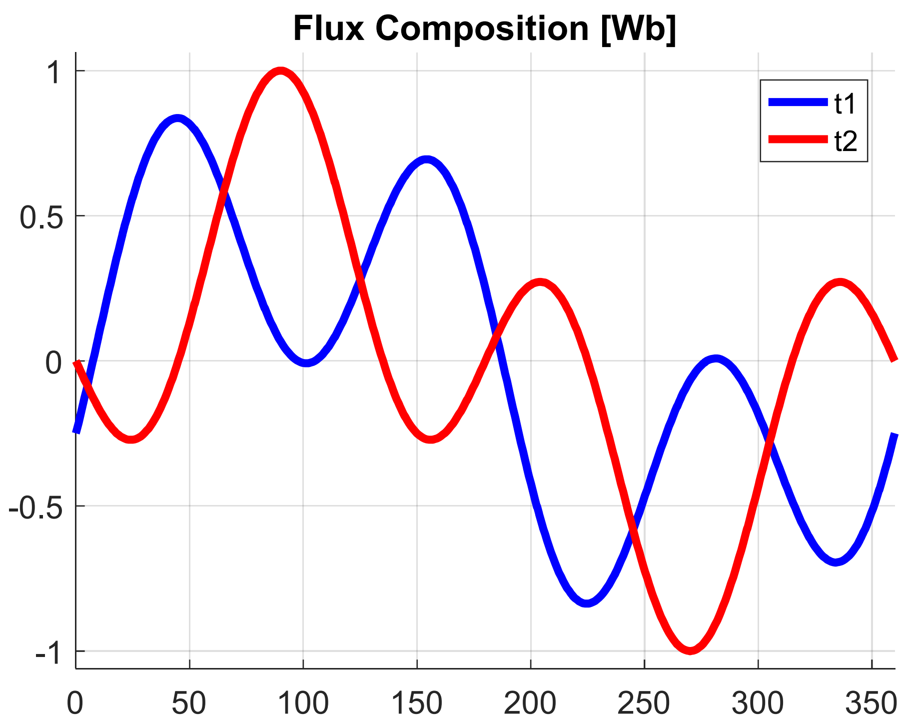

Figure 6.2-1 Flux Composition without Synchronization

A conservative choice is to take the two fluxes equal, and equal to half the nominal flux of the machine: this implies that for most of the times the machine will work in a sub-optimal condition but grants that the magnetic behaviour will be always linear and the control is not really dependant on the wireless communication that can be quite weak.

$$\varphi_{rd1} = \varphi_{rd3} = 0.5Wb \qquad \text{Eq. 146}$$

6.3 First Harmonic Torque and Third Harmonic Torque Compensation

As already mentioned, the first harmonic is in charge of transmitting the electrical power from the stator to the rotor: since no pulsating mechanism is wanted and used this implies that some torque will be produced.

In particular, if we maintain the field oriented condition explained in section 4.4 given a certain stator frequency and torque is straightforward the transmission of electrical power.

Let's now impose that the stator frequency of the first harmonic, ω_{01}, is a constant and its value will be discussed in the next chapter: in any case it is known by both the stator and the rotor side; furthermore, due to the synchronization of the timers of the two boards, even the angle is known by both the boards themselves.

Let's now recall the relation that, granting the field oriented condition, links the stator frequency ω_{01}, the torque produced T_1 and the power transmitted P_r([1]).

$$\omega_{01} = \omega_r + \frac{\alpha_{21} L_{m1} T_1}{\eta_{11} \varphi_{rd1}^2} - \frac{2 P_r L_{r1} \eta_{11}}{5 L_{m1} T_1} \qquad \textit{Eq. 147}$$

Assuming a different from zero torque T_1 it is possible to explicit those equations for the torque itself

$$\frac{\alpha_{21} L_{m1}}{\eta_{11} \varphi_{rd1}^2} T_1^2 - (\omega_{01} - \omega_r) T_1 - \frac{2 L_{r1} \eta_{11}}{5 L_{m1}} P_r = 0 \qquad \textit{Eq. 148}$$

Obviously, it is a second order equation that admits the following two solutions

$$T_1 = \frac{(\omega_{01} - \omega_r) \pm \sqrt{(\omega_{01} - \omega_r)^2 + \frac{8 \alpha_{21} L_{r1}}{5 \varphi_{rd1}^2} P_r}}{2 \frac{\alpha_{21} L_{m1}}{\eta_{11} \varphi_{rd1}^2}} \qquad \textit{Eq. 149}$$

Note that it makes sense to not ask for some torque in the first harmonic if the power is null: it is so have been implemented the solution with the sign minus.

$$T_1 = \frac{(\omega_{01} - \omega_r) - \sqrt{(\omega_{01} - \omega_r)^2 + \frac{8 \alpha_{21} L_{r1}}{5 \varphi_{rd1}^2} P_r}}{2 \frac{\alpha_{21} L_{m1}}{\eta_{11} \varphi_{rd1}^2}} \qquad \textit{Eq. 150}$$

It is straightforward that the torque so produced contributes to the overall torque T requested by the velocity regulator. In particular holds

$$3 T_3 = T - T_1 \qquad \textit{Eq. 151}$$

Now follows the Simulink implementation.

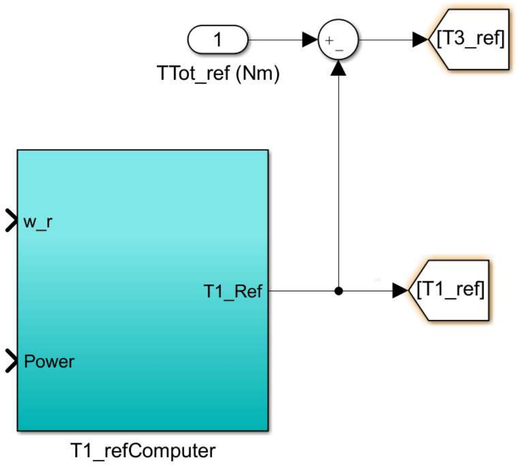

Figure 6.3-1 Outside-view of T1_Ref Computer with connected IO

The computation of the torque that must be delivered by the third harmonic is done with that sum in the left-high part of the scheme reported.

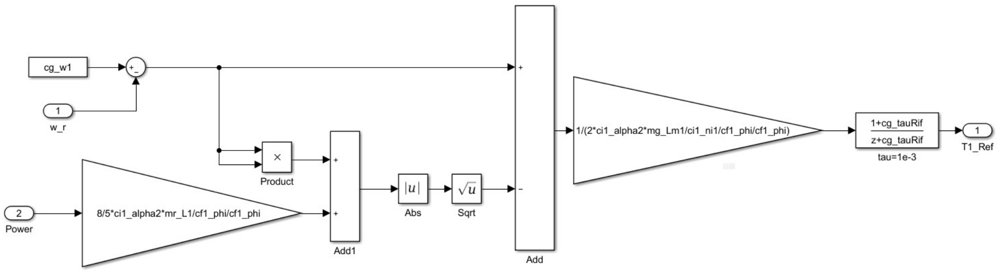

Figure 6.3-2 Inside-view of T1_Ref Computer

A low pass filter has been added in the implementation to have a smooth behaviour in the changing of the torque request by the first harmonic.

For what concerns the reference currents just briefly recall what is detailed described in section 4.7. In particular it holds for both the harmonics

$$i_{sd\#} = \frac{\varphi_{rd\#}}{L_{m\#}} \qquad \textit{Eq. 152}$$

$$i_{sq\#} = \frac{T_{\#}}{\eta_{1\#}\varphi_{rd\#}} \qquad \textit{Eq. 153}$$

Note that those two current references can be computed at the same time by both the stator and rotor boards: in particular this is useful for what concerns the first harmonic since is the one that is in charge to transmit the electrical power.

It is so straightforward that, once the power request has been transmitted and synchronized, the two controllers know all the four references and so can perform the proper feedforward actions since the flux reference is constant and known and the current reference, in particular the *q* component depends just on the power request.

For what concerns, instead, the third harmonic, no transmission is needed since, the "third harmonic machine" must acts like a usual induction machine: the rotor voltage of the third harmonic must be so always equal to zero.

Note that a zero voltage can be applied without knowing the frequency since a sinusoid of null amplitude is invariant with respect to the frequency.

This implies that none of the references for the third harmonic have to be transmitted to the rotor.

6.4 Harmonic Frequency Selection

In this section, the choice of the stator frequencies will be explained, and in particular the choice of the frequency of the first harmonic ω_{01}.

As already pointed out, this quantity must be constant and known by both the boards, since takes an important role in the low-level control and the wireless transmission introduces delays that are problematic to deal with. Let's now recall the expression of the torque that must be produced by the first harmonic.

$$T_1 = \frac{(\omega_{01} - \omega_r) - \sqrt{(\omega_{01} - \omega_r)^2 + \frac{8\alpha_{21} L_{r1}}{5\varphi_{rd1}^2} P_{r1}}}{2\frac{\alpha_{21} L_{m1}}{\eta_{11}\varphi_{rd1}^2}} \qquad \textit{Eq. 154}$$

From basic algebra is known that, to have a real result the square root must be positive and so, desiring a positive value for ω_{01}, it can be shown that the following inequality must holds

$$\omega_{01} > \omega_r + \sqrt{-\frac{8\alpha_{21} L_{r1}}{5\varphi_{rd1}^2} P_{r1}} \qquad \textit{Eq. 155}$$

Note that the power request from the rotor side P_{r1}, accordingly to the current' directions that we have assumed, is always negative since the rotor will never pump back energy in the rotor and so in the grid.

Note that, theoretically, there is no upper bound to the stator frequency but is good to maintain a reasonably low value to grant the possibility to produce the wanted flux and not have too strong back emf; it has to be remarked that, if the back emf is too big, the available voltage could be no more sufficient to control the currents at will.

Furthermore, that inequality must be considered at the maximum values, in absolute value, of both ω_r and P_{r1}: according to the machine parameters assumed, that will be reported lately, a reasonable value of ω_{01} is greater than $50 rad/s$.

The choice made is to impose

$$\omega_{01} = 100 rad/s \qquad \textit{Eq. 156}$$

For what concerns the third harmonic the selection of its stator frequency is the one adopted in a normal field oriented control and already reported in section 5.5.

$$\omega_{03} = \omega_r + \frac{\alpha_{23} L_{m3}}{9\eta_{13}\varphi_{rd3}^2} T_3 \qquad \textit{Eq. 157}$$

Since the rotor side acts like a short circuit in the third harmonic this value doesn't have to be transmitted.

6.5 Chapter References

[1] A. TILLI, A. BOSSO, C. CONFICONI A. HASHEMI, Integrated Control of Motion and Contactless Power Transfer for Doubly-Fed Induction Machine in Complex Rotary Apparatus, 20th IFAC Congress, 2017

[2] A. TANI, Slides of the seminar on multiphase modelling and control, UNIBO internal material, 2017

7 Full Knowledge Low-Level Control

7.1 MIMO Linear Quadratic Optimal Control

The low-level control, as already reported in the previous chapters, is in charge of making the system to track the references generated by the high-level control, that are strictly connected to the references given by the human operator.

Unfortunately, as pointed out in section 2.8, the model is strictly cross coupled as well as time varying. Even if the asymptotic stability is granted even with decoupled, single input single output, controllers, like PIs, the transient behaviour is really poor.

In order to achieve satisfying performances an optimal Linear Quadratic, also known as LQ, control has been implemented: in this way, the cross terms are taken in account to maximise the transient behaviour.

For the further discussion, we will assume that all the state is known even if the stator can know just the stator currents, while the rotor can measure just the rotor ones: the implementation of an observer to cope with these unknowns will be discussed later.

An LQ control is a well-known control strategy that looks for a stabilizing K, matrix of adequate dimension, that minimize the cost function that penalize both the input u and the state x weighted by two positive definite matrixes Q and R ([1]).

$$J = \int (x^T Q x + u^T R u) dt \qquad \textit{Eq. 158}$$

In reality K wasn't computed directly on matrix A, but, to ensure a fast convergence and a good transient behaviour, but on a less stable, or even unstable, matrix

$$A + \alpha I_4 \qquad \textit{Eq. 159}$$

In fact, computing the LQ optimal gain respect a more instable system lead to have a robust control respect variation and faster convergences. This is a well-known strategy to impose a response behaviour in an LQ solution.

Due to the time varying nature of A, it has been necessary to generate a set of possible A, according to the operative range of the machine, and for each of that an optimal K has been calculated and stored in look-up tables.

Note that K has a stabilizing function, that means that drives the feedbacked variable to 0: it is not suitable to feedback directly the state but its error respects the set point value.

To grant the convergence of the system to the setpoint value it is so necessary to feedforward a steady state output.

For a continuous time model, the state equation is obviously

$$\dot{x} = Ax + Bu \tag{Eq. 160}$$

We can compute the steady state value for u by imposing the time derivative of x equal to 0 and inverting the expression: this is quite simple since B is square, constant and not singular.

So u_{ref}, the steady state value of the output, is

$$u_{ref} = B^{-1}A(t)x_{ref} \tag{Eq. 161}$$

Unfortunately, A is time varying and so it is u_{ref}: in any case it is assumed, and seems reasonable, to consider the dynamic of variation of the matrix enough slow to make everything consistent even because, as shown in paragraph 2.8, just few elements of the matrix depend on time.

For what concern the implementation, both the stator and the rotor have the same controller; furthermore, even between the first and the third harmonics the difference consists just in the numerical values.

For these reasons, just one implementation will be reported: in particular it is reported the controller of the first harmonic of the stator.

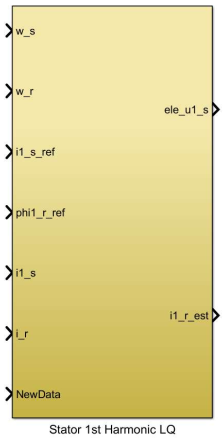

Figure 7.1-1 Outside-view Low Level Control

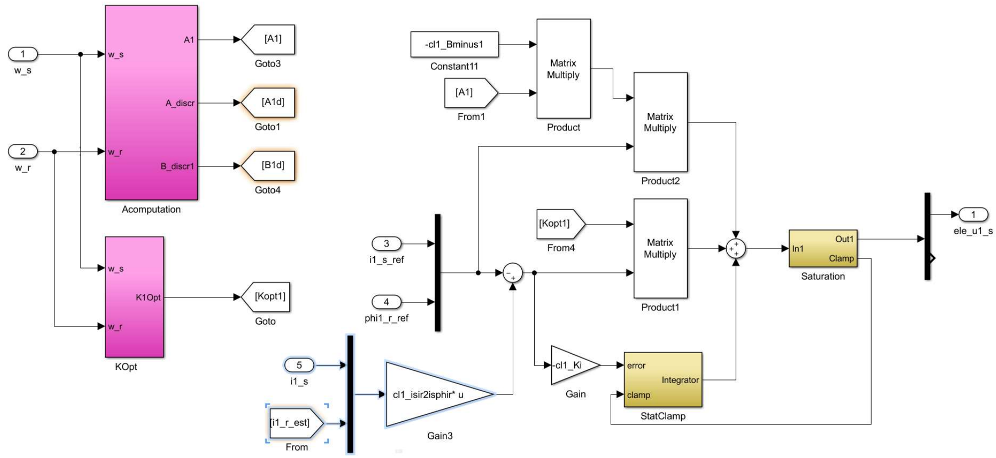

Figure 7.1-2 Inside-view Low Level Control

The first of the two blocks in purple computes, respectively, the dynamical matrix A, its discretization and the discretization of matrix B: those will be useful for the observer design.

In fact, for a linear model, it is possible to get a perfect linearization with the following equations:

$$A_d = e^{AT_s} \quad \text{Eq. 162}$$

$$B_d = (e^{AT_s} - I_4)BA^{-1} \quad \text{Eq. 163}$$

This has been implemented in Simulink with the following, easy, scheme.

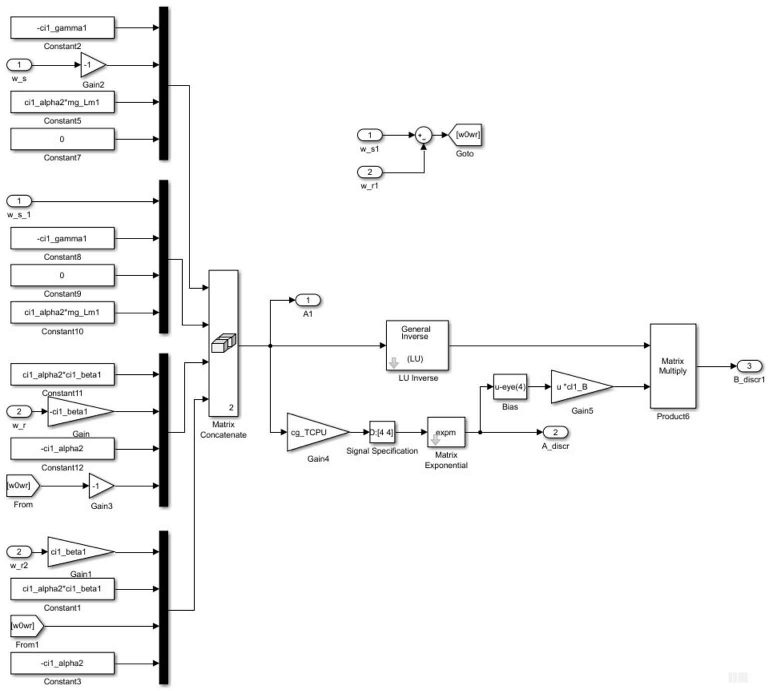

Figure 7.1-3 Inside-view of the A computation Block

The smaller purple block instead contains some look-up tables with the values of K, selected according to the stator frequency and the mechanical speed.

To grant stability and robustness to the control system an integral action has been added and tuned by hand. This integral term is also useful to cope with the errors that the observer, that will be discussed in the next paragraph, will introduce.

An extension of the anti-windup system has been implemented to prevent overshoots under saturation conditions: furthermore, since the rotor and the stator DC bus have different values, different saturation has been imposed to the signals.

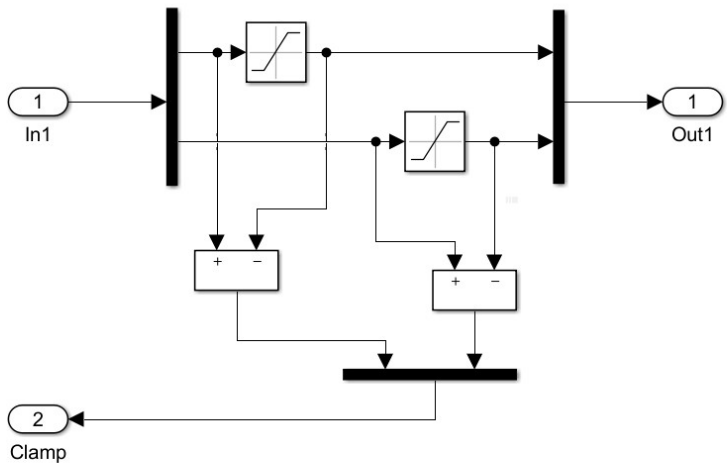

Figure 7.1-4 Inside-view Clamping Block (computes the Clamping)

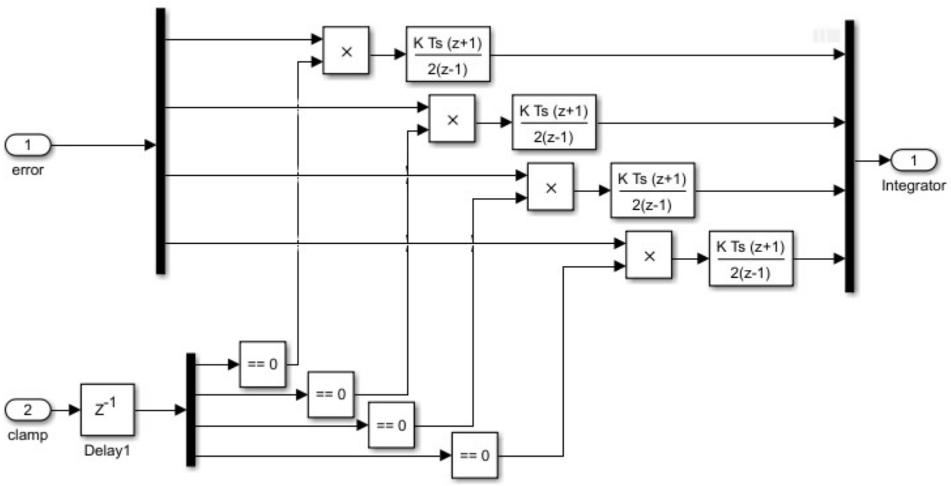

Figure 7.1-5 Inside-view StatClamp Block (computes the Integral Action)

7.2 Currents Observers

As already remarked the control is distributed between the stator and the rotor: this means that the stator can have direct measure only on the currents that flows on the stator windings as far as the rotor knowns directly just the rotor current. The information about the other side of the machine is available just when the Wi-Fi network send it successfully, that means no more that $1ms$.

On the other side, the control proposed is multiple input multiple output that implies that every state variable is accessible and used to determine the optimal output.

To cope with this problem, it is necessary to introduce an observer to both the rotor and the stator that estimates the current on the other side of the machine.

As already shown in the previous chapters it is possible to convert a continuous time model in a discrete one without any approximation in our case: we will exploit the discrete time model replica to set up an observer.

If we neglect the output injection for a generic state vector x, a discrete time model replica is

$$\hat{x}(t) = A_d\hat{x}(t-1) + B_d u(t-1) \qquad \textit{Eq. 164}$$

Since I am operating in state feedback plus some feedforward actions, to not incur in algebraic loops, I have to use the delayed input.

$$u(t) = K_{opt}(\hat{x}(t-1) - x_{ref}(t-1)) + u_{ff}(t) \qquad \textit{Eq. 165}$$

Where $u_{ff}$is the necessary feedforward action and x_{ref} is the state reference.

A sampling time of lag is unavoidable since the outputs are actuated at the beginning of the following task period. Due to that the output computed at time t will be applied at time t +1. Furthermore, as said, to not have algebraic loop, the output was computed with the estimated state at instance $t-1$.

This leads to have two sampling time of delay and a considerable loss in the phase margin of the control loop.

Let's now try to apply an input computed with the actual estimated state instead of the delayed one.

$$u(t) = K_{opt}(\hat{x}(t) - x_{ref}(t)) + u_{ff}(t) \qquad \textit{Eq. 166}$$

And so it results

$$\hat{x}(t) = A_d\hat{x}(t-1) + B_d u(t) \qquad \textit{Eq. 167}$$

Written like that is present an algebraic loop: since is a vectorial one Simulink or others software can't manage it very well and so stops the simulation. It is so necessary to solve it by hand.

In particular, substituting $u(t)$ it results

$$\hat{x}(t) = A_d\hat{x}(t-1) + B_d(K_{opt}(\hat{x}(t) - x_{ref}(t)) + u_{ff}(t)) \qquad \text{Eq. 168}$$

Now in this expression is no more present the input u: the algebraic loop is solved and the it is possible to explicit $\hat{x}(t)$.

$$\hat{x}(t) = \left(I - B_dK_{opt}\right)^{-1}(A_d\hat{x}(t-1) + B_d(-K_{opt}x_{ref}(t-1) + u_{ff}) \qquad \text{Eq. 169}$$

To this is now possible to add the integral action and the output injection effects.

So what is implemented is

$$\begin{aligned}\hat{x}(t) = \left(I - B_dK_{opt}\right)^{-1}(A_d\hat{x}(t-1) \\ + B_d\left(-K_{opt}x_{ref}(t-1) + u_{ff}(t) + u_{int}(t)\right) \\ + L(\hat{x}(t-1) - x(t-1))\end{aligned} \qquad \text{Eq. 170}$$

So in the very end what we have got is that at time t we apply to the system the output computed at $t-1$ obtained with the observed state of $t-1$: one sampling time of delay was removed.

In fact, in the very end of this computation what we have got is that the observer somehow “predicts” the future input since it will be applied with a single delay. In fact, everything can be resumed as

$$\begin{cases}\hat{x}(t) = A_d\hat{x}(t-1) + B_du(t) + +L(\hat{x}(t-1) - x(t-1)) \\ x(t) = A_dx(t-1) + B_d(K_{opt}(\hat{x}(t-1) - x_{ref}(t-1)) + u_{ff}(t-1))\end{cases} \qquad \text{Eq. 171}$$

Now let’s demonstrate the effectiveness of the proposed regulator in a rigorous mathematical way.

The demonstration is composed of two parts: in the first one we will prove that the estimated value converges to the steady state reference one. In the second part, instead we will prove that, with the proposed feed-back law drives the actual state of the machine to the set point.

To start the first part, let’s define the following error variables, assuming constant reference x_{ref} and so constant u_{ref}

$$\begin{cases}\tilde{\hat{x}}(t) = \hat{x}(t) - x_{ref} \\ \tilde{u} = u(t) - u_{ref}\end{cases} \qquad \text{Eq. 172}$$

Let’s remark again that the system, and in particular the matrix A, is time varying but with a dynamic that depends on the machine references, that are assumed to vary slowly: this makes consistent all the further considerations.

Substituting the error variables in the model replica reported in Eq. 167 we get

$$\tilde{\hat{x}}(t) = A_d\tilde{\hat{x}}(t-1) + B_d\tilde{u}(t) + ((A_d - I)x_{ref} + B_du_{ref}) \qquad \text{Eq. 173}$$

At steady state holds, since no variation happens what follows:

$$x_{ref} = A_d x_{ref} + B_d u_{ref} \tag{Eq. 174}$$

And so it results

$$(A_d - I)x_{ref} + B_d u_{ref} = 0 \tag{Eq. 175}$$

Note that this expression is totally equivalent to the one reported in Eq. 161 in which we have defined u_{ref}: obviously it can't be otherwise since the steady state input, so the input that is necessary to reach and maintain the steady state x_{ref}, can't vary if the system is expressed in continuous or discrete time.

The model replica error so it goes to simplify itself, and becomes

$$\hat{\tilde{x}}(t) = A_d \hat{\tilde{x}}(t-1) + B_d \tilde{u}(t) \tag{Eq. 176}$$

Now let's assume that the output error, $\tilde{u}(t)$ is computed with feedbacking the estimated state with some K. So it results

$$\tilde{u}(t) = K\hat{\tilde{x}}(t) \tag{Eq. 177}$$

Substituting it and explicating $\hat{\tilde{x}}(t)$ comes out

$$\hat{\tilde{x}}(t) = (I - B_d K)^{-1} A_d \hat{\tilde{x}}(t-1) \tag{Eq. 178}$$

Now it as to prove that the matrix $(I - B_d K)^{-1} A_d$ is stable: unfortunately, there is no mathematical trick that solves our problems but it has to be certificated numerically.

Fortunately, all the eigenvalues of $(I - B_d K)^{-1} A_d$ for both the first and third harmonics, for every ω_0 and ω_r in the range of our interest, are inside the unitary circle and so the system is stable.

So $\hat{\tilde{x}}(t)$ converges to 0 and this implies that the estimated values, with that previously defined input, converges to the refence values.

$$\hat{x}(t) \to x_{ref} \tag{Eq. 179}$$

Demonstrated this, we pass now to demonstrate that the real state $x(t)$ converges to x_{ref}.

Let's now define the error between the real state and the reference one, as

$$\tilde{x}(t) = x(t) - x_{ref} \tag{Eq. 180}$$

Obviously, the input definition can't vary since we have to feed both the real and the replica model with the same input.

The error model that comes out is

$$\tilde{x}(t) = A_d \tilde{x}(t-1) + B_d \tilde{u}(t-1) + ((A_d - I)x_{ref} + B_d u_{ref}) \tag{Eq. 181}$$

Again, as already proved $(A_d - I)x_{ref} + B_d u_{ref}) = 0$.

Now instead substitute even the definition of $\tilde{u}(t)$ and so comes out

$$\tilde{x}(t) = A_d \tilde{x}(t-1) + B_d K(\hat{x}(t-1) - x_{ref}) \qquad \textit{Eq. 182}$$

In the step before we have demonstrated that the estimation of the value of the state converges to the reference one.

That means that, asymptotically $\hat{x}(t-1) - x_{ref} \to 0$, that implies that the Eq. 182 simplifies and the system becomes autonomous.

$$\tilde{x}(t) = A_d \tilde{x}(t-1) \qquad \textit{Eq. 183}$$

Since A_d has been proved and makes physically sense to be always, for any stator and rotor frequency, stable, $\tilde{x}(t)$ will converge to 0.

This implies that

$$x(t) \to x_{ref} \qquad \textit{Eq. 184}$$

This means that, at steady state, the state converges to the reference desired value.

Note that it was not been proven that the estimated values of the state engage the real values, but tries to anticipate it.

In such a way, we have got better transient performances, even if we have not damaged the steady state stability.

7.3 Current Observer Implementation

Now let's consider it as an implementative point of view.

As first thing, it has been said that the goal is to estimate the currents on the other side of the motor; on the opposite our model has as state variables the stator currents and the rotor fluxes. It is so necessary a coordinate transformation.

The matrix that perform the transformation from the stator and rotor current to stator and rotor flux is

$$T_{isir2isphi} = \begin{bmatrix} 1 & 0 & 0 & 0 \\ 0 & 1 & 0 & 0 \\ L_m & 0 & L_r & 0 \\ 0 & L_m & 0 & L_r \end{bmatrix} \quad \textit{Eq. 185}$$

The values of L_m and L_r depends on the harmonic

The observer then estimates the stator current and the rotor flux: to recover to stator and rotor currents the inverse transformation, obtainable by inverting that matrix, must be applied.

These operations are performed by the two gains shown in Figure 7.3-1.

Note that even the known currents are estimated by the observer but in the control just the unmeasurable ones are used.

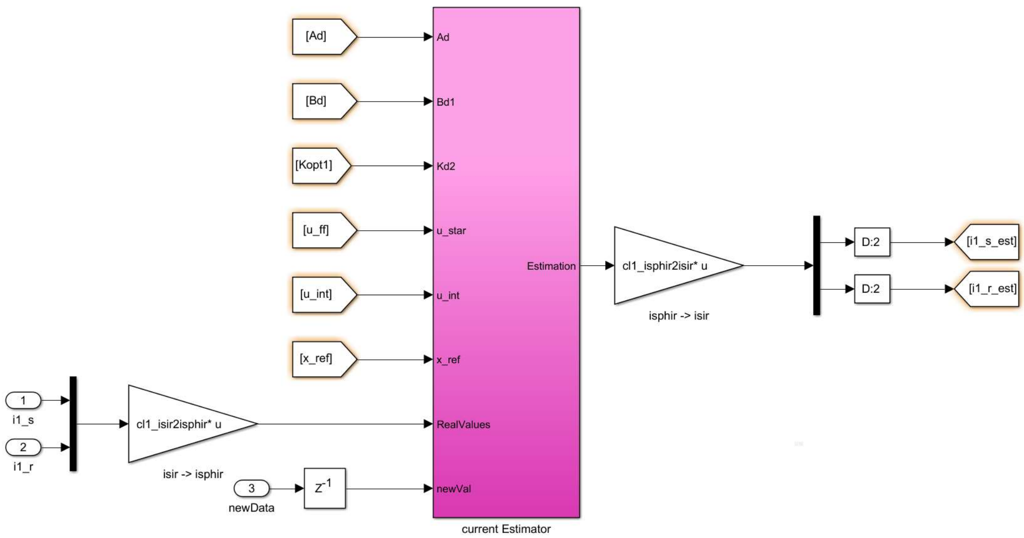

Figure 7.3-1 Outside-view Current Observer with connected IO

As said a complete information about the state, so the knowledge of the current flowing on the other side of the machine is available just once the Wi-Fi succeeds in transmitting the data: due to that it is possible to do output injection just when the new data is available.

When there is no new data the value of the 8-th input in Figure 7.3-2 is zero and so nulls the computed error between the estimated and current values.

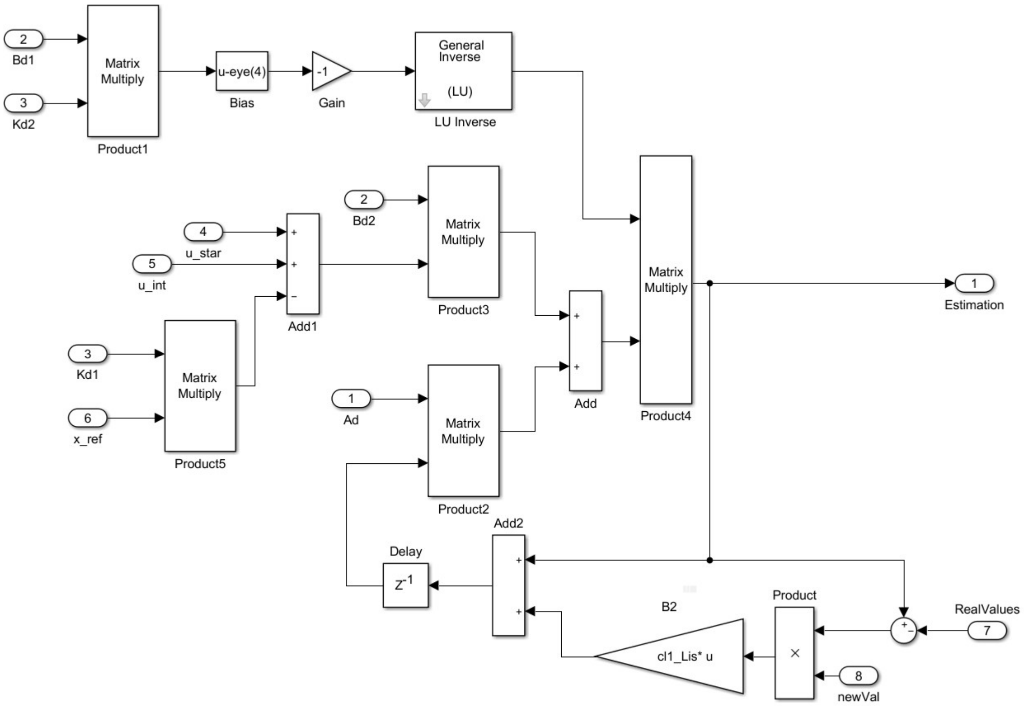

Figure 7.3-2 Inside-view Current Observer

7.4 Chapter References

[1] L. MARCONI, Notes of the course of System Theory and Advanced Control, personal notes, 2017

8 Low Level Control with Reduced State Knowledge

8.1 Feedforward Actions and Wi-Fi References Interpolation

In this section will be reported some different low-level controllers that acts without the knowledge of part of the state.

To cope with this problem all the following schemes exploits a feed forward action that, assuming perfectly known parameters and infinite sampling frequency, will drive the system to the desired reference state.

Since it is not possible, in a discrete time controller, to track immediately a reference, because the computed output will be actuated the next cycle, a time delay has been considered: in practice, the controller will try to track the two time step ahead reference.

Since it holds, in discrete time ([1], [2]),

$$x_{ref}(t+2) = A_d x_{ref}(t+1) + B_d u(t+1) \qquad \textit{Eq. 186}$$

Where $u(t+1)$ is the output applied at time $t+1$ but commuted at time t.

Usually it is not possible to forecast the future, but since all that quantities are referred to reference values, it is enough to delay them twice. In this way the reference that should be actual now, will be actual after two time step from now, and so that is the value of the reference state of two time step ahead.

It is so possible to invert the dynamical mode solving for $u(t+1)$: it comes out the feedforward actions necessary to track the generated reference.

$$u(t+1) = B_d^{-1}(x_{ref}(t+2) - A_d x_{ref}(t+1)) \qquad \textit{Eq. 187}$$

Two remarks have to be made: the first one is that is better to generate feasible references to have a better tracking, and that is why often, when the high-level control has been discussed, some filters where presents. The second remark, instead, is that, in a continuous time case with perfectly known parameters, the feedforward actions will be enough to track any feasible reference: in discrete time, instead is present in any case a feedback action in order to kill some little oscillation that pops out due to the discretization of the control command.

From these considerations follows that the controller needs a reference for the state at each sampling time and those values must be trackable: this means that at least must not be present discontinuities and in general it must be derivable as many times as the relative degree of the system. To get this is very easy at stator side since it is enough to filter the steps that the formulas generates.

Very different is at the rotor side since the rotor itself receives the information very sporadically due to the slowness of the Wi-Fi transmission: if no action will be performed the rotor controller should see a reference that at each Wi-Fi transmission makes some steps.

This leads to two problems: the first one is that a step is not a trackable reference, while the second one is that the references are not the same at each time step for the rotor and the stator, stuff that could lead to some oscillations.

To cope with these problems, both the stator and the rotor sample the references every cycle of the Wi-Fi and for the other cycle the just linearly interpolate respect the old value of the reference.

To improve the performances, I make transmit not the actual reference, expressed in Wi-Fi time, but the one step ahead one.

$$x_{ref}(t+1) = x_{ref}(t) + \frac{x_{ref}^{wifi}\left(t^{wifi}+1\right) - x_{ref}^{wifi}\left(t^{wifi}\right)}{\frac{T^{wifi}}{T_s}} \qquad \textit{Eq. 188}$$

Where $x_{ref}^{wifi}\left(t^{wifi}\right)$ is the actual data from the Wi-Fi and $x_{ref}^{wifi}\left(t^{wifi}-1\right)$ is the one received the Wi-Fi cycle before.

To compute the two steps ahead reference it is possible to just add the term on the left.

$$x_{ref}(t+2) = x_{ref}(t+1) + \frac{x_{ref}^{wifi}\left(t^{wifi}+1\right) - x_{ref}^{wifi}\left(t^{wifi}\right)}{\frac{T^{wifi}}{T_s}} \qquad \textit{Eq. 189}$$

Graphically happens in the discrete time domain that the actual reference converges to the Wi-Fi future one after $\frac{T^{wifi}}{T_s}$ little steps, of the duration if one T_s: obviously that is due to the fact that the controller is discrete.

In the figure below is reported an explicative example of how the interpolation works: to get the one and the two steps ahead references it enough to shift the red line to the left of one or two division.

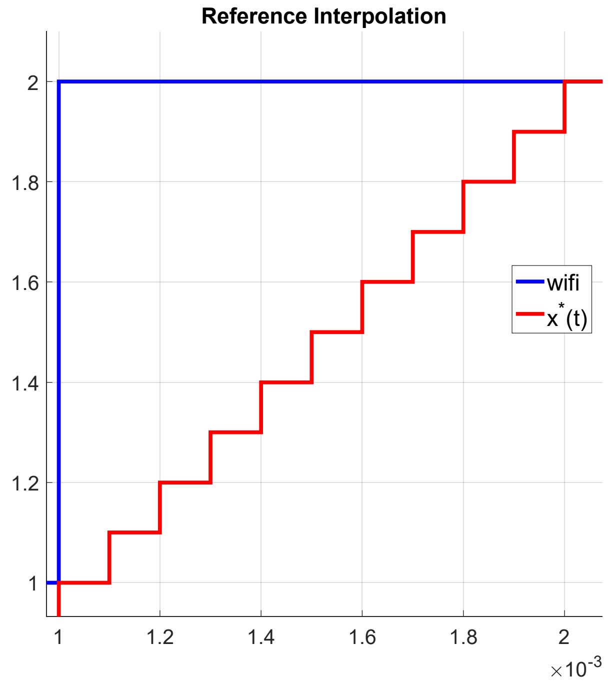

Figure 8.1-1 Reference Interpolation

Now it is reported the Simulink implementation.

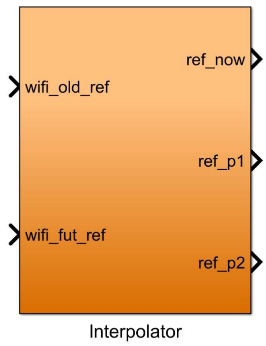

Figure 8.1-2 Outside-view Interpolator

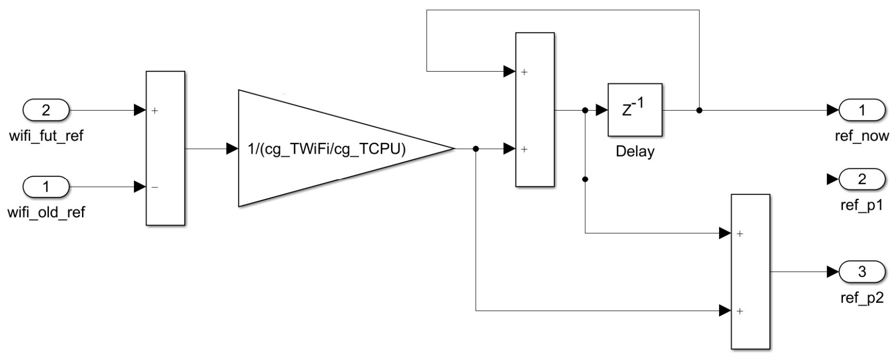

Figure 8.1-3 Inside-view Interpolator

8.2 Reduced LQ Controller with Feed-Forward Actions

The low-level control presented before has some disadvantages: the first one is that the observer is strictly influenced by the parameter uncertainties. In fact, even a little error on the values of the parameters can lead to a drift of the state estimation: moreover, the output injection can be done just sometimes due to the slowness of the Wi-Fi transmission. Furthermore, it must be implemented the observer shown before that can lead to a quite heavy computational payload.

That's why it has been decided to develop a low-level control that doesn't need the knowledge of the part of the state that can't be measured.

Let's now consider the system written in the measurable variable, so the rotor and stator currents. In particular if we analyse the matrixes A_i and B_i reported in section 2.9 we can individuate four 2x2 sub matrixes like

$$A_i = \begin{bmatrix} A_{isis} & A_{isir} \\ A_{iris} & A_{irir} \end{bmatrix} \qquad \textit{Eq. 190}$$

Where A_{isis} and A_{isir} represent respectively the effect of the actual state of stator and rotor currents over the future state of the stator currents and A_{iris} and A_{irir} the effect of the actual state of stator and rotor currents over the future state of the rotor current.

Similarly, B_i can be defined as

$$B_i = \begin{bmatrix} B_{isis} & B_{isir} \\ B_{iris} & B_{irir} \end{bmatrix} \qquad \textit{Eq. 191}$$

Where B_{isis} and B_{isir} represents respectively the effect of the actual value of stator and rotor voltages over the future state of the stator current and B_{iris} and B_{irir} the effect of the actual state of stator and rotor voltages over the future state of the rotor current.

It is now possible to individuate two measurable subsystems: for the stator is the one characterized by A_{isis} and B_{isis} and for the rotor by A_{irir} and B_{irir}.

In particular the stator subsystem has the following, continuous time, matrixes

$$A_{isis} = \begin{bmatrix} -\frac{R_s}{\sigma_1} & \omega_0 + L_m\beta_1\omega_r \\ -\omega_0 - L_m\beta_1\omega_r & -\frac{R_s}{\sigma_1} \end{bmatrix} \qquad \textit{Eq. 192}$$

$$B_{isis} = \begin{bmatrix} \frac{1}{\sigma_1} & 0 \\ 0 & \frac{1}{\sigma_1} \end{bmatrix} \qquad \textit{Eq. 193}$$

And the rotor one has

$$A_{irir} = \begin{bmatrix} -\alpha_2(1 + L_m\beta_1) & \omega_0 - (1 + L_m\beta_1)\omega_r \\ -\omega_0 + (1 + L_m\beta_1)\omega_r & -\alpha_2(1 + L_m\beta_1) \end{bmatrix} \quad \textit{Eq. 194}$$

$$B_{irir} = \begin{bmatrix} \frac{1 + L_m\beta_1}{L_r} & 0 \\ 0 & \frac{1 + L_m\beta_1}{L_r} \end{bmatrix} \quad \textit{Eq. 195}$$

With this knowledge, it is possible to compute an optimal linear quadratic gain for the two systems. Note that, since even the sub-matrixes are time varying according to ω_0 and ω_r, it will be necessary to generates some maps to contain the optimal gain to adapt to the values of the two angular speeds.

Obviously, a proportional feedback on part of the state is not enough to drive the overall system to the reference state since the cross terms of the system have been neglected. It has been implemented some feedforward actions to compensate the unknown part of the state in the way that has been discussed before.

Furthermore, to provide robustness to the parameter variation a hand tuned integral action has been added: the integral action in facts grants null error at steady state.

Now follows the Simulink implementation: as usual it transparent respect the harmonic order. There is instead a difference between the stator and the rotor, as outlined before. In any case it is just matter of the maps that have been stored and the variable connected to the feedback loop; nothing more changes.

For brevity so it is just reported the low-level control of the first harmonic of the stator current.

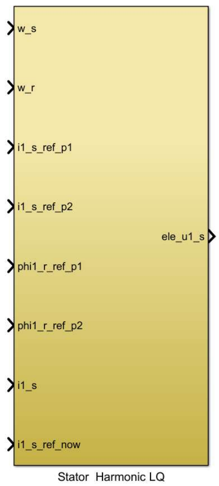

Figure 8.2-1 Outside-view Low-Level Control with Reduced LQ

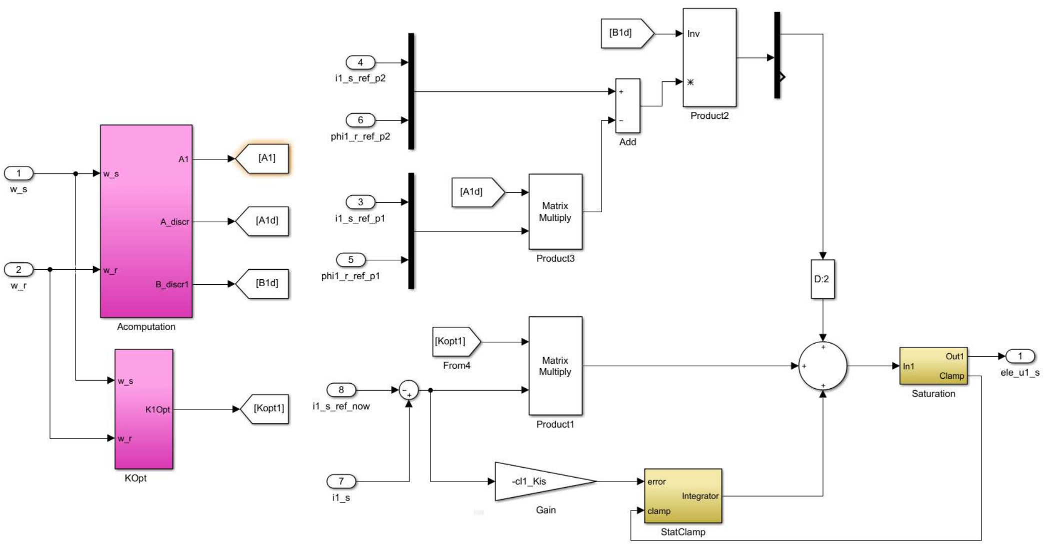

Figure 8.2-2 Inside-view Low-Level Control with Reduced LQ

8.3 PI Controller with Feed-Forward Actions

Up to now we have developed solutions that needs a quite huge amount of data stored in the flash memory of the board. This problem could be managed by reducing the number of points of the maps that contains the coefficients: the obvious drawback is that the matrix that in such a way is stored is no more the optimal LQ one but a sub-optimal one. Note that, since the system is already stable and the matrix stays positive definite, the stability is granted.

In any case in order to cope with the memory poorness of the present memory on the board it has been tried to substitute the, even reduced, LQ with a simple PI controller plus, as in the previous controller, some appropriate feedforward actions as explained in section 8.1.

The main idea is that, since the feedforward actions do the big part of the work, even a simple control can be enough to steer to zero the residual error due to the discretization.

The continuous time model taken in account is so something like

$$\dot{i}_{s\#} = -\frac{R_s}{\sigma_1} i_{s\#} + \frac{1}{\sigma_1} u_{s\#}(t) + d(t) \qquad \textit{Eq. 196}$$

For both the d and q component of the stator current; $d(t)$ is the residual error due to discretization.

Neglecting $d(t)$ and since the system is a single input single output system (SISO) it is possible to transform that state space representation in a more common transfer function and in particular came out ([2], [3])

$$G_s(s) = \frac{i_{s\#}}{u_{s\#}} = C(sI - A)^{-1}B \qquad \textit{Eq. 197}$$

$$G_s(s) = \frac{1}{\sigma_1 s + R_s} \qquad \textit{Eq. 198}$$

Similarly, for the rotor it is possible to write

$$\dot{i}_{r\#} = -\alpha_2(1 + L_m\beta_1)i_{r\#} + \frac{1 + L_m\beta_1}{L_r} u_{r\#}(t) + d(t) \qquad \textit{Eq. 199}$$

And so the rotor transfer function is

$$G_r(s) = \frac{1 + L_m\beta_1}{L_r} \frac{1}{s + \alpha_2(1 + L_m\beta_1)} \qquad \textit{Eq. 200}$$

Note that for both the stator and the rotor the order of the transfer function is one: this means that a simple PI controller is enough to reach any performance.

Assuming that the system, once applied the feedforward action, can represented by eight decoupled transfer functions (four for each harmonic, for each harmonic two

G_s and two G_r), the tuning of a PI controller is straightforward according to some desired crossover frequency and phase margin.

So the transfer function of the controllers are

$$R_s(s) = P_s + \frac{I_s}{s} \qquad \textit{Eq. 201}$$

$$R_r(s) = P_r + \frac{I_r}{s} \qquad \textit{Eq. 202}$$

The Simulink implementation is very similar to the reduced LQ controller: furthermore, it needs the same inputs.

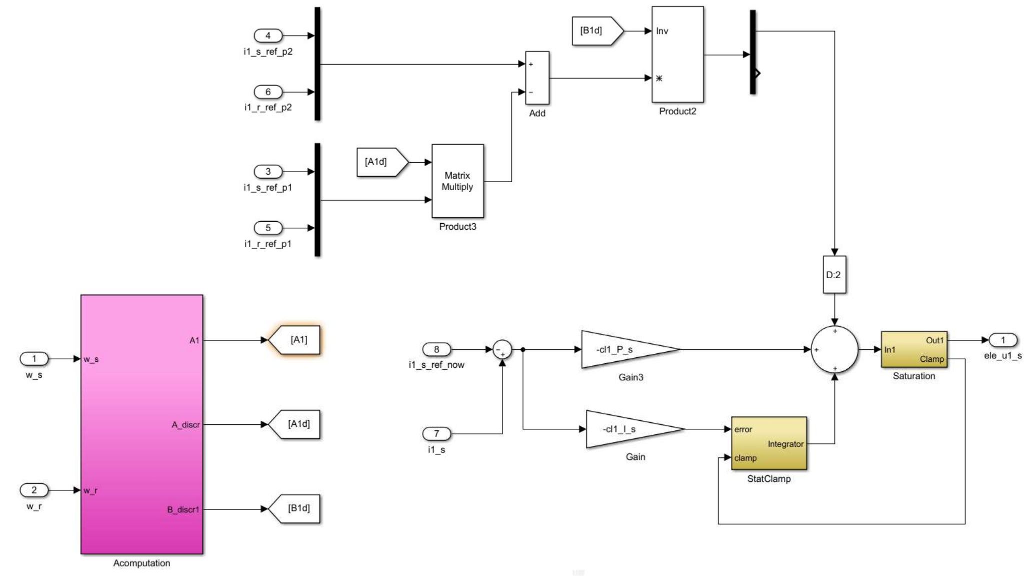

Figure 8.3-1 Inside-view Low-Level Control with PI Controller

8.4 Resonant Controller with Feed-Forward Actions

As shown in chapter 5 if the pulsating power solution is adopted, the references generated are sinusoidal.

It is well known that a PI controller can't follow exactly a sinusoidal reference, especially if it has high frequency. Luckily the frequency of the reference is known and decide by the implementer: we have referred to it in chapter 5 as $\bar{\omega}$ ([1], [4]).

This information is enough to tune a resonant controller: in fact, according to the internal model principle, to track exactly a signal the system has to have in the denominator polynomial the one generating the signal.

In practice in the open loop transfer function it must appear the Laplace transformation of a cosine that is

$$L(\cos(\bar{\omega}t)) = \frac{s}{s^2 + \bar{\omega}^2} \qquad \textit{Eq. 203}$$

Since in any case it is desirable to have zero steady state error still the integrator has maintained. So results that the continuous time regulators for both the rotor and the stator are

$$R_s(s) = P_s + \frac{I_s}{s} + \frac{R_s s}{s^2 + \bar{\omega}^2} \qquad \textit{Eq. 204}$$

$$R_r(s) = P_r + \frac{I_r}{s} + \frac{R_r s}{s^2 + \bar{\omega}^2} \qquad \textit{Eq. 205}$$

Obviously, these regulators must be discretized, and in particular the resonant part becomes unrecognizable after the discretization and its computation has been delivered to the software.

The Simulink implementation is the following.

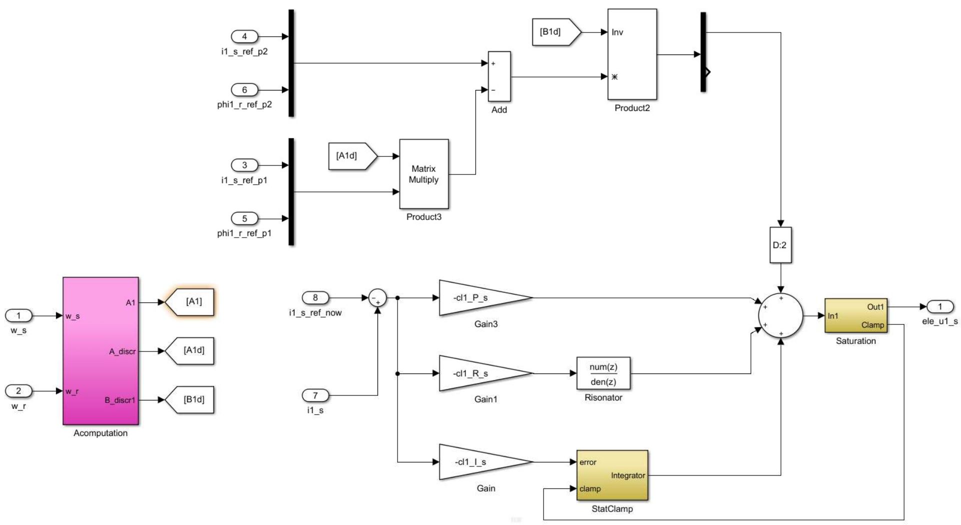

Figure 8.4-1 Inside-view Low-Level Control with Resonant Controller

8.5 Implementative strategies for matrix discretization

As mentioned in the first section of this chapter, and often recalled along it, some feedforward actions are basilar for the low-level control. Those are based on the inversion of the discrete time dynamical model that is, unfortunately, time varying.

On the other side, the continuous time model is well known and easily implementable, as reported in paragraph 7.2; this model has an exact discretization that can be carried out with the matrix exponential. In particular for a generic couple of matrixes A and B the exact discretization is

$$A_d = e^{AT_s} \qquad \text{Eq. 206}$$

$$B_d = (e^{AT_s} - I)BA^{-1} \qquad \text{Eq. 207}$$

The exact computation of the matrix exponential is a well-known heavy computational problem and some difficulties can appear in the practical implementation if that discretization is carried out.

The goal is to get a discretization that is not so heavy to be computed but still provides reliable and useful results.

It is now useful to recall the Taylor definition of the exponential that is ([5])

$$A_d = e^{AT_s} = \sum_{l=0}^{\infty} \frac{A^l T_s^l}{l!} \qquad \text{Eq. 208}$$

Can be easily seen that, it is possible to truncate the sum reported to a grade in with the result of the discretization is satisfactory.

For what concerns instead the discretization of B, its first formulation must be recalled and in particular holds

$$B_d = \int_0^{T_s} e^{At} dt \qquad \text{Eq. 209}$$

Substituting now the expression found before for the matrix exponential and solving the integral form turns out

$$B_d = \sum_{l=1}^{\infty} \frac{A^{l-1} B T_s^l}{l!} \qquad \text{Eq. 210}$$

Note that if we truncate the sum to the first element what is got is the Euler discretization where

$$A_d = I + AT_s \qquad \text{Eq. 211}$$

$$B_d = BT_s \qquad \text{Eq. 212}$$

From preliminary results, it turned out that this discretization is too poor to grant good results with the considered sampling time.

Furthermore, it is clear that the truncation can be performed at any number of iterations and the contribute of the i-th term is proportional to T_s^i: since T_s is quite small, it decreases the contribute of each term decrease very quickly.

According to this it has been decide to stop the discretization to the second order term: this choice grants reasonable computational time and a good discretization.

In the end the discretization that has been implemented is

$$A_d = I + AT_s + \frac{A^2 T_s^2}{2} \qquad \textit{Eq. 213}$$

$$B_d = BT_s + \frac{ABT_s^2}{2} \qquad \textit{Eq. 214}$$

Note that, in order to optimize the implementation, some terms are re-used: for example, the term ABT_s^2 can be obtained by multiplying the first order terms of A_d and B_d, AT_s and BT_s.

Finally, it has to be pointed out that the computation of matrix A_d must be done online: for what instead concerns the discretization of B it could be performed off-line if we use a first order approximation instead of a second order one. In other words, B_d can be computed offline if we neglect the terms from $\frac{AB\;_s^2}{2}$.

It can be argued that this computation is not very heavy but it has to be recalled that the matrixes A_d and B_d are computed in order to perform the necessary feedforward actions as explained in section 8.1: in particular for those is necessary the knowledge not of B_d but of its inverse.

So it follows that if the second order approximation is performed the inversion of the matrix must be performed online, operation that could result computationally heavy; if instead the first order approximation is used than even B_d^{-1} can be computed offline, and so some computational power can be saved.

In any case this decision can be performed properly only when the control hardware will be known.

Now follows the Simulink implementation.

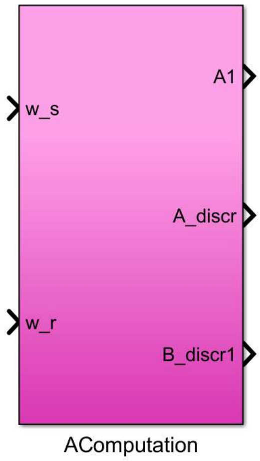

Figure 8.5-1 Outside-view AComputation

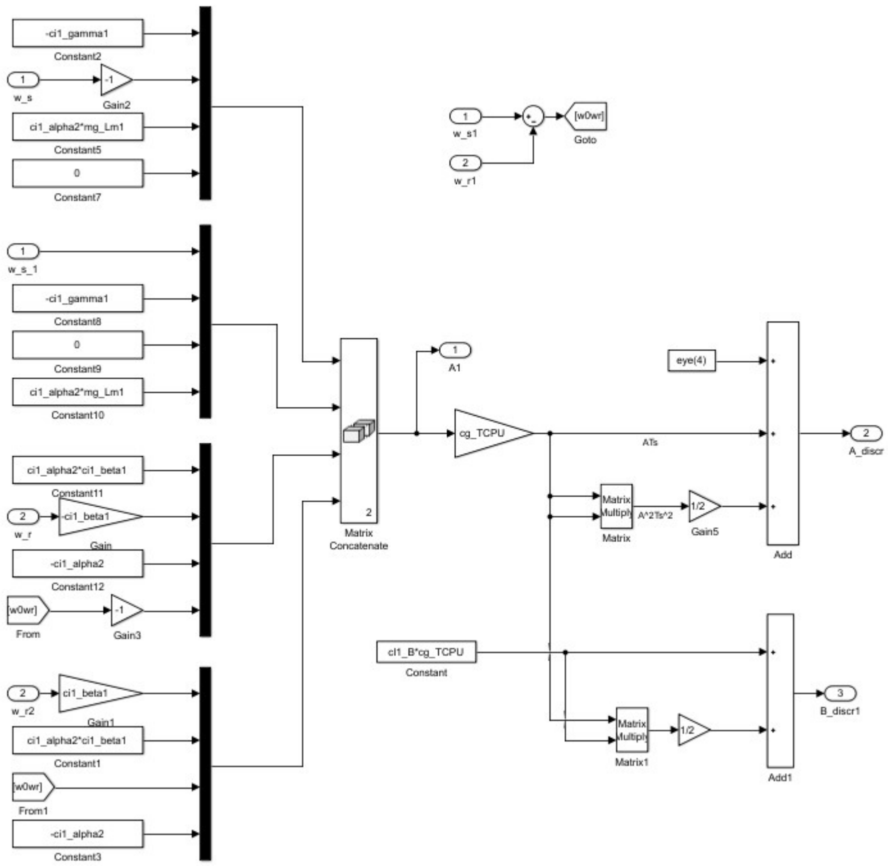

Figure 8.5-2 Inside-view AComputation

8.6 Chapter References

[1] L. MARCONI, Notes of the course of System Theory and Advanced Control, personal notes, 2017

[2] C. ROSSI, Notes of the course of Controlli 2, personal notes, 2014

[3] P. BOLZERN, R. SCATTOLINI, N. SCHIAVONI, Fondamenti di Controlli Automatici, McGraw-Hill, 2008

[4] L. ZARRI, Lectures slides of Electric Drives, personal notes, 2017

[5] N. KAZANTIS, C. KRAVARIS, Time-discretization of nonlinear control system via Taylor method, Computed and Chemical Engineering 23, 1999

9 Comparison between the Pulsating Torque and the Pulsating Flux Solutions

9.1 Controllers Chosen and Machine Parameters

In this section will be reported the results obtained by the mean of the Simulink simulations.

Before starting it has to be said which controller have been taken in account for the two possible high-level controls proposed.

For the pulsating torque high-level control has been selected as low-level controller the PI with feedforward actions: this choice has been done since the PI solution provides results that are just slightly worse with respect to the reduced LQ but it doesn't need to memorize lots of maps in flash memory.

For what concerns the oscillating flux the low-level control proposed is the resonant one for the first harmonic and the PI one for the third. In fact, for what concerns the power transmission it has been shown that sinusoidal references, with known frequency, are involved and only a resonant controller can grant perfect tracking. On the other side the velocity, and so the torque, tracking usually deals with ramps and steps, but without any foreknowledge about them: a PI controller has been shown to be enough robust and performing.

In the following sections, the results obtained with both the methodologies will be shown and compared and in the end some conclusion will be drawn.

At the time I'm writing, the machine has not been fully designed yet but, obviously, some parameters are necessary in order to carry out some simulations. Unfortunately, this Doubly Fed machine is not an ordinary one, since it is direct drive: this implies that mechanically is very slow ($60rpm$ as nominal speed) respect the usual electric machines that runs up to thousands of rpm.

According to this the parameters used are the ones of a machine that is 20 times bigger (in terms of power) than the real one: this because the dimensioning of the windings strictly depends on the currents, and so on the torque, and not on the speed since usually the Joule, thermal, losses are much bigger that the magnetic ones.

Furthermore, it has to be pointed out that the parameters found were referred to three phase DFIM and not to a five phase one and so the values of the inductances associated to the third harmonic are not present. It is known from the theory that the active value of them should be one ninth of the first harmonic one, but they have the same leakage value. A good trade-off should be to consider the third harmonics inductances as a third of the fundamental one.

In the following table the most salient parameters of the machine have been reported.

p	3	R_s	$0{,}036\ \Omega$	L_{s1}	26,45 mH	L_{s3}	8,8 mH
n_{Max}	$60\ rad/s$	R_r	$0{,}038\ \Omega$	L_{r1}	26,40 mH	L_{r3}	8,8 mH
DC_s	$800\ V$	DC_r	$600\ V$	L_{m1}	25,7 mH	L_{m3}	8,6 mH

Table 9-1 Electrical Machine Parameters

This parameters are referred to a Doubly Fed machine that can deliver $1kW$ of mechanical power and $3kW$ of electrical power.

Furthermore, an inertia of $15.2\ kgm^2$ has been thought reasonable since the mechanical size of the machine that should require so much electrical power.

9.2 Task Description

The test to which the control systems will be proved on is composed by four different section. We are assuming that at time $0s$, the start-up time the machine is stopped.

In the first part, that starts at time $0s$ and finishes at $1s$, the control has to flux the machine, no torque or power has been requested or has to be produced. The reference speed is at $0rpm$ just to not make discontinuous requests for the following part.

In the second section, the control manages to maintain the velocity equal to 0 while the power requested has been raised to $3kW$. A very steep ramp has been implemented since it is more realistic: in fact, when the electrical user turns on, the request of electric power changes so quickly that is almost like a step, since just the parasitic inductances and capacities smooth the outflowing current.

In any case a little smoothing has been carried out in order to have a feasible and reliable trajectory, task that, in the real machine, will be carried out by the active front end of the rotor inverter.

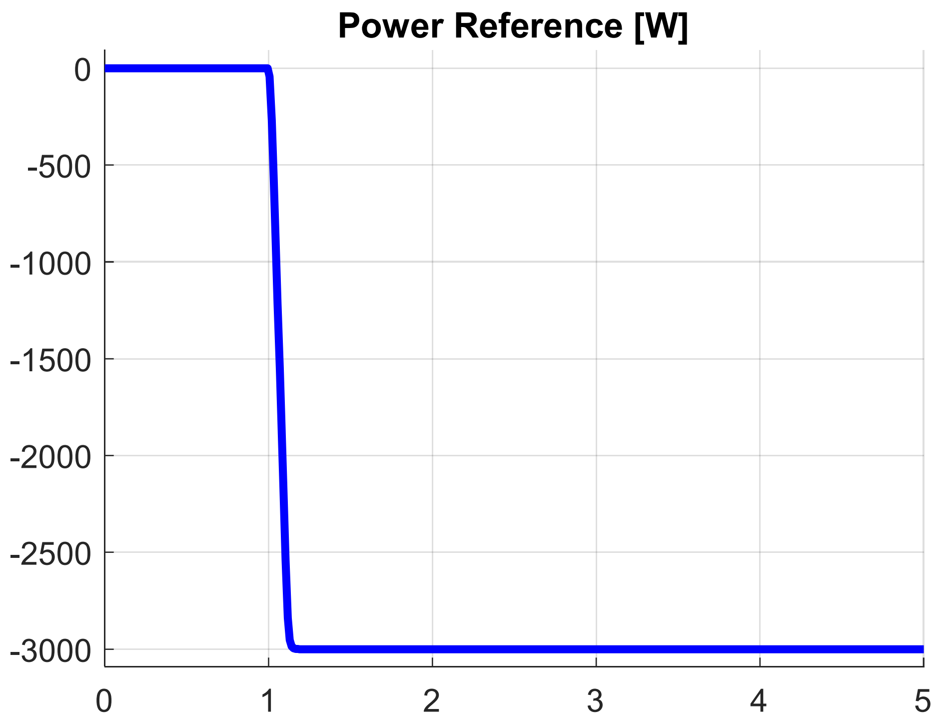

Figure 9.2-1 Test Power Reference

In the third section, that takes place from $2s$ to $4s$, still it is required to produce $3kW$ of electrical power but the velocity has been raised with a ramp from 0 to $60rpm$.

Finally, in the fourth part of the test, the machine is asked to maintain that velocity while it continues to transmit that power request. Note that is this last condition in which the machine will work prevalently.

The overall speed reference is reported in the following figure.

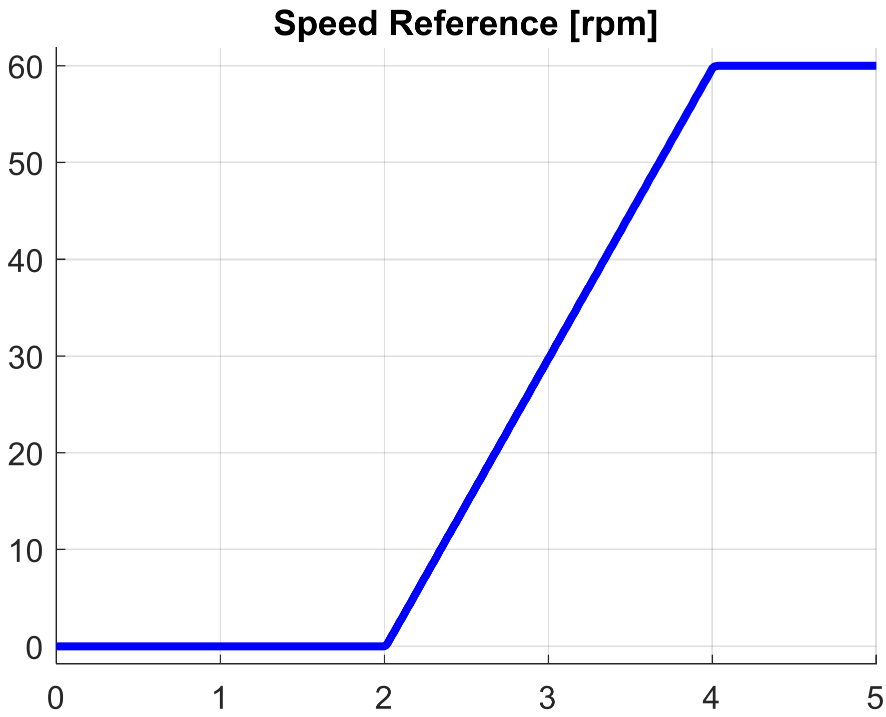

Figure 9.2-2 Test Speed Reference

9.3 Fluxing Phase

In this first phase the machine must be fluxed in order to have more reliable results once the motor starts to move or transmit power.

9.3.1 Fluxing Phase: Stator Currents and Voltage

In this phase, obviously both the q components of the first harmonic currents stays to 0 since no torque must be produced.

On the other side, a difference can be pointed out: in particular we can notice that the d component of the solution of pulsating flux rises to $35A$ while, in the solutions with pulsating torque it reaches a much smaller value: this is due to the fact that, since the pulsating torque solution needs much greater electrical frequencies the machine works with a lower flux to reduce the back emf.

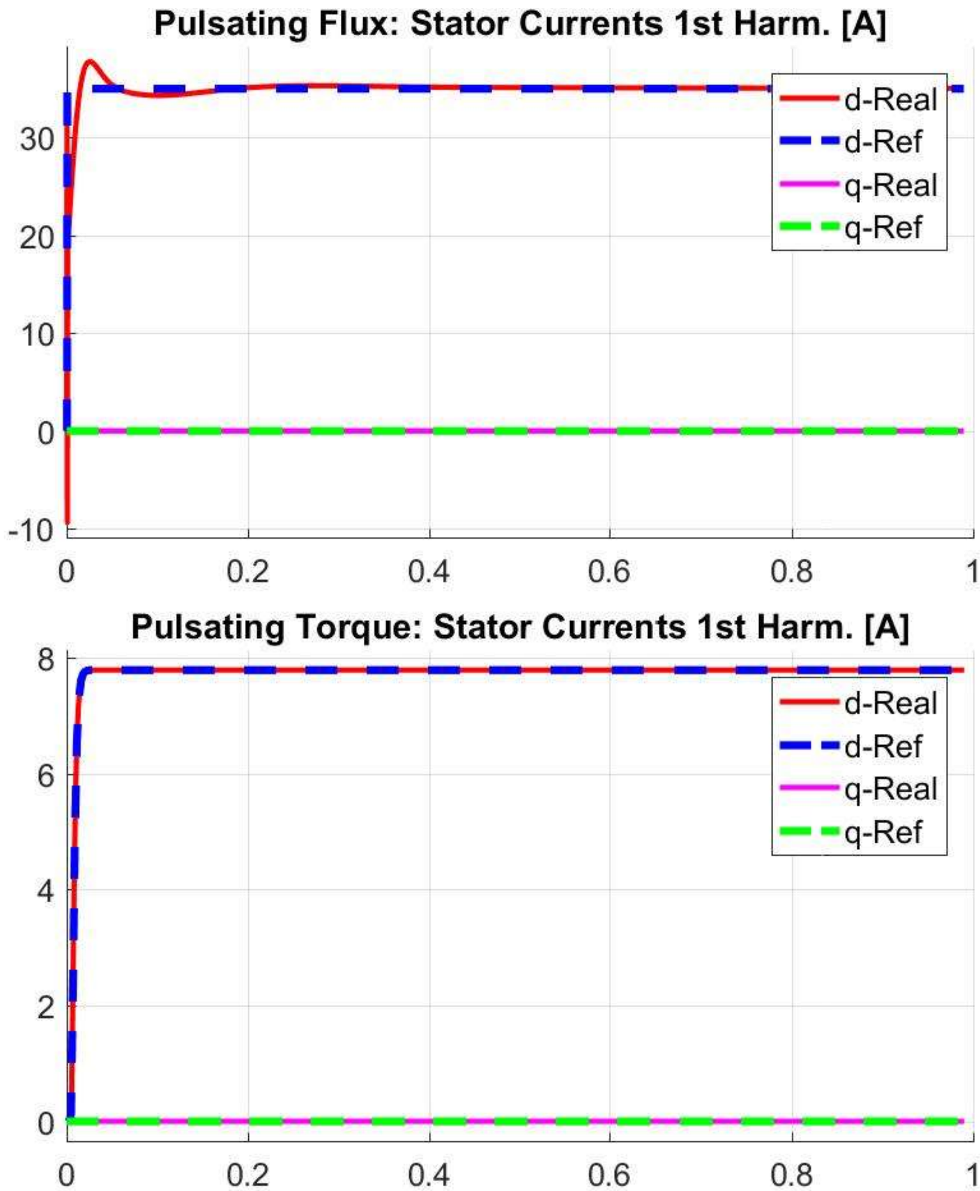

Figure 9.3-1 Fluxing Phase: Stator Currents 1st Harmonic

That choice is the same for the third harmonic and similar results appears: once again, since there is no torque, in both the solutions the q component is put to 0 while the d component has different values

Furthermore, it has to be pointed out the peak of the d current of the first solution: this is due to the anticipative solution adopted and described in section 5.4.

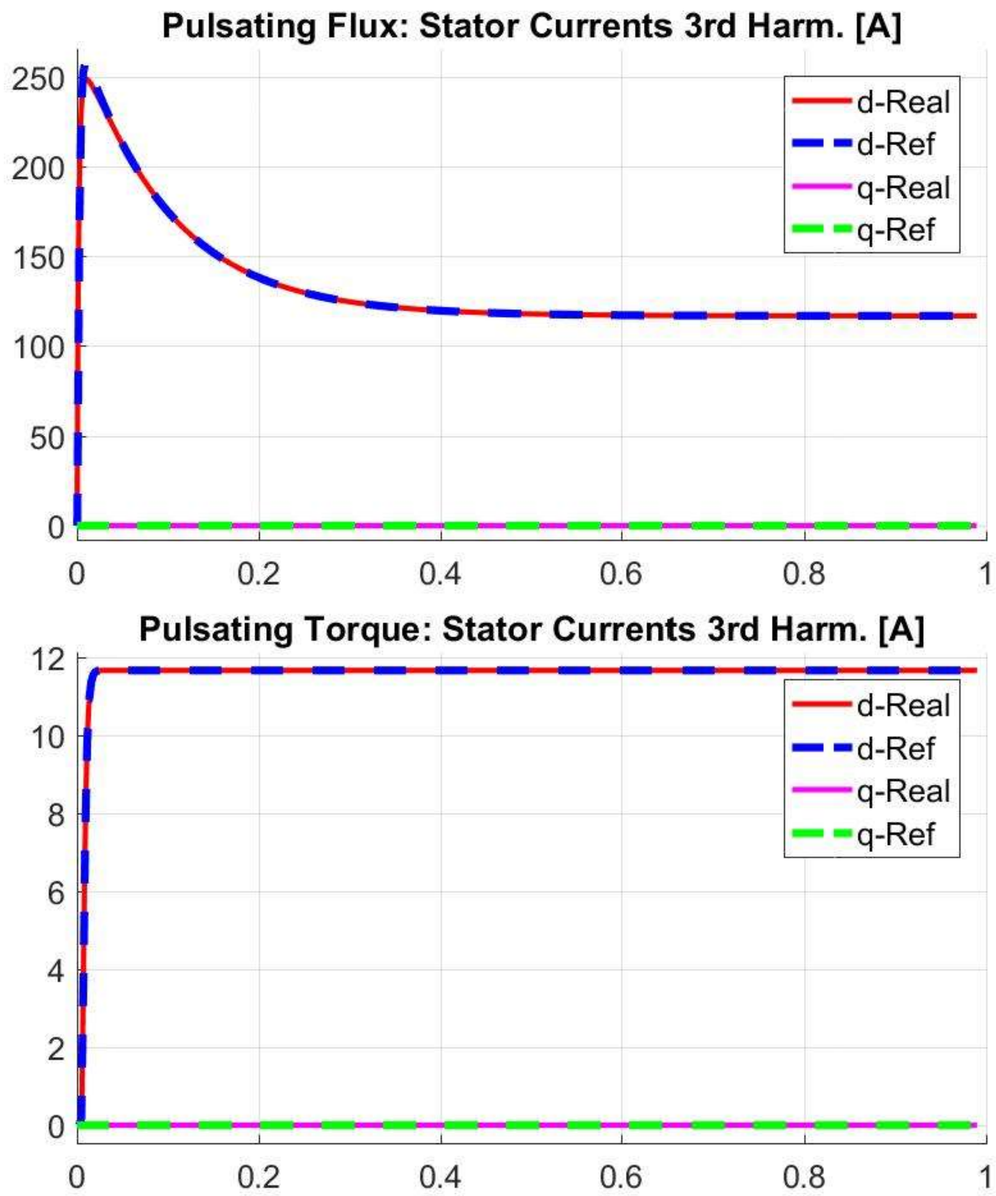

Fluxing Phase: Stator Currents 3rd Harmonic

Due to the very low resistance of the machine and the null stator frequency ω_0, and so the absence of back electro-motive force, even if certain amount of currents is circulating, less than $20V$ are needed.

The initial high peeks are instead due to the fast convergence of the currents to the reference values.

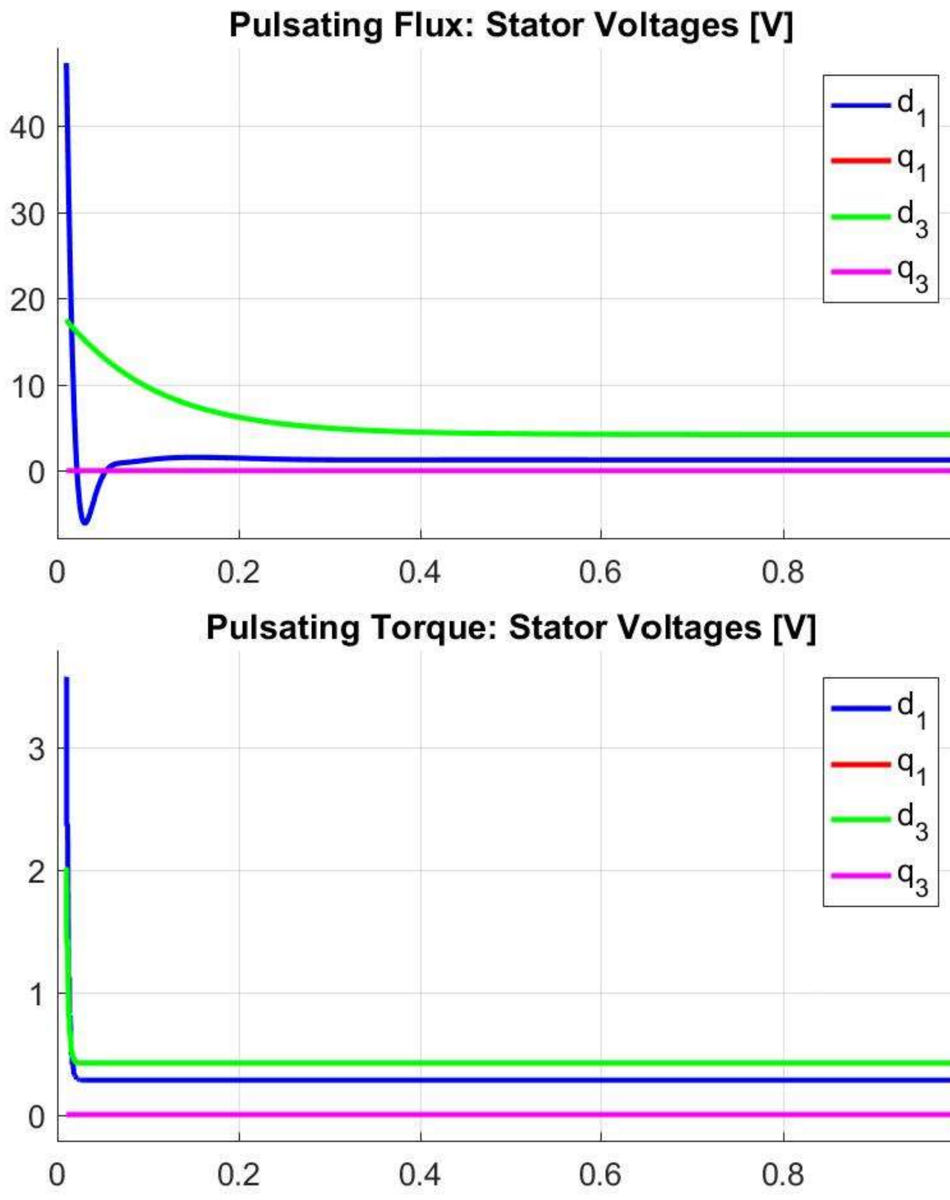

Figure 9.3-2 Fluxing Phase: Stator Voltages

9.3.2 Fluxing Phase: Rotor Flux

Let's now examine the behaviour of the rotor fluxes: for what concerns the first harmonic we see that the convergence is got $200ms$ but some different takes place between the two solutions.

First of all we have to point out that the pulsating torque solution expects very high stator frequency that means very high back emf. As already pointed out so the machine is highly defluxed in order to have enough voltage to control the current flowing in the rotor windings.

In second place, a little overshoot is present in the pulsating flux solution, but in any case, is limited and there is no rick of magnetic saturation.

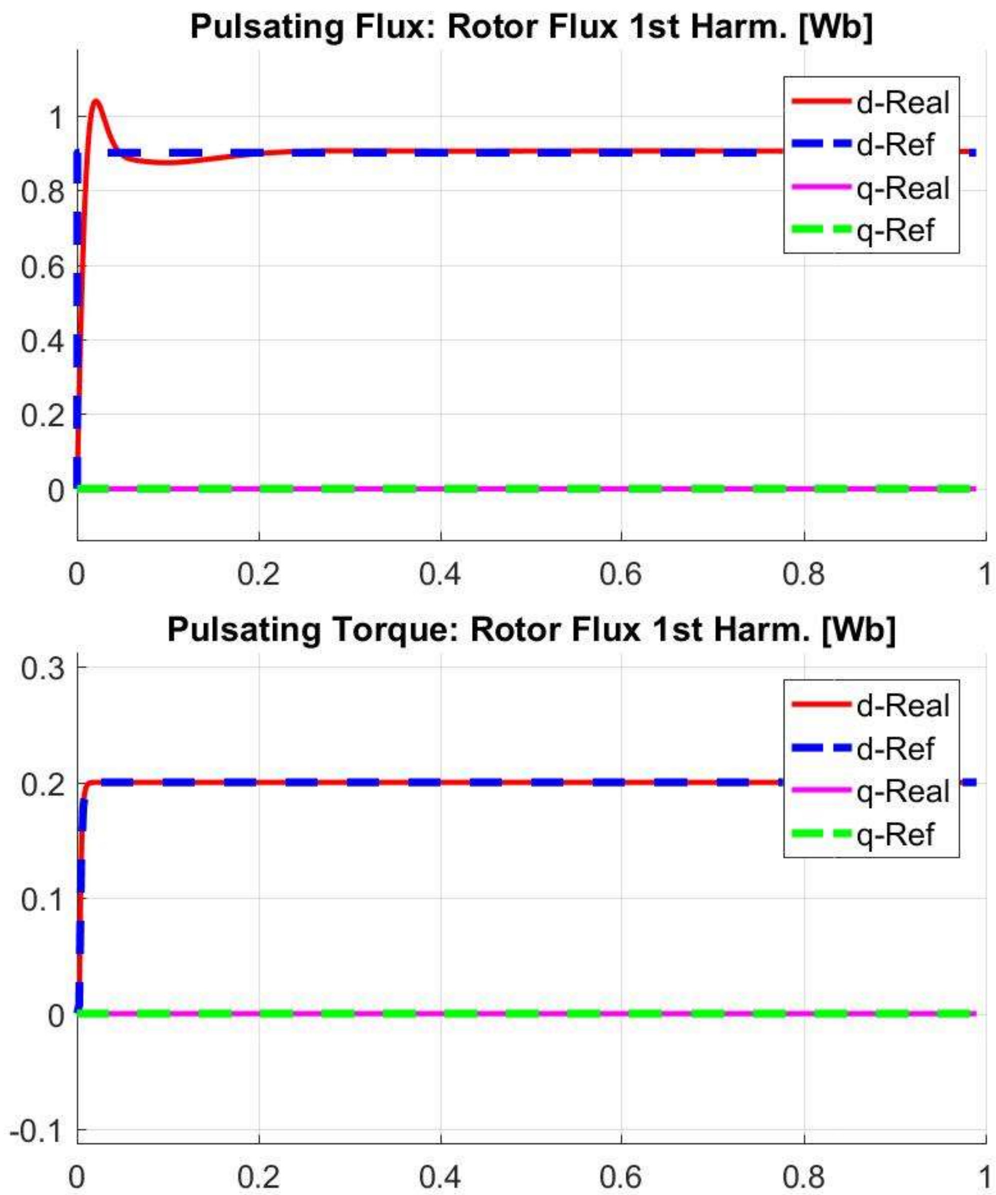

Figure 9.3-3 Fluxing Phase: Rotor Flux 1st Harmonic

For what concern, instead the third harmonic fluxing, in the pulsating flux control, it can be noticed that the dynamic is quite slower. This is due to two main reasons: the first one is that the mutual inductance of the third harmonic is quite smaller than the one of the first one.

On the other side, in comparison with the pulsating torque control, the flux is slower to reach the setpoint because the rotor is not controller. A faster dynamic is possible but with bigger peeks of currents and so it is not desirable.

In both the pulsating torque fluxes the reference tracking is almost perfect due in particular to the feed-forward actions.

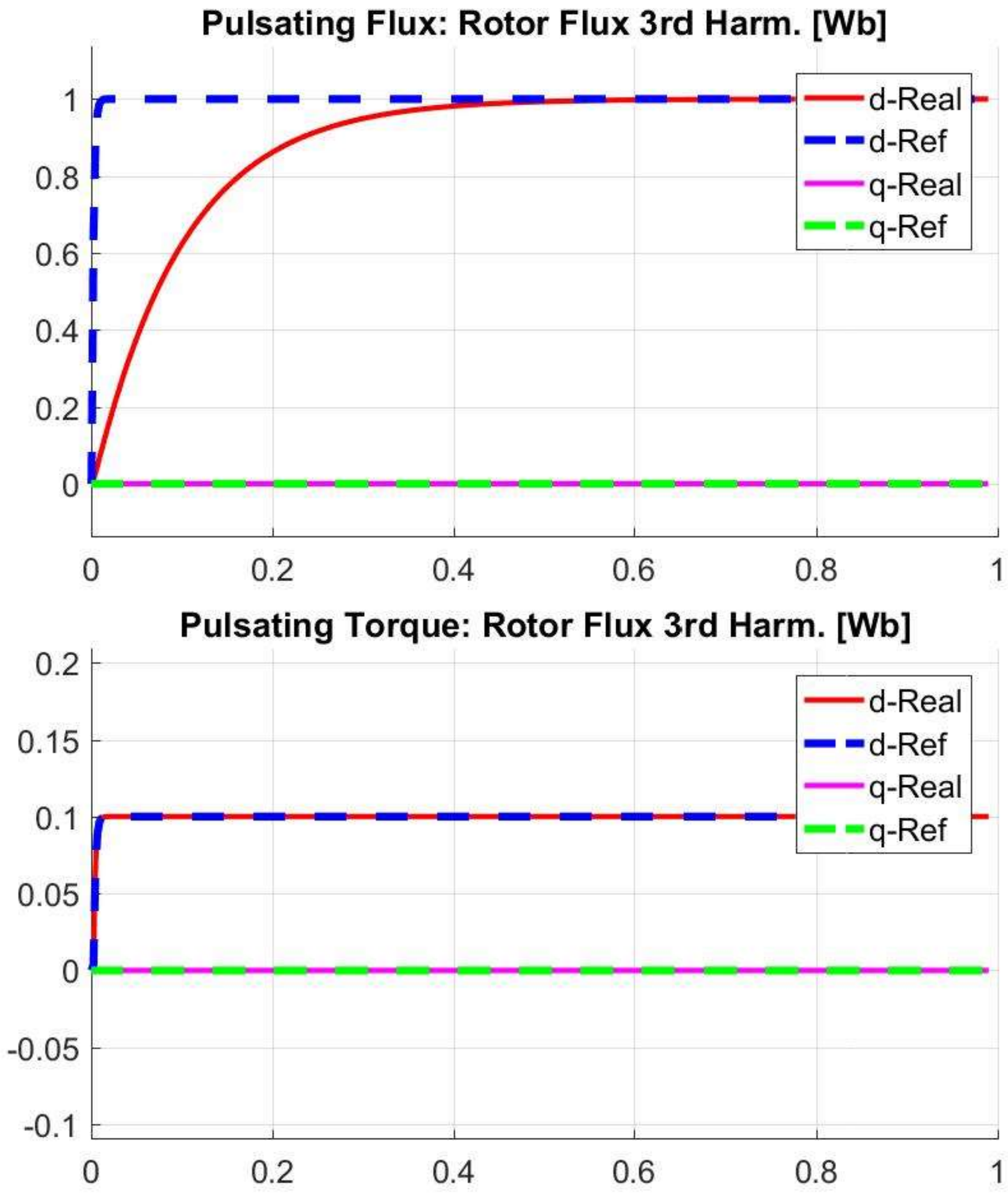

Figure 9.3-4 Fluxing Phase: Rotor Flux 3rd Harmonic

Since the torque solution works with much smaller fluxes, it can be explained the fact that the requested currents are lower.

9.3.3 Fluxing Phase: Rotor Currents and Voltages

It is well known that exists a relationship between the stator currents, the rotor fluxes and the rotor currents.

It is so not surprising that no strange behaviours take place there: all the rotor currents are so limited, except for a peek in the pulsating flux control on the d_3 component, that is obviously due to the fluxing of that harmonic.

Except this, all the currents are very close to 0.

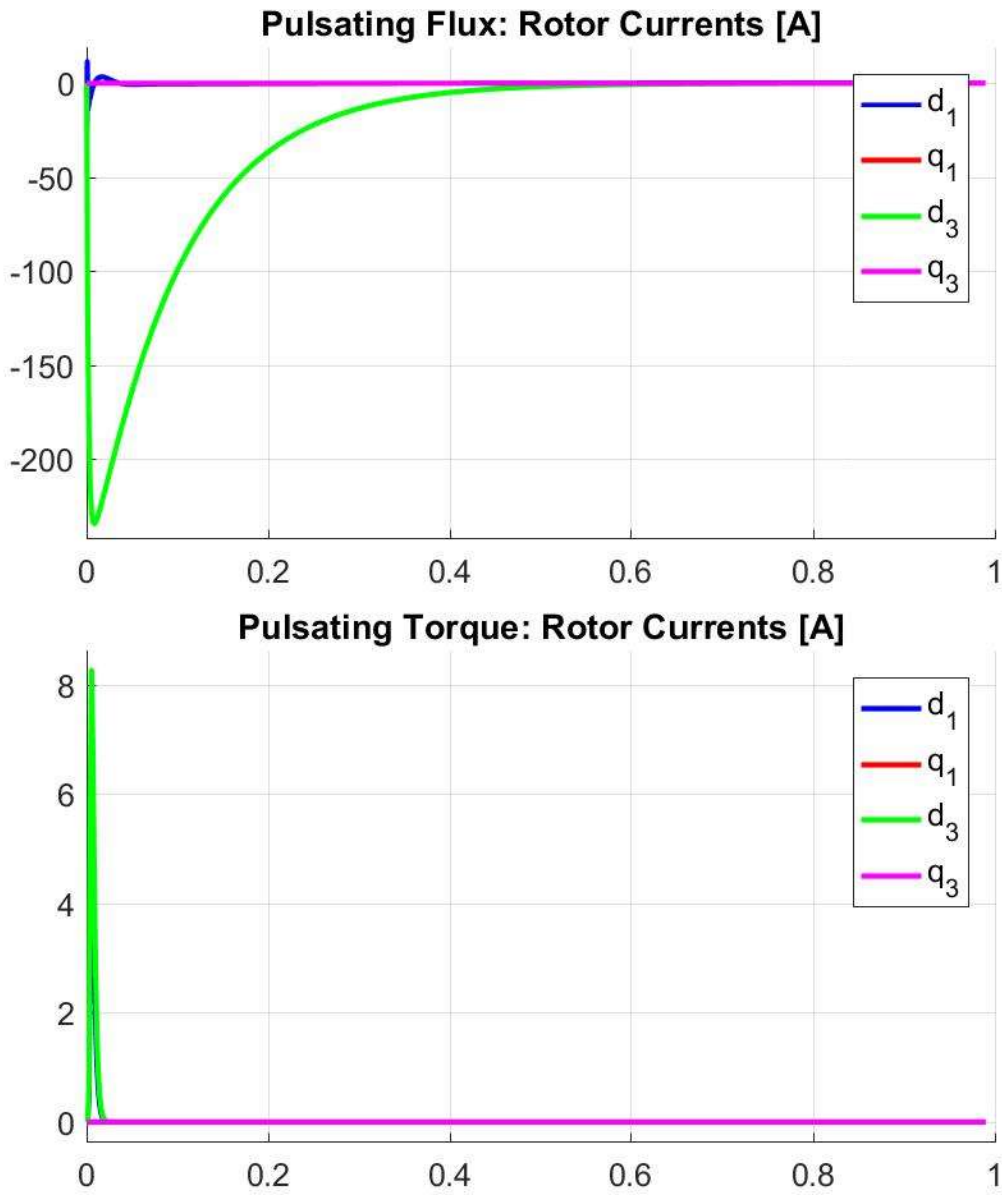

Figure 9.3-5 Fluxing Phase: Rotor Currents

Even on the voltages are present some peeks and in particular for the d_1 component of the pulsating flux control. This, as already remarked, is due to the fact that this control doesn't distribute currents and voltages as well as the pulsating torque one.

In any case the peeks last for less that $50ms$ and so are well admissible.

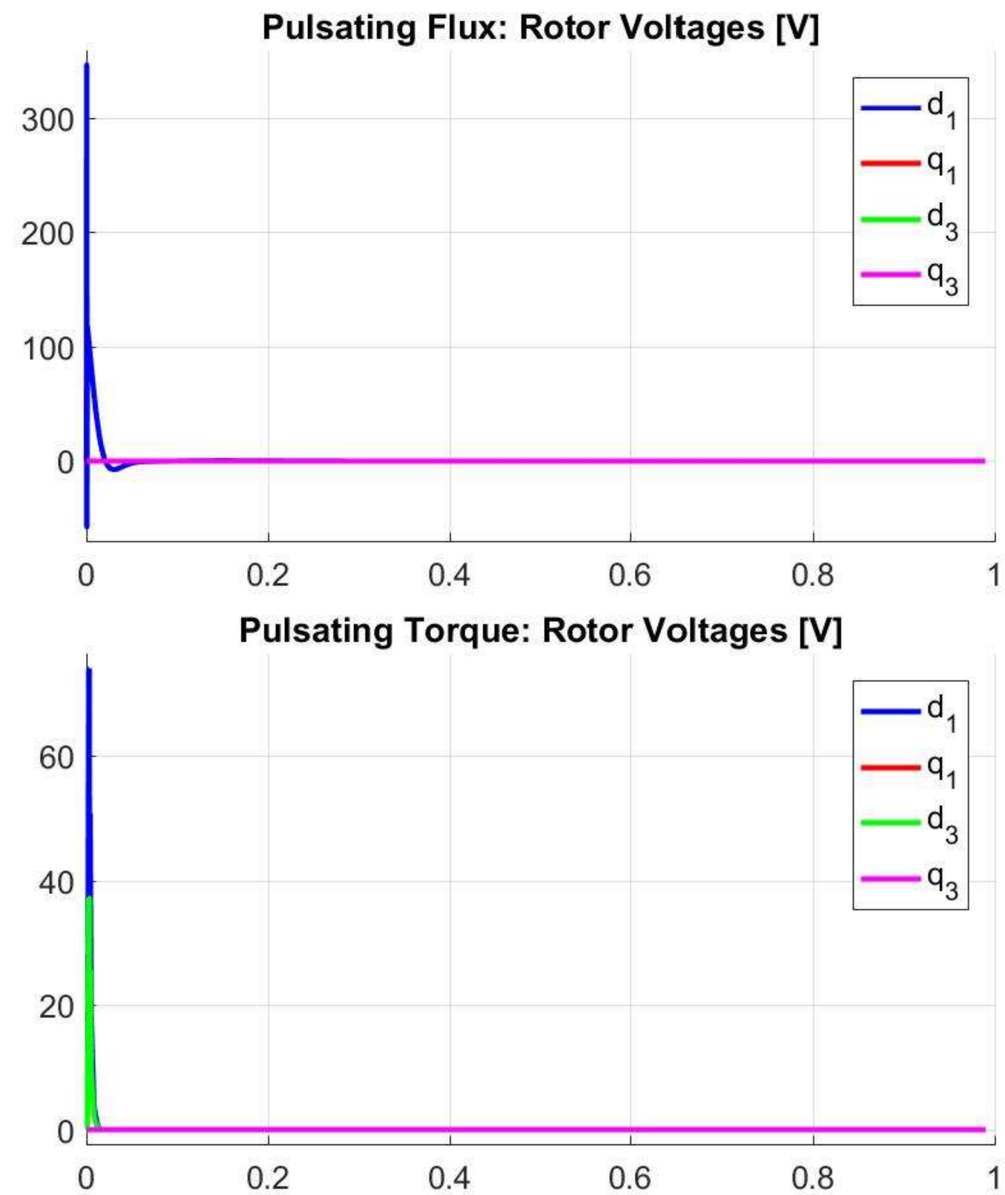

Figure 9.3-6 Fluxing Phase: Rotor Voltages

9.4 Null Velocity Setpoint

In this period, that last from $t = 1s$ to $t = 2s$, a null mechanical velocity is required to the rotor, but while some electrical power has to be transmitted from the stator to the rotor. Due to the power request, the modulations take place.

9.4.1 Null Velocity Setpoint: Velocity

As expected very different behaviour takes places in the two different controls: in fact, while in the pulsating flux the velocity reference is tracked perfectly.

In the pulsating torque, instead, a small, triangular, velocity ripple is present: the triangular shape makes sense since the velocity, neglecting the viscous friction, depends on the integral of the torque, that should like a square wave.

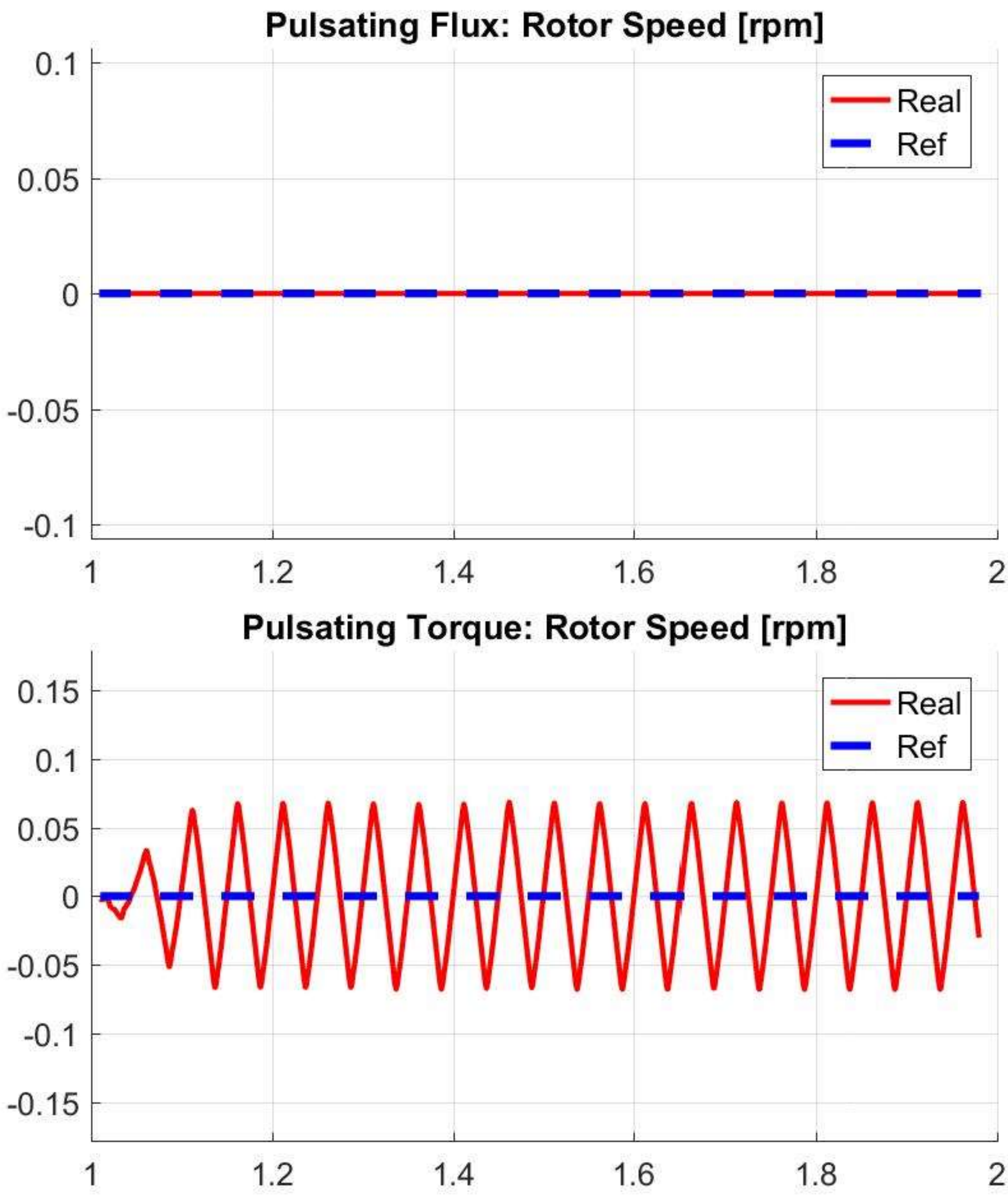

Figure 9.4-1 Null Velocity Setpoint: Rotor Speed

9.4.2 Null Velocity Setpoint: Power

Let's analyse a zoom of the complete plot since otherwise nothing could be seen.

As expected the pulsating flux solutions presents a behaviour of the power transmitted that is almost sinusoidal. A little error is present every two low peeks but it is due to the numerical approximation of the angle: in any case it last just for one sampling time and so doesn't represent a big issue.

For what instead concerns the pulsating torque control at steady state the setpoint is tracked perfectly and instantaneously, but at each inversion of the torque heavy oscillations appears with a big power error in the tracking. This is due to both the controller discretization and distribution.

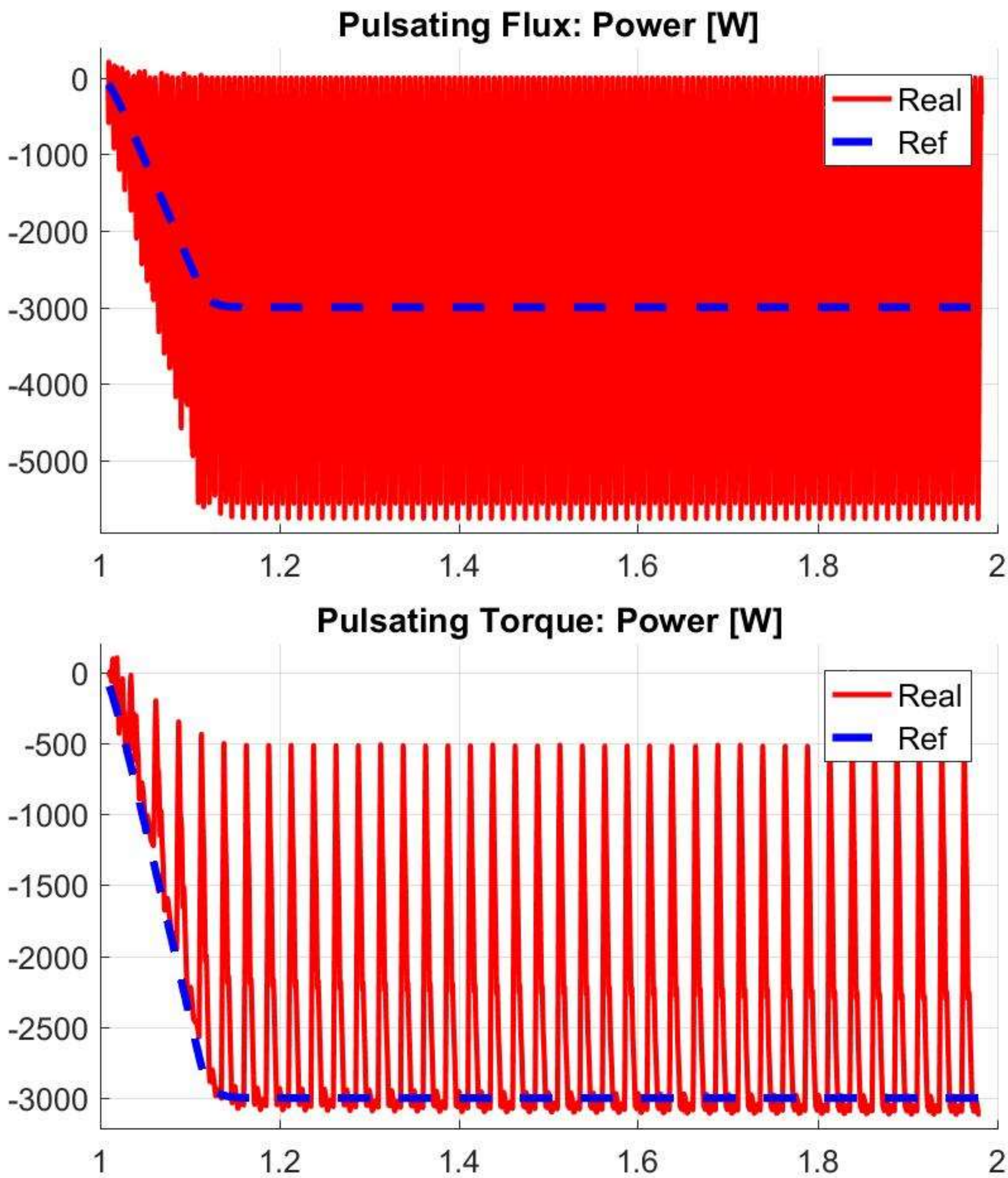

Figure 9.4-2 Null Velocity Setpoint: Rotor Power

9.4.3 Null Velocity Setpoint: Stator Currents and Voltages

For what concerns the stator currents we will see a behaviour that obviously is connected to what has been seen in the two previous sections.

In particular, for what concerns the first harmonic in the pulsating flux solution, it can be seen that the component sinusoidal reference is almost perfectly tracked. Furthermore, it increases with the time and then reaches a steady state amplitude: this is due to the augmenting of the request of the power from the rotor.

On the other side, for what concerns the control with pulsating torque, the q reference component of the current is, as expected, a square wave: the real currents follow it, but with some oscillations.

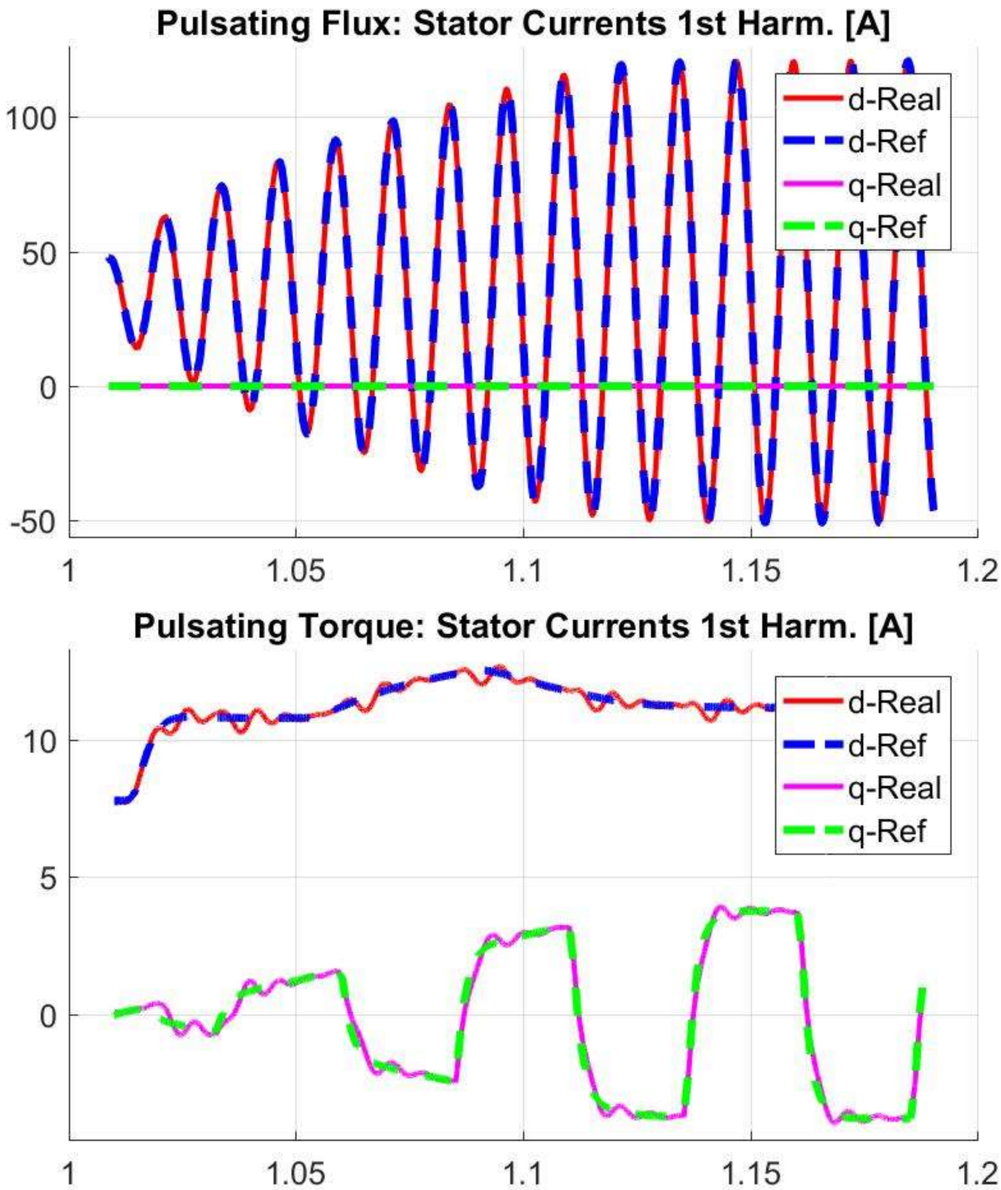

Figure 9.4-3 Null Velocity Setpoint: Stator Currents 1st Harmonic

For the pulsating torque solution, similar behaviour can be shown for the third harmonic where again, quite heavy oscillations take place. Note that, in any case they vanish and the steady state value is correct.

On the contrary, in the pulsating flux, the q component is equal to 0 since no torque is really necessary. It is just present the magnetizing current on the d axis.

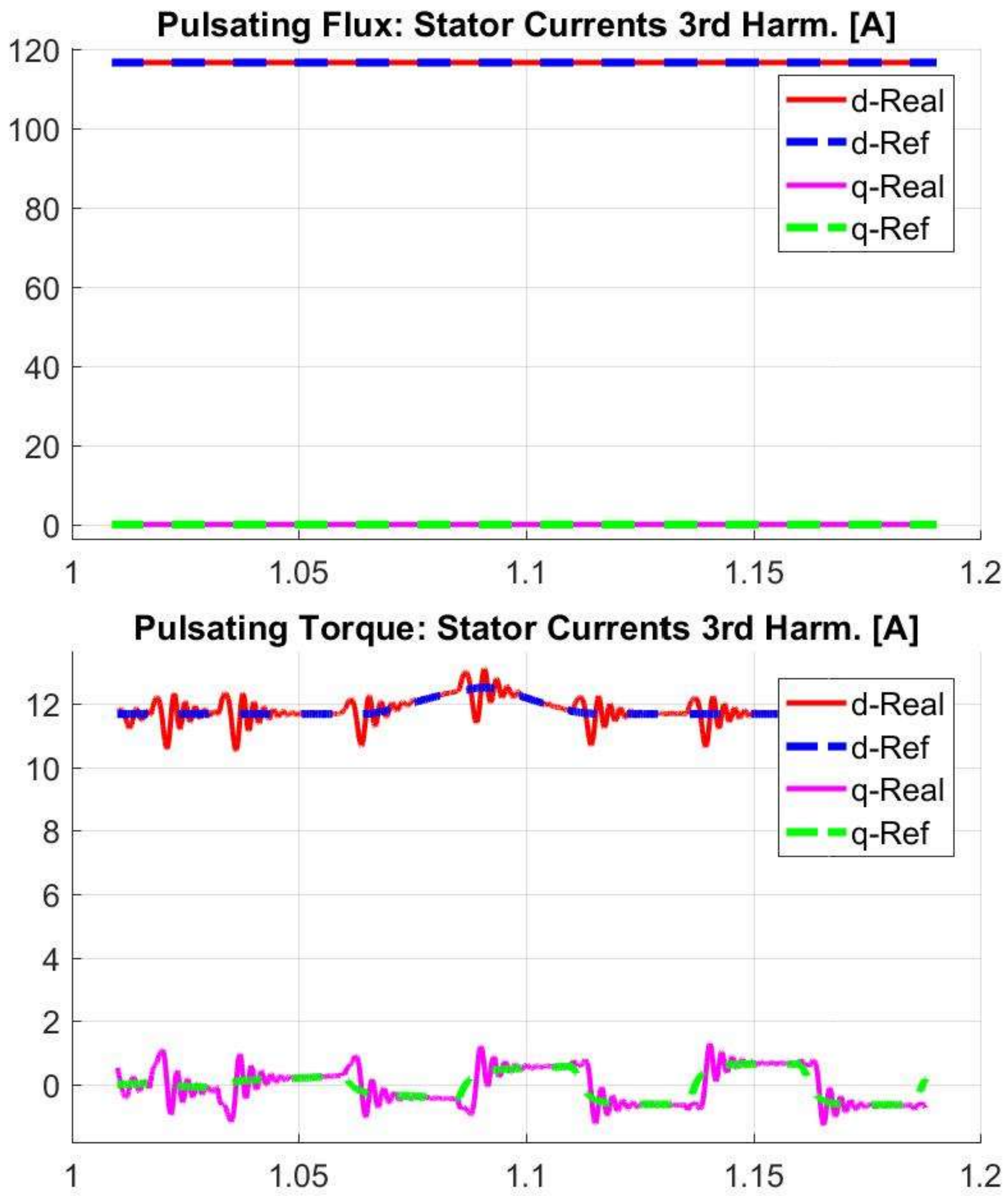

Figure 9.4-4 Null Velocity Setpoint: Stator Currents 3rd Harmonic

Now has to be underlined that, even if in the pulsating torque control, the currents have a sub-optimal behaviour their magnitude is up to ten times smaller respect in the pulsating flux solution.

On the other side, since the requested power, both mechanical and electrical, is the same come straightforward that the voltages will be much higher in the pulsating torque control. In particular the pulsating torque requests up to five time the voltage that the pulsating one needs.

Unlikely the currents, a high voltage request, if feasible, comes for free: in fact, no losses are connected to the voltage request since it doesn't change the switching frequency and no dissipations, like Joule losses, takes place if just voltages are applied.

This big difference find motivation in the fact that in the pulsating torque solution the stator frequency is much higher and so is the back emf.

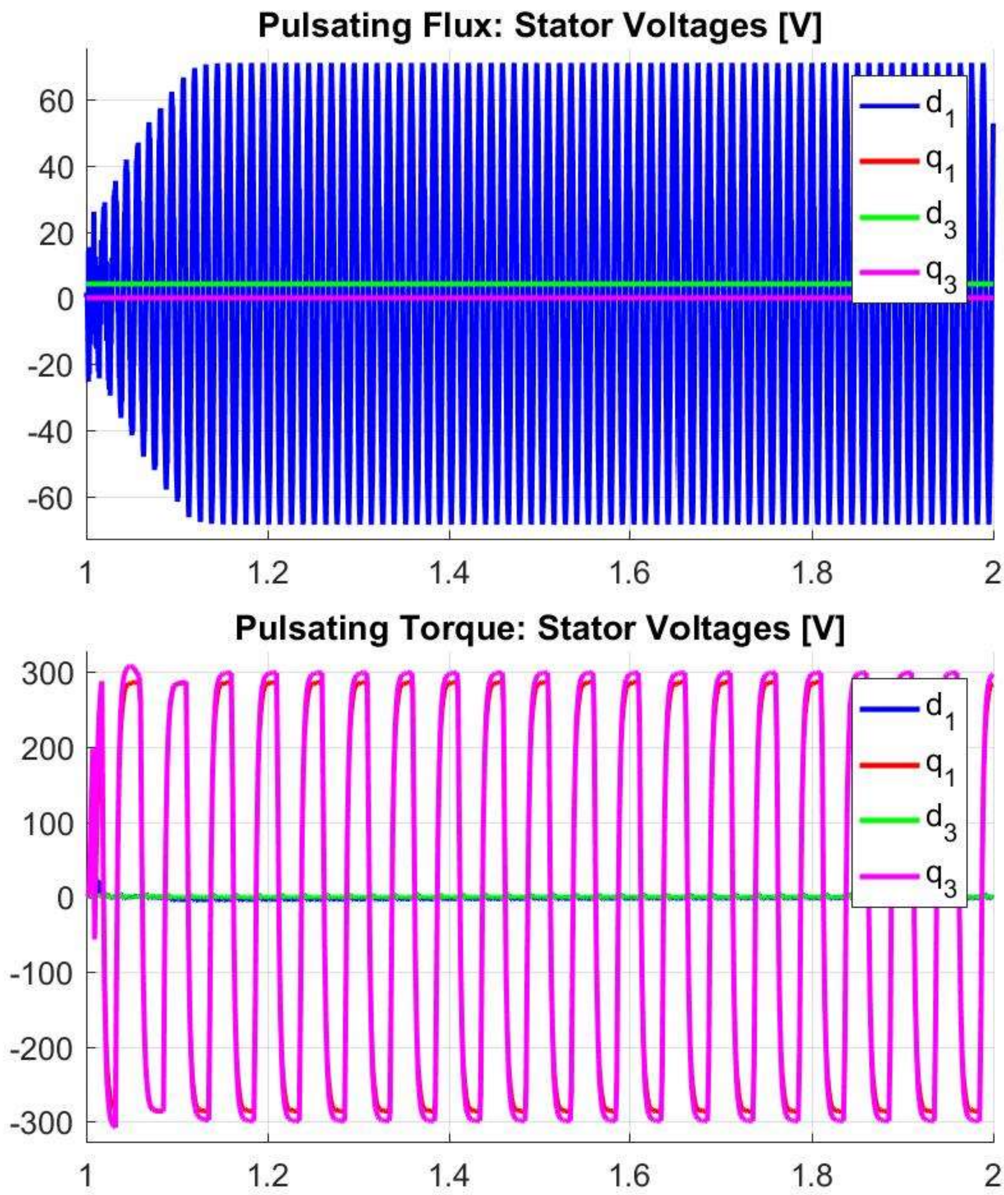

Figure 9.4-5 Null Velocity Setpoint: Stator Voltages

9.4.4 Null Velocity Setpoint: Rotor Flux

For what concerns the rotor flux in this part of the test can be shown that, in the control with pulsating flux, the reference is perfectly tracked: note that for the first harmonic the reference is a biased sine with an amplitude that increases since the power request itself increases while for the third is the nominal flux.

Instead for what concerns the pulsating torque solution, the reference is almost flat, but even there the control doesn't damp all the oscillations immediately: it just varies a little since, due to the error velocity, the torque request varies a little.

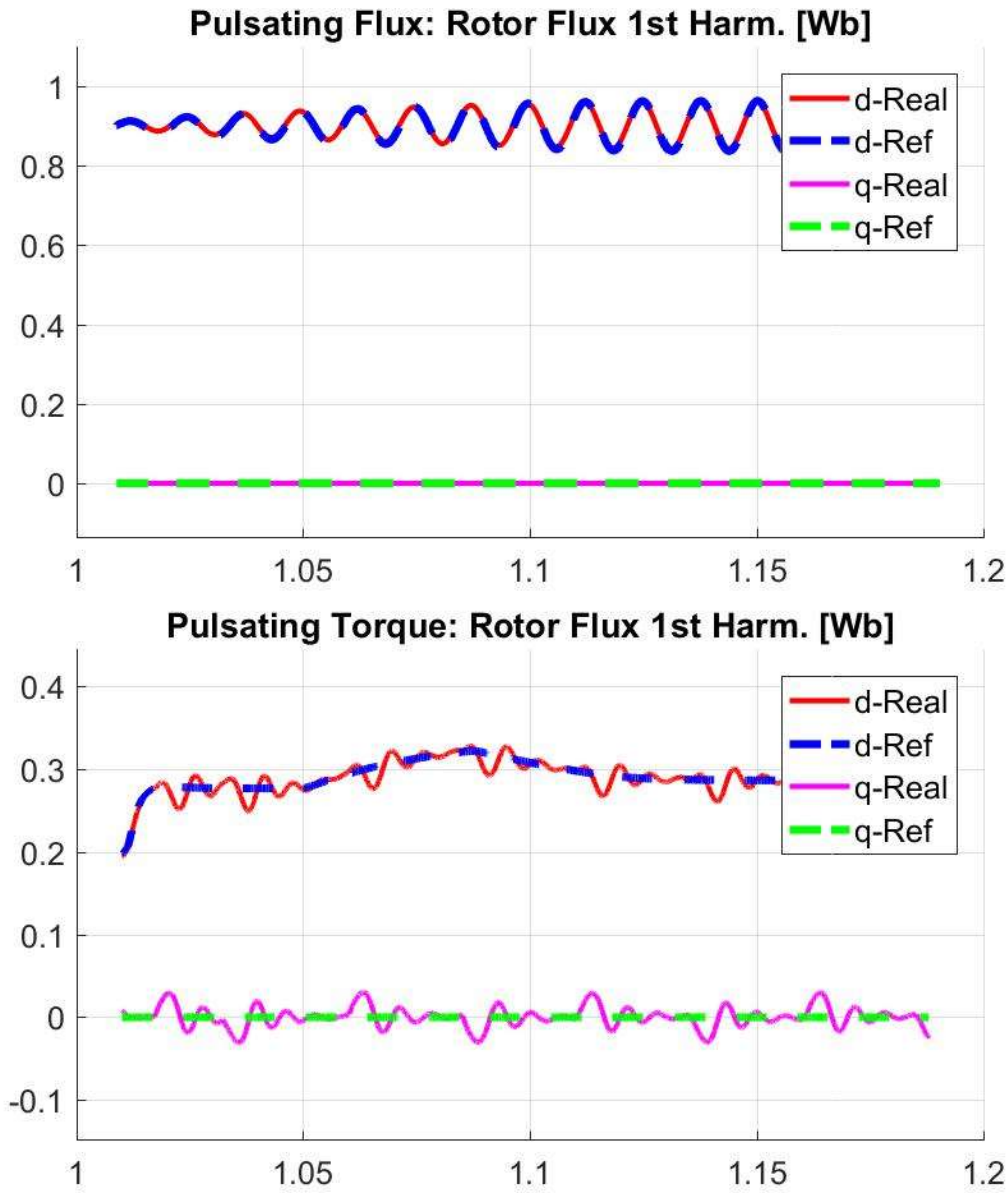

Figure 9.4-6 Null Velocity Setpoint: Rotor Flux 1st Harmonic

We have to point out that not only the d components of the flux oscillate but even the q ones: these last oscillations are in particular due to the oscillations in the stator currents.

Once again let's point out that those oscillation are vanishing and don't lead to any magnetic saturations since the maximum peek of the flux is less than a half of the rotor nominal flux.

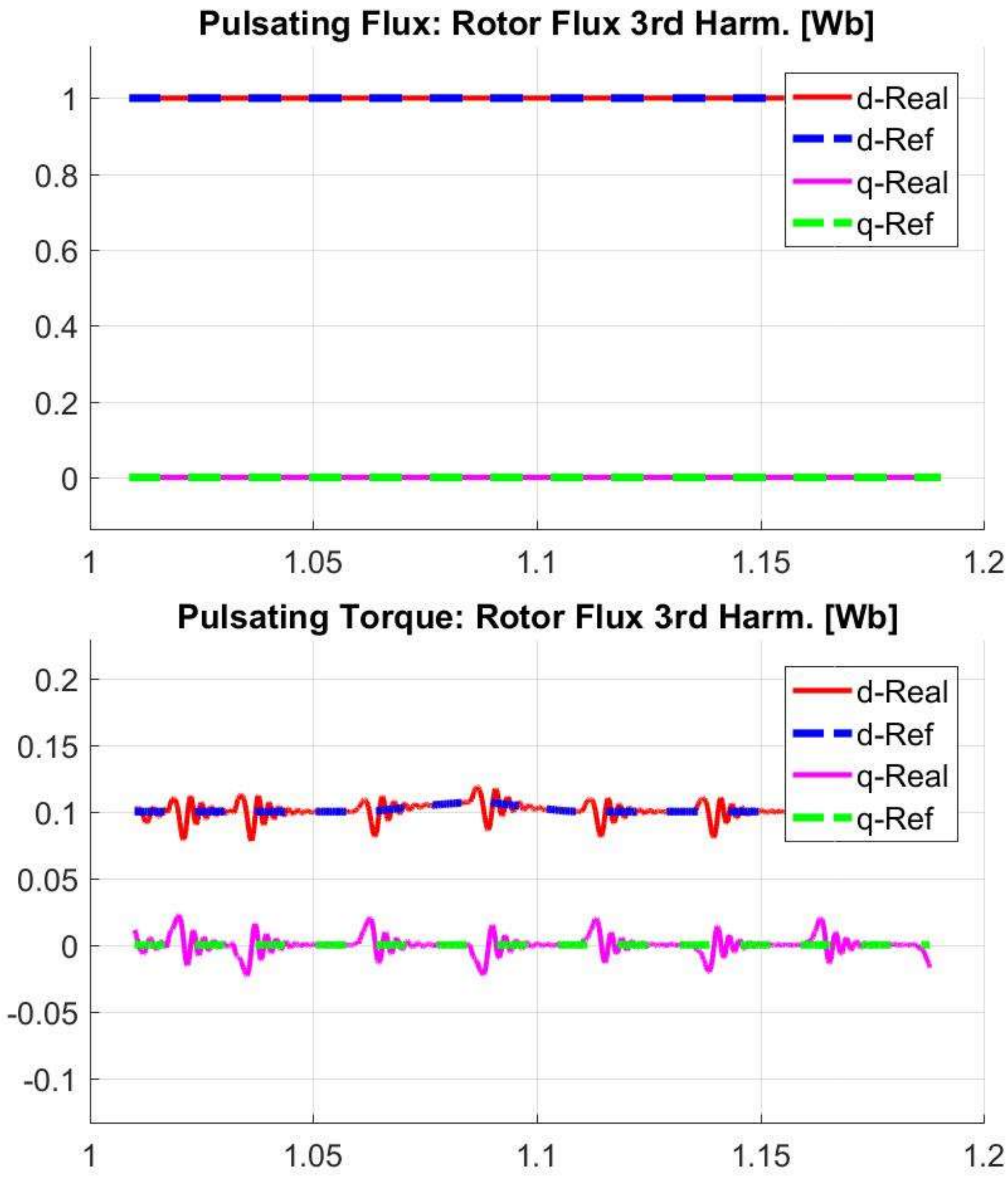

Figure 9.4-7 Null Velocity Setpoint: Rotor Flux 3rd Harmonic

As in the previous test section, the fact that the torque solution works with much smaller flux justify the fact that the requested currents are lower.

9.4.5 Null Velocity Setpoint: Rotor Currents and Voltages

Obviously, the oscillations, desired or undesired, of both the stator currents and rotor fluxes leads to some oscillations in the rotor currents.

Note that, in the pulsating flux control, the only current different from 0 is d_1, the one in charge of transmitting electrical power. Instead, the pulsating torque presents as obvious both q_1 and q_3 components of the currents different from 0 since both the harmonics are producing torque.

Furthermore, it has to be pointed out that, even if the steady state values of the currents of the second control are much lower than the ones of the first: the peek values differ of, more or less, $40A$.

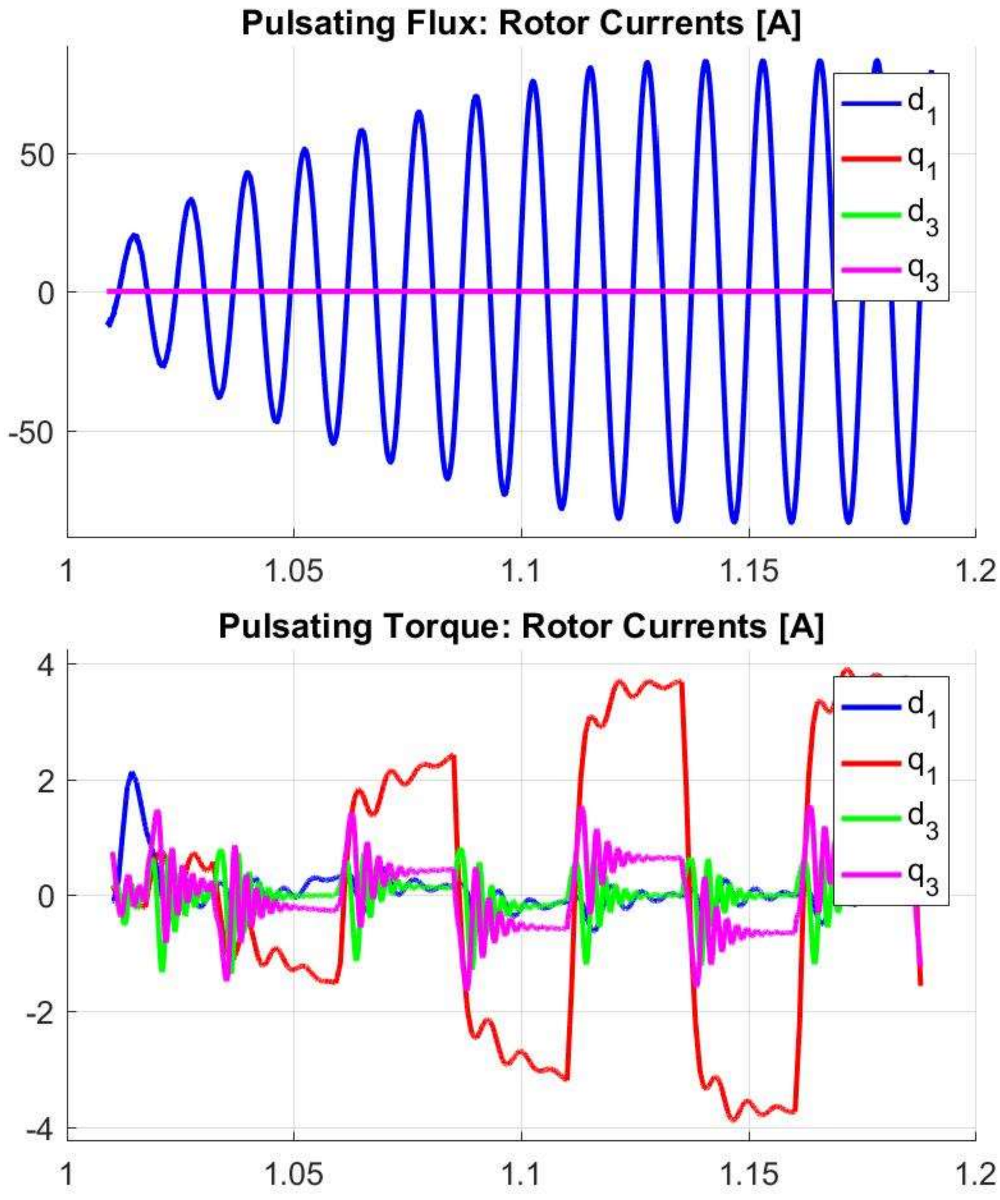

Figure 9.4-8 Null Velocity Setpoint: Rotor Currents

For what concerns, the voltages we notice that in the pulsating torque solution they are much higher, but this doesn't represent a big issue.

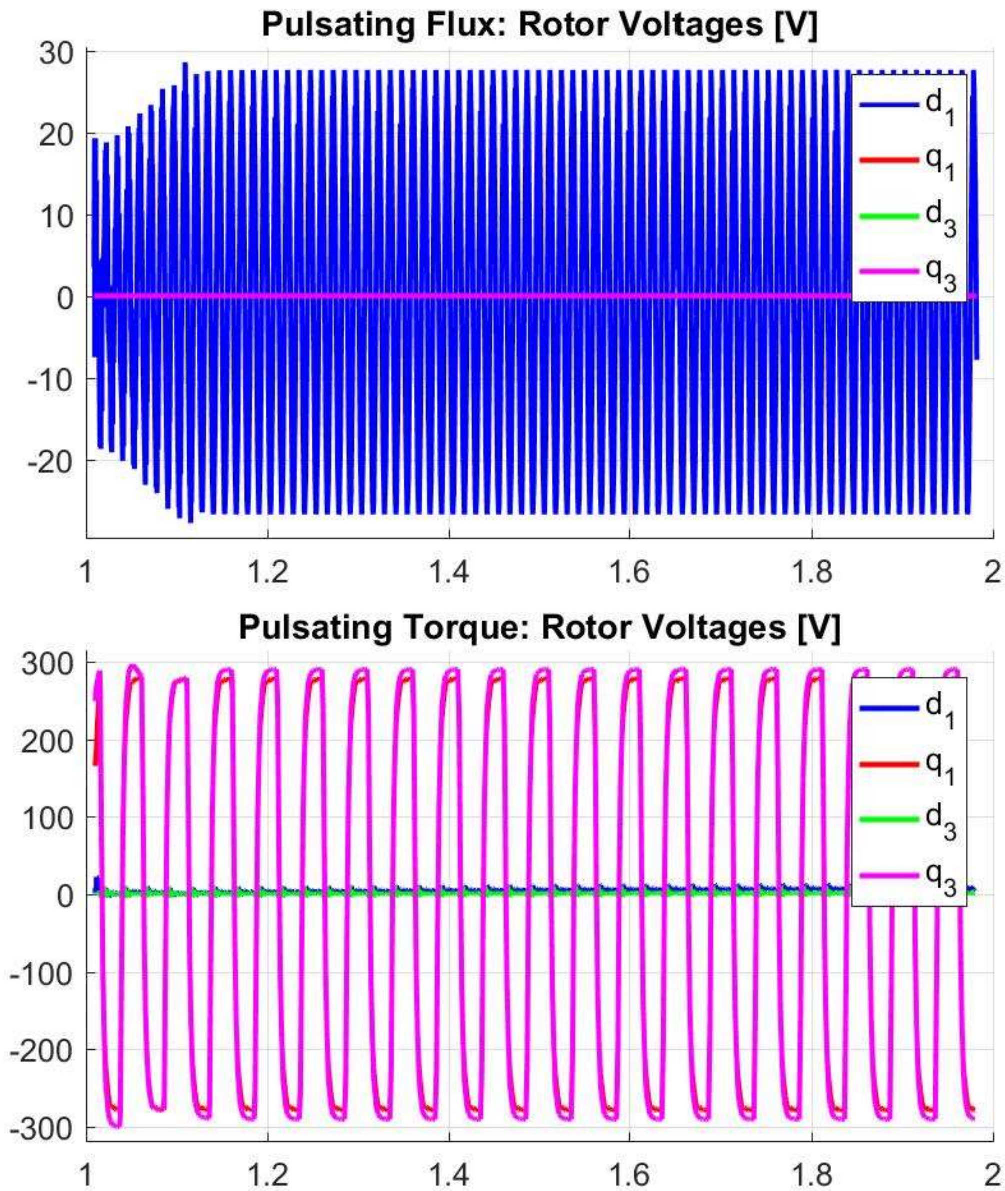

Figure 9.4-9 Null Velocity Setpoint: Rotor Voltages

9.5 Accelerating Setpoint

In this phase the machine is requested to accelerate from $0rpm$ to $60rpm$ in $2s$: it results that a quite big torque is necessary to perform such an action.

9.5.1 Accelerating Setpoint: Velocity

Let's now analyse the velocity behaviour of the machine when it is requested to accelerated. In this case the torque request is quite high, due to the high inertia of the rotor and so even the pulsating torque control doesn't modulate.

In both the control solutions so the reference is tracked almost perfectly.

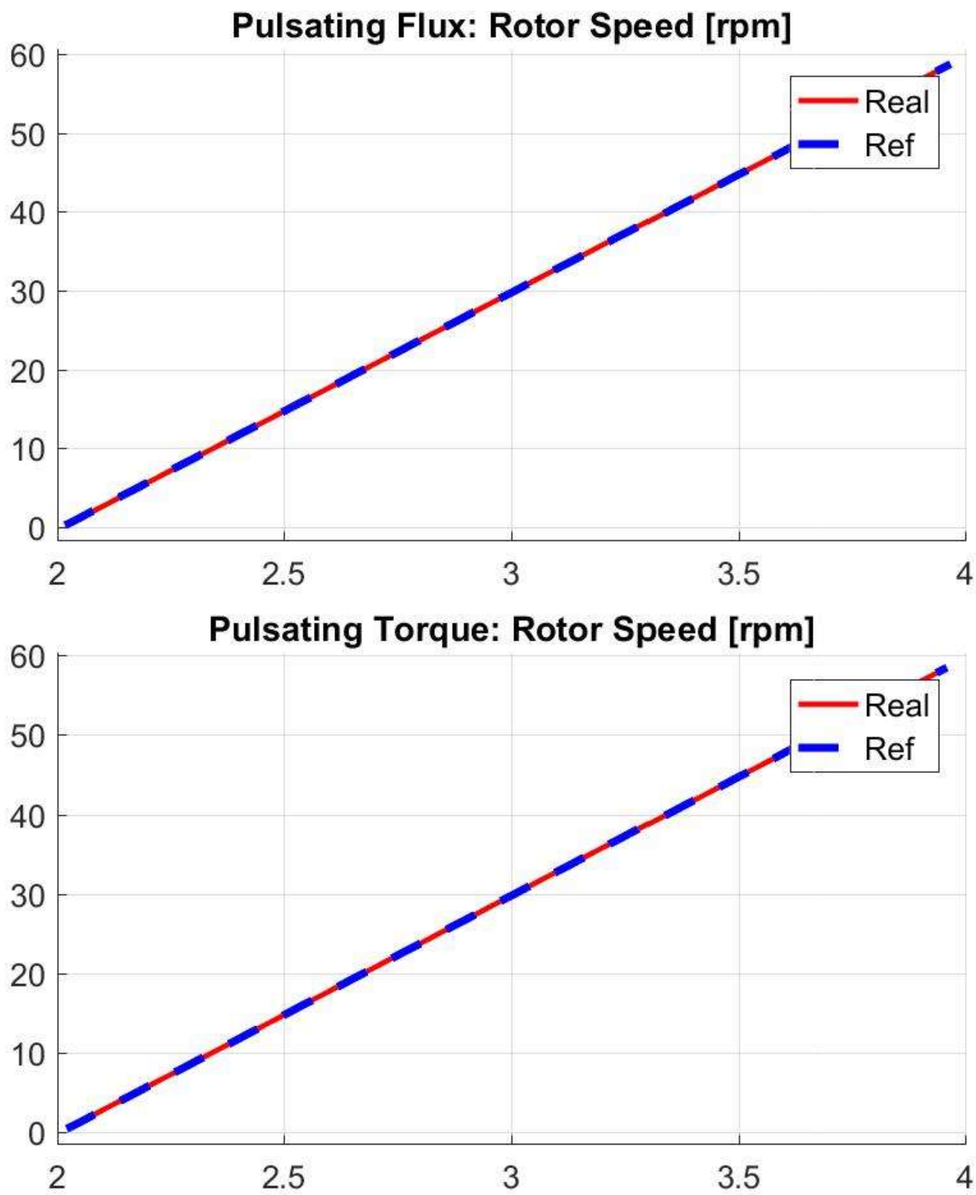

Figure 9.5-1 Accelerating Setpoint: Rotor Speed

9.5.2 Accelerating Setpoint: Power

For the power transmission can be noticed that the power in the pulsating flux solution continues to oscillates between 0 and $-6kW$, while in the pulsating torque one almost tracks perfectly the setpoint.

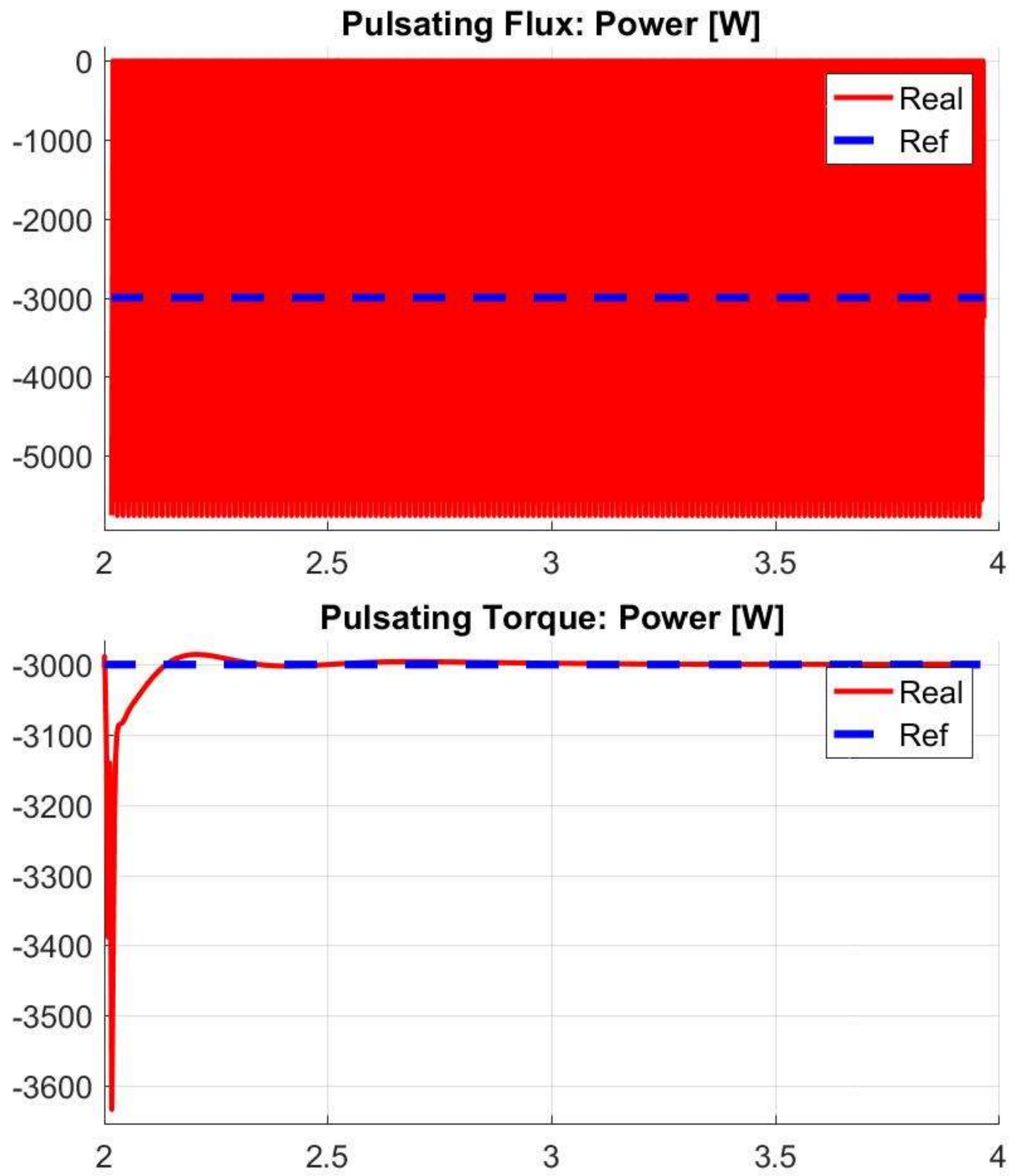

Figure 9.5-2 Accelerating Setpoint: Rotor Power

9.5.3 Accelerating Setpoint: Stator Currents and Voltages

Since the power and velocity don’t show any anomalous behaviour is expected to not have strange paths, and so it is.

In particular, we can point out that, in the pulsating flux solution, d_1 continues to oscillates to transmit power while q_1 tracks the 0 reference.

On the contrary, the pulsating torque control, request for some q component current since even the first harmonic contributes to produce torque.

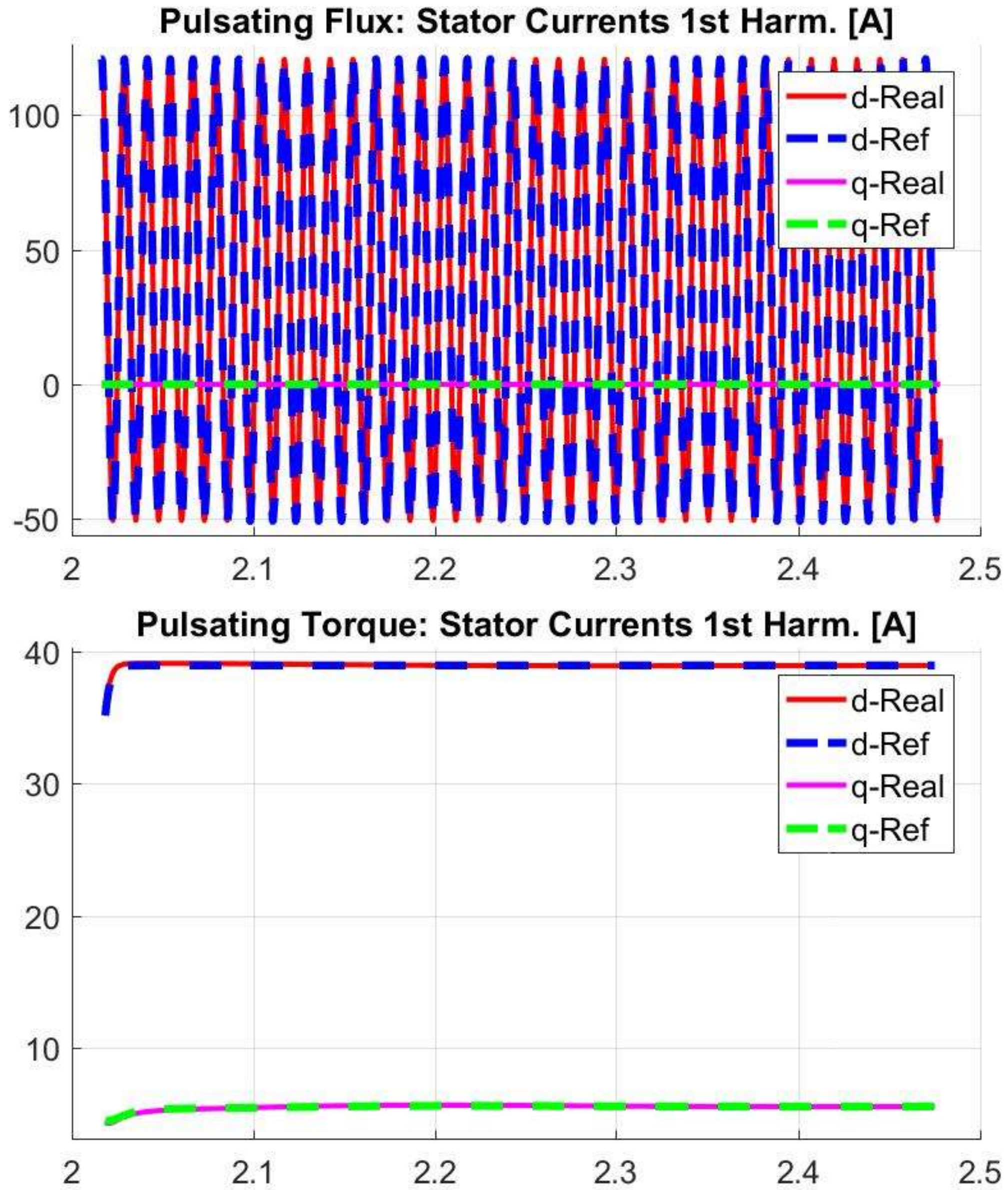

Figure 9.5-3 Accelerating Setpoint: Stator Currents 1st Harmonic

For what concerns the pulsating torque control similar consideration can be carried out for the third harmonic: the references are tracked without particular oscillations or error.

The same happens for the pulsating flux solution where, unlikely for the first harmonic, even the q component differs from 0 since this harmonic is in charge of produce the requested torque.

Finally, it has to be pointed out that, once again, the first solution requests currents that are even up to two orders of magnitude higher that the ones requested by the pulsating torque solution.

This is due once again due to the fact that the pulsating torque works with lower fluxes.

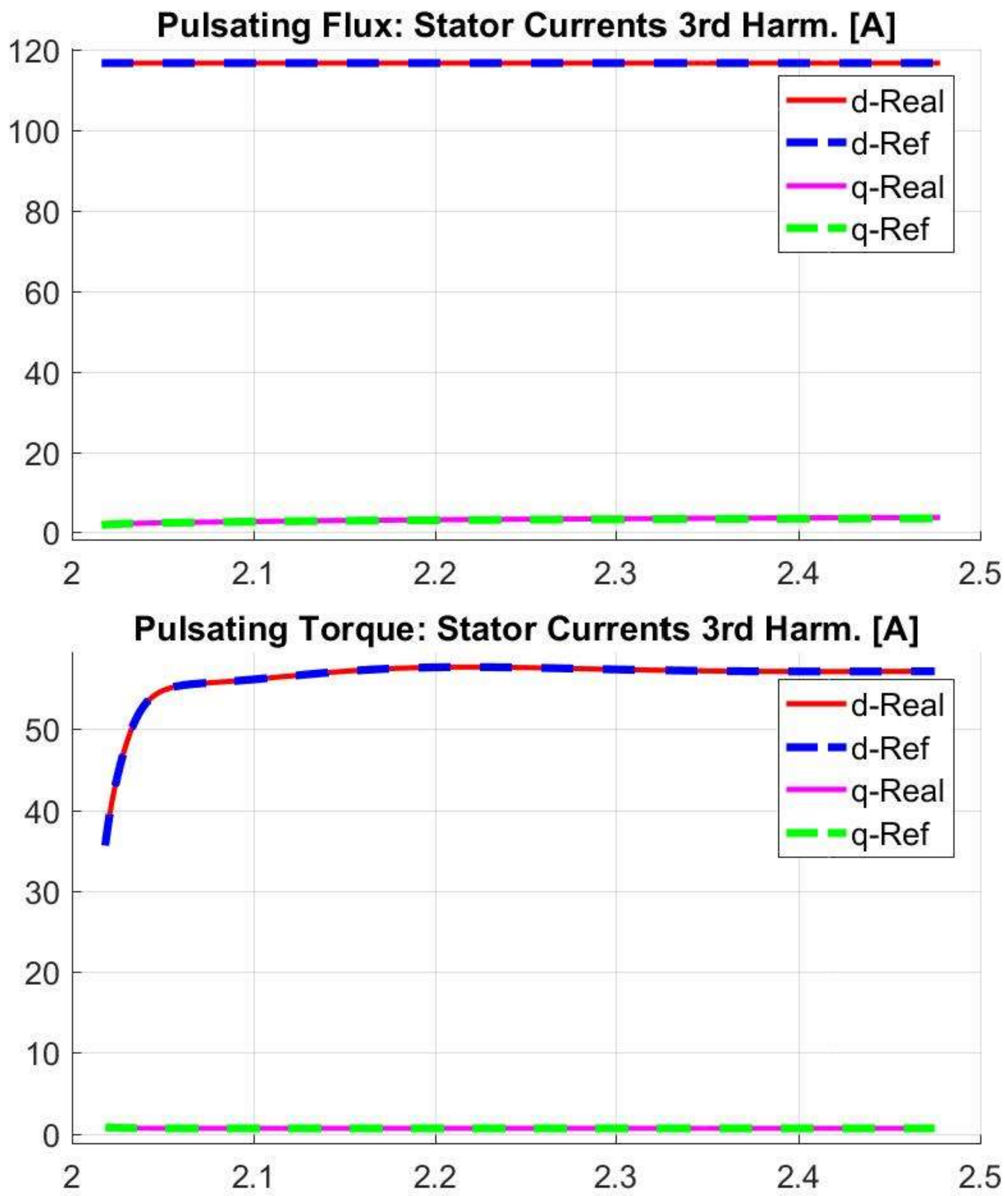

Figure 9.5-4 Accelerating Setpoint: Stator Currents 3rd Harmonic

On the contrary the requested voltages, as usual, are higher in the pulsating torque solution since the stator frequency is higher and so is the back emf.

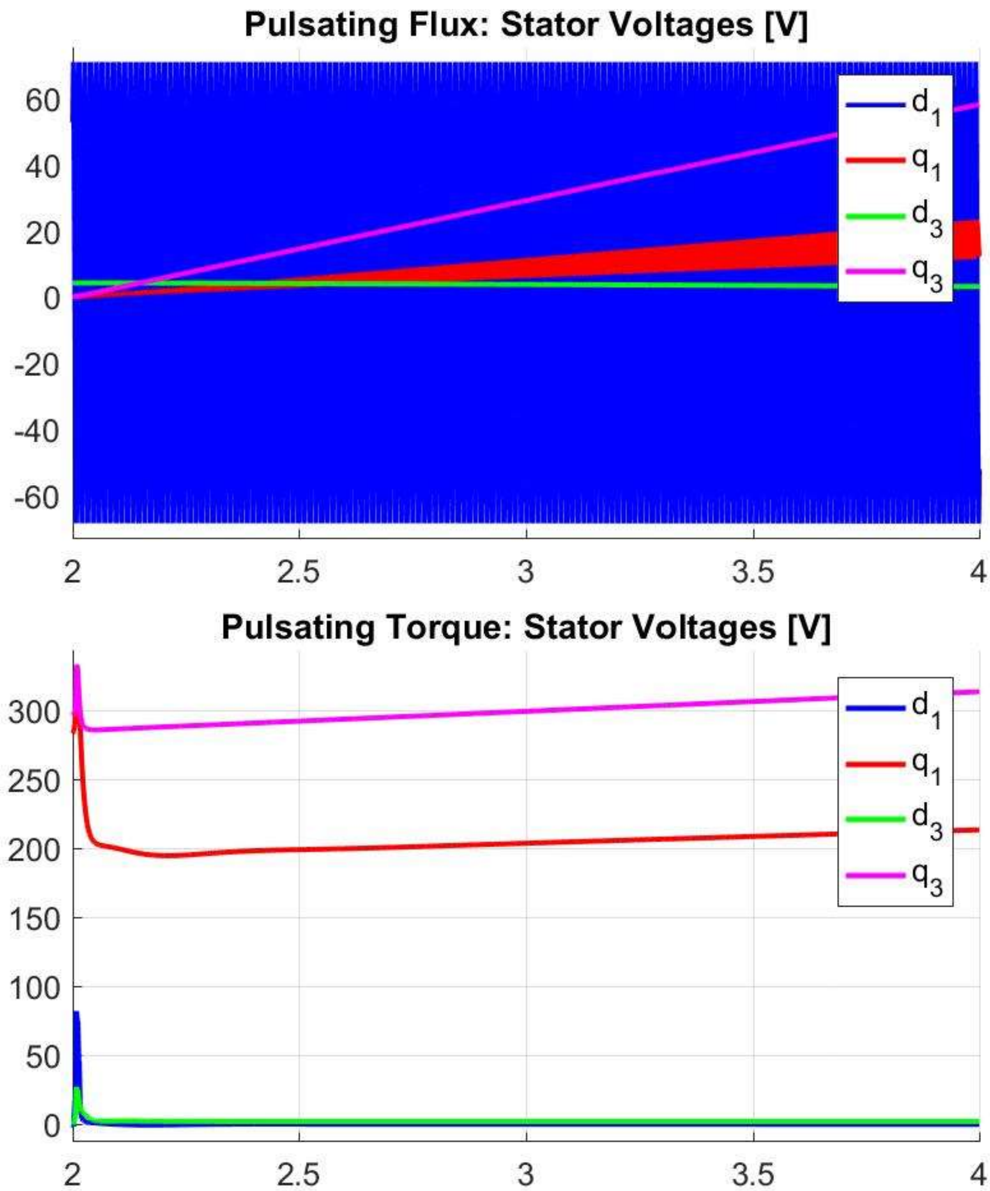

Figure 9.5-5 Accelerating Setpoint: Stator Voltages

9.5.4 Accelerating Setpoint: Rotor Flux

In this section, it is interesting to analyse the behaviour of the flux of the pulsating torque solution. In fact, since the torque request is quite high due to the acceleration requested, the flux can be increased without fear to saturate ω_0, that is the big problem connected to this solution: so the flux raises from $0.3Wb$ to $1Wb$ for what concerns the first harmonic.

The flux associated to the pulsating flux solution instead doesn't change behaviour respect the section before since the power request hasn't changed: just little oscillations come up on the increasing of the rotor speed.

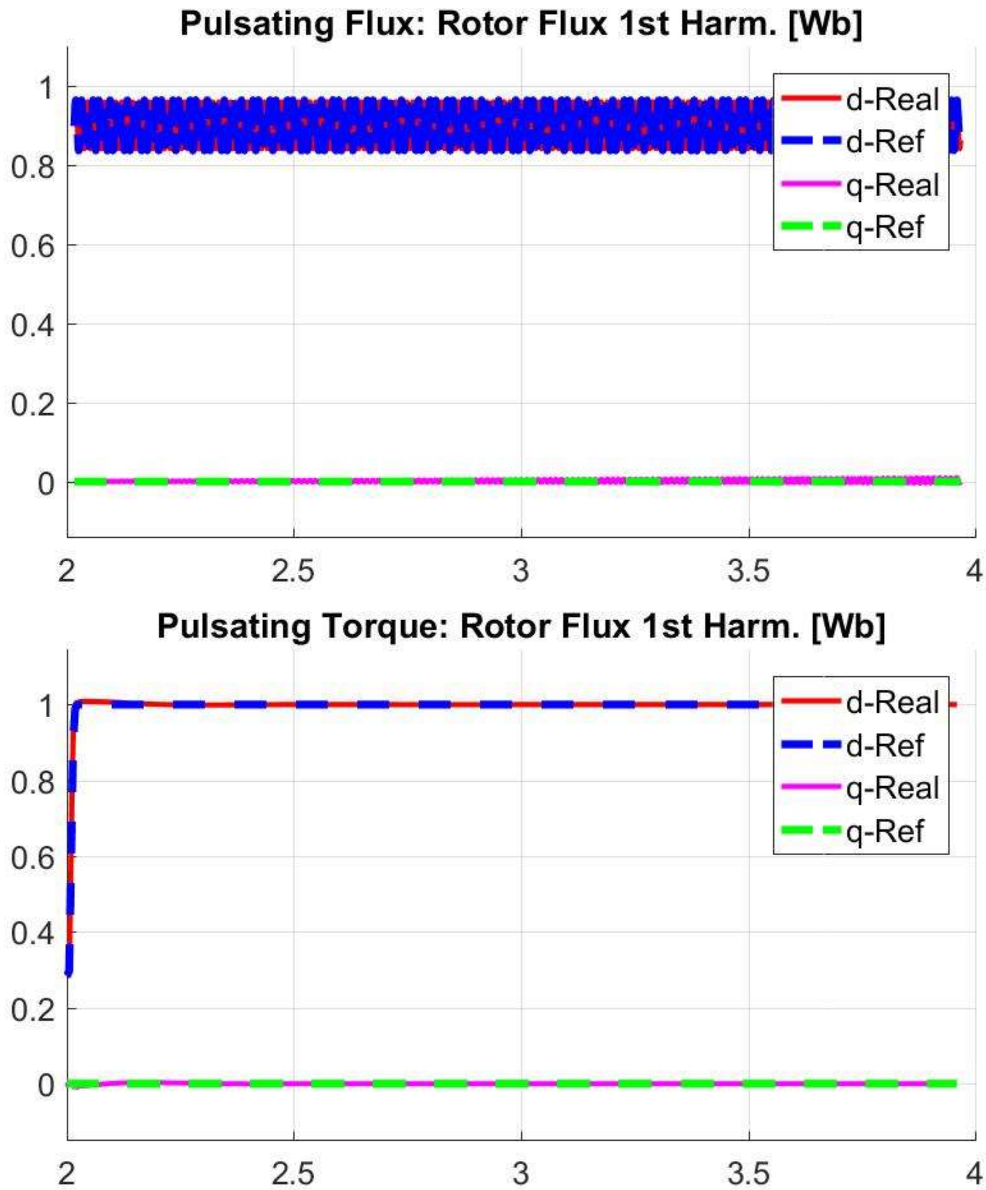

Figure 9.5-6 Accelerating Setpoint: Rotor Flux 1st Harmonic

For the pulsating torque control, similar argumentation can be carried out expect for the fact that the flux reference doesn't reach the nominal value since not enough torque is requested.

In the pulsating flux solution instead, the reference value doesn't change.

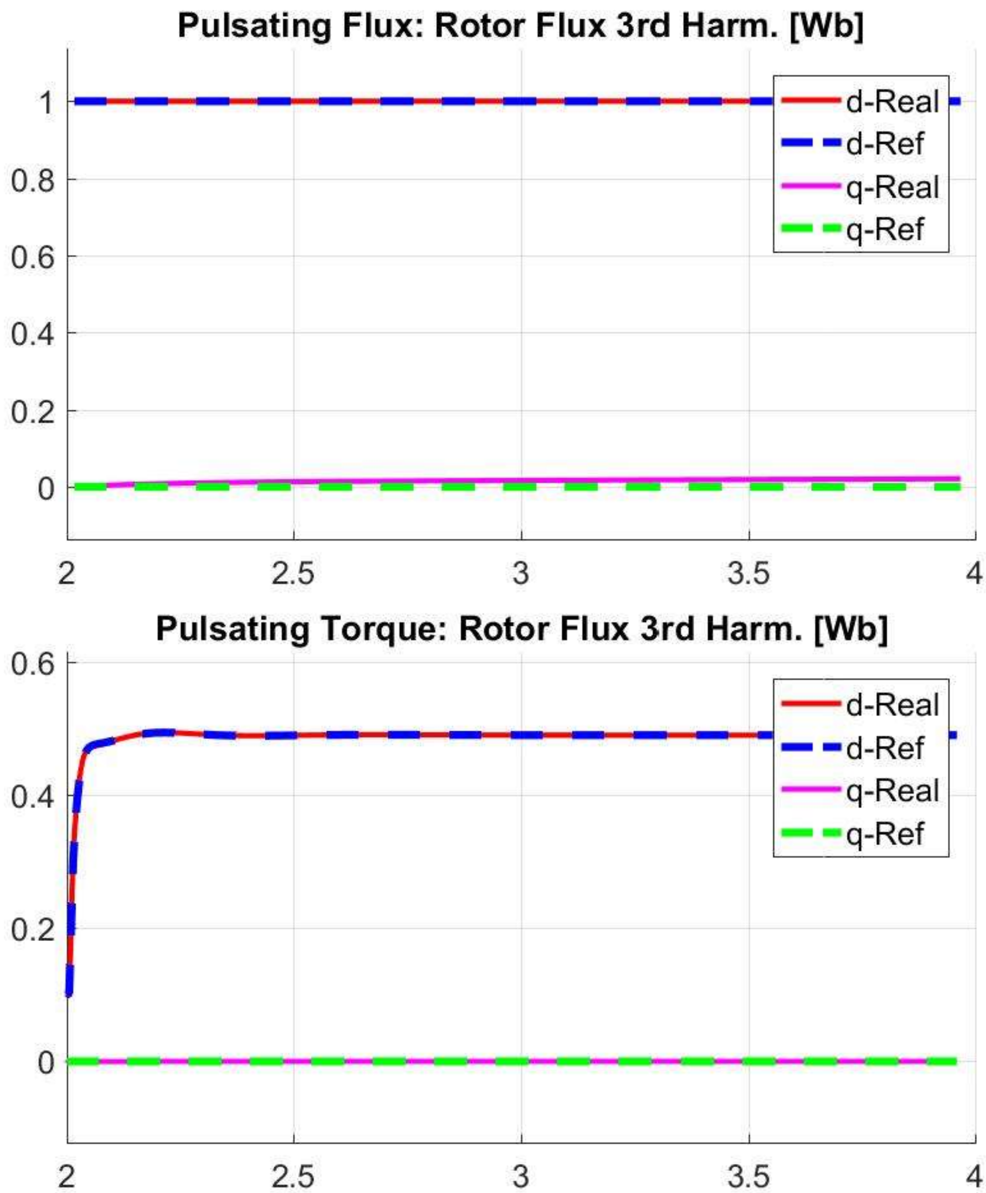

Figure 9.5-7 Accelerating Setpoint: Rotor Flux 3rd Harmonic

In both the controls technique and for both the harmonics the references are almost perfectly tracked.

9.5.5 Accelerating Setpoint: Rotor Currents and Voltages

The pulsating flux solution doesn't present a different behaviour respect the test section before.

Very different instead is the behaviour of the rotor currents in the pulsating torque solution that is directly connected to the flatness of the stator currents and rotor fluxes seen before. Even there no oscillations are present and the currents magnitude are very limited.

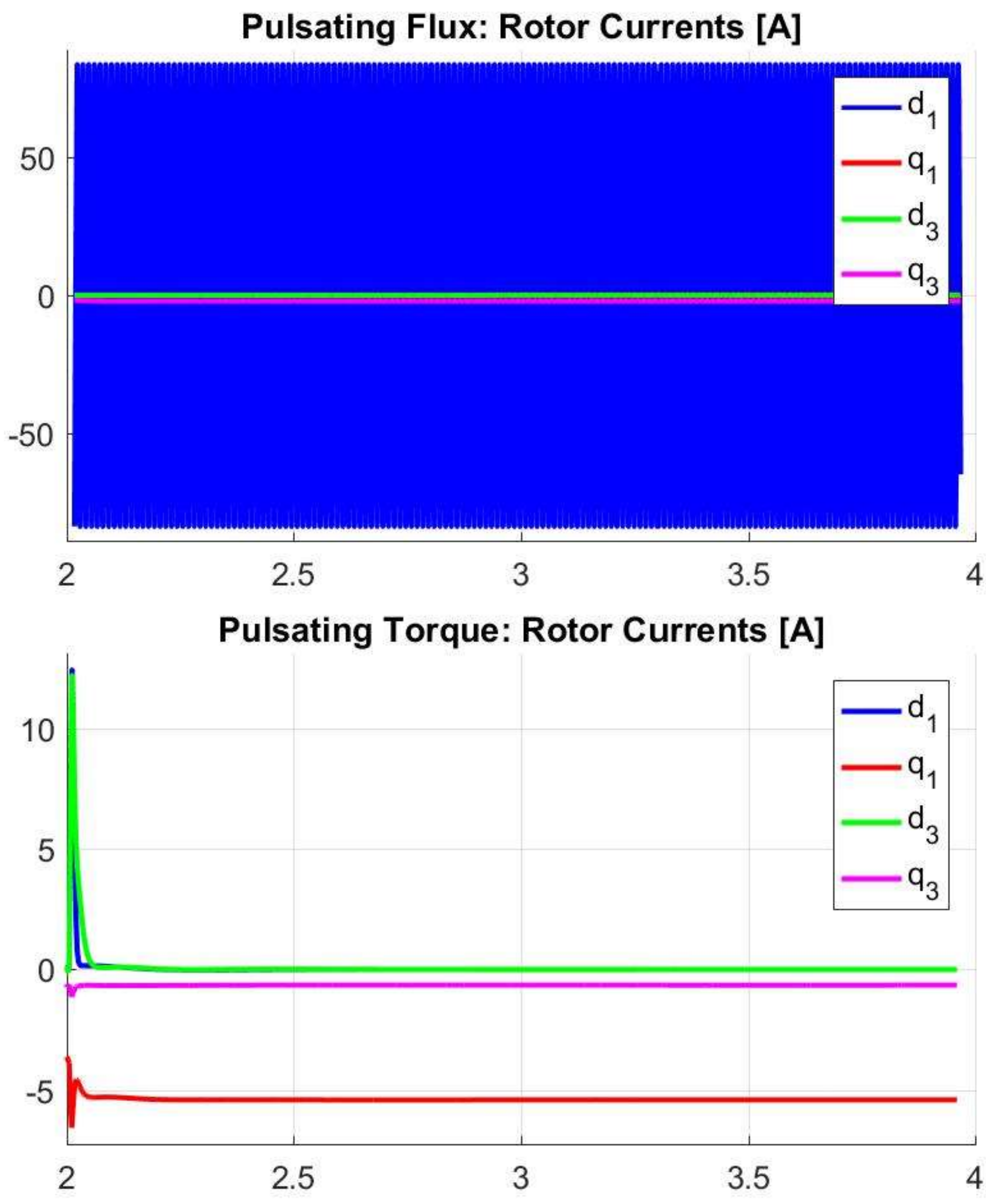

Figure 9.5-8 Accelerating Setpoint: Rotor Currents

In the pulsating flux solution, with respect to the rotor voltages, it can be seen that the oscillations that come out in the rotor flux have as counterpart, an oscillation of the voltage q_1.

More interesting are the voltages of the pulsating torque control: in fact, it is interesting that q_1 has a lower value respect the test part before: this is due to the fact that, since the flux is saturated to the nominal value of $1Wb$. This implies that the back emf is weaker and so less voltage is needed to inject the desired currents.

In any case the pulsating flux solution needs almost a tenth of the voltage of the pulsating torque one.

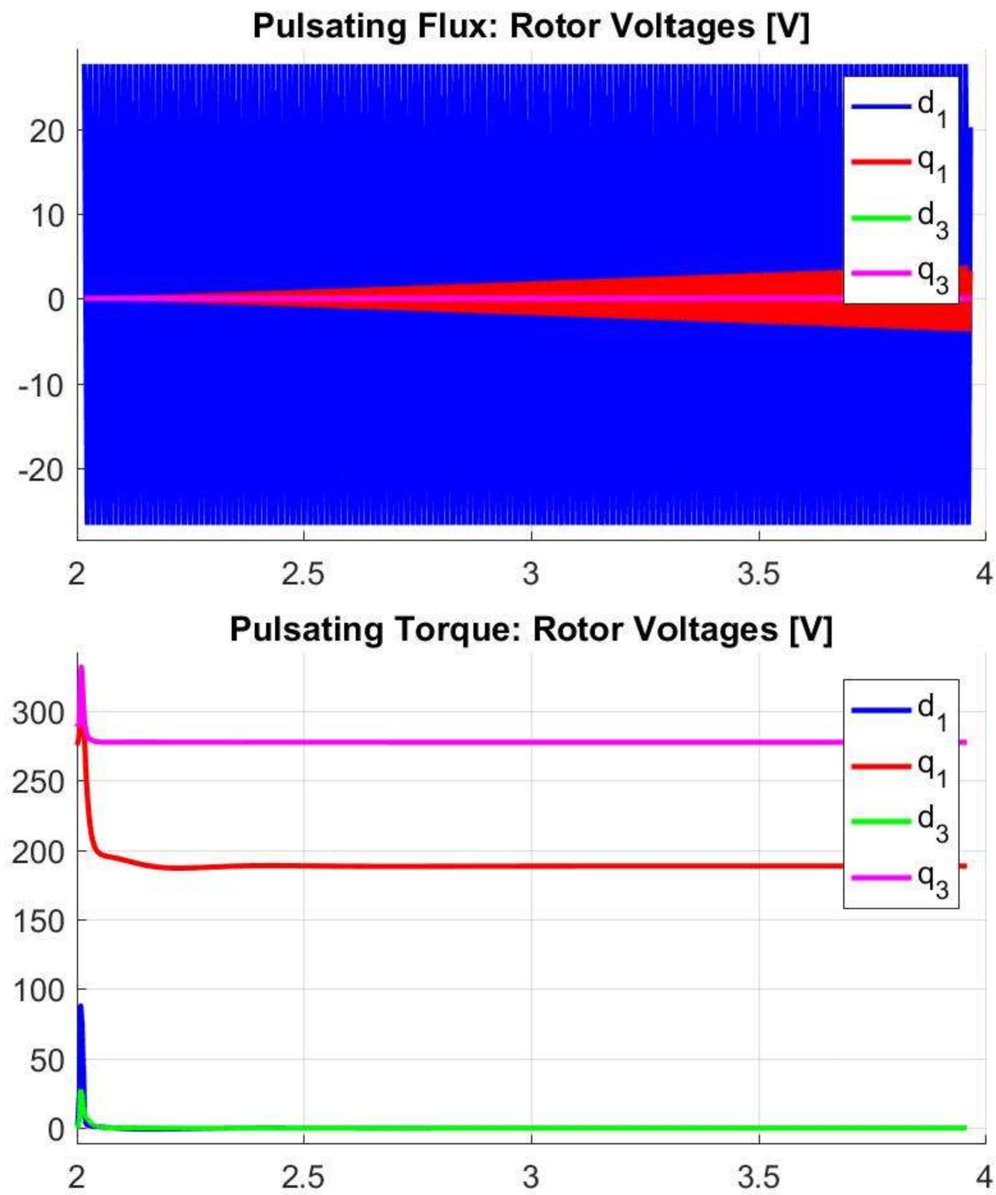

Figure 9.5-9 Accelerating Setpoint: Rotor Currents

9.6 Nominal Velocity Setpoint

In this section, the machine is asked to maintain the nominal speed of $60rpm$: the only torque requested is the one needed to compenstate the viscous friction.

9.6.1 Nominal Velocity Setpoint: Velocity

After the accelerating part, the rotor is asked to rotate to the nominal speed of $60rpm$. Note that no load torque is applied and so the pulsating torque control has to chopper the torque itself: as a consequence, obviously a ripple band appears, even if, as at the null velocity setpoint, is limited to one tenth of rpm.

Even in the pulsating flux control appears a little ripple band but that is due to the fact that, as seen before, the flux reference is not perfectly tracked and it has little oscillations.

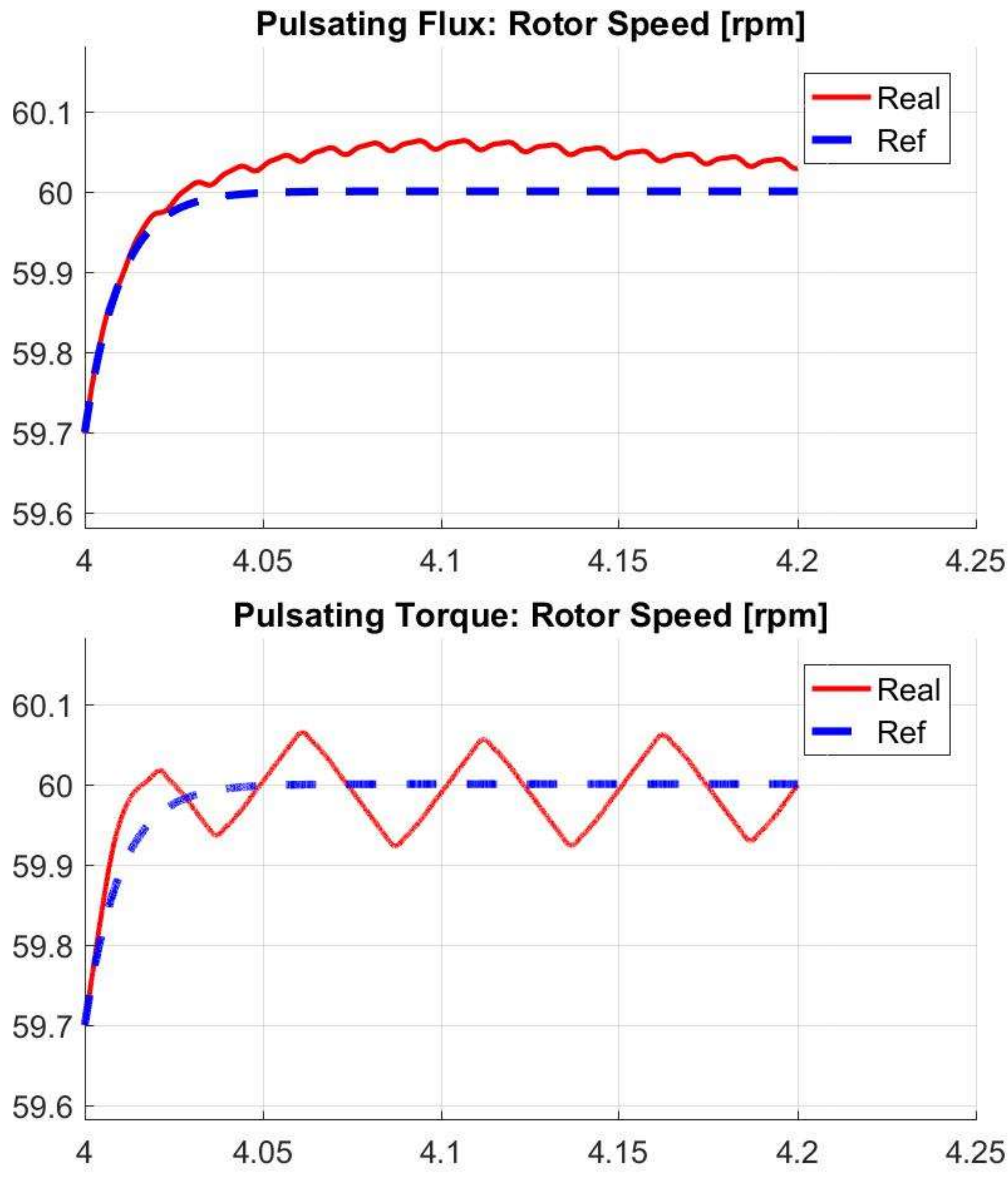

Figure 9.6-1 Nominal Velocity Setpoint: Rotor Speed

9.6.2 Nominal Velocity Setpoint: Power

For what concerns the power, it happens exactly what has been reported in paragraph 9.4.2: obviously in the pulsating flux the power is sinusoidal with mean value equal to $3kW$, the reference, while in the pulsating torque solution it stays exactly on the reference, once the transitory due to the torque inversion expires.

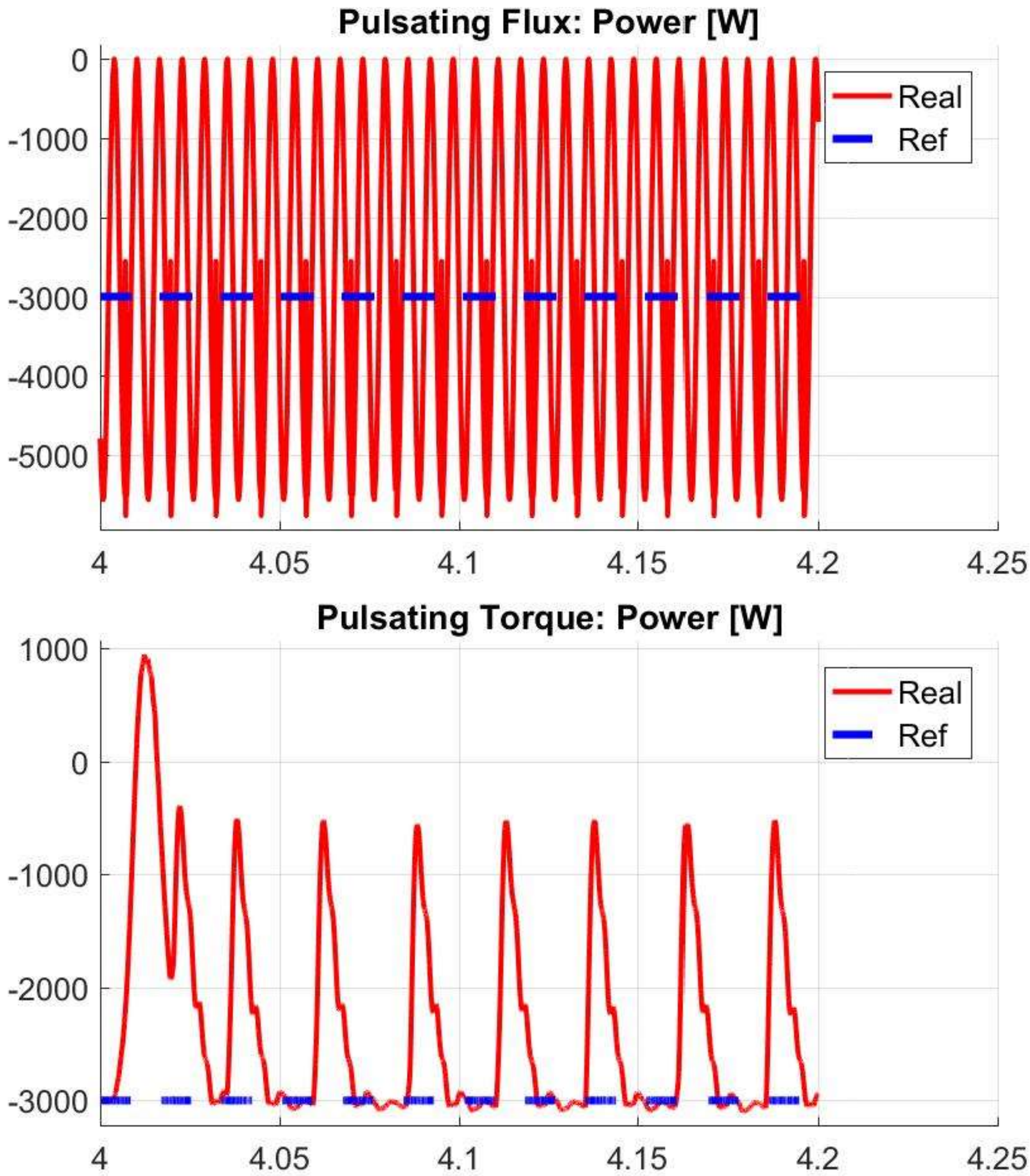

Figure 9.6-2 Accelerating Setpoint: Rotor Power

9.6.3 Nominal Velocity Setpoint: Stator Currents and Voltages

Nothing strange neither takes place in the stator current behaviour.

In particular in the pulsating flux solution the reference is perfectly tracked, while in the pulsating torque some little oscillations appear, even if they are bounded and vanishing.

Once again it has to be pointed out how much the stator currents are bigger using the pulsating flux control.

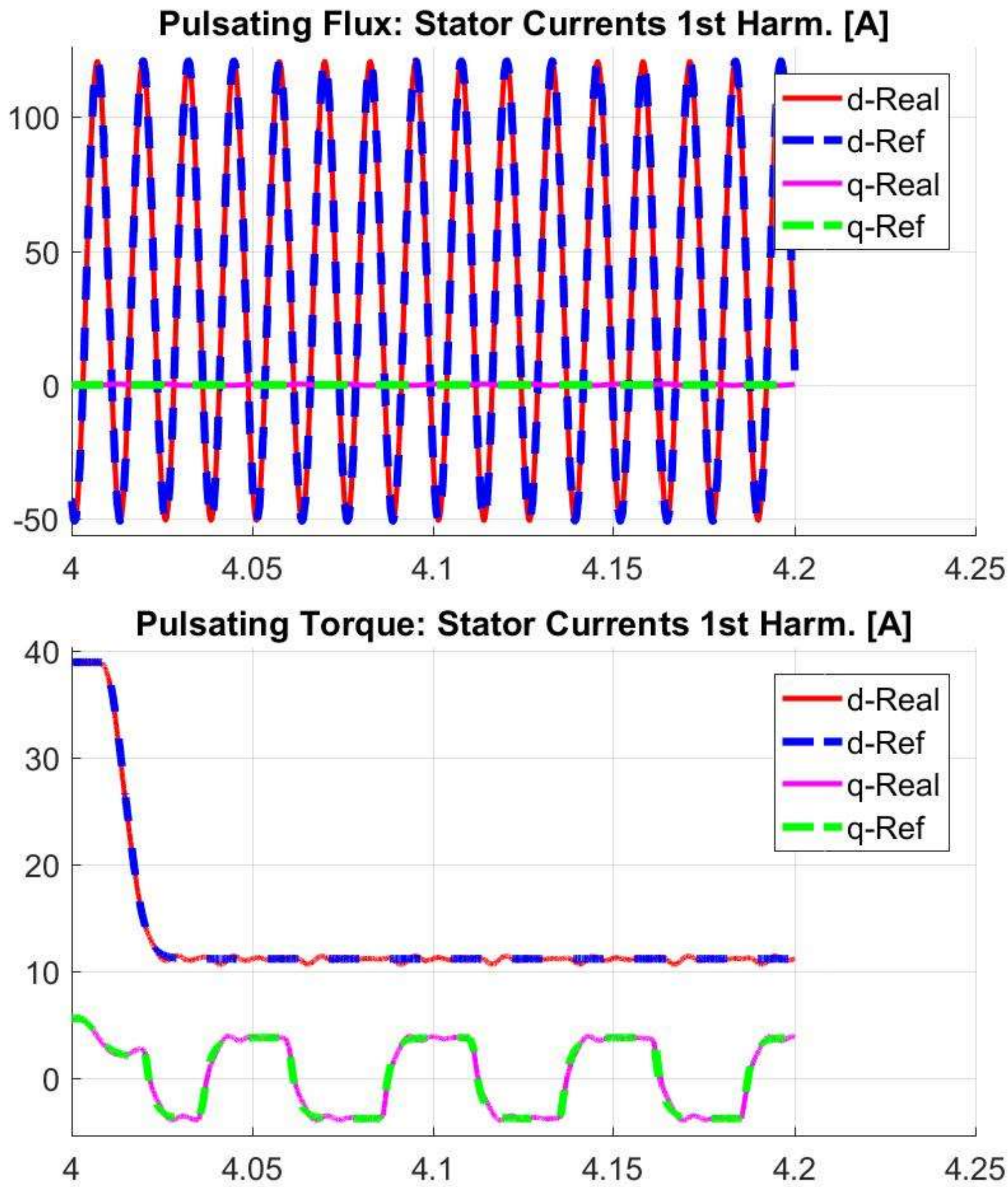

Figure 9.6-3 Nominal Velocity Setpoint: Stator Currents 1st Harmonic

As always, the third hamonic of the stator current in the pulsating torque has a really high d component since it is necessary to magnetize the rotor, while q is almost 0 since in this condition the only torque that must be produced is necessary to compensate the viscous friction.

Instead the pulsating torque control has much smaller currents, but with quite important oscillations.

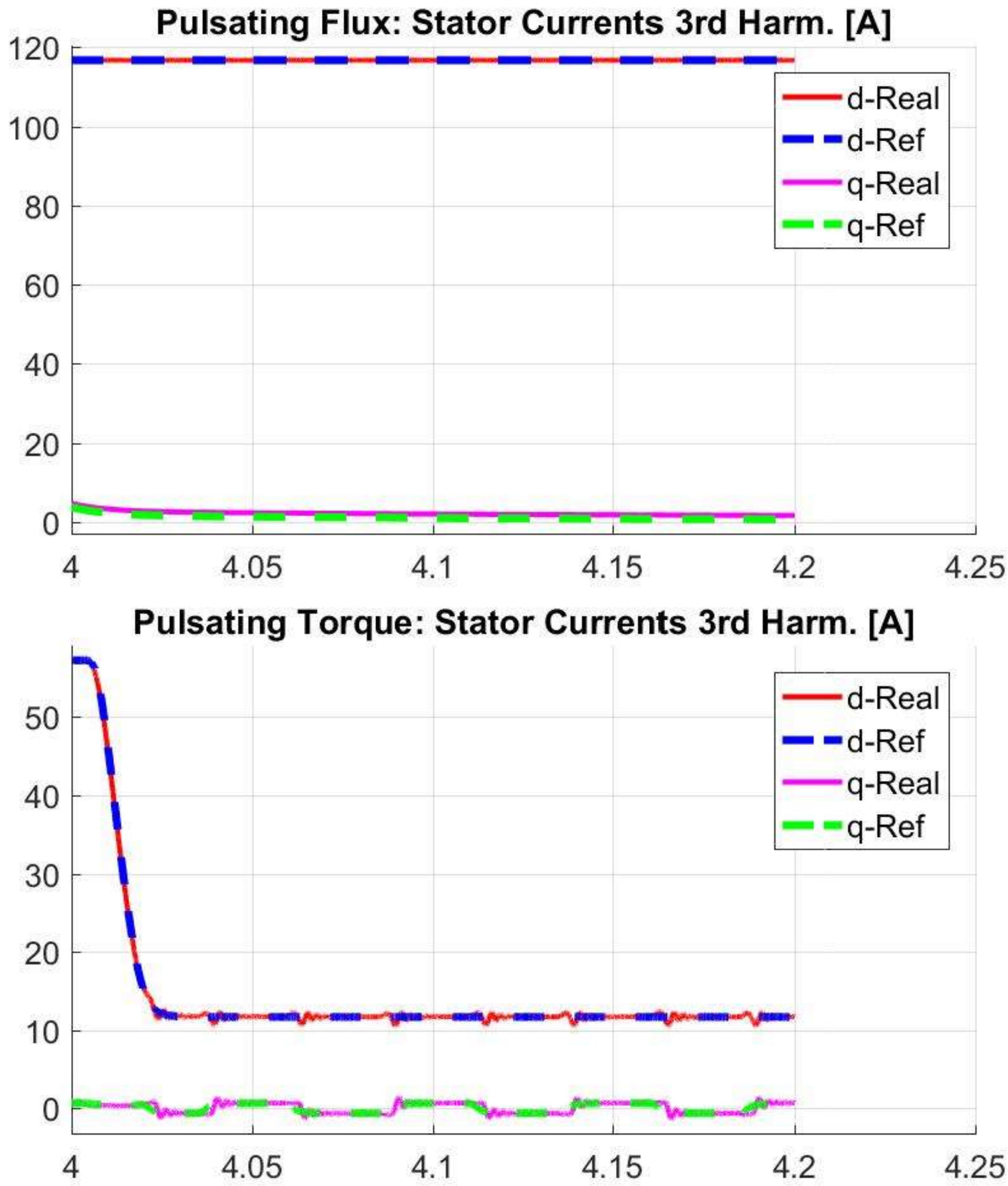

Figure 9.6-4 Nominal Velocity Setpoint: Stator Currents 3rd Harmonic

Since no load is applied and so the torque that must be produce is almost 0, the pulsating torque control has a really big back emf to be compensated since the stator frequency ω_0, is very high.

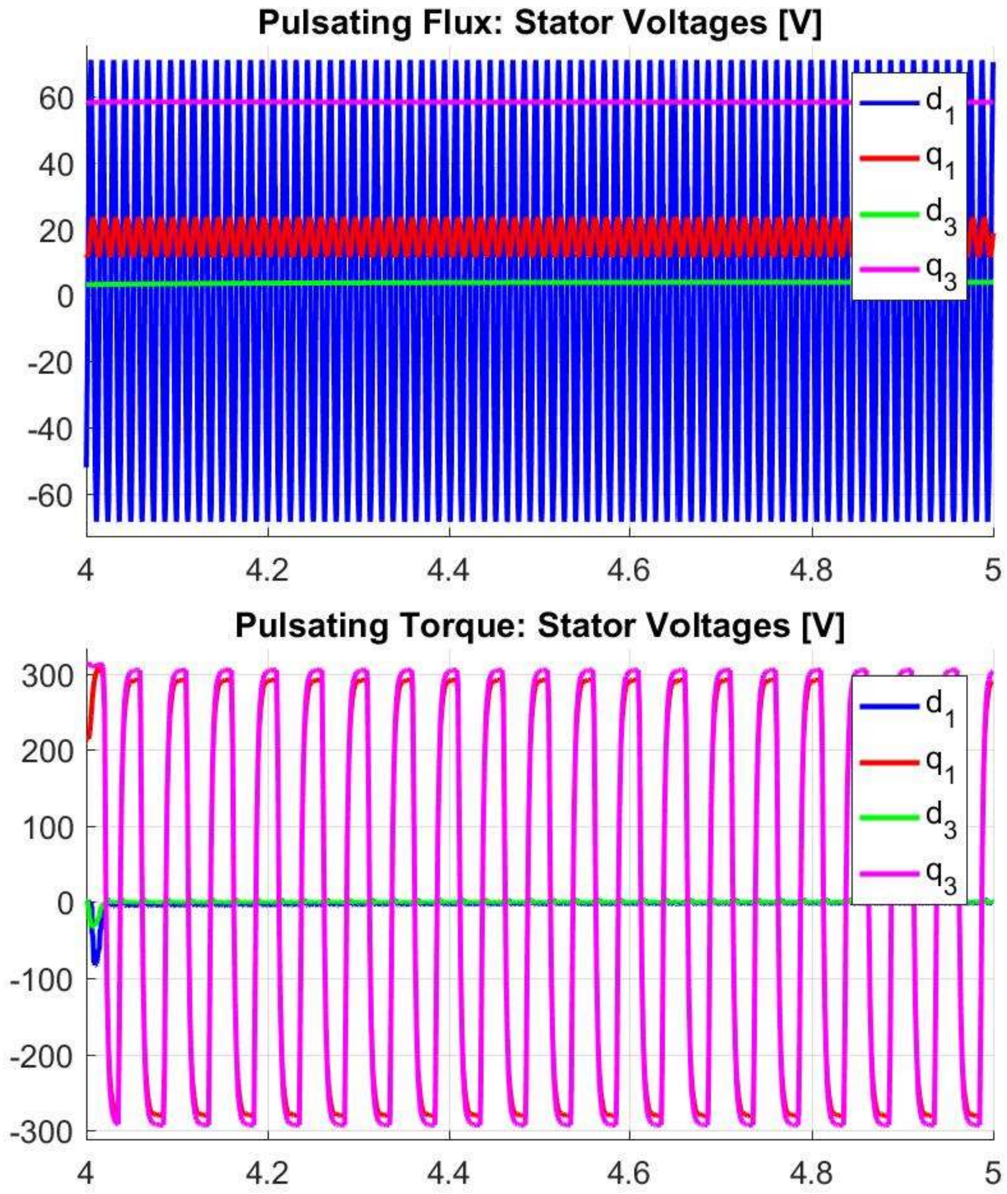

Figure 9.6-5 Nominal Velocity Setpoint: Stator Currents 1st Harmonic

9.6.4 Nominal Velocity Setpoint: Rotor Flux

For what concerns the first harmonic in the pulsating flux control it continues to have a good tracking of the sinusoidal reference. It has just to be pointed out a little disturbance on the q component that oscillates of some mWb around the reference.

Interesting is instead the behaviour of the flux in the pulsating torque solution: as first thing, it appears that the flux is reduced. This is done by the control to reduce the back emf since, seen that the torque needed to maintain the nominal velocity is quite small (and so ω_0 is huge).

Again some little oscillations are present when the torque changes sign.

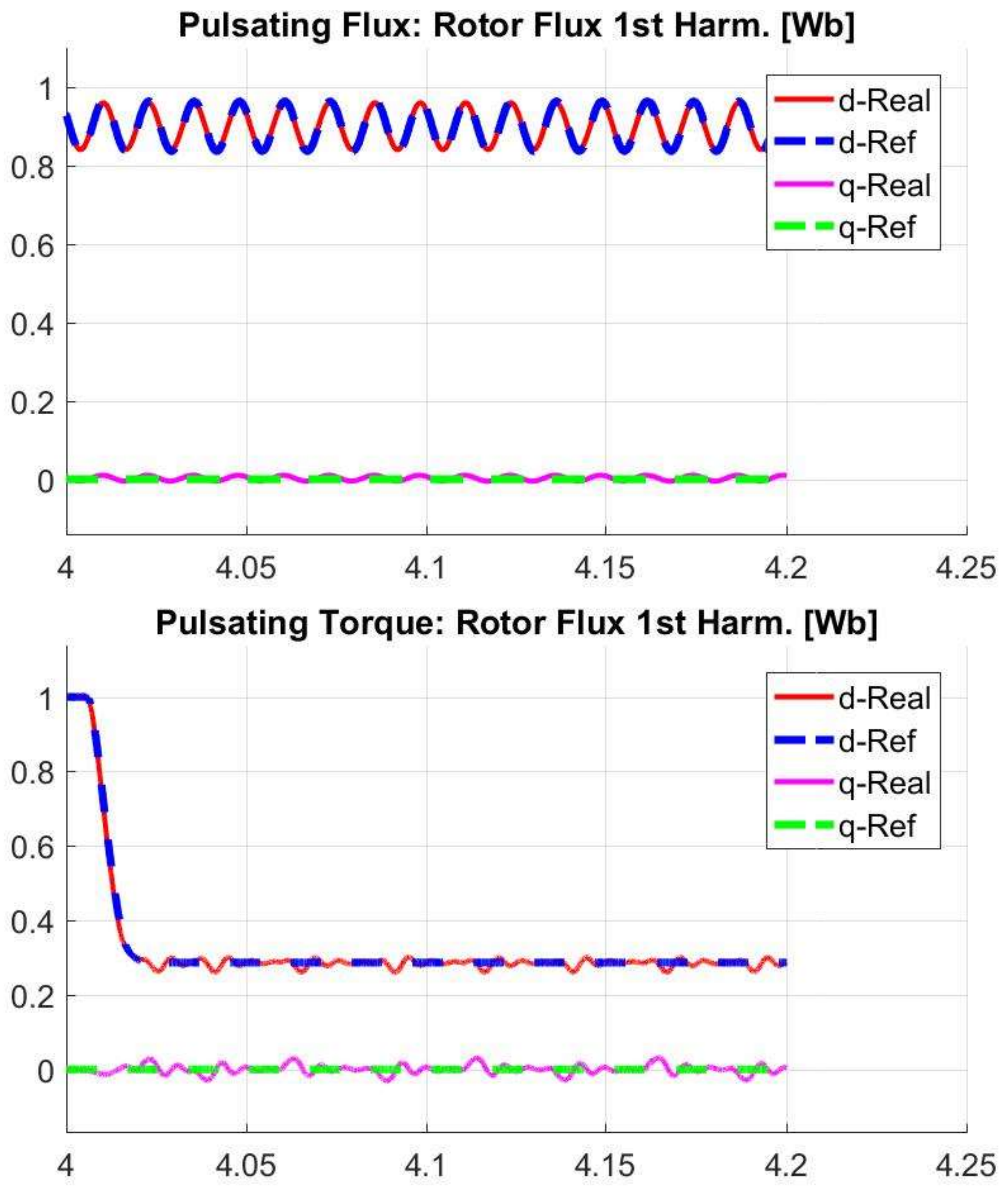

Figure 9.6-6 Nominal Velocity Setpoint: Rotor Flux 1st Harmonic

For the third harmonic of the flux in the pulsating torque control similar consideration can be carried out.

For what instead concerns the pulsating flux solution the nominal flux is maintained.

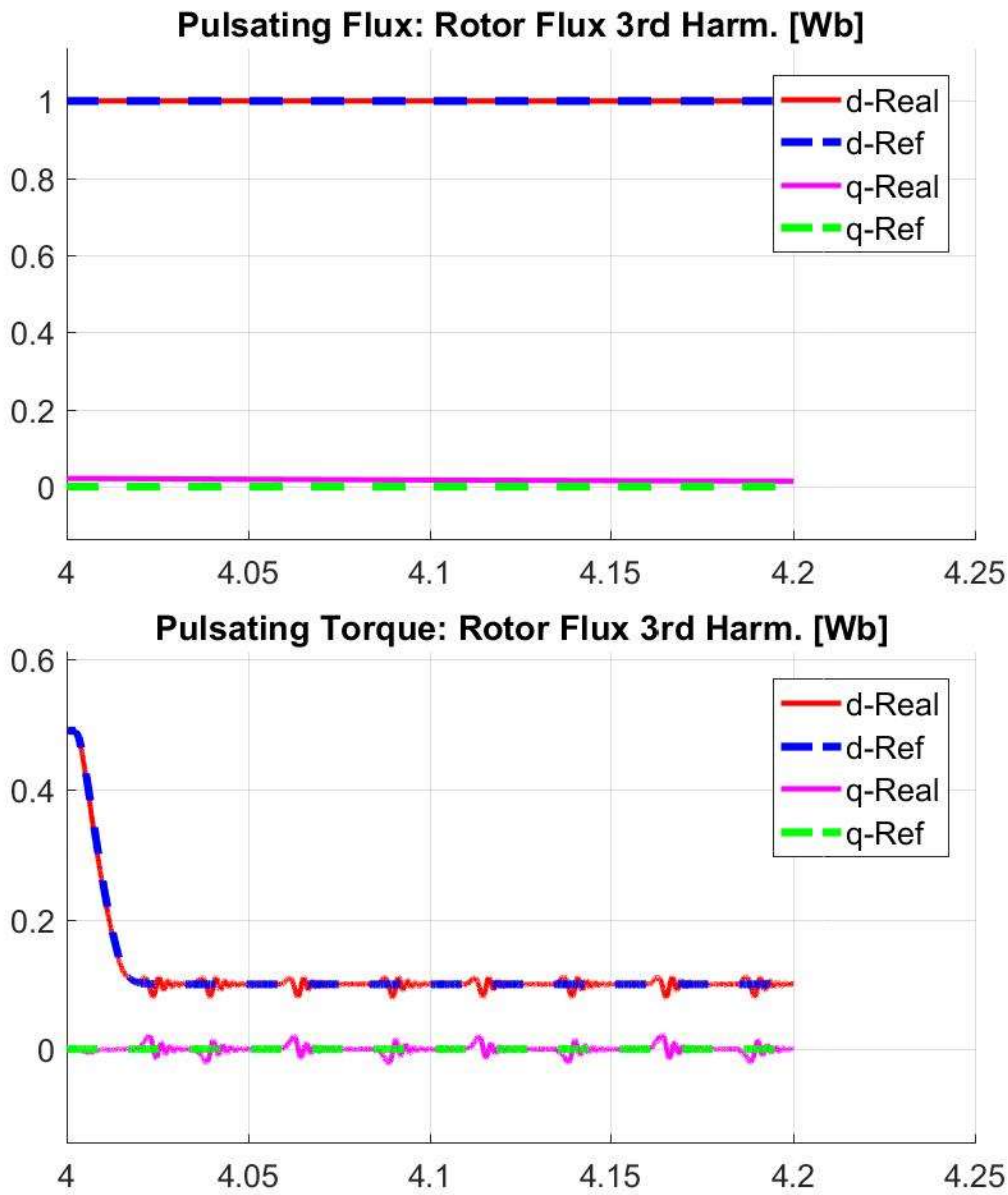

Figure 9.6-7 Nominal Velocity Setpoint: Rotor Flux 1st Harmonic

9.6.5 Nominal Velocity Setpoint: Rotor Currents and Voltages

In the pulsating torque control the decreasing of the flux can be also pointed out by means of the decrease of the d component of both the first and third harmonic: after, as the flux, it stabilizes around the steady state value, around with it oscillates a little when the torque is inverted.

For what concerns the pulsating flux solution instead the only relevant current is the d of the first harmonic that is in charge of transmitting the power.

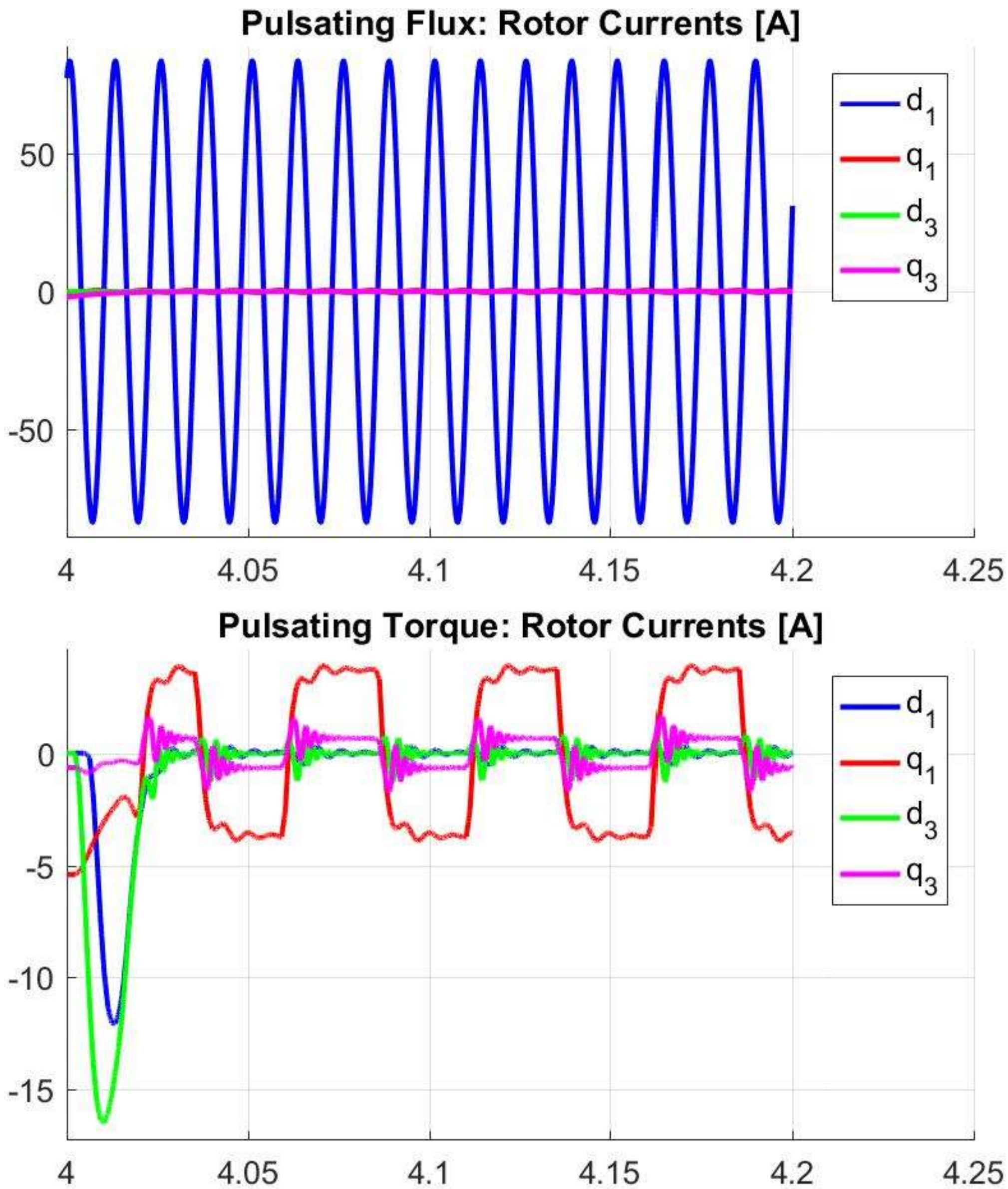

Figure 9.6-8 Nominal Velocity Setpoint: Rotor Currents

As in the null velocity setpoint the voltages of the pulsating torque solution are much greater since ω_0, and so the back emf, is bigger respect the pulsating flux control.

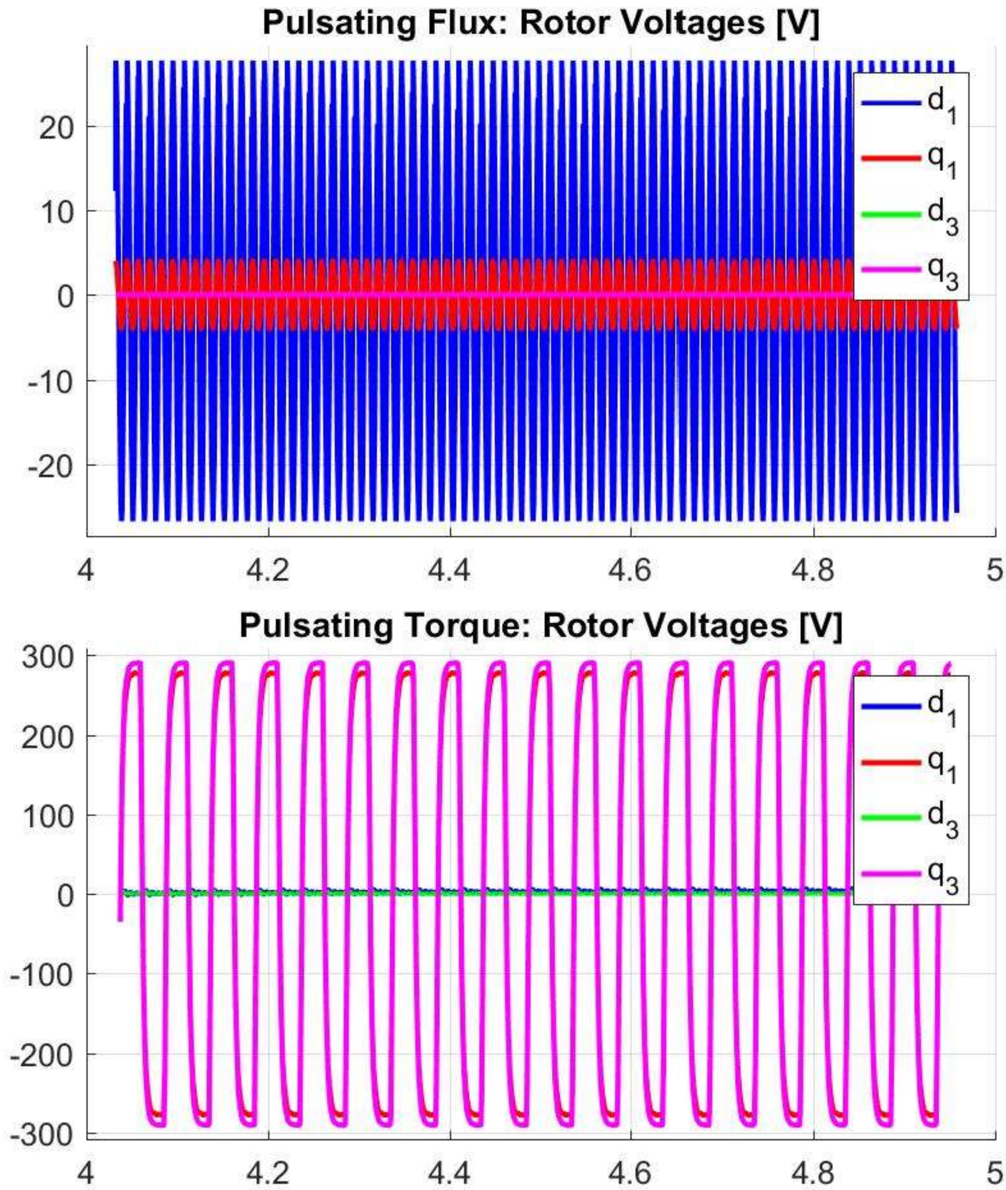

Figure 9.6-9 Nominal Velocity Setpoint: Rotor Voltages

9.7 DC-link Dimensioning

A crucial information to make the decision of which control apply for the doubly fed machine is the dimensioning of the DC-link. In the DC-link in particular is present a capacitor whose role is to smooth the choppering effects of the active rectifier and to supply the rotor devices.

The good dimensioning of this capacitance is fundamental to provide a good behaviour of the DC-bus voltage that must be as flat as possible.

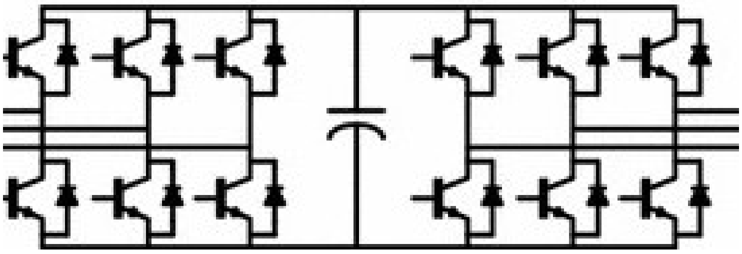

Figure 9.7-1 DC-link scheme

It is well known that the energy E stored in a capacitor is proportional to both the charge Q stored and the voltage between the armatures V.

$$E = \frac{1}{2} QV \qquad \textit{Eq. 215}$$

The fundamental equation that defines the capacitance is

$$C = \frac{Q}{V} \qquad \textit{Eq. 216}$$

Substituting it in the previous equation it is possible to show that

$$E = \frac{1}{2} CV^2 \qquad \textit{Eq. 217}$$

Now let's focus for a while on E and in particular on its variation: it is well known that it can be represented as

$$\Delta E = \int P_C dt \qquad \textit{Eq. 218}$$

Where P_C is the power flowing in the capacitance. This quantity is obviously related to the power P_r coming from the active rectifier, and so from the DFIM rotor and the power P_L absorbed by the load.

So it results

$$\Delta E = \int_{t1}^{t2} (P_r - P_L) dt = \frac{1}{2} C(V^2(t_2) - V^2(t_1)) \qquad \textit{Eq. 219}$$

Let's assume the power needed by the electrical load as constant to the reference value of $3kW$.

For what concerns the pulsating flux solutions, since has been shown that the references are well tracked, analytical solution can be found out. In particular has been shown in section 5.1 that the power delivered has, assuming a reference equal the need of the load, to m an expression like

$$P_r = P_L \frac{1 + \cos 2\overline{\omega} t}{2} \qquad \textit{Eq. 220}$$

Where $\overline{\omega}$ is in our simulations $500\ rad/s$: this implies that P_r has period

$$T_{P_r} = \frac{2\pi}{2 * 500} = 6{,}3ms \qquad \textit{Eq. 221}$$

Let's point out now that the maximum negative difference from the reference voltage happens at half the period, when ends the upper part of the cosine.

So the missing energy results to be

$$\Delta E = \int (P_r - P_L) dt = P_L \int_0^{\frac{\pi}{2\overline{\omega}}} \left(\frac{1 + \cos 2\overline{\omega} t}{2} - 1 \right) dt \qquad \textit{Eq. 222}$$

Solving the integral comes out

$$\Delta E = -P_L \frac{\pi}{4\overline{\omega}} = -P_L \frac{T_{P_r}}{2} \qquad \textit{Eq. 223}$$

Substituting the proper values results

$$\Delta E = -9.42J \qquad \textit{Eq. 224}$$

Let's now assume that we don't want that the voltage oscillates more than the 1% respect the nominal value that we can assume of $600V$. So results that

$$\begin{gathered} V(t_1) = 600V \\ V(t_2) = 594V \end{gathered} \qquad \textit{Eq. 225}$$

It is so possible to dimension the capacitance with

$$C = \frac{2\Delta E}{V^2(t_2) - V^2(t_1)} = 2{,}6mF \qquad \textit{Eq. 226}$$

That appears to be a good and reasonable results: note that, being more tolerant about the voltage ripple, like for example the 3% or 5%, this capacitance could become even smaller than $1mF$.

For what concerns the pulsating torque solution, no analytical solution is easy to find out. Let's so measure the missing energy ΔE from a graph: for sake of simplicity let's assume that the real power has a triangular shape.

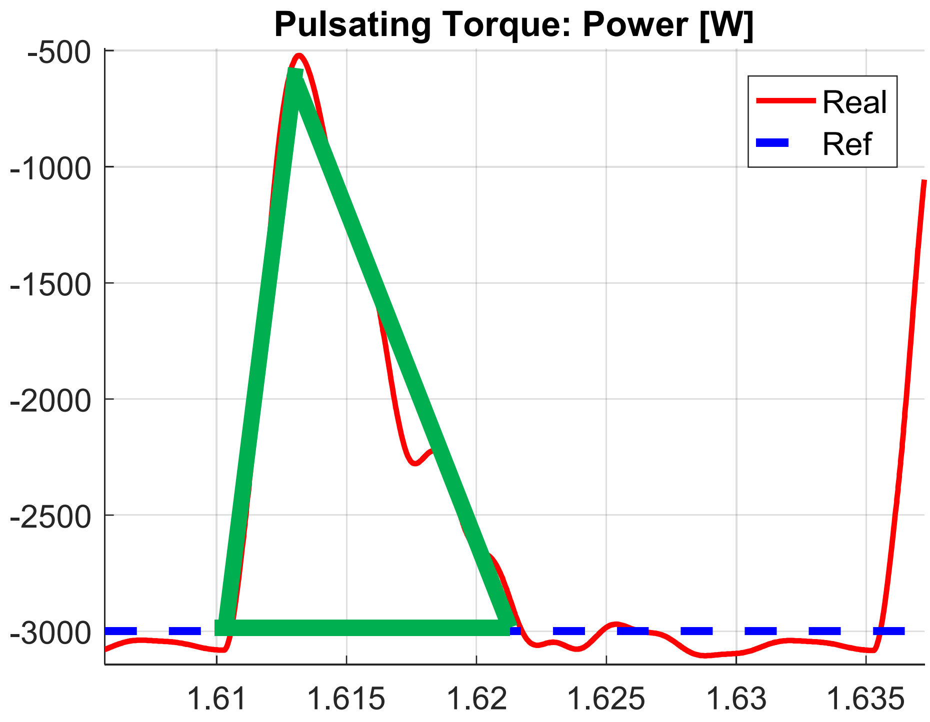

Figure 9.7-2 Pulsating Torque Power

Under this assumption, doing some approximative measurements on the graph it comes out

$$\Delta E = -12J \qquad \textit{Eq. 227}$$

And so the capacitance that is needed to satisfy the same requests as before is about

$$C = \frac{2\Delta E}{V^2(t_2) - V^2(t_1)} = 3{,}5mF \qquad \textit{Eq. 228}$$

9.8 Comparison Conclusions

Let’s now carry out some conclusion about this first comparison.

As a first remark, it has to be underlined that both the controls could be adapted for a three phase doubly fed induction motor, that could be cheaper than a five phase one. In particular let’s notice that the pulsating torque control should require less re-elaboration since that should consist in almost only in a change of parameters.

For what concerns the mechanical behaviour of the machine, it has been shown that the overall velocity reference is tracked almost perfectly by the pulsating flux solution while a ripple band appears in the pulsating torque control when the speed reference is constant or in any case the torque request is low.

This ripple band is quite small in our case and so could be acceptable: let’s notice that this derives from the assumption of a big carousel mounted on it that acts like a low pass filter on the torque. If we had assumed a much smaller inertial load the resultant ripple will increase up to unacceptable values; furthermore, a smaller load could invalid even the assumption of stiffness of the mechanical system and the pulsating torque could generate some, undesirable, oscillations.

For what concerns, instead, the sizing of the converters two aspects has to be taken in account: the DC-link and the current magnitude. About the first one it has been shown that there is not a big difference in the size of the capacitance that must be used in the rotor converter: furthermore, since commercial components will be used, probably the same capacitance bank will be used.

For what concerns the currents magnitude instead, it has been shown that the pulsating torque solution up to four times less current: this obviously could let to use cheaper and smaller electrical switches, likes IGBTS or MOSFET.

10 Comparison between the Pulsating Flux and the Independent Frequencies Solutions

10.1 Control and Task Description

In this chapter will be compared the simulative results obtained with the pulsating flux and the independent frequencies high level control that has been deeply explained in chapters 5 and 6.

Has low level control has been implemented, for the pulsating flux, the resonant controller with feedforward actions, while the simple PI, again with feedforward actions, has been shown to provide satisficing results for the independent frequencies control.

The task that is asked to the control to be accomplished is quite similar to the one shown in the previous chapter but with some differences.

As before is present an initial phase, that lasts $1s$, in which the machine is fluxed: in this phase, no power or torque is required and so the rotor should remain still and no electrical power flows from the stator to the rotor.

In the second place, is present a phase, of again $1s$, in which still no motion is required but the electrical power request rises up to the nominal value of $3kW$: this phase is very similar to the one proposed in the chapter before.

Since is an electrical load, it makes sense the model this request like a very steep slope: in fact, the electric domain has time constant that are typically very small and this justify the fact that any load absorb almost immediately the nominal power.

Quite different is instead the acceleration that is required as third phase of the test: here in fact the machine is requested to reach the nominal speed of $60rpm$ in just $0.5s$. This makes since it has to be shown that the machine is capable to reach high levels of torque to get high accelerations to get a fast start up of the machine. Still $3kW$ of electrical power is requested by the rotor to the stator.

Finally, the system is asked to maintain the nominal velocity while transmitting the same amount of power.

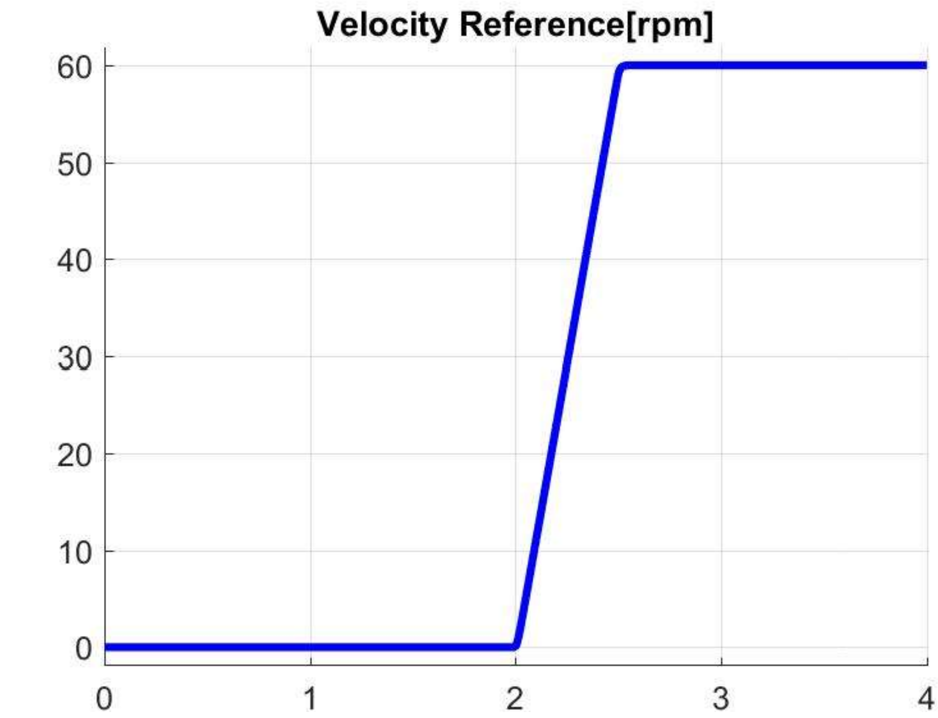

Figure 10.1-1 Velocity Reference

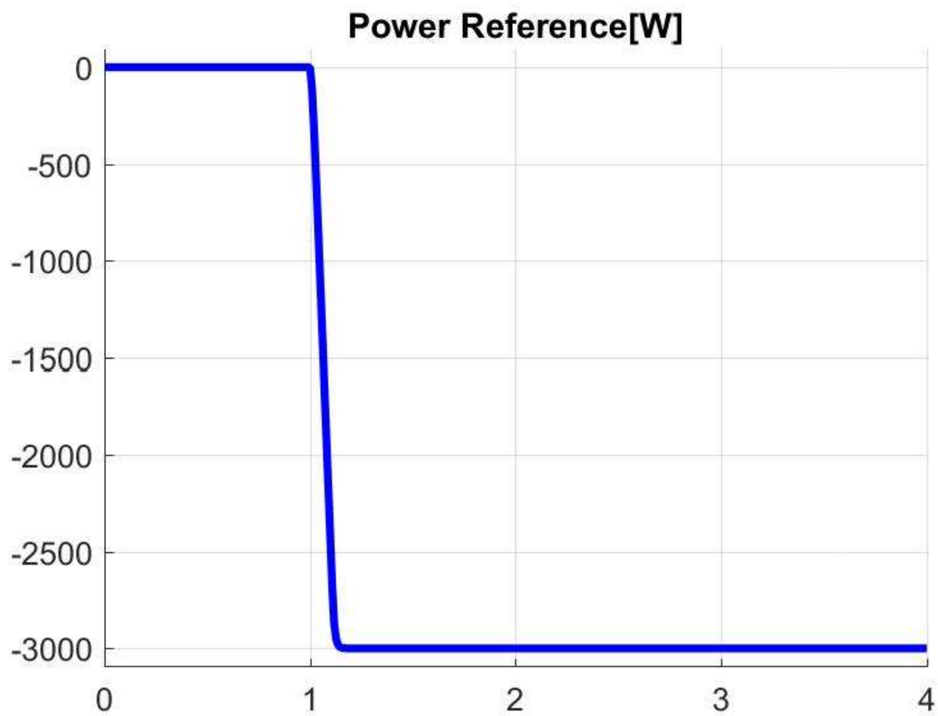

Figure 10.1-2 Power Reference

10.2 Velocity

As first thing, we will analyse the mechanical speed behaviour of the rotor under the two different controls.

As can be seen both the controls are capable to track almost perfectly the trajectory: that is due to the fact that both the high-level controls have the third harmonics that works just as a motor. The tracking is very good even during the acceleration grant to the feed forward action on the inertia that have been provided.

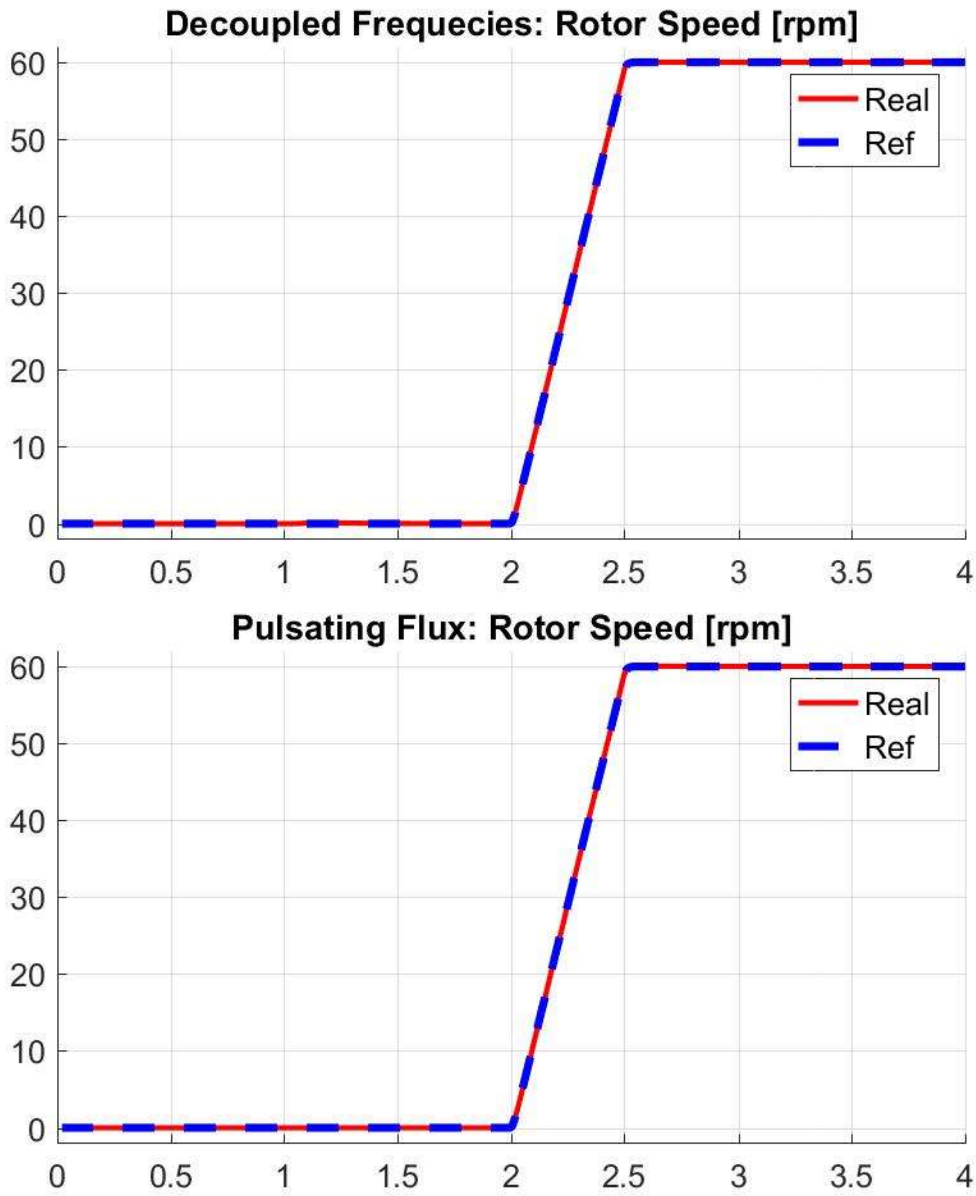

Figure 10.2-1 Rotor Speed

10.3 Power

The other critical overall point is the power request. Here it is possible to see how much the two algorithms works in a different way.

In facts, as expected, the decoupled frequencies control tracks immediately and at the exact value the power request. Just a little error in the tracking appears when the rotor starts moving and looks like it is proportional to the mechanical speed itself: this make sense since, even the coordinates transformation from $d - q$ to $abcde$ relies on the mechanical angle, that a discrete time system must assume constant during the sampling period.

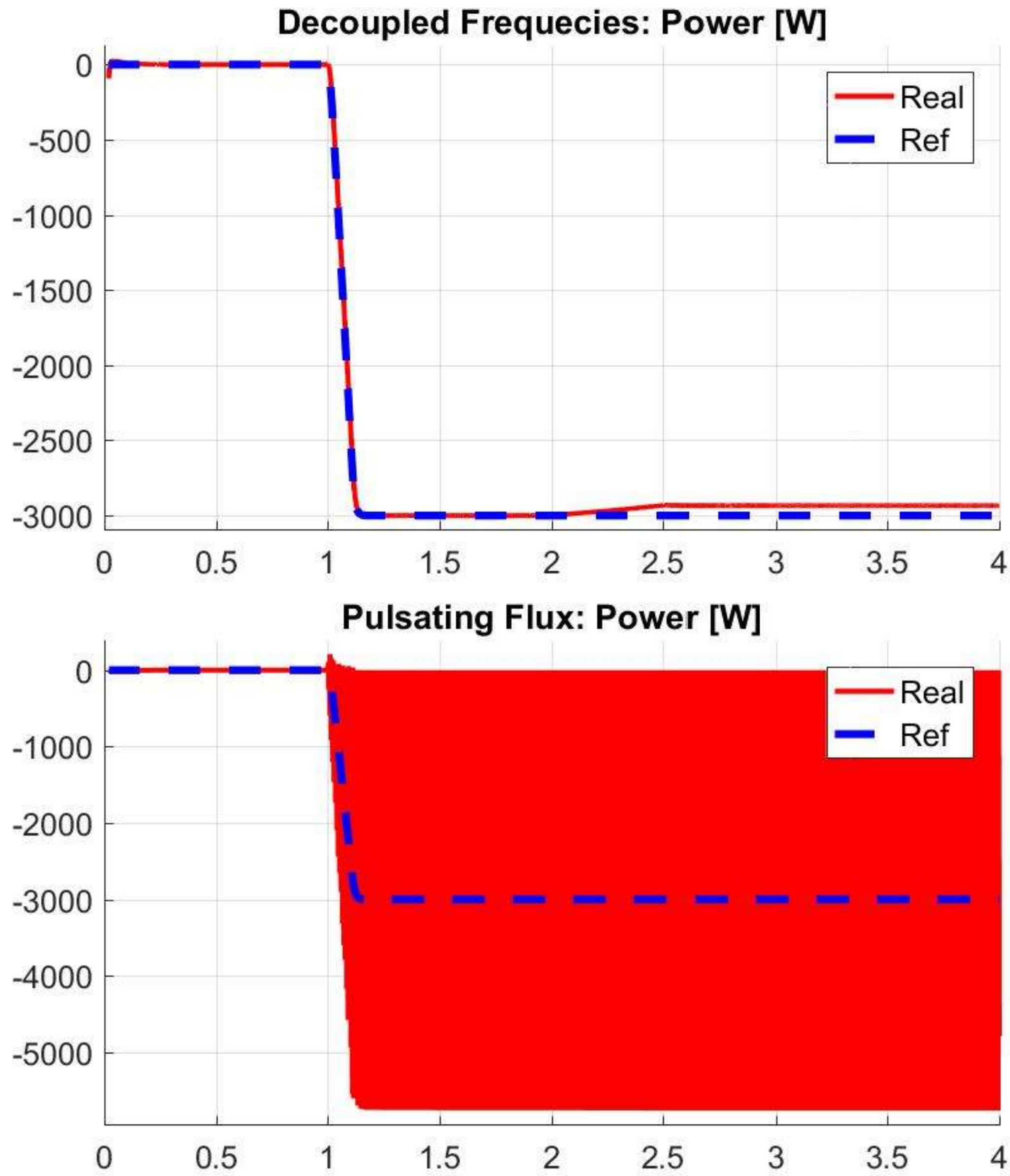

Figure 10.3-1 Power

A little tracking error is present even during the increment of the power request: this makes sense since the theory grants null error with constant references: in any case the error is very small to be negligible and can be easily coped by the control of the active front-end on the rotor side.

For what instead concerns the power in the oscillating flux solution, the transmitted power oscillates between 0 and the double of the request, so $6kW$.As in the comparison before, every two period of the power, and so every period of the flux, there is one spike due to the discretization of the angle.

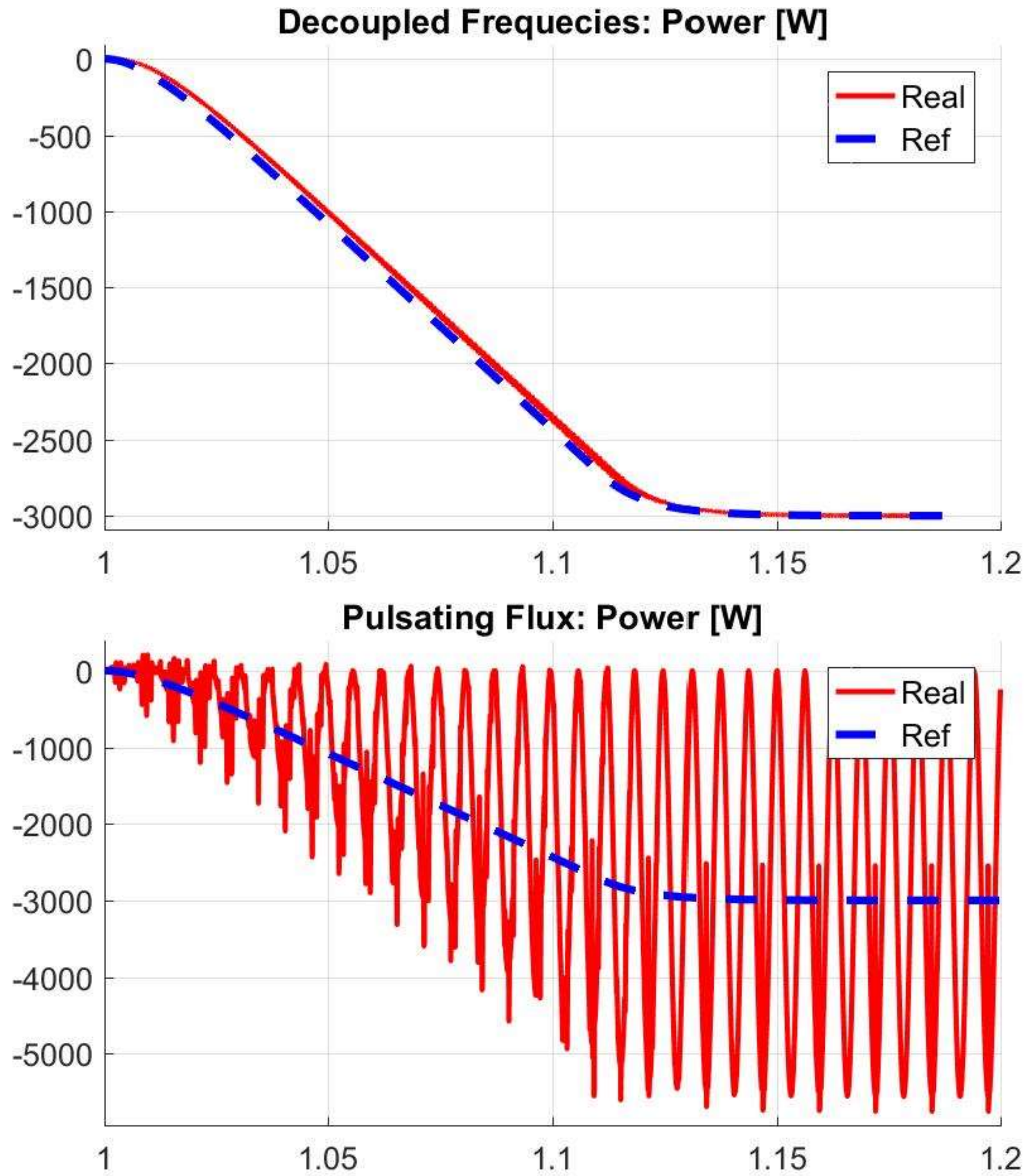

Figure 10.3-2 Power: zoom

10.4 Stator Currents and Voltages

The analysis of the stator currents is the most delicate one since it involves directly the torque produced by the machine.

For what concerns the first harmonic currents, as an overall view, it is possible to see that the magnitude is much lower in the decoupled frequency control. This is because the currents in the pulsating flux solution is in charge to change both the flux and its derivative.

Since the power transmitted is proportional to the amplitude of the oscillation, and since the machine is fluxed by the stator, the d component of the current starts to oscillates with an enlarging amplitude when the power request rises.

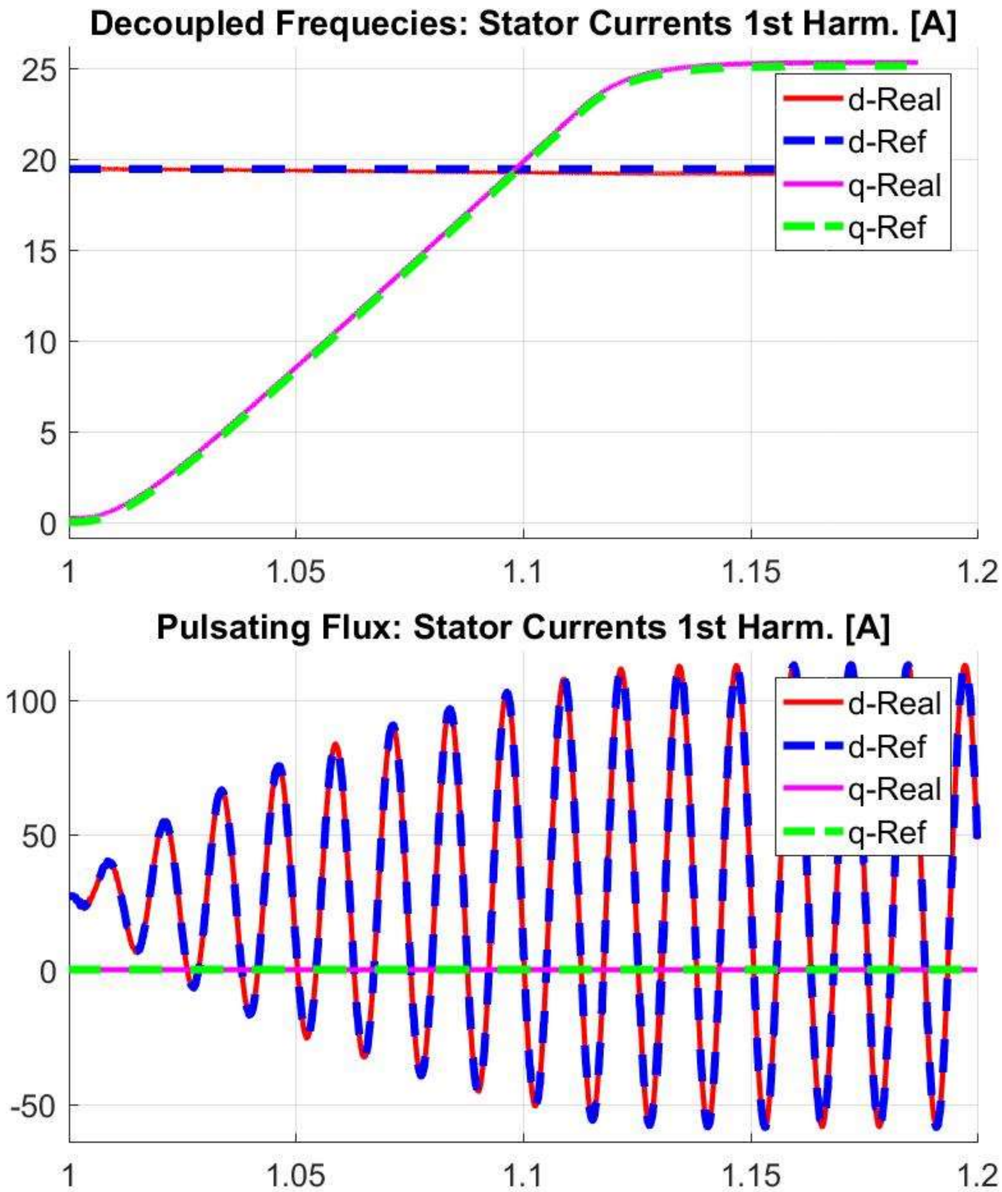

Figure 10.4-1 Stator Currents 1st Harmonic: zoom

Let's now focus on the q component of the current: as expected in the pulsating flux solution it remains equal to 0 since no torque is requested to the first harmonic in this solution.

It is interesting instead to analyse the behaviour of the q component in the independent frequencies control. During the fluxing phase (the first second), as expected it remains equal to 0.

After that, the power request rises, and so it' necessary to raise the torque of the first harmonic too since is the one devoted to transmit power from the stator to the rotor.

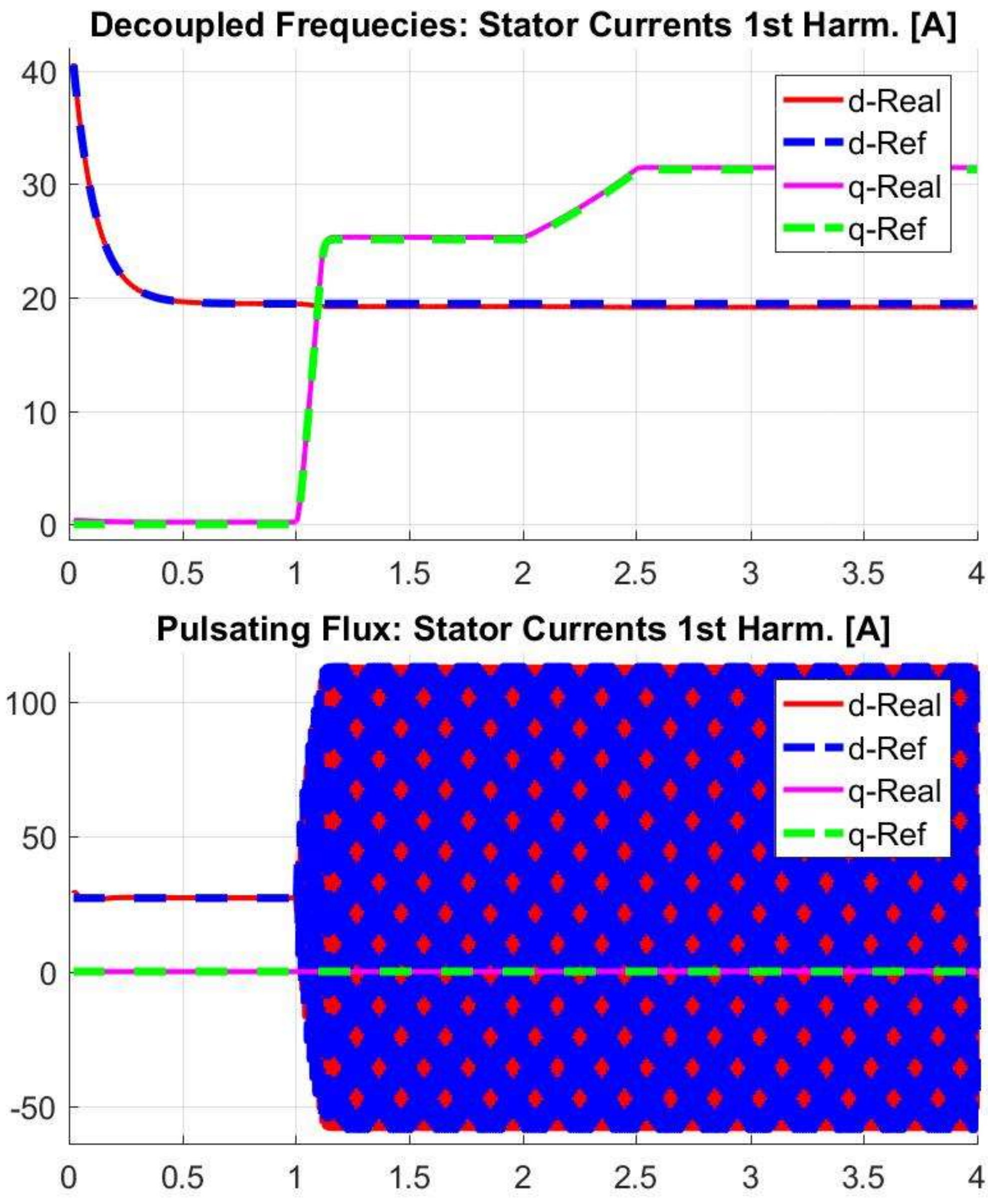

Figure 10.4-2 Stator Currents 1st Harmonic

Once the power request has reached the setpoint value the q current stays still up to the acceleration takes place: here again the q component of the first harmonic current raises again but due to a different reason.

In fact, this increase it is not due to the increasing of the power request but to the increasing of the mechanical speed of the rotor itself: from the figure below in fact is possible to observe how, give a certain amount of power to transmit, the torque that must be produced by the first harmonic varies.

Once the speed setpoint is reached the q current settle again to a constant value.

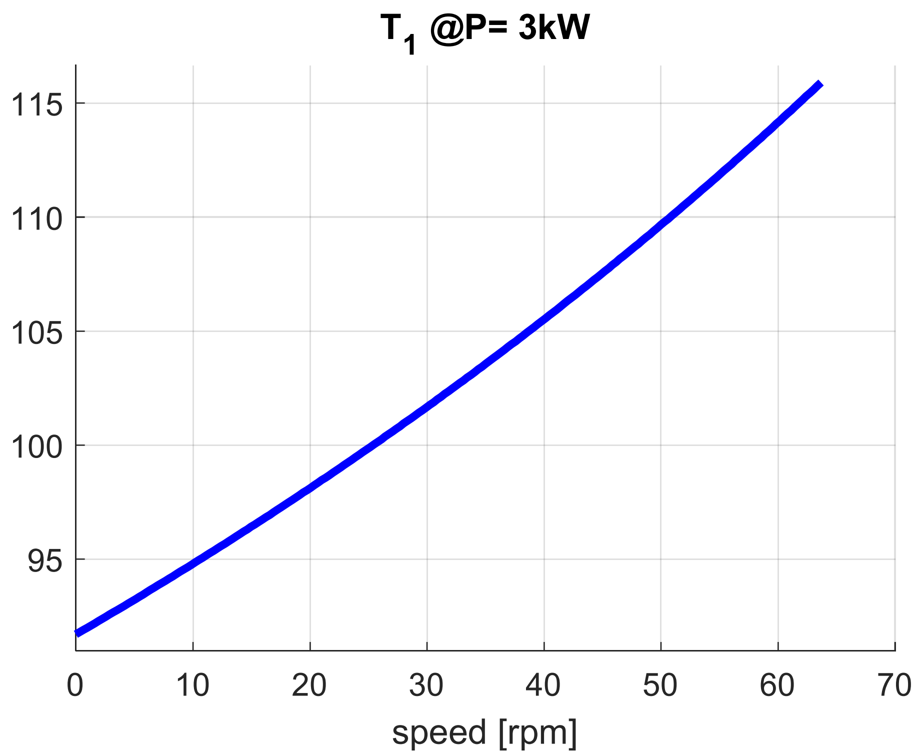

Figure 10.4-3 Torque of the first Harmonic versus Mechanical Speed ($P = 3kW$)

For what concerns the third harmonic, that in both the control solutions acts like a standard induction machine, we can find similar behaviour.

In both the cases it is present an initial peek in the d component of the currents: this has been done in order to faster the flux convergence.

For what concerns the decoupled frequencies control, it is possible to see that, when the power request rises, the q component rises too: this is because, since the first harmonic needs to produce some torque to transmit power, the third one has to compensate since no torque is required to stay still in our application. Similar consideration can be applied to the nominal speed part.

In the accelerating part, instead the q component drastically decrease since quite a lot of torque is required and so the third harmonic has no more to compensate.

For what concerns instead, the pulsating flux *q* component it has some relevant values just when the machine has to be accelerated, since a quite high amount of torque is required.

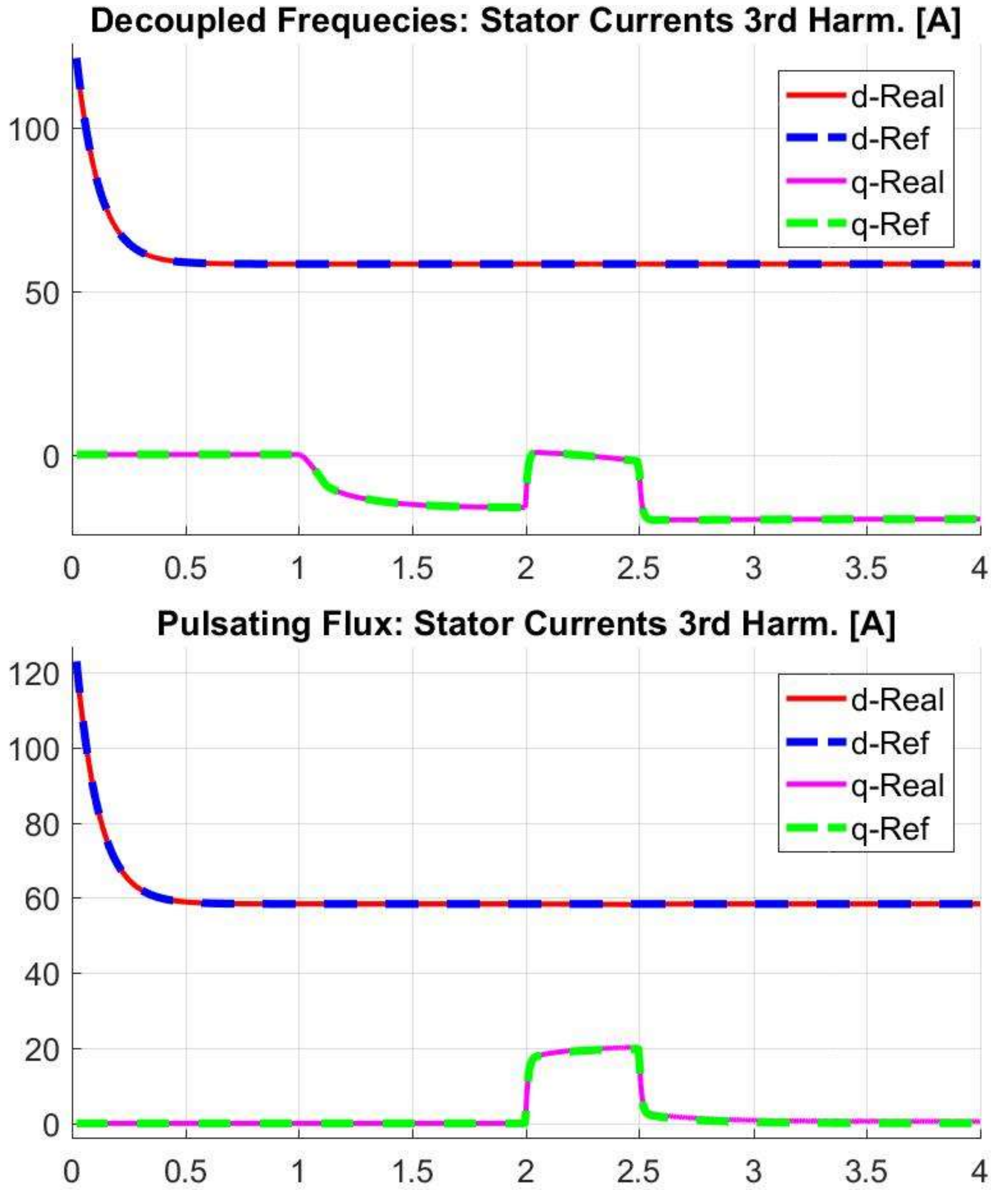

Figure 10.4-4 Stator Currents 3rd Harmonic

For sake of completeness the stator voltages are now reported.

It has to be pointed out that none of them are extremely high and the have similar magnitudes.

It is notable that, in both the control scheme, the q components of the voltages must compensate the back emf. Due to that, the q_3 voltages are equal to 0 up to the rotor is requested to accelerate since both the rotor speed and the torque request are null. The component q_1 is different from zero instead from the beginning in the decoupled frequencies control since for the first harmonic the stator frequency is fixed and different from 0.

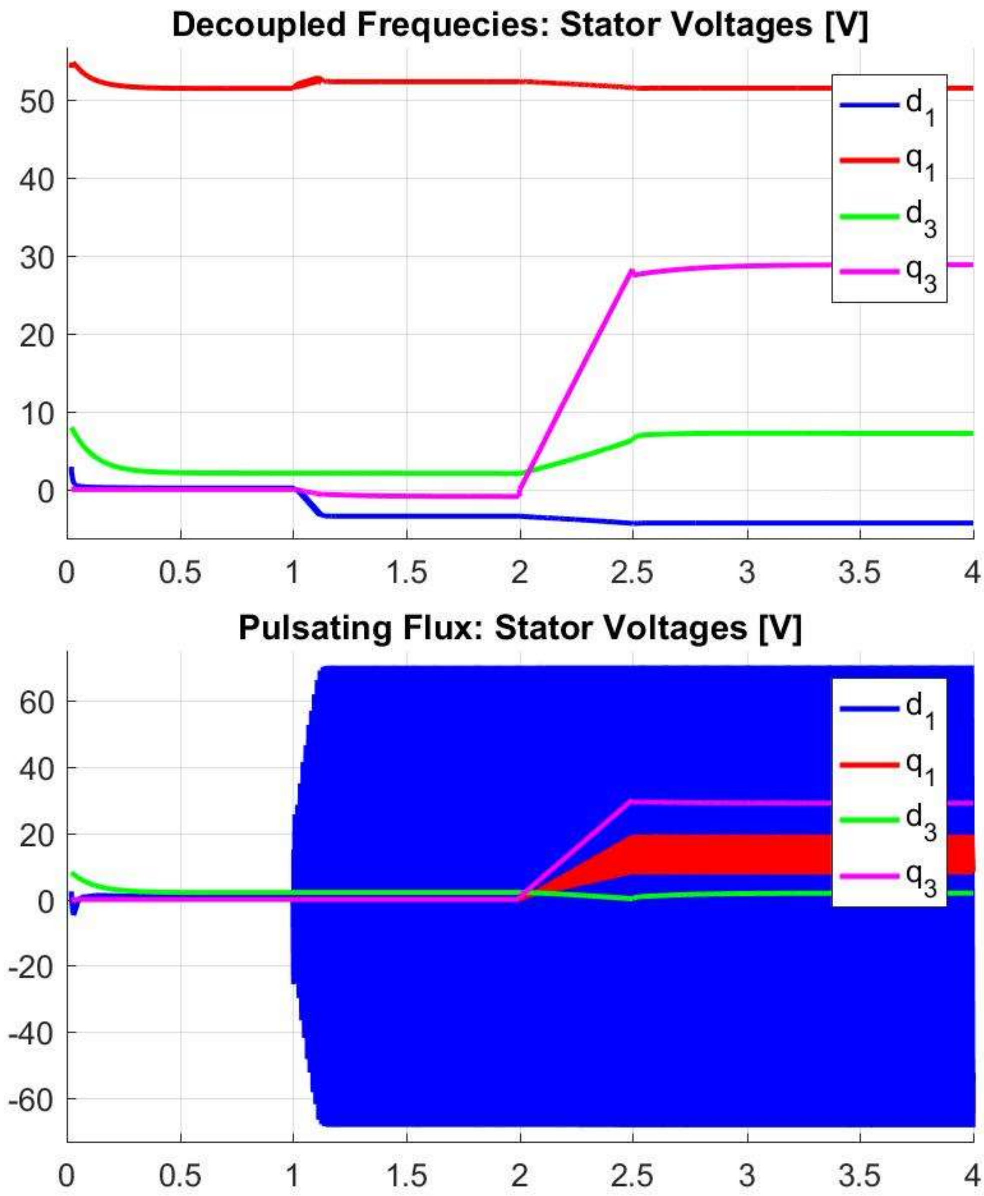

Figure 10.4-5 Stator Voltages

10.5 Rotor Fluxes

For what concerns the rotor fluxes in the independent frequencies control it can be seen that the constant setpoint is reached and maintained along during all the test for both the harmonics. Just in the third harmonic appears a quite remarkable mismatch in the tracking of the q component of the flux: again, this is fault of the discretization of the angle during the rotation.

For what concerns, instead, the pulsating flux solution, is remarkable the behaviour of the first harmonic flux: in fact, during the first second, while the machine is fluxed, the flux reaches the setpoint ($\overline{\varphi}$). After that, since the power request rises, it starts oscillating.

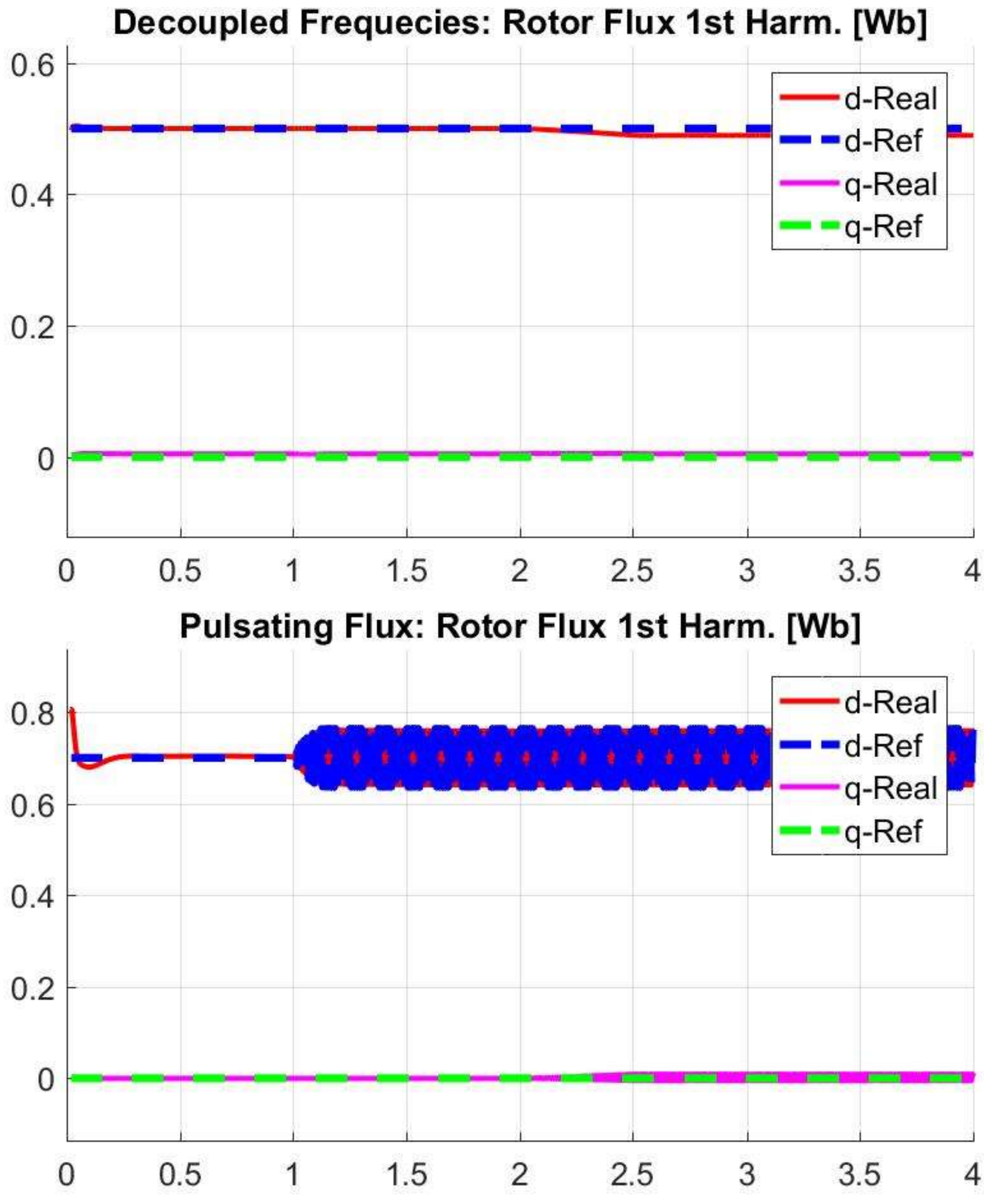

Figure 10.5-1 Rotor Flux 1st Harmonic

Here is reported a zoom of the phase in which the power request rises. As expected, the flux in the independent frequencies solution stays stills and this just proves the effectiveness of the low-level control design.

For what concerns, instead, the pulsating flux solution it is possible to see how much the amplitude of the sinusoidal flux increases according to the rising of the power request. Furthermore. it is possible to underline how much the resonant controller is capable to track the sinusoidal reference almost perfectly.

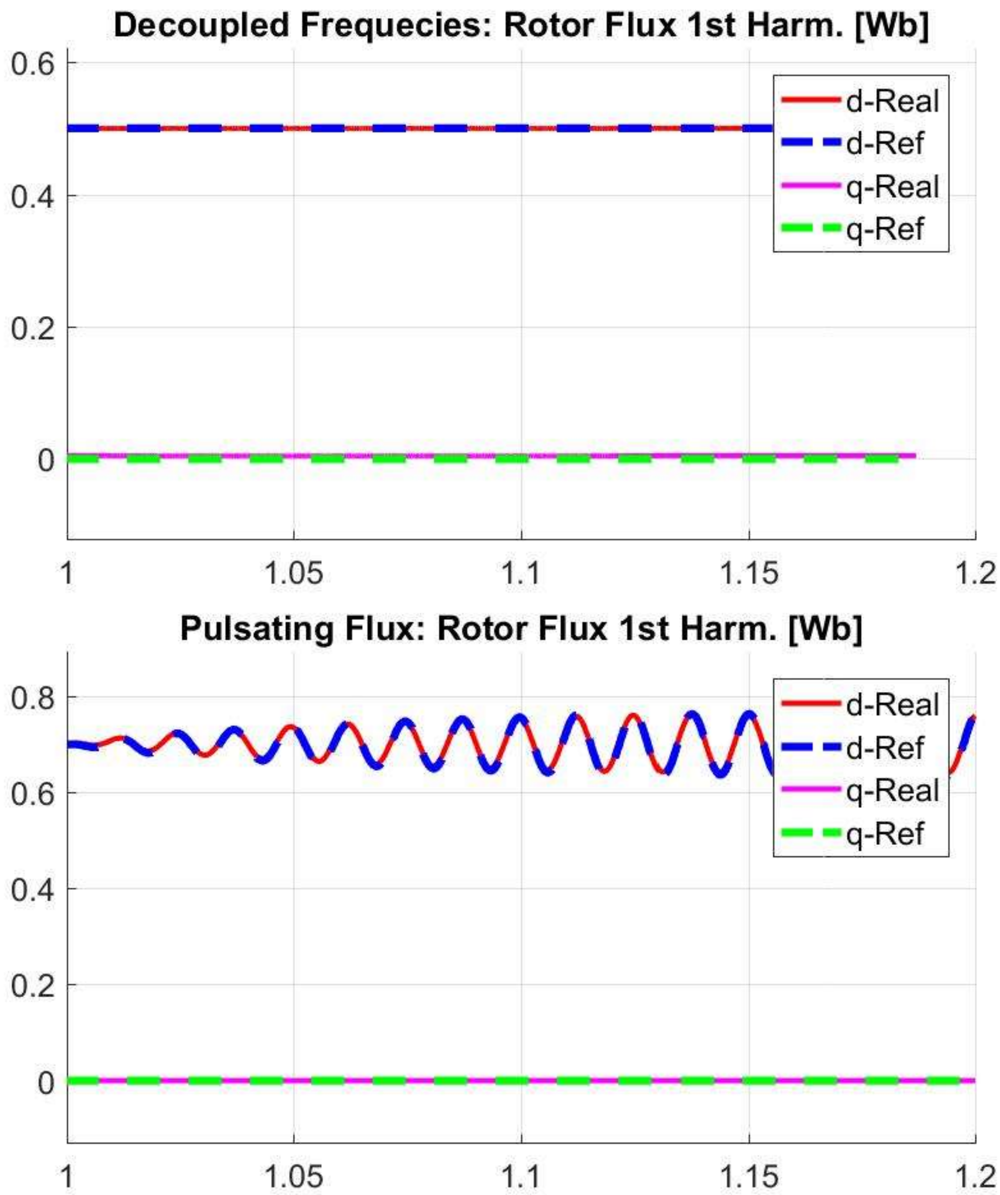

Figure 10.5-2 Rotor Flux 1st Harmonic: zoom

The third harmonic flux in the pulsating flux solution acts very similar to the one in the decoupled frequencies solution: in facts, it reaches the setpoint and almost track it perfectly.

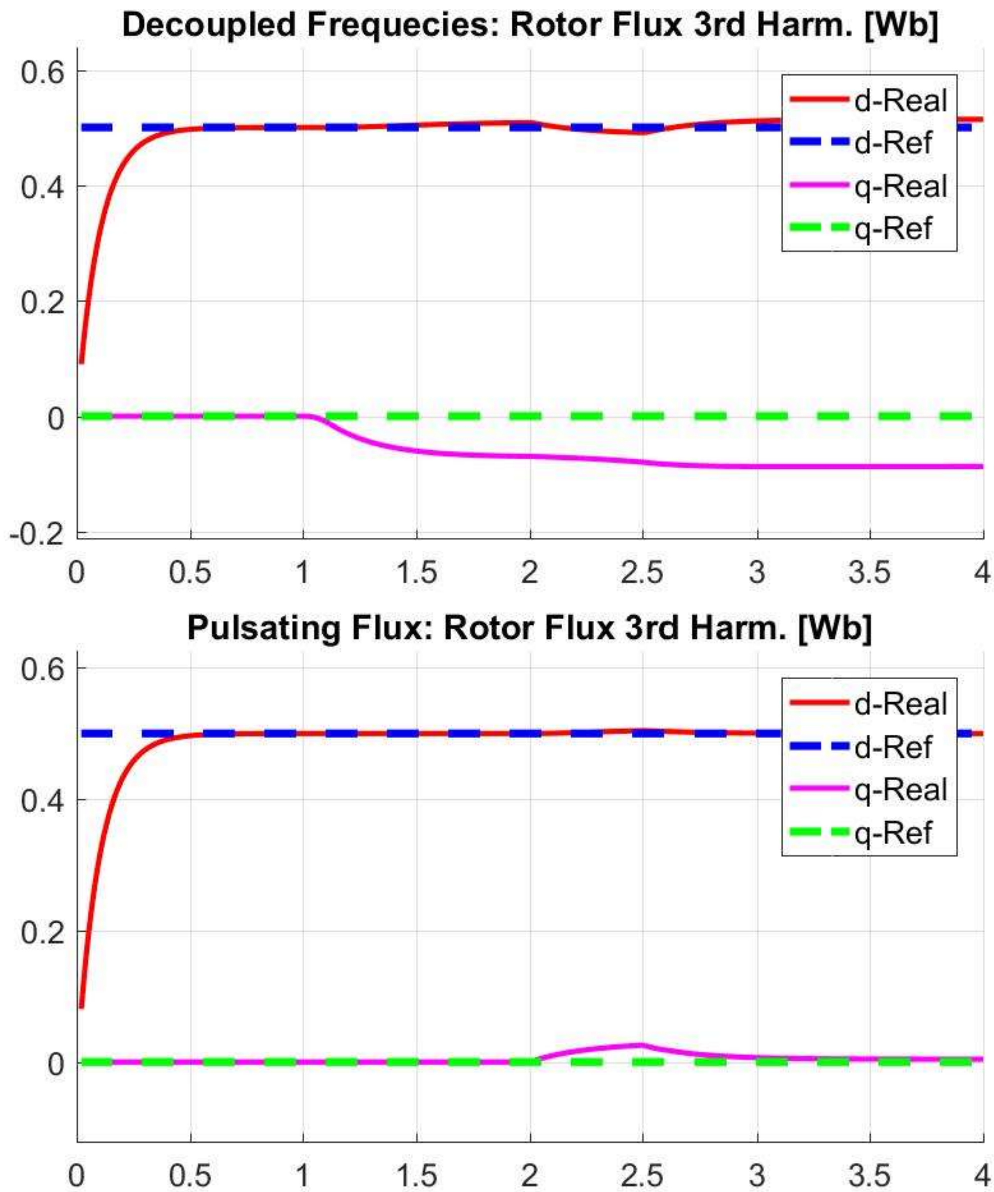

Figure 10.5-3 Rotor Flux 3rd Harmonic

10.6 Rotor Currents and Voltages

Given the behaviour of the stator currents and of the rotor fluxes, the behaviour of the rotor currents is straightforward since these three quantities are linearly coupled.

It has to be remarked that, after the conclusion of the fluxing phase, in both the control the d components of the rotor currents are equal to 0: this is due to the fact that the machine is fluxed from the stator in both the control strategies. The only exception is d_1 in the pulsating flux solution, that start to oscillate accordingly to the rise of the power request.

For what concerns the q components of the currents, both the controls present a specular behaviour respect the q components of the stator currents: this is a direct consequence of the fact that $\varphi_{rq\#}$ is asked to be null.

For what concerns the overall magnitudes it is possible to underline, as for the stator currents, that the pulsating flux solution needs much higher currents respect the independent frequencies one.

Obviously, this is due to the power request that makes oscillates the flux: to obtaining an oscillating flux is necessary an oscillating stator currents that implies an oscillating rotor current.

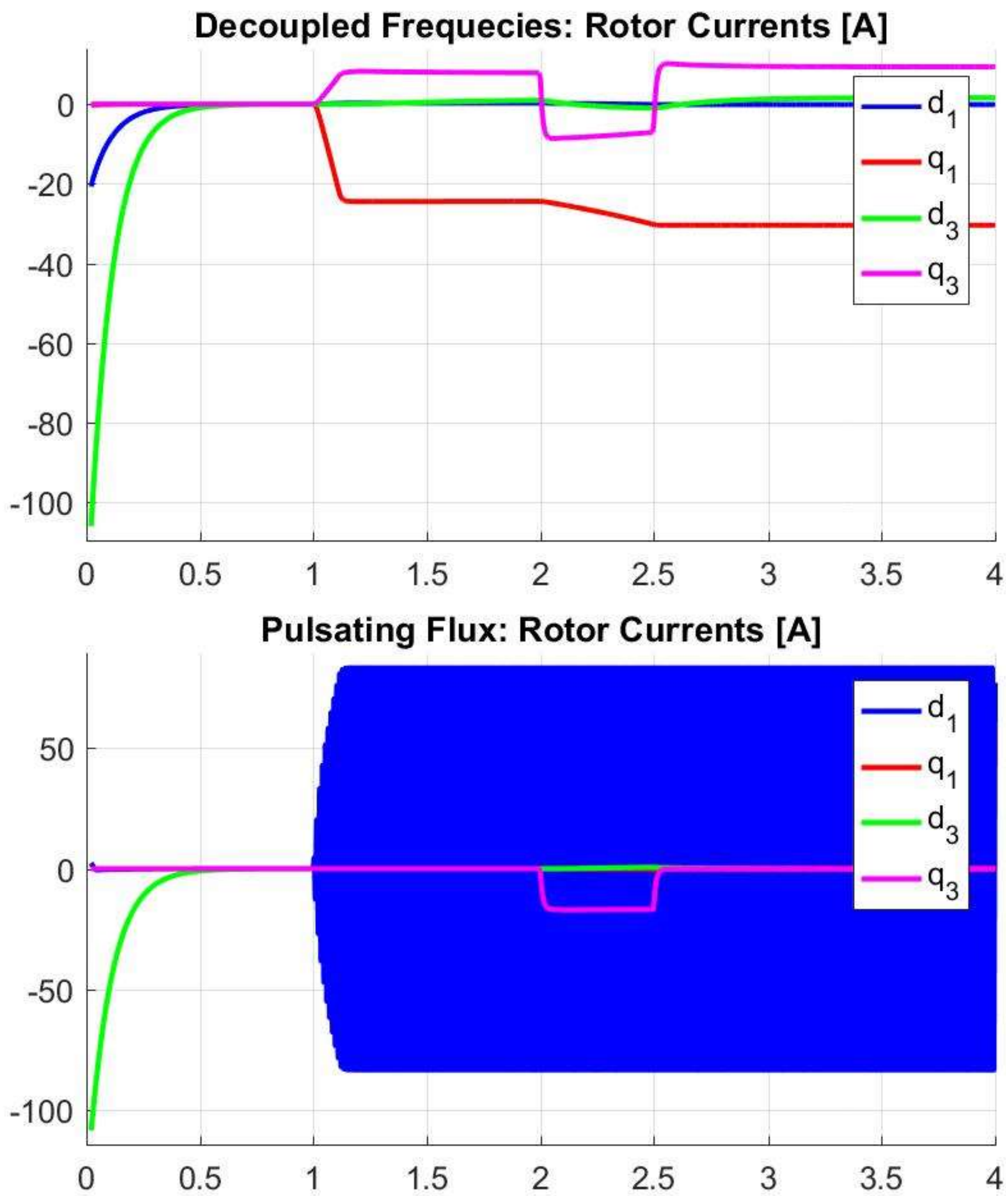

Figure 10.6-1 Rotor Currents

For what concerns the voltages no significant peaks appear and in any case they are quite far from the limits.

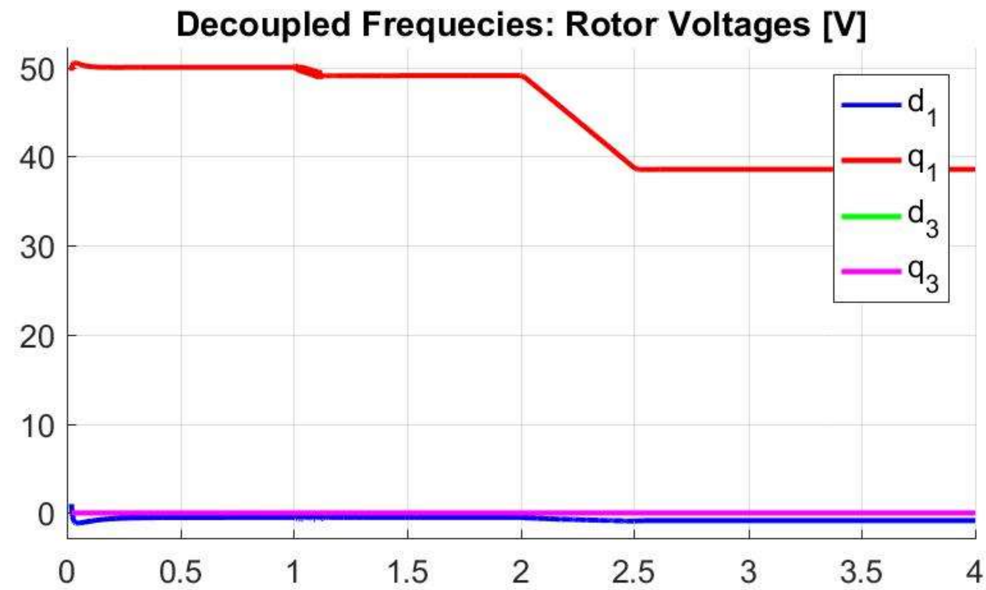

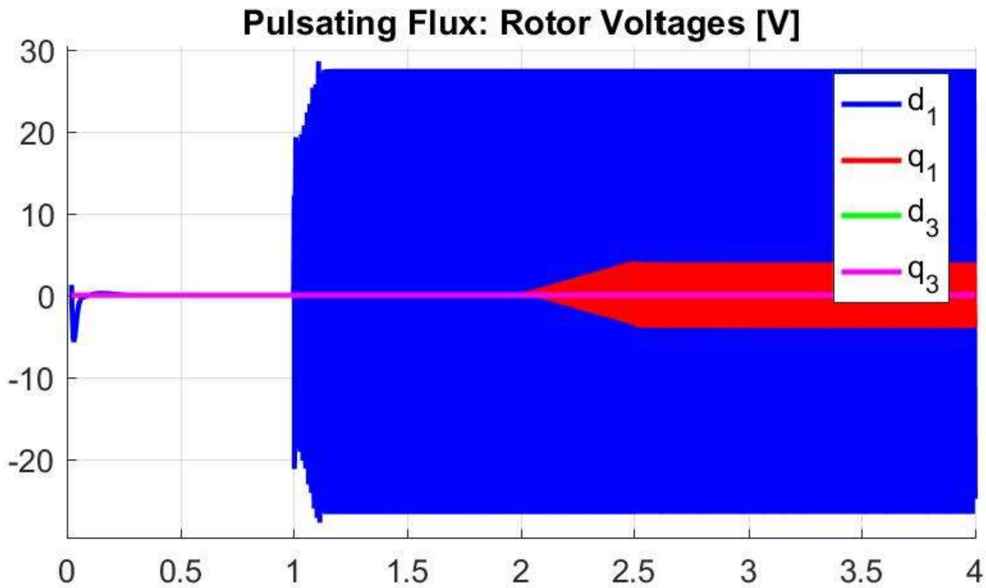

10.7 Comparison Conclusion

Let's now take some conclusion about the two control strategies compared in this chapter.

As first thing, it has to be pointed out that both the control schemes are capable to satisfy the requests and track the references. In particular, for what concerns the mechanical speed, the reference is tracked almost perfectly.

The power reference, so the amount of power that is asked to be transmitted from the stator to the rotor, is instead satisfied exactly with the independent frequencies control while at the mean value over half the period in the pulsating flux solution.

Due to that, obviously, the pulsating flux solution requires a DC-Link of at least $2.6mF$, as calculated in section 9.7, while, theoretically, the independent frequencies control doesn't need any. To this affirmation must added that, some capacitance is, in any case needed, in order to cope with the load peaks requests and to permit to the active rectifier that works as front end of the rotor back to back converter, to work properly.

For what concerns the dimensioning of the converters instead some differences come out: in particular it has to be pointed out that the pulsating flux solution requires much greater currents, up to three times. This could affect the dimensioning of the converters.

11 Conclusions

In this thesis, it has been shown how it is possible to exploit a five phase doubly fed induction machine to transmit power from the stator to the rotor that can lodge some high power requesting electrical equipment, like electric drives or robotic manipulators.

In particular, three high-level policies have been developed, allowing transmission of both electrical and mechanical power to the rotor in order to move the carousel mounted over the rotor and feed the drives that are placed on it.

In particular, the first two controls are based on the synchronism of the fluxes of first and third harmonic: this leads to the suppression of an important degree of freedom, like the stator frequency, in one of the two harmonics that leads to the necessity of using some modulation strategy to get, at mean value, the reference that are requested.

In any case, this synchronization leads also to two important advantages: the first one is that the two fluxes associated to the harmonics compose in such a way to get a lower peak in the resultant one, thing that makes possible to rise them to have a quicker dynamic response. The second, and most important one, is that is possible to adapt the two possible control schemes for a three phase machine.

The first control designed provides to the mechanical load the torque that is required as mean value: in this way, the limitation that rises to grant the synchronism of the fluxes is avoided.

As drawback, some ripple in the velocity appears and, when the torque sign changes even the track of the power is no more good and so a quite big DC-link is required. The second drawback of this control strategy is that no more applicable if the inertial load is lightweight since the velocity ripple will become much greater and the rotor itself could resonate due to the poor stiffness of the load itself. The third drawback of this control method is that a great number of data must be exchanged between the rotor and the stator: this is due to the fact that both the harmonics concur in the power and torque transmission and no a priori knowledge over the references shapes is available.

The second control developed, instead, satisfy the power request as mean value while the torque is satisfied exactly: in order to obtain this result, the flux is made oscillates in order to exploit the voltage and, then, the power provided through its derivative.

As drawback, in order to have a pulsating flux, is necessary a big amount of current; furthermore, since the power structurally oscillates, a large DC-link is necessary, too.

The third method to control the machine instead is based on the de-synchronization of the two fluxes, and so it is reliable only on a five phase machine.

This control avoids the limitation introduced by synchronization, and it is so possible to transmit the right amount of electrical and mechanical power instantaneously, without any modulation strategy: this implies that any reliable profile of the velocity and of the power reference can be tracked almost perfectly.

As results of this choice just a very small DC-link will be needed that will become dependent on the electrical load, while the currents magnitude remains quite small, that implies a smaller size of the two converters needed.

Since it is possible to rely on a five phase machine, it is possible to use this last methodology to achieve the goals of this thesis since it doesn't present heavy drawbacks. Further development will concern the physical implementation of the control described on the real machine that has to be delivered yet.

Appendix A: Symbols

Symbol	Meaning
$\#_s$	Stator variable
$\#_r$	Rotor variable
$\#_{\#d}$	d-axis variable
$\#_{\#q}$	q-axis variable
$\#_{\#\#1}$	First harmonic variable
$\#_{\#\#3}$	Third harmonic variable
$\#_{ref}$	Reference value
$\#^{wifi}$	Wi-Fi transmitted value
$\boldsymbol{u}, \boldsymbol{v}, \boldsymbol{V}$	Voltage
$\boldsymbol{i}$	Current
$\boldsymbol{\varphi}, \boldsymbol{\phi}$	Flux
$\boldsymbol{P}$	Electrical Power
$\boldsymbol{T}$	Torque
$\boldsymbol{\omega_0}$	Fundamental electrical stator frequency
$\boldsymbol{\omega_r}$	Fundamental electrical rotor frequency
$\boldsymbol{\omega_m}$	Mechanical Speed
$\boldsymbol{v_{real}}$	Generic vector in the world reference frame
$\boldsymbol{v_{dq}}$	Generic vector in the Clarke Park reference frame
$\boldsymbol{v_a} \quad \boldsymbol{v_b} \quad \boldsymbol{v_c} \quad \boldsymbol{v_d} \quad \boldsymbol{v_e}$	Phases of a vector in real world
$\boldsymbol{v_{d1}}\ \boldsymbol{v_{q1}}$	d-q values of the first harmonic of a generic vector in Clarke Parke
$\boldsymbol{v_{d3}}\ \boldsymbol{v_{q3}}$	d-q values of the third harmonic of a generic vector in Clarke Parke
$\boldsymbol{v_n}$	Value of the neutral of a generic vector in Clarke Parke
$\boldsymbol{i_{sd1}}, \boldsymbol{i_{sq1}}, \boldsymbol{i_{sd3}}, \boldsymbol{i_{sq3}}$	d-q components of the stator currents of first and third harmonic
$\boldsymbol{\varphi_{rd1}}, \boldsymbol{\varphi_{rq1}}, \boldsymbol{\varphi_{rd3}}, \boldsymbol{\varphi_{rq3}}$	d-q components of the rotor magnetic flux of first and third harmonic
$\boldsymbol{L_s}$	Stator windings inductance
$\boldsymbol{R_s}$	Stator windings resistance
$\boldsymbol{L_r}$	Rotor windings inductance
$\boldsymbol{R_r}$	Rotor windings resistance
$\boldsymbol{L_m}$	Mutual inductance
$\boldsymbol{p}$	Number of pole pairs
$\boldsymbol{\alpha_2}, \boldsymbol{\beta_1}, \boldsymbol{\gamma_1}, \boldsymbol{\sigma_1}, \boldsymbol{\eta_1}$	Equations parameters

$\boldsymbol{J}$	Inertia of the rotor
$\boldsymbol{b}$	Viscous friction of the rotor
$\boldsymbol{G_m}$	Mechanical transfer function
$\boldsymbol{A, A_i}$	A Matrix of the state space Representation
$\boldsymbol{B, B_i}$	B Matrix of the state space Representation
$\boldsymbol{C}$	C Matrix of the state space Representation
$\boldsymbol{x(t), z(t)}$	Generic States
$\boldsymbol{\overline{\omega}}$	Frequency of the pulsating flux
$\boldsymbol{\overline{\varphi}}$	Pulsating Power flux bias
$\boldsymbol{k(P)}$	Amplitude of the oscillation of the flux
$\boldsymbol{k_u}$	Voltage proportional gain
$\boldsymbol{\overline{P}}$	Mean Power Transfered
$\boldsymbol{G_{phi_{rd3}}}$	Flux transfer function
$\boldsymbol{\tau_\varphi}$	Flux imposed time constant
$\boldsymbol{\hat{x}}$	Estimated state
$\boldsymbol{A_d}$	Discrete state matrix A
$\boldsymbol{B_d}$	Discrete state matrix B
$\boldsymbol{K_{opt}}$	Optimal state feedback matrix
$\boldsymbol{u_{ff}}$	Feedforward input
$\boldsymbol{T_s}$	Sampling time of the task
$\boldsymbol{L}$	Output injection matrix
$\boldsymbol{Q}$	LQ weights of the states
$\boldsymbol{R}$	LQ weights of the outputs
$\boldsymbol{u_{ref}}$	Stady State Voltage
$\boldsymbol{\hat{\hat{x}}}$	Error between the estimated value and the real one
$\boldsymbol{T_s}$	Sampling time of the controller
$\boldsymbol{T^{wifi}}$	Period of the wifi transmission
$\boldsymbol{t^{wifi}}$	Wi-Fi Instant
$\boldsymbol{A_{isis}, A_{isir}, A_{iris}, A_{irir}}$	Sub Matrixes of A_i
$\boldsymbol{B_{isis}, B_{isir}, B_{iris}, B_{irir}}$	Sub Matrixes of B_i
$\boldsymbol{d(t)}$	Residual error due to discretization
$\boldsymbol{R_s(s)}$	Stator Regulator
$\boldsymbol{R_r(s)}$	Rotor Regulator
$\boldsymbol{P_s}$	Proportional gain of the stator controller
$\boldsymbol{I_s}$	Integral gain of the stator controller
$\boldsymbol{P_r}$	Proportional gain of the rotor controller
$\boldsymbol{I_r}$	Integral gain of the rotor controller
$\boldsymbol{R_s}$	Resonant gain of the stator controller

R_r	Resonant gain of the rotor controller
E	Energy stored
Q	Charge of the capacitance
C	Capacitance
P_C	Power flowing in the capacitance
P_L	Power to the load